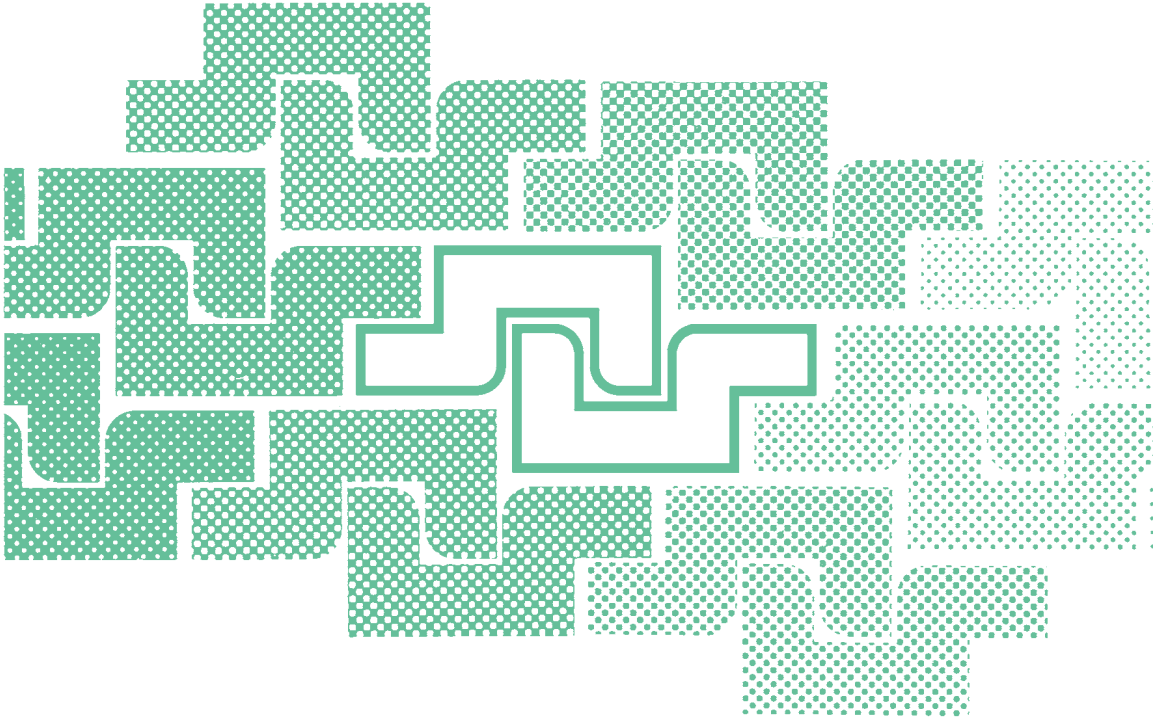

Environmentally Friendly Coastal Protection

Edited by

Claus Zimmermann, Robert G. Dean,
Valeri Penchev and Henk Jan Verhagen

NATO Science Series

IV. Earth and Environmental Sciences – Vol. 53

Environmentally Friendly Coastal Protection

NATO Science Series

A Series presenting the results of scientific meetings supported under the NATO Science Programme.

The Series is published by IOS Press, Amsterdam, and Springer (formerly Kluwer Academic Publishers) in conjunction with the NATO Public Diplomacy Division.

Sub-Series

I. Life and Behavioural Sciences	IOS Press
II. Mathematics, Physics and Chemistry	Springer (formerly Kluwer Academic Publishers)
III. Computer and Systems Science	IOS Press
IV. Earth and Environmental Sciences	Springer (formerly Kluwer Academic Publishers)

The NATO Science Series continues the series of books published formerly as the NATO ASI Series.

The NATO Science Programme offers support for collaboration in civil science between scientists of countries of the Euro-Atlantic Partnership Council. The types of scientific meeting generally supported are "Advanced Study Institutes" and "Advanced Research Workshops", and the NATO Science Series collects together the results of these meetings. The meetings are co-organized by scientists from NATO countries and scientists from NATO's Partner countries — countries of the CIS and Central and Eastern Europe.

Advanced Study Institutes are high-level tutorial courses offering in-depth study of latest advances in a field.
Advanced Research Workshops are expert meetings aimed at critical assessment of a field, and identification of directions for future action.

As a consequence of the restructuring of the NATO Science Programme in 1999, the NATO Science Series was re-organized to the four sub-series noted above. Please consult the following web sites for information on previous volumes published in the Series.

http://www.nato.int/science
http://www.springeronline.com
http://www.iospress.nl

Series IV: Earth and Environmental Series – Vol. 53

Environmentally Friendly Coastal Protection

edited by

Claus Zimmermann
University of Hannover,
Germany

Robert G. Dean
University of Florida,
Gainesville, FL, U.S.A.

Valeri Penchev
Bulgarian Ship Hydrodynamics Centre,
Varna, Bulgaria

and

Henk Jan Verhagen
Delft University of Technology,
Delft, The Netherlands

Springer

Published in cooperation with NATO Public Diplomacy Division

Proceedings of the NATO Advanced Research Workshop on
Environmentally Friendly Coastal Protection Structures
Varna, Bulgaria
25–27 May 2004

A C.I.P. Catalogue record for this book is available from the Library of Congress.

ISBN-10 1-4020-3300-1 (PB) Springer Dordrecht, Berlin, Heidelberg, New York
ISBN-13 978-1-4020-3300-1 (PB) Springer Dordrecht, Berlin, Heidelberg, New York
ISBN-10 1-4020-3299-4 (HB) Springer Dordrecht, Berlin, Heidelberg, New York
ISBN-13 978-1-4020-3299-8 (HB) Springer Dordrecht, Berlin, Heidelberg, New York
ISBN-10 1-4020-3301-X (e-book) Springer Dordrecht, Berlin, Heidelberg, New York
ISBN-13 978-1-4020-3301-8 (e-book) Springer Dordrecht, Berlin, Heidelberg, New York

Published by Springer,
P.O. Box 17, 3300 AA Dordrecht, The Netherlands.

Printed on acid-free paper

Printed in the Netherlands.

CONTENTS

PREFACE

Coastlines have been and still are the centre lines of civilization around the world with still increasing pressure from both sides, the hinterland and the sea, with all its foreseeable and unforeseeable impacts through nature or mankind. While response of nature to such impacts is flexible in the way that all morphological changes with all the consequences are tolerated as part of the system, man cannot tolerate short-term or long-term changes without being threatened in its physical and economical existence.

Therefore, tools and techniques for coastal protection have been developed to keep the status quo of the coast whereever possible. In nearly all cases the desired effects on increased protection and reduction of risk to life were obtained with extensive costs and with creation of new or extended problems to the coastal environment in the near or far field.

Since the coastline is only part of a complex system, which extends quite a distance inland and to the sea, i. e. the coastal zone, coastal engineering has to be part of the coastal zone management process. Here, the ideas and proposals for coastline stabilization, coastal protection and maintenance have to be assessed under economic, environmental – and with increasing importance – sociological aspects. As a result, additional ideas have to be introduced into the conventional engineering and modelling practice by the coastal engineer. New techniques are to be developed in modelling and execution to finally introduce "environmentally friendly" solutions.

The objectives of the Advanced Research Workshop (ARW) on Environmental Friendly Coastal Protection Structures were:

- *to contribute to the critical assessment of existing knowledge in the field of coastal and environmental protection;*
- *to identify directions for future research in that area;*
- *to promote close working relationships between scientists from different countries and with different professional experience.*

The latest trends in research in coastal and environmental protection have been summarized and developed during the meeting. Seventeen papers are presented in this book, including 8 key-notes, and 9 selected participant presentations, attempting to cover as completely as possible all related aspects – coast, engineering structures, water, sediments, ecosystems – and their complicated interactions.

Coastal protection will remain a task with increasing importance, but analysis of risks to man and environment has to be the essential effort in this work.

This meeting already helped to promote further collaboration of the scientists in the field of coastal and environmental protection.

SUMMARY
OF THE ADVANCED RESEARCH WORKSHOP

C. Zimmermann, V. Penchev

The Advanced Research Workshop was focused on discussions of latest trends in research in coastal protection, emphasizing on environmental impact of coastal structures. The Scientific Program included 1 plenary and 4 scientific sessions, each followed by broad discussions. Eight key-notes have been presented by the invited key-speakers. 18 presentations have been delivered by the other participants, including 14 oral and 4 poster papers. Special meetings of 3 Thematic Work Groups (WG) were held on the last day of the meeting. Scientific sessions and WG meetings were cross-linked, and not over-lapped, in order to provide interdisciplinary approach and avoid repetitions during discussions. An attempt has been made to cover as completely as possible all related aspects – beach, water, engineering structures, sediments, ecosystems, and their complicated interaction.

The Plenary session was entitled "Coastal Protection for the next 100 Years" and was focused on the latest trends and basic approaches in coastal protection. An opening key-note address has been introduced by Prof. C. Zimmermann, Co-Director of the ARW where an **overview of the up-to-date knowledge** has been presented, and **identification of directions for future research** has been addressed. State-of-the-art in **research related to beach nourishment as a basic means of sustaining the world's beaches** has been presented by Prof. Robert G. Dean from University of Florida. Latest achievements and **innovations in coastal protection** have been discussed in the key-paper of Ms. Joan Pope, Technical Director of Coastal and Hydraulics Lab., US Army Engineer Research and Development Center. During discussions, participants identified the needs to ensure the availability of an **adequate understanding of the physics underlying coastal and nearshore processes**, and the associated **information/data resources** to provide guidance for future decisions related to coastal morphological changes. This scope also encompasses effects of relative **sea level change** and **reduction in sediment supply**, each which can induce erosional pressure on the beach and nearshore systems and each of which can be due to both natural and/or anthropogenic causes.

Classical and unconventional coastal protection methods have been discussed during the first scientific session. Two key-papers have been presented by Dr. Marcel van Gent (WL Delft Hydraulics, Netherlands) and Mr. Henk Jan Verhagen (Delft University of Technology, Netherlands). Presentations have been focused on **recent methods for investigation and design of "non-sandy" coastal structures, including hydrodynamic interactions, strength, stability, and failure aspects**. Key papers have been supported by 4 presentations by other participant. Discussions were focused on critical assessment of the recent level of research in this area. Some practical aspects related to providing **guidance for structure performance**, and basic information to decision makers have been also discussed.

A second scientific session was dedicated to **numerical & physical modelling** of coastal structures. Key-papers addressed basic issues of advanced methods & tools in numerical

C. Zimmermann et al. (eds.), Environmentally Friendly Coastal Protection, 7-8.

simulations in coastal hydraulics & sediment transport, as well as of **integrated hydraulic-environmental modelling** (Dr. J.A. Roelvink, WL Delft Hydraulics, Netherlands). Special attention was paid to **effects on hydrodynamics and morphology, modelling of silt transport, water quality and primary production,** as well as on **ecological evaluation** based on lumped parameter systems , mean or other statistical parameters. Discussion concentrated on the modern computational techniques that make it very possible to make mathematical descriptions of nearly all processes and to compute hydrodynamic behavior in detail. Regarding the **interaction of water and sand and/or mud beds**, including the aspects of **water quality modelling**, mathematical models are much more complicated, but still very possible. Need of more **interdisciplinary integration** in development of both numerical and physical models was underlined. The continuous need for **calibration and verification of mathematical models** using physical models was stressed.

Third scientific session was focused on research on some **environmentally friendly coastal protection methods**, where a beach is required at all, no negative impact on water quality is provided, rock emplacement on the beach is avoided, and aesthetic properties are preserved. Research achievements in **modelling of artificial coastal reefs** have been presented in the key-paper of Dr. V. Penchev, Coastal Hydraulics Dept., BSHC, Bulgaria. It was stressed that application of reefs and submerged sills (most often in conjunction with beach nourishment) is a sensitive engineering solution that requires more knowledge and further research on **mechanism of wave breaking**, and **longshore currents generated in protected area**. Similar aspects have been discussed also in the papers presented by 3 of the invited participants. Application of **modern computational tools** in studying non-traditional coastal protection structures has been examined during discussions.

General aspects of advanced coastal defense strategies have been discussed during the last scientific session. Environmentally friendly approaches in coastal protection, **including assessment of associated impacts** have been addressed in the paper presented by Dr. G. Rozynski, Institute of Hydro-engineering, Poland, as well as in the presentations of some of the invited participants. Discussions were focused on the **impact of coastal protection structures on local habitats**, as well as on the **integration of physical, biological and social points of view for ICZM**.

The meetings of the 3 Thematic **Work Groups** (WG)**,** respectively WG1: Coastal Morphology, WG2: Engineering Structures / Hydrodynamic Interactions, and WG3: Environmental Aspects/Integrated Modelling took place during the last day of the meeting. All the presentations and discussions have been summarized, and recommendations for further research have been proposed. A final **Round Table** took place before the closing, where the achievements of the meeting have been summarized by the ARW Co-Directors.

The workshop was held in a friendly atmosphere that allowed broad exchange of scientific information and expertise among various sectors (hydraulics, morphology, environmental protection, risk assessment), and nations, related to the central topic.

Chapter 1

Key-Notes

ENVIRONMENTAL FRIENDLY COASTAL PROTECTION STRUCTURES THE ENDLESS STRUGGLE OF THE ENGINEER AGAINST WATER, WAVES AND EROSION – OPENING ADDRESS –

Claus Zimmermann
University of Hannover, Franzius-Institut for Hydraulic, Waterways and Coastal Engineering
Hannover, Germany

1. Coastal Colonisation and Requirement for Protection against the Sea

Major parts of the world population live and work at or near coasts (Fig. 1) which are subject to constant attacks from short-term and long-term changing water levels, storms, waves and currents. Together with geomorphologic and seismic activities such attacks result in permanent changes of coastlines. While nature reacts quite flexibly to such variations and changes, humans attempt to maintain its position. In doing so, tools and methods have been developed over centuries to fight against the sea and fix the coastline or even extend it, Fig. 2. Growing coastal populations and metropolitan areas with increasing industrial complexes and infrastructures demand protection against the hazards from the sea, i.e. the action of the coastal engineer.

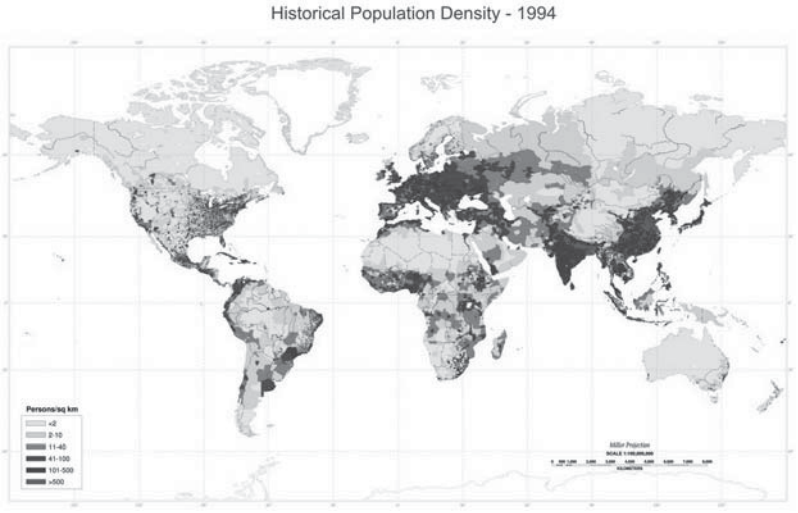

Figure 1: Coastal Population around the World

C. Zimmermann et al. (eds.), Environmentally Friendly Coastal Protection, 11-24.

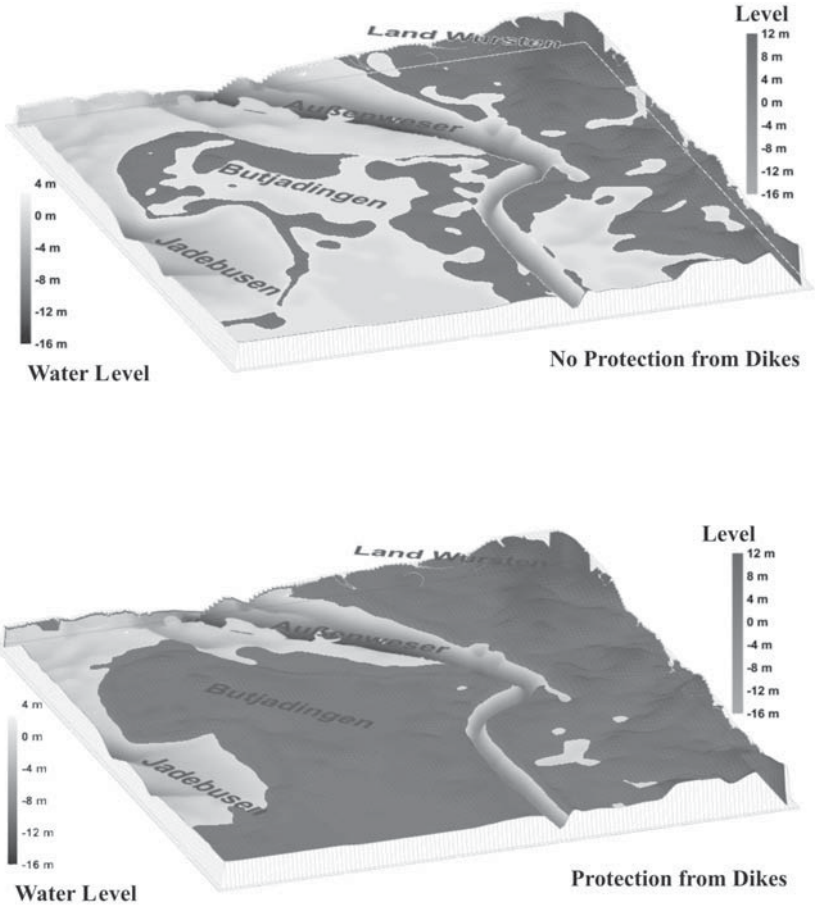

Figure 2: North Sea Coastal Areas without and with Coastal Protections Today

2. Coastal Variability and Reaction of Men

There is a wide variation of coasts and their morphologies around the oceans. Rocky cliffs like in the fjords of Scandinavia, the West Coast of the United States of America or long stretches of the Mediterranean showed only marginal changes for generations. They require negligible activities for protection of settlements and infrastructures, Fig. 3.

Figure 3: No Coastal Protection Required at Rocky Cliffs
(Adelmann, K., California Coastal Records Project, 2004)

But major parts of the coastal population have settled along shallow coasts and estuaries with often extreme tidal activities, Fig. 4. Shallowness with reefs, bars and sandy shoals in most cases is a result of long-term intrusion and deposition of mostly sandy sediments from rivers. Most prominent examples are the constantly changing deltaic plains of the Mississippi, Nile, Ganges, and Yellow River deltas. Apart from geomorphological degradations, the tide, wind and wave induced longshore currents result in permanent accretion and erosion of sands and beaches which, with the additional action of aeolian sand transport, sand or dune fronting features in major parts of the world's coastline (Bird, 1986).

Figure 4: Coast at Low and High Tides

Since longshore and cross-shore variations at shallow, sandy coasts may occur in a few years periods, human's settlements and activities are constantly in danger and require engineering reactions. Such reactions to the undesired changes depend on the stress acting on the coastline from both sides. From the hinterland it is the human activities and social

habits that push against the coastline and even shift it, by building structures, infrastructures, farming, etc. including control of discharges and drainage. From the sea, water levels and waves varying with tides and only statistically predictable storm conditions result in regional water levels and waves, local currents and sediment erosion and accretion. For the appropriate engineering reactions and precautions numerous tools have been developed over generations to a fairly high standard, considering safety, long-term changes, including climate, and environmental sustainability.

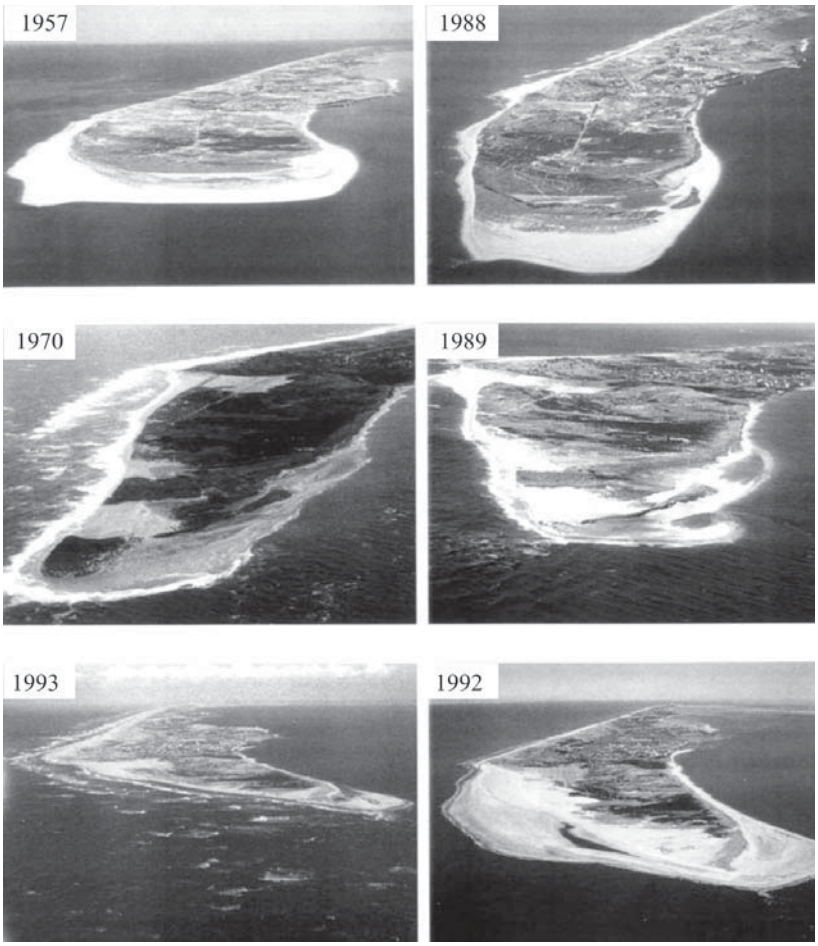

Figure 5: Morphological Changes of a Dune Island at the North Sea Coast within 35 Years (Zeug, G., German Aerospace Center, 2000)

Figure 6: Stress to Coasts from Human Activities and the Sea

3. Stress on Coasts from the Sea

Tides and winds are the predominant stress factors to coasts. Superposition of high tidal waves with extreme storm events (Hurricanes, Typhoons) in many cases increase local average water levels by several metres which are intensified in estuaries and bay areas by reflections and constrictions, Fig. 7.

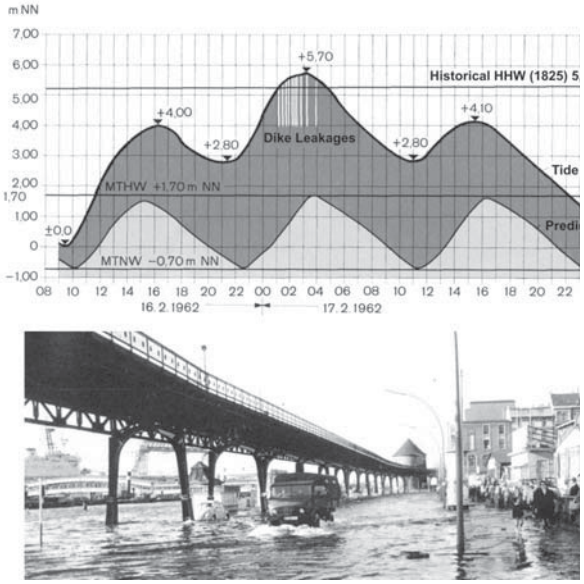

Figure 7: Storm Tide Water Levels Upstream of an Estuary (Elbe, Hamburg)

While wind induced waves in fetch limited estuaries and bays have only minor effects on coast lines and artificial structures, open coasts are subject to heavy wave attacks which increase with rising water levels and depths, Fig. 8. Since wind induced water levels and thus wave heights result from statistical processes, design criteria for the reacting engineer can only be obtained by using probabilistic methods, Fig. 9. Social consent is also required to assume certain levels of safety standard for selection of probable design wave heights or overflows and thus the risk for the hinterlands.

Figure 8: Storm Waves at a Sea Wall

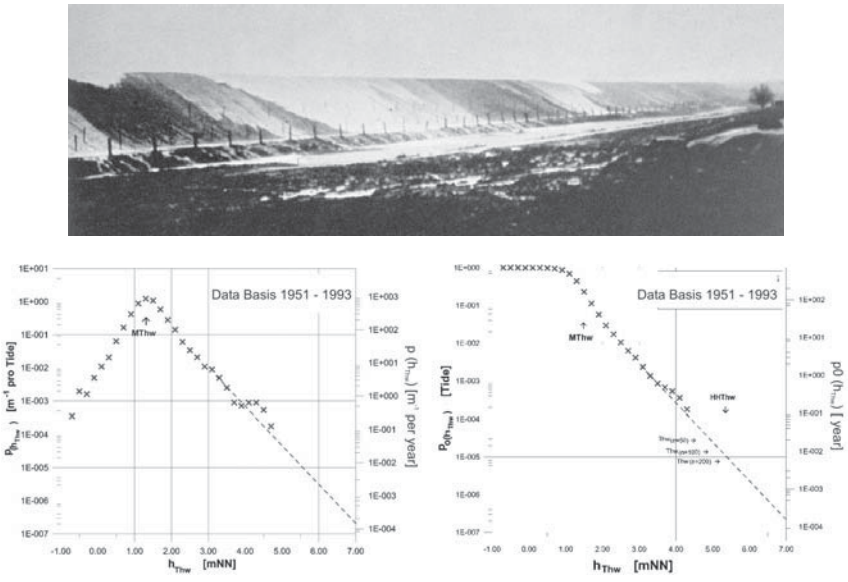

Figure 9: Probability of Wave Overflow as a Basis for Design Levels

4. Stress on Coasts from the Hinterland

Securing the population along coasts against regular flooding and in many cases even extending settling areas into the sea means fixing of a certain defence line which always reduces water levels affected coastline lengths and thus the flooding areas and volumes. As a result, local water levels increase due to tidal and surge wave reflections, while wind waves will also increase and, therefore, increased structural safety levels are required.

Additional stress to the coast arises from growing tourism and beach dwellings with high pressure for direct access to beaches and unobstructed views over the sea, Fig. 10. Negligence of the not exactly predictable changes and variabilities in the coastline request often for immediate action of authorities and coastal engineers. Stress on protection standards in recent decades increased dramatically because of exponentially growing investments in housing, industrial complexes and infrastructures in flood prone areas, Fig. 11.

Figure 10: Hazards to Settlements along Coasts

Figure 11: Non-Stress-Resistant Infrastructures behind Coastline

Such high risk potential requires the definition and evaluation of the second parameter as given in the definition of risk:

Risk = Probability of Recurrence * Level of Damages

Where damages are the result of failures of any protections at the coast.

5. Coastal Engineering Reaction and Tools for Coast Protection

Fighting against water and waves commenced in ancient times began with settlings on artificial wharfs and construction of dikes and sea wall, Fig. 12.

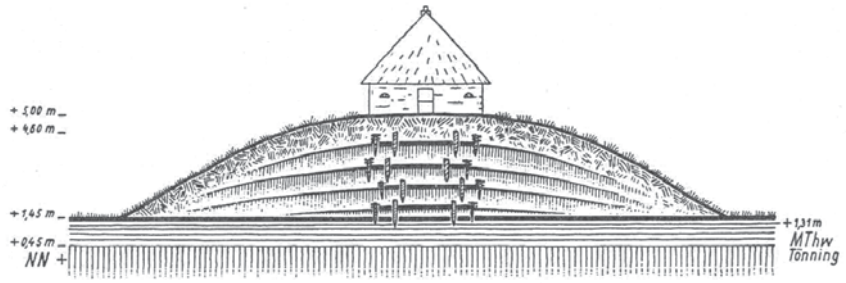

Figure 12: Ancient Wharfs and Dikes, Sea Walls

To stop regression of sandy coastlines and prevent shipping channels from sedimentation, groynes perpendicular to the coasts were built to reduce or even prevent longshore currents and longshore sediment transport, Fig. 13.

Figure 13: Groynes

Preventing erosions on limited coastal reaches results in the leeward part of the coast often being subject to strong erosion thus requiring further coastline protections, a phenomenon arising also for larger and smaller breakwaters which protect harbours and harbour channels against waves, currents and sedimentation, Fig. 14.

Figure 14: Lee Erosions Past Groynes and Breakwaters

For the stabilisation of sandy coasts including cliff coasts, the development of detached breakwaters above mean water level and under water, acting as artificial reefs, has shown good results, Fig. 15.

Figure 15: Detached Breakwaters

However, despite such "hard and rocky" reactions successfully prevented beach erosion and degradation, they are often considered as not consistent with the natural coastal deformation processes. Therefore, beach sand replenishment and nourishment has been developed as a more soft and "environment friendly" coastal protection tool, Fig. 16.

Figure 16: Beach Nourishment of Eroding Coast

For the temporary protection of coastlines exposed to storm surges, which is mainly along heavily populated estuaries, storm surge barriers have been developed and are built in many parts of the world, Fig. 17. In some cases, large tidal rivers are closed during limited (< 12 > 36 hours) storm periods, cutting peak surge water levels and preventing waves from attacking dikes and infrastructures in the hinterland. River discharges and ship traffic can pass at low tides and under no storm conditions to the then protected harbours and cities.

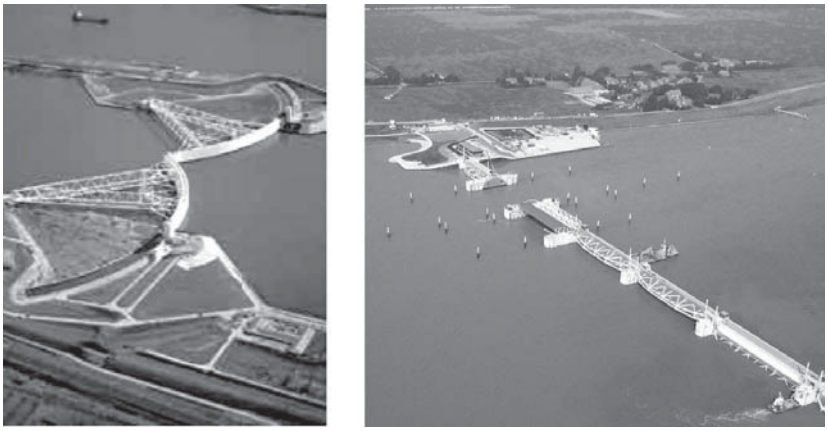

Figure 17: Storm Surge Barriers as Temporary Coastal Protection

The effect of forelands and islands in front of coasts at risk to waves and storm surges reducing wave heights due to shoaling, wave breaking and diffraction has been realised only in recent years, Fig. 18.

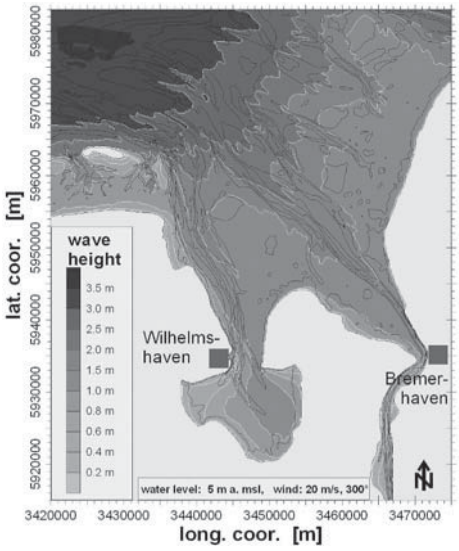

Figure 18: Wave Height Reductions over Forelands

Such tools for the protection of coastlines, structures and infrastructures - often in various combinations - have been proven as very successful; although acquiring large investments and continuing maintenance and adjustments.

6. Coastal Zone Sustainability and Environment Friendliness of Coast Protection - The Challenge of Coastal Zone Management

Considering the different stress factors to a coastline and the wide requirements on protection and from environment and the society, the need for an overall systematic approach for local and regional situations including careful and extensive analysis of risk (Fig. 19) is obvious.

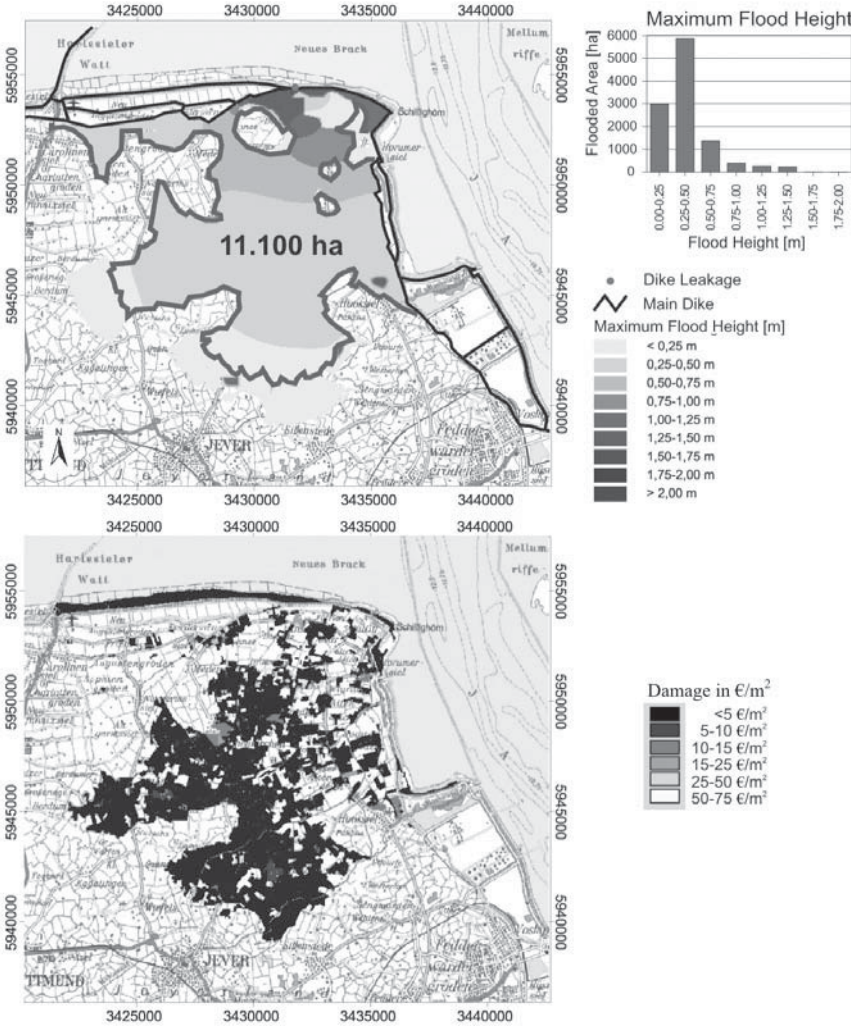

Figure 19: Hinterlands at Flood Risk and Level of Probable Damages

This means management of the coastal zone as a whole, including application of risk analysis to the coastal environment and the hinterland to be protected with sufficient and

available tools. In the eyes of the engineer such tools are "environment friendly" while they meet also reliable protection, Fig 20 and Fig. 21.

But the unsolved question remains as to how and who is to define "environment friendly".

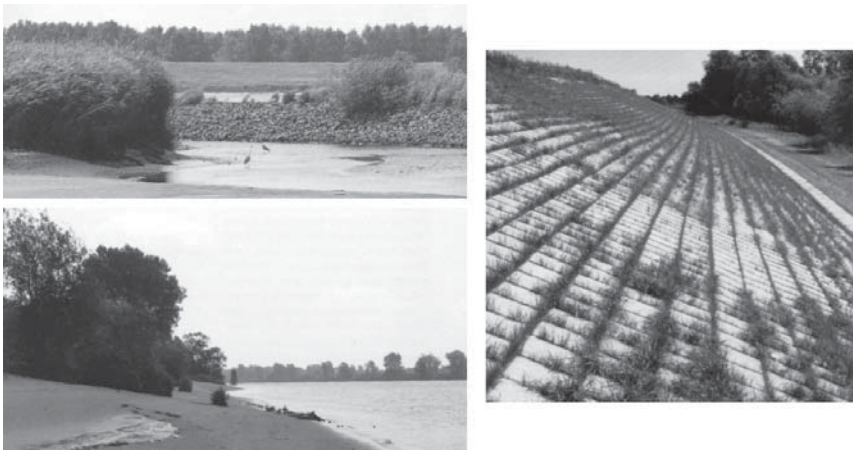

Figure 20: Landscaping of Dikes and Revetments for a Friendly Environment

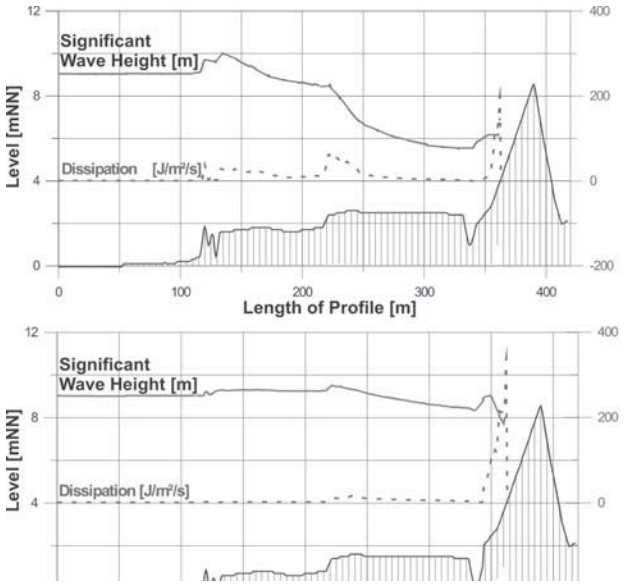

Figure 21: Protection of Forelands and Restauration of Wetlands will reduce Wave Loads on Coastlines and Protection Structures

This NATO Workshop has brought together coastal scientists and engineers from coastal countries and different domains. It provides an overview of up-to-date knowledge and identifies directions for Future Research. There is substantial promotion of International and Interdisciplinary Relationships. This is necessary since coastal protection on a local and global scale will remain the challenge for all future generations and with increasing importance.

References

Bird, E.C.F. (1986). "Coastline Changes", John Wiley & Sons Ltd., Chichester, England

Dean, R.G., Dalrymple, R.A. (1991). "Water Wave Mechanics for Engineers and Scientists," World Scientific Publishing Co. Pte. Ltd., Singapore

Department of the army, U.S Army corps of engineers (2001). "Coastal Engineering Manual," CEM, Washington, DC 20314-1000, United States

Elsner, A., Mai, S., Meyer, V., Zimmermann, C. (2003). "Integration of the flood risk in coastal hinterland management," Proc. of the Int. Conf. Coast Gis, Genua, Italy

Kramer, J. (1989). "Kein Deich - Kein Land - Kein Leben: Geschichte des Küstenschutzes an der Nordsee," Verlag Gerhard Rautenberg, Leer, Germany

Mai, S., Zimmermann, C. (2002). "Diked Forelands and their Importance in Coastal Zone Management," Proc. of the Hydro 2002 Conference, Kiel, Germany

Mai, S., Zimmermann, C. (2003). "Risk Analysis - Tool for Integrated Coastal Planning," Proc. of the 6th Int. Conf. on Coastal and Port Engineering in Developing Countries COPEDEC, Colombo, Sri Lanka

Nordstrom, K., Psuty, N., Carter, B. (1990). "Coastal Dunes: Form and Process," John Wiley & Sons Ltd., Chichester, England

Schiereck, G.J. (2001). "Introduction to Bed, Bank, and Shore Protection - Delft University Press - Phase III," Delft University Press, Delft, Netherlands

Soulsby, R.L. (1997). "Dynamics of Marine Sands," Thomas Telford Publications, London, England

BEACH NOURISHMENT: BENEFITS, THEORY AND CASE EXAMPLES

Robert G. Dean
Department of Civil and Coastal Engineering, University of Florida
Gainesville, FL, U.S.A.

Abstract

Beaches provide a wide range of societal benefits including storm protection, recreation, and habitat for a number of species. However, many beaches are under natural and/or human induced erosional pressures. The engineer is left with few choices to address this erosional pressure: (1) Correct the erosional cause which is usually practical only if the cause is human related, (2) Retreat from the shoreline, (3) Armor the shoreline, and (4) Beach nourishment which comprises the placement of large quantities of good quality sand in the nearshore system. In many cases, beach nourishment is the only practical environmentally friendly approach of those identified. Emphasis is directed to the benefits of beach nourishment and methodology which identifies the critical design factors. The application of a simple numerical model to predict the performance of two case examples is illustrated.

1. Beaches, Beach Erosion and Available Engineering Options

Beaches provide many benefits to society and the natural system. These benefits include storm protection to upland structures, recreational opportunities especially in urban settings and habitat for a number of species. Many of the World's shorelines are eroding at varying rates due to both natural and/or anthropogenic causes. Due to the attractiveness of shorelines for commercial and residential sites, erosion is of increasing concern and methods are often sought to address this issue.

There are surprisingly few options to deal with an eroding shoreline: (1) Correct the cause of the erosion, (2) Retreat from the shoreline, (3) Employ structures, and (4) Beach nourishment. The ideal option would be to correct the cause of erosion; however, this is usually only possible in limited cases in which the cause is due to anthropogenic activities, such as harbor development that interrupts the net longshore sediment transport, trapping of sand in constructed upland reservoirs, sand mining, inducement of ground subsidence through withdrawal of hydrocarbons or other ground fluids, etc. In the case of interruption of longshore sediment transport, correcting the cause requires reinstatement of the net longshore sediment transport. Retreat from the shoreline is only practical on shorelines that are relatively undeveloped and this option is increasingly less attractive with the trend of coastal development. Examples of the structural option include construction of groins and/or coastal armoring such as seawalls or revetments, each of which has some adverse effects. Groins trap sand from the littoral system, thus stabilizing the beach; however, in

C. Zimmermann et al. (eds.), Environmentally Friendly Coastal Protection, 25-40.

the process, the erosional stress is transferred to the downdrift beaches. Properly constructed coastal armoring will protect the upland; however, when placed on a receding shoreline, the beach will narrow and gradually disappear. Thus, of the four options available, in many cases beach nourishment is the only option that is "environmentally friendly". If the nourishment is constructed of sediments similar to the native sediments, any disruption to the ecology of the beach system will be temporary and the benefits of the beach will replicate those of a natural but wider beach. The following section focuses on the broad benefits of a wide beach.

1.1 Benefits of Beach Nourishment

The primary benefits of beach nourishment include: Storm damage reduction, recreation, and habitat, each of which is discussed below.

1.2 Storm Damage Reduction

A wide beach is a very effective energy absorber. This is especially significant in low lying areas such that severe storms can impact upland structures. The effectiveness of wide beaches in reducing structural damage has been demonstrated through both field studies conducted after storms and by application of accepted coastal engineering principles as discussed below.

Damage surveys following major storms have documented the storm damage reduction due to wider beaches. Figure 1a presents the results of a survey by Shows (1978) of the damage experienced by 540 structures after Hurricane Eloise which impacted the western shoreline of Florida in 1975. The "CL" shown in this plot is a permitting jurisdictional "Control Line" established by the State of Florida and is oriented approximately parallel to the shoreline. The steeply sloping damage curve is a reflection of the wave energy absorbed by the additional beach width fronting the individual structures. The effect of beach nourishment is to place a wave absorber (the beach) seaward of upland structures thereby reducing the wave heights and energies occurring at any upland location. Figure 1b presents the results of a beach nourishment project that adds 50 feet (15 m) to the beach width. The reduction in damage is evident. As an example, shifting the damage curve by 50 feet reduces the damage in Figure 1b by approximately $ 50,000 (1976 dollars) for a structure located 100 feet (33 m) from the Control Line.

Rogers (2001) has conducted an analysis of the effectiveness of six North Carolina beach nourishment projects in reducing impacts by Hurricanes Dennis and Floyd which occurred in 1999. The two categories of damage to structures were "destroyed" and "threatened by erosion", the latter generally signifying partial undermining of the foundation. The six nourished beaches included three which had been designed by the U.S. Army Corps of Engineers and which incorporated a substantial dune in the design.

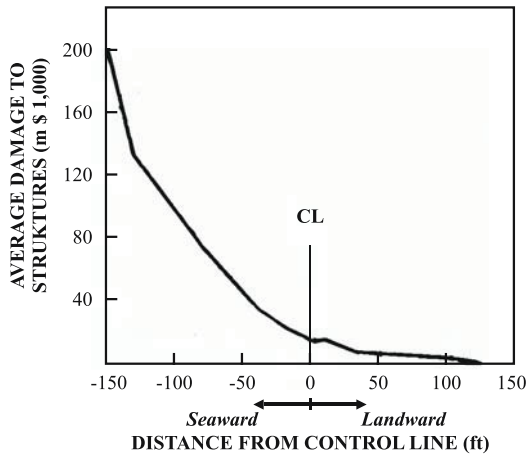

(a) Average Damage per Structure vs Distance From Control Line

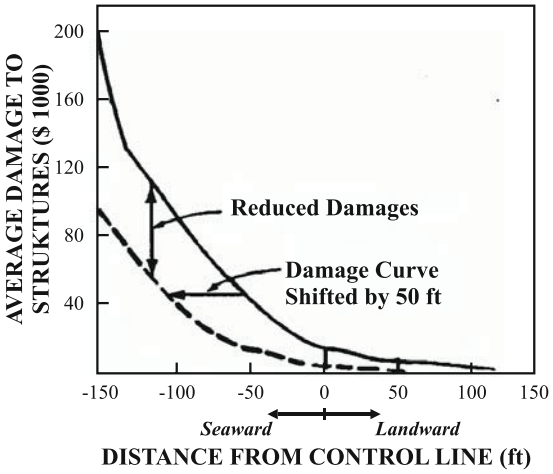

b) Effect of Shifting the Damage Curve by 50 ft (15 m)

Figure 1: Illustrating the Damage vs Distance From the Control Line and the Damage Reduction Resulting From an Additional 50 feet (15 m) Beach Width

The other three projects included two private projects and a beach disposal operation adjacent to a navigational channel. These latter projects were not as substantial as those designed by the Corps of Engineers and did not incorporate a dune feature. Hurricane Floyd which occurred two weeks after and was stronger than Hurricane Dennis was rated as having a 75 year return period and caused a maximum storm tide of 3 m. These two hurricanes impacted approximately 500 km of shoreline and caused 968 structures to be rated as either “destroyed” or “threatened by erosion” in the 300 mile shoreline of North Carolina. For those structures located behind the substantial dunes constructed as part of the three Corps of Engineers projects described earlier, no structures were listed in either

of these two impacted categories. Although structures located landward of the other three nourishment projects did not fare as well as those protected by the three more substantial projects with dune features, it was concluded that these projects provided significant protection and damage reduction to the upland structures.

Approximate computational methods can be applied to estimate the reduction in damage potential as a result of additional beach width. Dean (2000) has applied the Dally, et al. (1985) model of wave height reduction over bathymetry/topography that can include the contribution of a beach nourishment project.

$$\frac{\partial EC_G}{\partial y} = -\frac{K}{h}\left[EC_G - (EC_G)_S\right], \textit{ Waves Breaking}$$
$$\frac{\partial EC_G}{\partial y} = 0, \textit{ No Breaking} \tag{1}$$

in which E is the wave energy density ($E = \rho g \frac{H^2}{8}$), ρ is mass density of water, H is the wave height, C_G is group velocity, K is a constant (taken here as 0.17), the subscript "s" denotes a stable value of the quantity in the parenthesis, and $H_S = \alpha\left(h + S\right)$ where α is a proportionality factor (≈ 0.4), S is the storm tide, h is the local water depth related to the mean water level and y is directed onshore. Eq. (1) has the characteristic that waves will shoal in accordance with the conservation of wave energy in the absence of breaking and that waves breaking over a uniform depth will stabilize at a wave height which is approximately 0.4 times the water depth. Waves commence breaking where the ratio of wave height to total water depth is approximately equal to 0.78.

1.3 Recreational Amenities

In many cases, coastal armoring has been constructed to protect upland structures. As noted, on an eroding shoreline, the beach width available for recreation will diminish until recreational opportunities are very limited. Nourishment can restore the recreational amenities of a beach. An example is Miami Beach, Florida where, prior to the beach nourishment project, which occurred during the period 1976 to 1981, the beach was extremely narrow and hazardous in places to walk along at high tide. As the beaches eroded, so did the tourism base and the economy of this area. The nourishment project has revitalized the economy of the area such that as of 1991, there were 20 million visitors annually to this 16 km beach which is more than twice the number of the combined visitations to the three most heavily visited National Parks in the United States. The total income attributed to the U. S. economy by beach tourists is $260 billion with $60 billion in Federal taxes (Houston, 2002).

1.4 Beaches as Habitats

Beaches also serve as habitats for several species including birds and sea turtles. Sea turtles are an endangered species in the United States and require a certain beach width for successful nesting. Coastal armoring constructed to limit coastal retreat will result in gradual narrowed beaches such that sea turtle nesting habitat is impaired. Many such beaches have been nourished in the United States and the overall effect on turtles has been favorable. In Florida, nourished beaches are monitored for three years to document effects

on nesting sea turtles. If the nourishment material provides a good "match" to the native sediments, usually, there is a reduction in nesting activity for the first year after nourishment followed in later years by no discernible effect of the nourishment. A total of 316 km of so-called "index beaches" have been monitored in Florida for sea turtle nesting activity since 1989. Figures 2 and 3 present the results of this monitoring for the Loggerhead and Green Turtle species, the first and second most numerous species in Florida. On average, the Loggerhead nests are spaced at approximately 8 m along the 316 km monitored. The increase of Green turtle nests (Figure 3) is very dramatic. These turtles and their eggs were harvested for food until about 50 years ago.

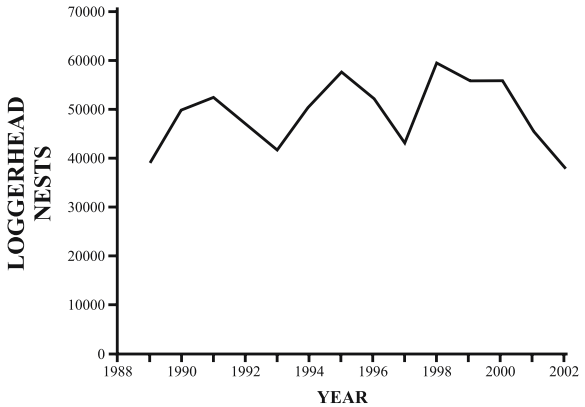

Figure 2: Variation With Time of Numbers of Loggerhead Turtle Nests Along 316 km of Florida's Sandy Shoreline

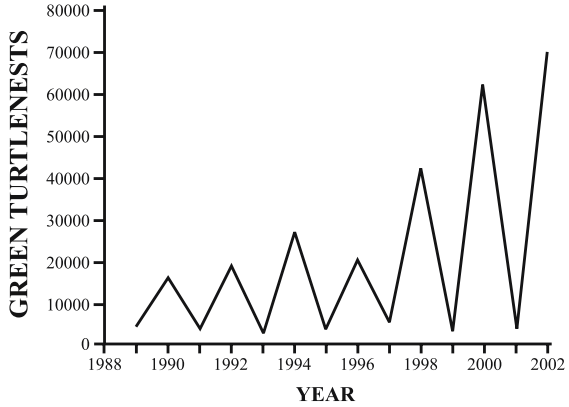

Figure 3: Variation With Time of Numbers of Green Turtle Nests Along 316 km of Florida's Sandy Shoreline

2. Sediment Transport Mechanics of Nourished Beaches

Nourished beaches respond to the same forcing as natural beaches, primarily waves, tides and associated currents. Nourished beaches represent a planform perturbation (or "bulge") and thus are out of equilibrium and the nourished profile is usually placed at a slope that is steeper than equilibrium. Thus nourishment induces both longshore and cross-shore (seaward) sediment transport components as illustrated in Figure 4.

Analytical and numerical models have been developed to represent the mechanics of the induced longshore and cross-shore sediment transport components. Longshore and cross-shore processes are usually treated separately with some justification provided by the cross-shore time scales usually being shorter than the longshore processes. The paragraphs below first review an analytical theory for the longshore processes followed by some results obtained from this theory.

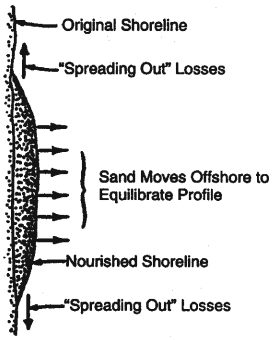

(a) Plan view showing "spreading out" losses and sand moving offshore to equilibrate profile.

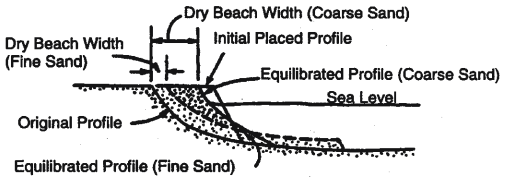

(b) Elevation view showing original profile, initial placed profile and adjusted profiles that would result by nourishment with coarse and fine sands.

Figure 4: Sand Transport to Adjacent Beaches and Adjusted Profiles Associated with Nourishment with Coarse and Fine Sands

2.1 The Pelnard Considère Theory

The Pelnard Considère Theory (1956) is a second order equation based on combining the equation for sediment conservation (continuity equation)

$$\frac{\partial y}{\partial t} + \frac{1}{(h_* + B)} \frac{\partial Q}{\partial x} = 0 \tag{2}$$

with the linearized form of the following equation for longshore sediment transport

$$Q = K \frac{H_b^{2.5} \sqrt{g / \kappa}}{8(S-1)(1-p)} \sin 2(\beta - \alpha) \tag{3}$$

In the above equations, y is the cross-shore coordinate to some contour, usually mean sea level, t is time, Q is the longshore sediment transport rate, x is the longshore coordinate, h_* is the depth of closure, B is the berm height such that $(h_* + B)$ is the vertical dimension of active profile motion, K is the so-called sediment transport coefficient (dimensionless and of order unity), H_b is the breaking wave height, g is gravity, κ is the ratio of breaking wave height to breaking water depth (≈ 0.78), S is the ratio of sediment density to water density and p is the sediment porosity.

Eq. (2) considers the beach profile to be in equilibrium and to move landward and seaward in response to divergences and convergences, respectively without change of form, see Figure 5.

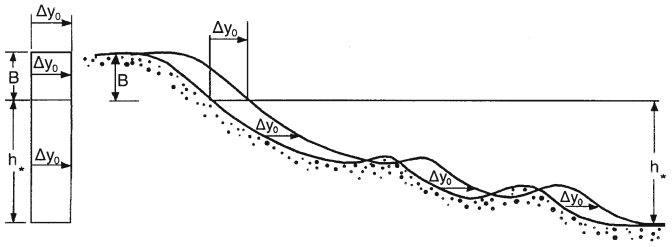

Figure 5: Profile Translation, Δy_0, Associated With Volume Density Addition, V, Compatible Sands

The Pelnard Considère (PC) equation is

$$\frac{\partial y}{\partial t} = G \frac{\partial^2 y}{\partial x^2} \tag{4}$$

which is recognized as the heat conduction equation. The quantity G is termed the "longshore diffusivity", has dimensions of Length^2/Time and is given by

$$G = K \frac{H_b^{2.5} \sqrt{g / \kappa}}{8(S-1)(1-p)(h_* + B)} \tag{5}$$

such that the longshore diffusivity is greater for larger breaking wave heights. The role of G is shown clearly by rewriting the *PC* equation in the following form

$$\frac{\partial y}{\partial (Gt)} = \frac{\partial^2 y}{\partial x^2} \tag{6}$$

such that for any project, the evolution at any time is related only to the product of time and longshore diffusivity. If two beach nourishments are constructed with scaled initial planforms of length ℓ, the following form

$$\frac{\partial y}{\partial(Gt / \ell^2)} = \frac{\partial^2 y}{\partial(x / \ell)^2} \tag{7}$$

establishes a non-dimensional time Gt / ℓ^2 and a non-dimensional length x / ℓ. Thus two projects constructed with scaled initial planforms will evolve with scaled planforms, but with rates depending on the scaled time, Gt / ℓ^2.

Many valuable approximate results can be established based on solutions to the Pelnard Considère theory as reviewed later in this paper. The interested Reader is referred to the original paper or to a number of other sources for additional results: Le Mehaute and Brebner (1961), Larson, et al. (1997) and Dean (2002).

2.2 Equilibrium Beach Profile Concepts

Under the action of constant water level and wave forcing, beaches tend to approach a constant profile, termed the equilibrium beach profile (EBP). Bruun (1954) first identified the following EBP form

$$h(y) = Ay^{2/3} \tag{8}$$

in which h is the water depth at a distance, y from the shoreline and A is a so-called profile scale parameter which depends on sediment size (or sediment fall velocity) as shown in Figure 6 and in Table 1. Because the A parameter increases with sediment size, beaches composed of coarser sediments will be steeper that those with finer sediments. EBP concepts and applications are very useful for evaluating the effects of nourishment with sediments that are different sizes than the native. As illustrated in Figure 7, depending on the nourishment sediment size, D_F, relative to the native, D_N, and volume of nourishment added per unit beach length, three types of nourished profiles are possible: intersecting, non-intersecting and submerged. Intersecting profiles require sediments that are coarser than the native; however sediments coarser than the native can result in non-intersecting profiles. Compatible sediments result in non-intersecting profiles and submerged profiles require sediments that are finer than the native. Although we will not examine the details of the applications of equilibrium beach profiles to beach nourishment, some of the results will be discussed.

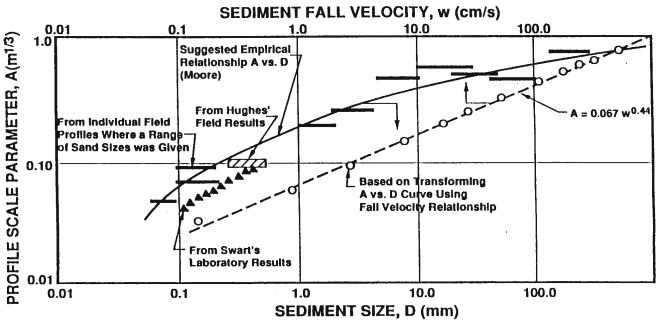

Figure 6: Variation of Beach Profile Scale Parameter, A, With Sediment Size, D, and Fall Velocity, w From Dean (1987)

Table 1: Variation of sediment scale parameter, A with sediment size, D

D(mm)	0.00	0.01	0.02	0.03	0.04	0.05	0.06	0.07	0.08	0.09
0.1	0.063	0.0672	0.0714	0.0756	0.0798	0.084	0.0872	0.0904	0.0936	0.0968
0.2	0.100	0.103	0.106	0.109	0.112	0.115	0.117	0.119	0.121	0.123
0.3	0.125	0.127	0.129	0.131	0.133	0.135	0.137	0.139	0.141	0.143
0.4	0.145	0.1466	0.1482	0.1498	0.1514	0.153	0.1546	0.1562	0.1578	0.1594
0.5	0.161	0.1622	0.1634	0.1646	0.1658	0.167	0.1682	0.1694	0.1706	0.1718
0.6	0.173	0.1742	0.1754	0.1766	0.1778	0.179	0.1802	0.1814	0.1826	0.1838
0.7	0.185	0.1859	0.1868	0.1877	0.1886	0.1895	0.1904	0.1913	0.1922	0.1931
0.8	0.194	0.1948	0.1956	0.1964	0.1972	0.198	0.1988	0.1996	0.2004	0.2012
0.9	0.202	0.2028	0.2036	0.2044	0.2052	0.206	0.2068	0.2076	0.2084	0.2092
1.0	0.210	0.2108	0.2116	0.2124	0.2132	0.2140	0.2148	0.2156	0.2164	0.2172

Notes:

(1) The A values above, some to four places, are not intended to suggest that they are known to that accuracy, but rather are presented for consistency and sensitivity tests of the effects of variation in grain size.

(2) As an example of use of the values in the table, the A value for a median sand size of 0.24 mm is: $A = 0.112\ \mathrm{m}^{1/3}$. To convert A values to $\mathrm{ft}^{1/3}$, multiply by 1.5.

2.3 Results From Solutions to the Pelnard Considère Equation and Application of Equilibrium Beach Profile Concepts

Several valuable results from the PC equation and solutions thereof and equilibrium beach profiles are reviewed below.

Background Erosion: Many beach nourishment projects are constructed in response to a pre-existing erosion rate, e, (here, termed "background erosion rate") which can be natural or due to anthropogenic causes. The *PC* equation being linear, establishes that the solution for a beach nourishment project can be added to the solution for background erosion, occurring separately. Denoting $y_T(x,t)$ as total shoreline change and $y_0(x,t)$ and $y_B(x,t)$ as the solutions in the absence of background erosion and only the background erosion, respectively, the following applies

$$y_T(x,t) = y_0(x,t) + y_B(x,t) \tag{9}$$

Project Longevity on a Long Straight Beach: Consider a project with initial rectangular planform of length, ℓ, constructed on a long straight beach with no background erosion. It can be shown that the time required for a certain percentage, $X\%$ of the volume to be transported out of the nourishment area (Figure 4a) can be represented by

$$t_{X\%} = K_{X\%} \frac{\ell^2}{H_B^{2.5}} \tag{10}$$

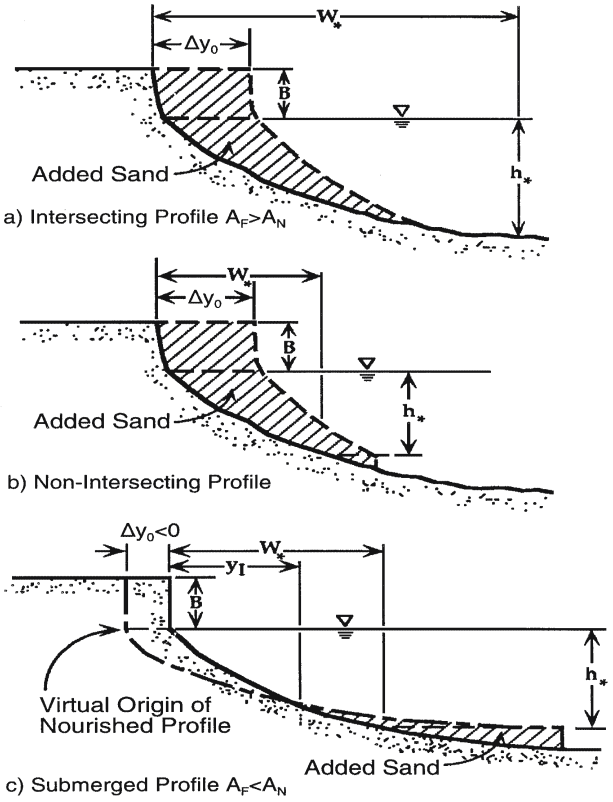

Figure 7: Three Generic Types of Nourished Profiles. Adapted from Dean (1991)

As an example consider $X = 50$, such that the result pertains to 50% of the volume remaining within the nourishment area, The quantity $K_{50\%}$ is

$$K_{50\%} = 0.18 \text{ years } \text{m}^{2.5} / \text{km} \tag{11}$$

such that the time t is in years, the project length, ℓ is expressed in kilometers and the breaking wave height, H_B is in meters. This relationship demonstrates the significance of

project length. As an example, the time required for a project with length, $\ell = 1$ km, acted upon by a breaking wave of height of 1 m to "lose" one-half of its volume to the adjacent beaches is 0.18 years, approximately two months. If the same wave height acted on a nourishment project with a length of 10 km, the half-life would be 18 years! Of course, if a background erosion was present in the nourishment area as is usually the case, Eq. (10) would require modification. However, we have seen that we could address the background erosion through superposition.

Independence of Project Evolution to Storm Sequencing: It can be shown from the *PC* equation that the evolution of a project depends only on the cumulative wave loading, that is the evolution is independent of the sequencing of storms that caused the evolution, and only depends on the cumulative wave energy flux on the project up to a particular time.

Existence of a Representative Wave Height: Although in nature, waves vary with time, at any time the evolution of a project can be shown to be same as if a particular constant wave height had acted on the project. This equivalent wave height, H_{eq}, is expressed as

$$H_{eq} = [(\overline{H_B^{2.5}})]^{0.4} \tag{12}$$

Increasing Renourishment Intervals: For the case of no background erosion or weak background erosion, the required renourishment intervals to maintain a certain minimum volume within the nourishment area increase with renourishment number. The explanation for this is that as the earlier nourishments evolve, they behave as longer and longer projects and thus evolve more slowly with time. The overall evolution rate therefore decreases with time and renourishment number. Somewhat surprisingly, for quite high background erosion rates, the required renourishment intervals decrease with time although the explanation is more complicated than is warranted for presentation here.

Stationary Project Centroid For Compatible Sediments: The evolution of nourishment projects constructed with sand compatible with the native sediments on a long straight beach are surprisingly insensitive to wave approach angle. This result is very valuable to the designer of beach nourishment projects on long straight beaches as it allows the designer to concentrate efforts on quantifying the wave height characteristics, which are usually better known than the wave directions. Usually, the effects of wave direction will simply reduce the evolution rate moderately.

Planform and Total Plan Area Evolution Resulting From Nourishment With Sand Compatible With or Coarser or Finer Than the Native: It has been noted that nourishment with compatible sand results in a planform anomaly centroid that is stationary. If the nourishment sand is finer or coarser than the native, the centroid anomaly migrates updrift and downdrift, respectively.

In addition to affecting the planform centroid, equilibrium beach profile (EBP) concepts can be applied to investigate the effects on the total planform resulting from nourishing with sediments compatible with or coarser or finer than the native. Total plan area as referenced here is the sum of the dry beach areas inside and outside of the project area. Nourishment sands coarser than, compatible with and finer than the native evolve with increasing total plan areas, constant total plan areas and diminishing total plan areas, respectively. Here, the initial total plan area is considered to be that subsequent to equilibration.

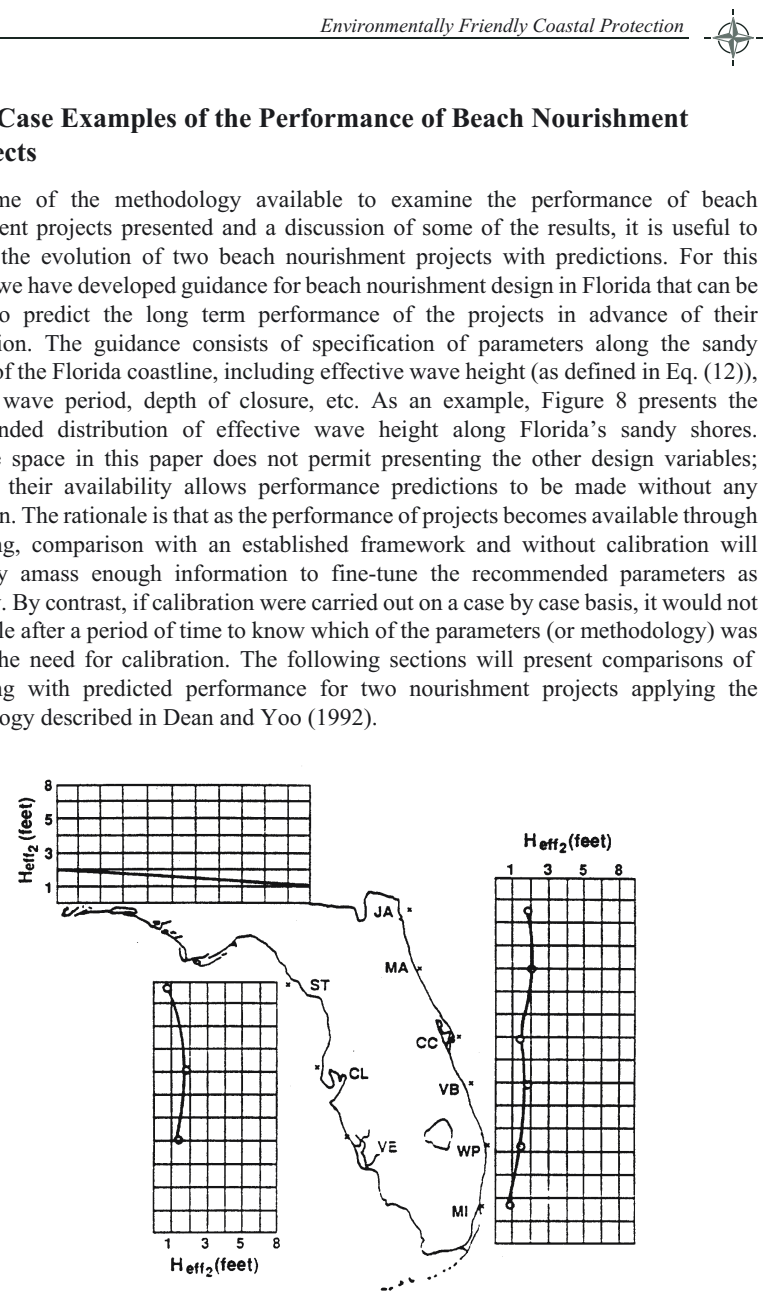

Figure 8: Effective Wave Height Variation Around the State of Florida
(Note: 3.28 feet = 1 m)

3. Two Case Examples of the Performance of Beach Nourishment Projects

With some of the methodology available to examine the performance of beach nourishment projects presented and a discussion of some of the results, it is useful to compare the evolution of two beach nourishment projects with predictions. For this purpose, we have developed guidance for beach nourishment design in Florida that can be applied to predict the long term performance of the projects in advance of their construction. The guidance consists of specification of parameters along the sandy portions of the Florida coastline, including effective wave height (as defined in Eq. (12)), effective wave period, depth of closure, etc. As an example, Figure 8 presents the recommended distribution of effective wave height along Florida's sandy shores. Available space in this paper does not permit presenting the other design variables; however, their availability allows performance predictions to be made without any calibration. The rationale is that as the performance of projects becomes available through monitoring, comparison with an established framework and without calibration will eventually amass enough information to fine-tune the recommended parameters as necessary. By contrast, if calibration were carried out on a case by case basis, it would not be possible after a period of time to know which of the parameters (or methodology) was causing the need for calibration. The following sections will present comparisons of monitoring with predicted performance for two nourishment projects applying the methodology described in Dean and Yoo (1992).

3.1 Delray Beach, Florida

This project was constructed initially in 1973 after attempts to protect a coastal highway with revetments failed twice. The nourishment history is shown in Table 2 and comparisons of the measured and predicted performances is presented in Figure 9 where background erosion rates of zero and 2 feet per year (0.6 m/year) are shown.

Three features of Figure 9 merit discussion: (1) There is reasonably good agreement between the measurements and predictions, (2) There are times when the predictions overpredict the performance and other times when the performance is underpredicted. This is due, in part, to the variability in wave conditions (primarily wave height which mobilizes the sediment and drives the evolution). Due to this variability, a single wave height can only be correct on average for representing the long-term forcing, and (3) Some surveys indicate more volume within the project area than preceding surveys, even in the absence of beach nourishment in the intersurvey period. The theories that have been discussed are unable to predict this increase. The two possible explanations for this increase include sand waves which are known to exist in the nearshore but for which there is not a complete understanding or simply survey errors.

Table 2: Nourishment History at Delray Beach, Florida

Nourishment Date	Volume Added (Millions of m^3)	Cumulative Volume Added (Millions of m^3)
1973	1.25	1.25
1978	0.54	1.79
1984	0.99	2.78
1992	0.79	3.57
2002	0.78	4.35

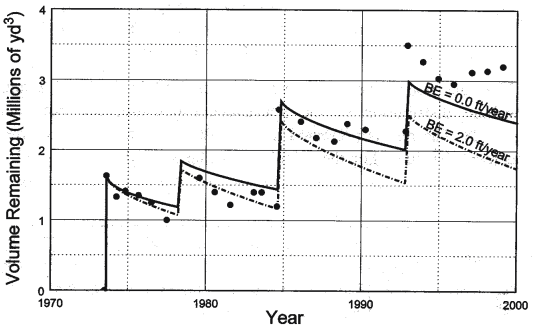

Figure 9: Comparison of Measured and Predicted Performance of Delray Beach, FL Beach Nourishment Project

3.2 Perdido Key, FL

Perdido Key, Florida was nourished in 1989 with 4.5 million m^3 over a length of approximately 7 km. In addition, approximately 3 million m^3 of sand was placed in water depths of approximately 6 m. As seen in Figure 10, this project is situated adjacent to a deepened inlet (Pensacola Pass) which complicates the analysis considerably. Monitoring results are available for approximately 8 years. The Project area is shown in Figure 10 and the measured volumetric evolution within the project area is compared with the predicted project evolution in Figure 11.

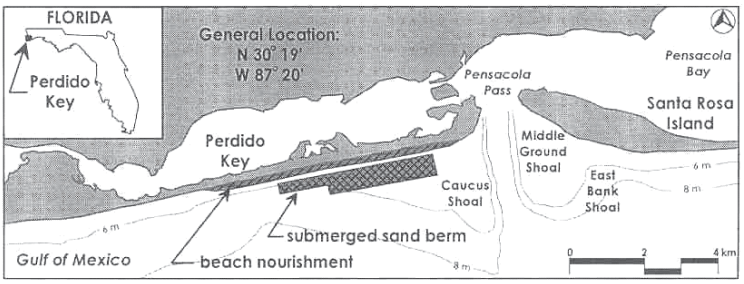

Figure 10: Project Area and Nourishment on Perdido Key, FL

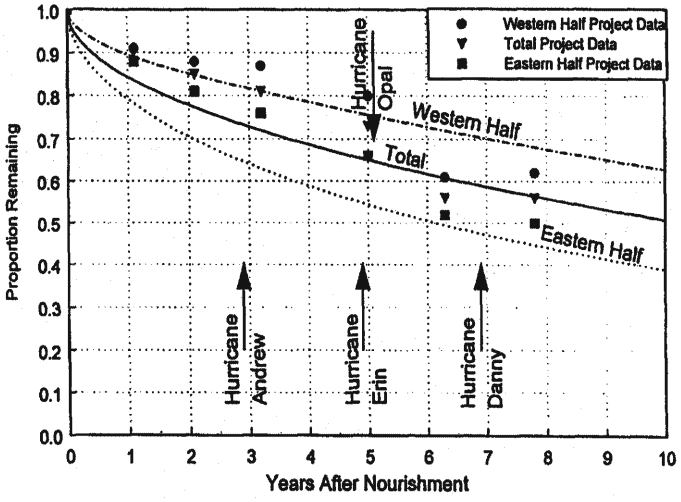

Figure 11: Comparison of Measured and Predicted Volumes Remaining Within Project Area for Perdido Key Beach Nourishment Project. The Lines and Symbols Represent Predictions for the two Project Halves and the Total Project

This project adjacent inlet was considered as a sink in the formulation, that is, the shoreline was assumed "pinned" at the inlet (eastern end of the Project). This results in an asymmetric evolution with more rapid losses from the Project area for the eastern half than for the western half. Also of interest is that during the eight years of monitoring, this area

was subjected to a fairly large number of hurricanes and tropical storms, with some of them being rather severe. Since the predictions agree reasonably well with the measurements, it is likely that the specified effective wave height for this project is too large for average conditions.

4. Summary

Of the available methodologies for addressing beach erosion, beach nourishment is the only "environmentally friendly" approach which can both provide protection to upland structures and maintain a beach that is suitable for recreation and natural habitat, such as for sea turtles. Beaches are also valuable for recreation and in areas of favorable climates and warm water, can provide a valuable source of income to the local economy.

Design of beach nourishment projects usually considers the alongshore sediment and cross-shore sediment transport separately due, in part to the shorter time scale for the cross-shore sediment transport.

References

Browder, A. E., and R. G. Dean (2000) "Monitoring and Comparison to Predictive Models of the Perdido Key Beach Nourishment Project, Florida, USA", *Coastal Engineering,* Vol. 39, 173–191

Bruun, P. (1954) "Coast Erosion and the Development of Beach Profiles", *Technical* Memorandum *No. 44,* Beach Erosion Board

Dean, R.G. (1977) "Equilibrium Beach Profiles: U.S. Atlantic and Gulf Coasts", *Ocean Engineering Technical Report No. 12*, Department of Civil Engineering and College of Marine Studies, University of Delaware

Dean, R.G. (1987) "Coastal Sediment Processes: Toward Engineering Solutions", Proceedings*, Coastal Sediments*, ASCE, 1–24

Dean, R. G. (1991) "Equilibrium Beach Profiles: Characteristics and Applications", *Journal of Coastal Research*, 7(1), 53–84

Dean, R.G. (1995) "Beach Nourishment Planform Considerations", *Proceedings, Coastal Dynamics 95*, American Society of Civil Engineers, 533–546

Dean, R. G. and C.- H. Yoo (1992) "Beach-Nourishment Performance Predictions", Proceedings, Journal of Waterway, Port Coastal and Ocean Engineering, American Society of Civil Engineers, Vol. 118, No. 6, pp. 567 – 586

Dean, R. G. (2002) "Beach Nourishment: Theory and Practice", World Scientific Press, New Jersey, 399 Pages

Houston, J. R. (2002) "The Economic Value of Beaches", Proceedings of the 15th Annual Conference on Beach Preservation Technology, Florida Shore and Beach Preservation Association, Tallahassee, FL, pp. 31 – 42

Larson, M., H. Hanson and N.C. Kraus (1997) "Analytical Solutions of One–Line Model for Shoreline Change Near Coastal Structures", *Journal of Waterway, Port, Coastal and Ocean Engineering*, American Society of Civil Engineers, 123(4), 180–191

Le Mehaute, B. and A. Brebner. (1961) "An Introduction to Coastal Morphology and Littoral Processes", *Report 14*, Civil Engineering Department, Queen's University, Canada

Moore, B. (1982) "Beach Profile Evolution in Response to Changes in Water Level and Wave Heights", *M.S. Thesis*, University of Delaware, Newark, DE

Pelnard–Considère, R. (1956) "Essai de Théorie de l'Evolution des Formes de Rivage en Plages de Sable et de Galets", *4th Journees de l'Hydraulique, Les Energies de la Mer*, Question III, Rapport No. 1

Shows, E. W. (1978) "Florida's Setback Line – An Effort to Regulate Beachfront Development" Coastal Management Journal, Vol. 4, Nos. 1 – 2, pp. 151 – 164

INNOVATIONS IN COASTAL PROTECTION

Joan Pope, William R. Curtis
Coastal and Hydraulics Laboratory,
U.S. Army Engineer Research and Development Center,
Vicksburg, MS, U.S.A.

Abstract

Shore protection strategies include adjusting the activities of man (management) and adjustments to the physical system (engineering). Engineering activities fall into three classes: coastal hardening (armoring), reducing the transport and loss of littoral sediment, and adding sediment to the littoral system. Innovations in shore protection should consider and address the processes causing the specific erosion of concern. Several demonstrations of innovations in shore protection approaches and strategies are currently being conducted in the United States. Future shore protection projects should require better assessment of the long-term cause and effect of the erosion and engineering treatments, rather than building an immediate solution to the symptom.

1. Introduction

The coastal zone is highly dynamic, spatially variable, and is affected by littoral and non-littoral physical processes. The social-economic interests of mankind are often in conflict with sustaining a healthy coastal zone. There is the expectation that human ingenuity can resolve erosion problems, yet such actions may adversely impact the natural attractiveness and ecology of the coastal setting. Selection of a functional shore protection alternative requires an understanding of the physical phenomena causing the erosion and the recognition that the coast will never be a stable system. No action is without potential impact and no solution is permanent.

Coastal erosion problems occur over a range of coastal settings including sandy, cohesive, wetland, engineered shores, and various combinations. In some settings littoral processes interact with a geologically inherited coast that is presently in an erosive or unstable state. Limited sediment supply, irregular underwater topography, ground water seepage patterns, water level changes, and changes in storm patterns may be natural contributors to the erosive trends. Human activities can also aggravate the processes causing erosion by changing the sediment supply through poor coastal development practices and a lack of appreciation for the normal range of beach variability.

2. Current State of the Practice of Shore Protection

Various generic alternatives for assessing and addressing coastal erosion are discussed in the context of their applicability and appropriateness. Strategies for Coastal Zone Management range from doing nothing and abandoning human activities to modifying

C. Zimmermann et al. (eds.), Environmentally Friendly Coastal Protection, 41-56.

development practices and adopting integrated and holistic management policies that focus on regional sediment management. Engineering solutions range from increasing the supply of littoral sediments (e.g., beach fill, near shore disposal, sand by-passing) to slowing the loss of sediment (e.g., breakwaters, groins, reefs, sills, dewatering), to the extreme of coastal armoring (e.g., seawalls, bulkheads, revetments). Each class and solution has merit depending upon the situation and in many cases combinations of approaches are appropriate.

3. The State-of-the-Art of Shore Protection

Standard approaches for mitigating coastal erosion hazards are described in Pope (1997) and incorporated in the U.S. Army Engineers *Coastal Engineering Manual* (CEM), Part V-3 "Shore Protection Projects" (Basco and Pope 2001). Table 1, extracted from the CEM, presents a classification scheme for organizing and considering shore protection approaches. Responses to coastal erosion of flooding hazards either involve changing the natural physical system (via armoring, beach stabilization, or beach restoration) or changing man's activities (adapting or accommodating) or combinations of both. This hierarchy is based on the functional intent of the design, its configuration and placement, and construction materials. All traditional and non-traditional structural approaches can be grouped and classified via this hierarchy.

Over the past century, design of shore protection strategies have evolved significantly reflecting a better understanding of the natural system, improved design tools, and environmental sensitivity. Through the 1960s, most shore protection activities in the United States involved the construction of shoreline armoring works either as large seawalls or revetments. Starting in the 1960s the use of beach nourishment become more common, including the construction of large-scale projects such as the Miami Beach fill in the 1970s. In recent years, there has been growing interest in the incorporation of beach stabilizing structures such as breakwaters and groins to moderate or reduce the loss rates for placed beach fill.

4. Innovations and the Future

An innovation is a non-traditional approach, construction method, material, configuration, shape, concept, device, that has a sound engineering basis and value added over similar traditional methods. Observed trends in shore protection innovations directly influence the physical process causing the local erosion problem while minimizing environmental and aesthetic impact. Proper implementation of innovation requires education of policy makers, developers, and the public or the innovation could become an environmental or economic impediment.

In terms of construction materials there have been significant advances in the quality and durability of geosynthetic materials that can be used as a filter material or as containers (e.g., for sand-filled tubes and bags). There have also been advances in the use of precast concrete units, interlocking units, and field construction techniques. Promising examples of concept or functional innovations for mitigating coastal hazards are:

Table 1a: Alternatives for Coastal Hazard Mitigation

Approach	**Changes to the Natural, Physical System**							
Class	**Armoring Structures**			**Beach Stabilization Structures and Facilities**				
Type	**Seawall**	**Bulkhead**	**Dike/Revetment**	**Breakwaters**	**Groins**	**Sills**	**Vegetation**	**Groundwater Drainage**
Geometry (configurations) or location	• Vertical • Curved • Gravity	• Crib • Stepped/Terraced • Cantilevered • Tie-Backed	• Sloped	• Headland • Detached • Single • System • Submerged (reef-type)	• Normal • Angled • Single • System (field) • Notched • Permeable • Adjustable • Shaped (*T* or *L*)	• Shoreline • Submerged • Perched beach • Intertidal • Submerged		• Beachdrain • Bluff dewatering • Interior drainage
Materials of construction	• Concrete • Rock	• Sheet-pile - steel - timber - concrete - aluminum	• Earth • Rock revetment • Geotextiles (bags) • Gabions	• Rock • Precast concrete units • Sheet-pile types - steel - concrete - timber - etc. • Geotextiles bags			• wetland • Submerged • Aquatic Vegetation • Mangrove	• System of pipes and pumps with sumps

Table 1b: Alternatives for Coastal Hazard Mitigation

Approach	**Changes to the Natural Physical System (continued)**		**Changes to Man's System**			**Changes in Both**		**No Change**
Class	**Beach Restoration**		**Adaptation and Accommodation**			**Combinations**		**Do Nothing**
Type	**Beach Nourishmgent**	**Sand Passing**	**Flood Proofing**	**Zoning**	**Retreat**	**Structural and Restoration**	**Structural and Restoration and Adaptation**	
Geometry	• Subaerial • Dune • Feeder • Profile • Underwater berms	• Bypassing • Backpassing	• Elevated structures • Raise grade • Sandbags • Flow diversion	• Setbacks • Land use restrictions • Public lands (Institutional)	• Individuals • Communities • Infrastructure • Move structures	• Any combination of 1, 2, or 3 alternatives	• Any combination of all alternatives except retreat	Let nature take its course
Materials	• Borrow sites • Dredged material • Artificially made	• Littoral traps • Smooth out hot-spots • Downdrift material returned updrift	• Single-family homes on timber piles					

1. Improvements to beach fill retention through the use of sand retaining structures for mitigating localized losses in hot spots or project transition areas;
2. Improved sand bypassing through project area;
3. Shoreline stability through use of submerged, broad-crested structures, shore-attached headland or "tuned" structures, highly transmissive breakwaters and permeable and adjustable groins;
4. Alternative beach fill materials (mixed sediments, underwater placement, coarser-grained, artificial sand);
5. Alternative construction materials such as recycled materials, geosynthetics, thermoplastics and composites;
6. Interlocking and uniquely shaped armor or structural units;
7. Ground water management;
8. Use of vegetation and other bio-engineering approaches;
9. Wave energy modification through bathymetric modification or other geometric adaptations.

5. United States National Shoreline Erosion Control Development and Demonstration Program

The National Shoreline Erosion Control Development and Demonstration Program was authorized by the United States of America Congress under Section 227 of the Water Resources and Development Act of 1996 (WRDA 96). For brevity, the program is referred to as Section 227. Section 227 demonstrates and evaluates a variety of innovative or non-traditional shoreline erosion control methods in a variety of coastal settings at prototype-scale. The Section 227 program effort has three primary objectives. First, is to assess and advance the state of the art of coastal erosion control technology. Technology is assessed for the value added of selected innovative methods over traditional methods in the context of structural stability, functional project performance, environmental impact and lifecycle cost. Second, is to encourage and achieve the development of innovative solutions to the coastal erosion control challenge and to use the program's authority to demonstrate and evaluate the effectiveness of various devices and methods in both the laboratory and at prototype-scale in the field. Third, is to communicate findings to the coastal management and engineering communities (Pope, Curtis, and Turk 2001).

Support is provided by Section 227 for the planning, design, construction, monitoring and evaluation of innovative shoreline protection applications at selected demonstration sites. Twelve projects are located on the shores of the Atlantic, Pacific, and Gulf Coast and the Great Lakes. The program also sponsors monitoring and evaluation of two projects constructed outside of Section 227. In addition to project prototype-scale project evaluation, Section 227 provides support for the evaluation and documentation of existing or previously existing innovative applications (e.g., Kraus and Rankin 2004).

Demonstration project locations meet selection criteria mandated by the program authority. In addition, several criteria were established based on previous experience with

a low-cost shore protection demonstration program conducted in the 1970s called Section 54 (USACE 1981). These additional criteria address the necessity to monitor and evaluate project functional performance in given physical setting and include:

1. Minimize the potential for negative environmental and societal impacts;
2. Be experiencing shoreline erosion at a manageable rate;
3. Have sufficient length of shoreline to demonstrate the functional performance of applied technology;
4. Have suitable control sections or pre-project monitoring records;
5. Have identifiable spatial and temporal scales associated with localized coastal processes.

Demonstration project locations are indicated in Figure 1. Table 2 lists general project information for each demonstration site including specific location, project objectives and status.

Figure 1: Demonstration project locations

6. Demonstration Projects

Each Section 227 demonstration site was selected based on a number of criteria, but also with consideration of the site's potential value as a prototype-scale experimentation site. Upon selection of the site, significant effort was expended in defining the cause of the erosion and developing alternative strategies for mitigating the erosion. An emphasis was put on developing, engineering, and testing alternative functional approaches that would be suitable for that specific site. Only a few demonstration projects are described in this section. The reader is referred to the program website at http://chl.erdc.usace.army.mil/section227 for program information and a description of all the demonstration sites.

Table 2: Section 227 Demonstration Project Description

Location	Erosion Challenge	Engineering Solution
Seabrook Harbor, New Hampshire	Channel bank erosion and harbor shoaling in by tidal currents	Thermoplastic or composite sheet pile retaining structures
Cape May Point, New Jersey	Dune erosion and sediment retention in groin cells	Narrow-crested precast concrete reef units to create perched beach
Chesapeake Bay, Maryland and Virginia	Sandy beach and wetland habitat erosion in fetch and depth limited waves	Evaluation of shoreline stabilization structures previously constructed including groins, breakwaters, sills and headlands
Miami Beach, Florida	Erosional hot-spot in beach nourishment project caused by focusing of wave energy	Wide-crested submerged reef of integrated porous concrete units and articulated concrete mat
Alligator Point, Florida	Erosion of fine-grained sandy beach influenced by large transverse bars	To be determined
Jefferson County, Texas	Erosion of cohesive bed and dune terrace overwash	Low-volume beach nourishment and clay-core dune
Sacred Falls, Oahu, Hawaii	Pocket beach erosion	Y-head structures to emulate natural morphologic features
Ventura County, California	Sandy beach erosion	Sand-filled geotextile containerized reef
Martinez, California	Wetland substrate erosion caused by wind and vessel generated waves and estuarine tidal currents	Bioengineered branch-box breakwater matrix
Cape Lookout, Oregon	Dune erosion and overwash	Dynamic cobble berm and geotextile tube core dune
Allegan County, Michigan	Coastal bluff erosion caused by perched groundwater	Horizontal and vertical drain dewatering system
Sheldon Marsh, Ohio	Cohesive bed and sand barrier spit erosion	Effectively wide-crested submerged breakwater (submerged and detached submerged breakwater matrix)

6.1 Cape May, New Jersey

Cape May Point is a 1.8-km-long beachfront community located on the southern tip of New Jersey. Cape May Point is particularly vulnerable to storm damage due to exposure to waves from both the Atlantic Ocean and Delaware Bay. Wave heights average 0.6 m in the summer and 1.2 m in the winter with much higher waves occurring during storms. The mean tide range is 1.2 m. Net longshore sediment transport is predominantly wave induced and is directed from east to west with an average transport rate on the order of 153,000 cu m/year. Existing shore protection structures along the shoreline at Cape May Point include a series of nine groins at ~150-300 m spacing and a rubble revetment armoring the shoreline in the easternmost groin cell (Figure 2). The groins have stabilized the shoreline, which has shown some variability over the last 40 years ranging from 0.9 m of erosion per year to 0.9 m of accretion per year.

The shoreline of Cape May Point is vulnerable to storm damage through wave attack, erosion, and inundation. During the early part of this century, the complex tidal/wave/current interaction of the Delaware Bay and the Atlantic Ocean led to persistent

long-term shoreline erosion at Cape May Point. This unstable shoreline necessitated repeated local action in the form of construction and rehabilitation of numerous groins, beach nourishment, dune construction, and seawall fortification since the 1930s. These actions have made much of the shoreline relatively stable, fluctuating between periods of erosion and accretion. The extensive man-made dune system that has been developed over the years along the western portion of Cape May Point has been particularly effective is providing shore protection for that area. However, while these efforts have for the most part "held-the-line" in most shoreline sections with regard to erosion, that "line" is at a critical position. There is virtually no buffer to deal with forces due to storm events, which can severely damage the area. An especially critical area is at the eastern portion of Cape May Point where recent significant erosion has left the deteriorating stone revetment and residential structures highly vulnerable to storm damages.

Figure 2: Groin cells, Cape May Point, New Jersey

In 1994, approximately 305 m of Beachsaver^{TM} Reef was installed in two of the nine groin cells. The modular reef system consists of individual units 3 m in length and weighing 20-ton (Figure 3). At MLW, the crest of these reefs varies from +0 to 0.6 m below mean sea level. Volumetric measurements between May 1994 and May 1995 showed an increase in sand volume in each cell (Herrington, Bruno, and Ketteridge 1997). Since then, closing off the seaward ends of the groin cells with the reef units has reduced the cross-shore loss of sand from the cells.

To mitigate future storm damage and coastal erosion at Cape May Point, the site has been selected as a demonstration project under Section 227. The objective of the experiment is to compare the sand-retention performance of the narrow-crested, submerged Beachsaver^{TM} Reef with a less obtrusive, low profile precast concrete sill. The project will be augmented by the addition of beach fill. Success will be determined by the retention of the added volume of sand. While the Beachsaver^{TM} Reef is a proprietary, and rather complex structure, the sill is a modified version of a standard "Double-T" panel used for structural deck construction (Figure 4). In this application, the Double-T panels, each 9 m in length and weighing close to 30-ton, will be inverted (the deck becoming the base and the stems becoming sill walls) and placed end to end. While the Beachsaver^{TM} Reef modules are 1.8 m in height, and obstruct a significant portion of the water column, the Double-T is only 0.8 m in height. It may be hypothesized that the sill would have little

effect on the local wave field at its installed depth of 3 m below the mean low water level as compared to the Beachsaver^{TM} Reef, with its higher crest elevation. It appears that the majority of the offshore transport occurs as bedload movement at the ends of the groin cells, and that both structures should act as sills that retain sand and increase beach width.

Figure 3: Beachsaver^{TM} Reef unit

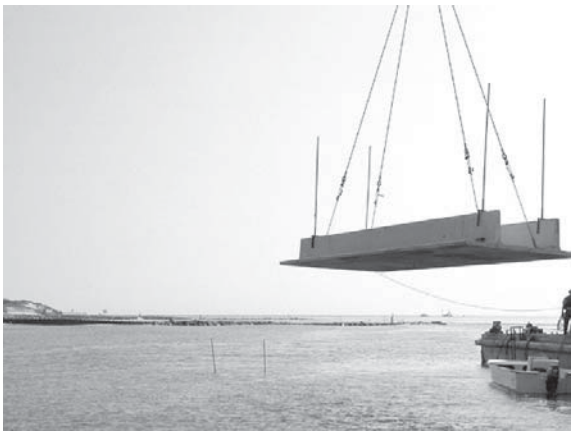

Figure 4: Placement of Double-T sill unit, Cape May Point, New Jersey

6.2 Jefferson County, Texas

The project location fronts the McFaddin National Wildlife Refuge 49 km west of the Texas / Louisiana border. Beaches at the demonstration area consist of a thin sand veneer over mud (Figure 5). Wave heights average between 0.76 and 0.91 m in the summer and between 1.2 and 1.4 m in the winter, with much higher waves occurring during storms.

Mean tide range is 0.39 m. Net longshore sediment transport is predominantly wave induced and bi-directional with an average transport rate on the order of 38,000 to 114,700 cu m/year westward. The average long-term shoreline erosion rate is approximately 1.5 m, annually. Since 1980, the road has been closed due to coastal erosion and storm overwash. Shore protection structures constructed to protect the roadway no longer exist.

Figure 5: Exposed clay and organic sediments, Jefferson County, Texas

Storms erode the thin layer of sand, exposing the mud to further erosion. During storms, beach sediment is washed over the low-laying dune and deposited in a wetland area landward of the beach (Figure 6). Overwashed sediment is not recovered from the wetland and therefore, lost to the beach profile. The beach profile has limited post-storm recovery due to a deficit of sediment in the littoral system.

The primary objectives of the project are to minimize erosion of the exposed cohesive sediment and to minimize sand overwash. These objectives will be accomplished by constructing experimental beach nourishment templates contained by geotextile tube groin cells, and dune construction. The 762-m-long dune is designed to withstand a 5-year return period storm. Part of the dune will be constructed with a clay core underlying a sand veneer. The remaining dune will be constructed of sand. Fronting half of the engineered dune corridor is beach nourishment divided into four experimental cells of varying fill volume and grain size. The objective of the nourishment is to investigate the longevity of minimal fill volumes (15 to 30 cu m/m) combined with native beach sand ($0.17 \text{ mm} < d_{50} < 0.21 \text{ mm}$) or sand larger than what is naturally present on the active beach profile ($0.31 \text{ mm} < d_{50} < 0.40 \text{ mm}$). A geotextile tube groin separates each experimental cell (Figure 7). The function of the tube is to contain the experimental areas. It is noted that groin structures designed for the purpose of trapping and retaining sand from the littoral system in this area would not be functional due to the normal sand deficit.

Figure 6: Overwash fan encroaching on wetland, Jefferson County, Texas

Figure 7: Geotextile tube groin construction, Jefferson County, Texas

6.3 Allegan County, Michigan

A 16 km reach of a Lake Michigan bluff located in Allegan County, Michigan, consists of interlayered till, fluvial, and lacustrine deposits. A sandy beach fronting the bluff provides a buffer from the moderate wave energy climate of southeastern Lake Michigan

(Figure 8). There is no tidal influence, but water levels can fluctuate over a 1.8 m range. At present, lake levels are not encroaching on the toe of the bluff. The cause and effect of coastal bluff instabilities in the study area has been monitored over the past several years.

Figure 8: Wide beach fronting unstable bluff, Allegan County, Michigan

Groundwater adds weight to the soil, disrupts the soil skeleton, exerts seepage pressure on the soil particles, and reduces contact between soil particles when the bluff is saturated and pore pressure is high. As a result, the ability of the soil to resist slope movements is reduced and the probability of slope failure is increased. Soil engineers have known these effects for many years and the installation of drainage systems in terrestrial bank systems is common practice. However, a lack of quantitative monitoring of slope performance before and after dewatering, particularly in a coastal setting, has limited the rigorous application of effective stress analysis for coastal bluffs. Additional design and monitoring information is needed to reveal the benefits of this process beyond the level of anecdotal information.

Bluffs in the study area are composed of interlayered sand and clay and show significantly greater numbers and sizes of slumps, greater movement rates, and more rapid recession than do bluffs composed dominantly of sand or clay. Deep, curved (but not arcuate) failure surfaces develop in interlayered sand and clay. Several years of displacement monitoring in the study area have shown that slow-moving slumps and mass movements are inactive during summer and fall months, but move significantly during the winter and spring, regardless of storm activity or Lake Michigan water level. Although periodic high wave activity cannot be dismissed as a factor, it is clear from the monitoring data that accelerated displacement occurs during periods of bluff face freezing while the toe is protected from wave attack by shoreline ice (Figure 9). The more rapid movement continues into the spring when the bluff face thaws and the discharge of ground water

maintains elevated pore pressures. When the excess pore water is naturally drained, bluff movement stops. Shallower, planar movements occur only during the late winter and spring months. Where the bluff is dominated by till, there is insufficient ground water storage capacity to create a confined system during a bluff-face freeze. However, perched ground water is stored in bluff-top sand layers. During periods of thaw and spring rain, seeps from this bluff-top sand saturates the displaced soil to create the equivalent of a condition where saturated till flows on top of over consolidated, unsaturated till. When ground water seeping stops, bluff movement stops also.

Figure 9: Frozen perched groundwater seeps on bluff face,
Allegan County Michigan

The fact that minor rises in perched ground water levels lead to significant bluff movement forms the basis for the proposed demonstration project. By removing excess ground water before incipient bluff instability occurs via implementation of a bluff dewatering system, slope movements should be greatly reduced or eliminated. The objective of this demonstration project is to show that the dewatering of shoreline bluffs is an inexpensive, non-invasive, and effective method of erosion control. The per-foot cost of bluff dewatering will ultimately be less than one-third that of the per-foot cost for traditional stone revetments or steel-sheet pile structures. This mitigation method does not directly interfere with the littoral processes, as do traditional beach or nearshore structures.

6.4 Miami Beach, Florida

The City of Miami Beach is located on the southeast Florida coast in Dade County. The project site extends along the shoreline for approximately 762 m, with a southern limit of 63rd Street. The Dade County shoreline consists of a barrier island with a bay behind it. Whereas the typical barrier island is a sand dune moving progressively over the bay sediment, the Dade County barrier island (i.e., Miami Beach) probably developed on a shallow sandstone reef where mangroves grew and trapped additional sediments creating a stable island. A series of three reef lines (with areas of sand in between) exist offshore of the project site. These reef lines vary in relief (rises in elevations above adjacent sandy areas) from low relief (<1 m) to high relief (>3 m). The continental shelf offshore of the project site is relatively narrow with the shelf break located only a few kilometers from the shoreline.

Analysis of the wave hindcast data indicates that the incident direction of wave energy along the Dade County shoreline is bimodal. Northeasters produce large waves incident from a steep northerly angle during much of the fall and winter months, and the easterly/southeasterly trade winds produce smaller but more persistent waves from the eastern and southern sectors during the rest of the year. The direction of peak wave energy is from the northern sectors, as evidenced by southerly net sediment transport, but the wave energy incident from the southern sectors is significant. The mean tide range is 0.77 m with spring tides of 0.93 m above the mean low water level. The U.S. Federal Emergency Management Agency estimates storm surge return period in the area as 1.04 m (5 year), 1.61 m (10 year), 2.01 m (20 year), 2.59 m (50 year) and 3.11 m (100 year).

The shoreline recession rate in the demonstration project site ranges from 4.27 to 7.62 m, annually (excluding the effects of beach fill). Shoreline recession in this area is in direct correlation to local impacts of tropical and extratropical storm events. The 63rd Street demonstration project site can be described as an "erosional hot spot" within the beach nourishment project designed for hurricane storm damage and flood protection (Figure 10). The authorized beach nourishment project is designed to provide a specific level of storm damage reduction and recreation benefits through the establishment and maintenance of a beach nourishment design template. Monitoring indicates that shoreline recession at the demonstration project site exceeds the rates experienced on adjacent shorelines.

The primary objective of the demonstration project will be to reduce the volume of sediment lost from the hot spot to maintain template dimensions between renourishments, while minimizing impact to the longshore transport of sediment to adjacent beaches. This objective will be accomplished by application of a wide-crested and highly transmissive reef submerged in the surf zone. Reef units will be an integration of precast concrete Reef Balls™ and articulated concrete mat. Figure 11 shows a conceptual design of a single integrated unit. Units will be placed to construct a 12-m-wide reef spanning the demonstration project area. In addition to shoreline stabilization, the reef is designed to enhance the local underwater habitat as the structure emulates the natural hard bottom and reefs found in other areas of the south Florida nearshore. This demonstration project will also document the performance of other methods implemented to maintain the Miami Beach beach nourishment design template at two other erosional hot spots (e.g., use

submerged rubble-mound reef for wave attenuation, and headland structures for sediment retention (Figure 12)).

Figure 10: Erosional hot spot, 63rd Street, Miami Beach, Florida

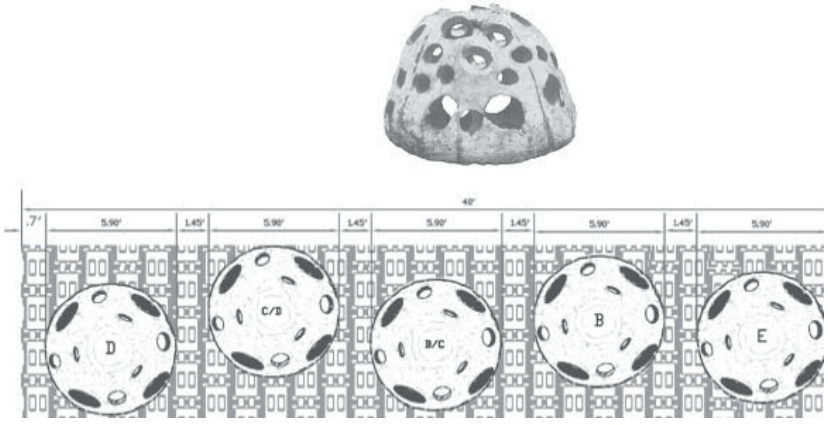

Figure 11: Top: Reefball™. Bottom: Conceptual design of single integrated Reefball™ and articulated concrete mat unit

Figure 12: Headland structures, Miami Beach, Florida

7. Summary

General trends in coastal shore protection innovations are to use methods that are less obtrusive and more "natural" and that the solution be based upon understanding of the root cause of the erosion. Specific areas of innovation include:

- Alternate sand sources and beach nourishment placement protocols though use of mixed sediments, underwater placement, coarse-grained sediments, and artificial sand and sand retaining structures;
- Modification of incident wave conditions through use of reefs and sills and bathymetric modifications and other geometric adaptations;
- Reduction of net sediment loss though use of breakwater variations (broad-crested, submerged, tuned-structures, and alternative materials), groin variations (adjustable, permeable, and alternative materials), improved regional sediment management strategies, and groundwater management;
- Vegetative-structural combinations.

8. Conclusion

Through the Section 227 Program, the U.S. Army Corps of Engineers has a unique opportunity to investigate innovative or non-traditional shoreline erosion control technologies as a research and development initiative. Extensive monitoring is being conducted at each demonstration site and the findings used to develop design guidance. The program is structured to provide information at various technical levels to organizations and individuals with coastal protection interests. To date, several demonstration projects and technical transfer efforts are underway. Complementary research programs and independent research initiatives serve the coastal manager by addressing coastal erosion challenges in new and innovative manners and thus advance the state-of-the-practice of shore protection.

References

Basco, D., and Pope J., 2001, "Shore Protection Projects," *Coastal Engineering Manual*, Engineer Manual 1110-2-1100, Part V, Chapter V-3, U.S. Army Corps of Engineers, Washington, DC

Herrington, T.O., Bruno, M.S., and Ketteridge, K.E., 1997, "Monitoring study of the Beachsaver Reef at Cape May Point, New Jersey," Technical Report TR-2751, Davidson Laboratory, Stevens Institute Of Technology, Hoboken, NJ

Kraus, N.C. and Rankin, K.L., 2004, "Functioning and Design of Coastal Groins: The Interaction of Groins and the Beach - Processes and Planning," *Journal of Coastal Research* SI(33)

Pope, J., 1997, "Responding to Coastal Erosion and Flooding Damages," *Journal of Coastal Research* 1(3), (704-710)

Pope, J., Curtis, W.R., and Turk, G.F., 2001, "Shoreline Protection Disaster Preparation and Response Strategies: The National Shoreline Erosion Control Demonstration Program", *Proceedings from American Society of Civil Engineers Conference on Coastal Disasters*

U.S. Army Corps of Engineers, 1981, "Low-Cost Shore Protection - Final Report on the Shoreline Erosion Control Demonstration Program (Section 54)", U.S. Army Corps of Engineers, Washington, DC

CLASSICAL, INNOVATIVE AND UNCONVENTIONAL COASTLINE PROTECTION METHODS

Henk Jan Verhagen
Coastal Engineering Section, Delft University of Technology
Delft, The Netherlands

Abstract

The purpose of this paper is to give a state of the art overview of a number of recent developments in structures for shoreline protection. In other presentations the need for coastal protection structures is discussed, as well as solutions including "soft" technology like beach nourishment (see the papers of R. Dean and J. Pope).

Regarding loose armour, new developments can be reported on the stability of rock in shallow water conditions. This topic will be elaborated in more detail in the presentation of M.Van Gent.

In case the required rock size becomes too large, usually concrete elements will be used. Many elements exist, a recent PIANC working group has identified 217 different elements, but most of them are applied only seldom. Recent developments in concrete elements are the Core-Loc (developed by the US Army Corps of Engineers) and the Xbloc (developed by Delta Marine Consultants in the Netherlands). Both blocks have specific advantages in making a stable slope protection; the drawback of such blocks is the complicated shape, which makes them more costly.

One of the advantages of block like Core-Loc and Xbloc is that they can be applied as a single layer. Recent research has shown that simple concrete cubes can also be applied in a single layer; however, special attention must be paid to the placing density as well as to the rock size in the secondary layer.

Another development is the use of extreme heavy aggregates; by using magnetite specific densities up to 4000 kg/m^3 can be achieved. The main advantage of using heavier densities is that the weight of the individual block may reduce by a factor of 5. Consequently thinner layers are possible, and also lighter construction equipment can be used.

An alternative for rock and concrete structures is through the use of geofabrics. In fact there are many kinds of variations using sandbags. Geotextile technology makes it possible nowadays to create geofabrics with wide ranges of required strengths and filter properties. Although there is still some debate on the durability of geofabrics, in general it is accepted that by use of the material under water, durability is no longer a problem. Basically three types of geotextile structures are relevant in shoreline protection. Of course the classical sandbag is applied, but in large sizes. Large open bags of 1 m^3 are often used for the creation of temporary dams, while closed bags are often placed as an underwater revetment or as a hidden protection only to become active in case of calamities.

C. Zimmermann et al. (eds.), Environmentally Friendly Coastal Protection, 57-71.

Another recent development in geofabrics is the application of Geocontainers and Geotubes. Geocontainers are huge bags (order of 250 m^3), placed in situ using a split hopper barge. With Geocontainers relatively steep underwater structures can be constructed with mainly sand. Geotubes are long tubes, with a diameter in the order of 5 m and a length in the order of more than 100 m. The Geotubes are filled in situ.

Both types are mainly applied under conditions where sand is available, but rock has to be imported, and in consequently rather expensive.

A last development to be discussed is the tendency to go to more simple constructions. Especially for small scale structures it is sometimes attractive not to make an advanced and precise design, but to make it more simple by over dimensioning some elements and accepting damage. On the long run this may be a less expensive solution.

1. New Developments Related to Concrete Armour Units for Breakwaters

Traditional rubble mound breakwaters are protected with armour consisting of large rock. Unfortunately for big waves, the required rock size becomes so large that it is often a problem to find these rocks. Therefore as an alternative employed for many years, concrete elements have been used. Basically one may distinguish two tendencies in the development of concrete elements:

- Keep the element as simple as possible, to lower production and placing costs. The drawback is that the quantity of concrete is not minimal. This approach leads to the application of concrete cubes;
- Maximize the permeability and the internal friction. The drawback is that this leads to complicated shapes and costly production, but a low material quantity. This approach has led to many units, like the Tetrapod, the Accropode, the Core-Loc and the Xbloc. All of these blocks are commercial developments and patented, although some patents have expired. Recently PIANC has published a catalogue with most of the concrete elements (PIANC-MarCom 2004).

With the Accropode a new development has started to make these elements suitable for placement in a single layer. This saves a considerable amount of material, and also reduces the total placing time. The drawback is that the shape becomes even more complicated, and also the placement must be done with care. Especially attention must be paid to the placement of the first layer at the toe of the breakwaters.

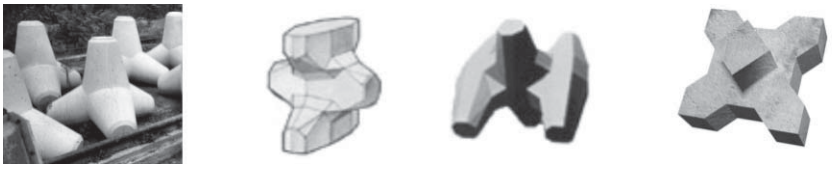

Tetrapod Accropode Core-Loc Xbloc

Figure 1: Various concrete elements for breakwaters

Some years ago in South Africa, the Dolos, a very slender concrete element has been developed. This element was quite light, but extremely stable and has been applied for a number of breakwaters. Unfortunately, because of the slenderness of the element, there was an unexpected high risk of breaking the legs.

Based on the experiences with the Accropode and the Dolos in the previous decade a new block has been developed by the US Army Corps of Engineers, the Core-Loc. This block is very stable, and can be applied in a single layer (Melby and Turk, 1997). Placement has to be done carefully, according to strict guidance of engineers of Core-Loc.

Last year, Delta Marine Consultants, from the Netherlands, has presented a new block, the Xbloc, which according to model tests, is nearly as stable as the Core-Loc, and can also be applied in a single layer without problems. According to Delta Marine Consultants the advantages of this block are easier manufacturing and less strict placing regulations (Reedijk et al., 2003).

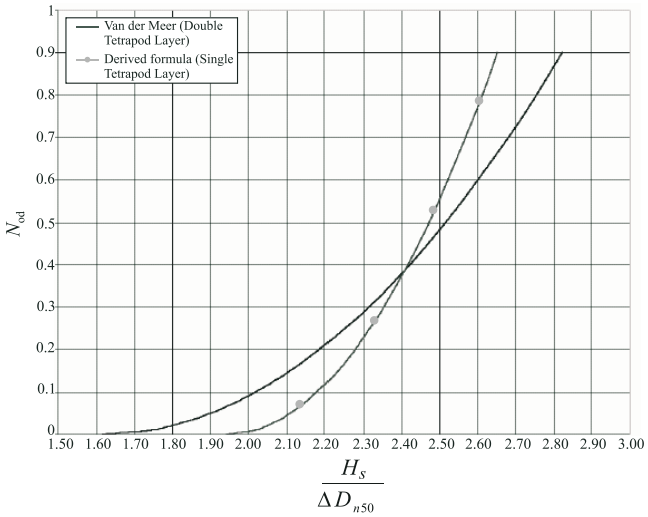

Figure 2: Stability of a single layer and a double layer of Tetrapods (DeJong, 2003)

Although the Xbloc is smoother than natural rock, the overtopping is less. This is mainly caused by the fact that the block has a higher void ratio than natural rock (recent research by Klabbers (2004)).

Recent research in Delft has shown that also some older elements can be applied in a single layer configuration. Model tests with Tetrapods and with Cubes have shown that with both elements a stable construction can be achieved (Bagheloe, 1998; Van Gent et al., 1999 and Van Den Bosch et al., 2002). The packing density of the armour layer has be as such that $n_v < 0.4$ (n_v is the void ratio). The placement density of the single layer has to be higher that in case of a double layer, and the secondary armour has to be slightly larger to prevent damage to the secondary layer.

In his research, DeJong (2003) found that the damage to the secondary layer for armor void ratios on the order of 0.3 was not caused by washing out of the material, but mainly because of sliding and displacement. The experiments demonstrated that the erosion of the secondary layer is a function of the incident wave height rather than the armour layer packing density or the wave steepness. The general conclusion was that with a sufficient packing density of $n_v < 0.4$ and a normal designed secondary layer, the construction is stable, but that a somewhat different stability curve must be used (see figure); the erosion in the secondary layer will never be more than three times the D_{n50} of the secondary layer.

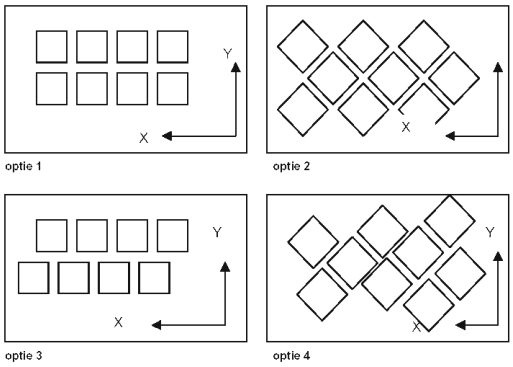

Figure 3: Dumping options for cubes on a slope (Verhagen et al., 2002)

Both for cubes as well as for Tetrapods the required placement density can be achieved by individual placing with cranes. Normally Cubes are dumped from a position around the waterline (this saves much time); it was found that the required placement density can be achieved also by dumping, provided the water depth is not more than approximately five times the block size. Also it was found that dumping in diagonal lines gives a much higher placing accuracy than dumping in parallel lines. Option 2 (see figure) gives the best results (Verhagen et al., 2002). This implies that dumping from a side-dumping barge is usually not a good option.

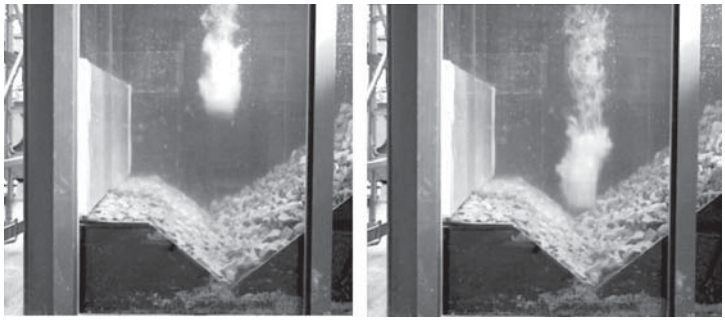

Figure 4: Dropping of a block in the laboratory (Verhagen et al., 2002)

During the initial tests it was also clear that when the blocks were dropped from above the waterline, quite some air was entrained. Blocks with much entrained air deviated less from the vertical path than blocks without air. So this gave the impression that dropping from above water would possibly result in more accurate dropping than in the case the blocks were just dipped into the water. See figure. In addition, the rotation of the blocks was investigated in these initial tests. The conclusion was that all blocks did tilt somewhat, but that they did not really started to rotate.

2. The Use of Heavy Aggregates

Nearly all stability equations for armour units use as stability number the parameter ($H / \Delta D$). Because the density of the material is included in this parameter, it implies that an increase of density will also increase the stability. In the past this stability number had been validated for variations of density of a range between 2400 and 2800 kg/m^3. However, it is also possible to use extremely heavy aggregates, and to produce concrete with a density in the order of 4000 kg/m^3. Because it was not clear beforehand that the stability relations are still valid for these values, some tests with extra heavy cubes have been conducted (Triemstra, 2000, 2001). The advantages are not only that the same stability can be achieved with a much smaller block, but also with a lighter block. This seems somewhat contradictory but can be explained easily. Because the density is 1.6 times larger, the blocks can be 1.6 times smaller, which means that the volume is $1.6^3 = 4$ times smaller which means that the weight per block is 4/1.6 = 2.5 times less.

The result is that, although the material cost per kg is higher (because of the costly aggregate), the total concrete cost may be lower; however, there are more additional benefits. Because the blocks are lighter, the cranes can also be lighter. Also the spread of the crane can be less. In summary, a considerable saving can be achieved.

Example: A simple breakwater in 10 m waterdepth will require an Xbloc of approx. 6 tons. Assume the breakwater is 5 m above water level; then the total height is 15 m and the width of the slope 22.5 m. With heavy aggregates only 2.5 tons is needed. For placing the 6 tons block over a distance of 22.5 m a 120 tons crane is needed. For placing 2.5 tons blocks on the same slope only a 40 tons crane is needed. The average price of such a crane is only one third of the price of a 100 ton crane. Additional benefits are the smaller storage yard for the blocks, the easier transport, etc.

3. Overtopping of Breakwaters

A long-term research programme on overtopping of sloping structures has resulted recently in a new set of guidelines for run-up and overtopping (Van der Meer, 2002). The formula has the overall shape of:

$$Q^* = a\sqrt{\frac{\tan\alpha}{H/L}}.\exp\left(bR^*\right) \tag{1}$$

In which Q^* and R^* are the dimensionless overtopping and the dimensionless crest height, respectively. The slope of the structure is given by α, H and L are the wave height and

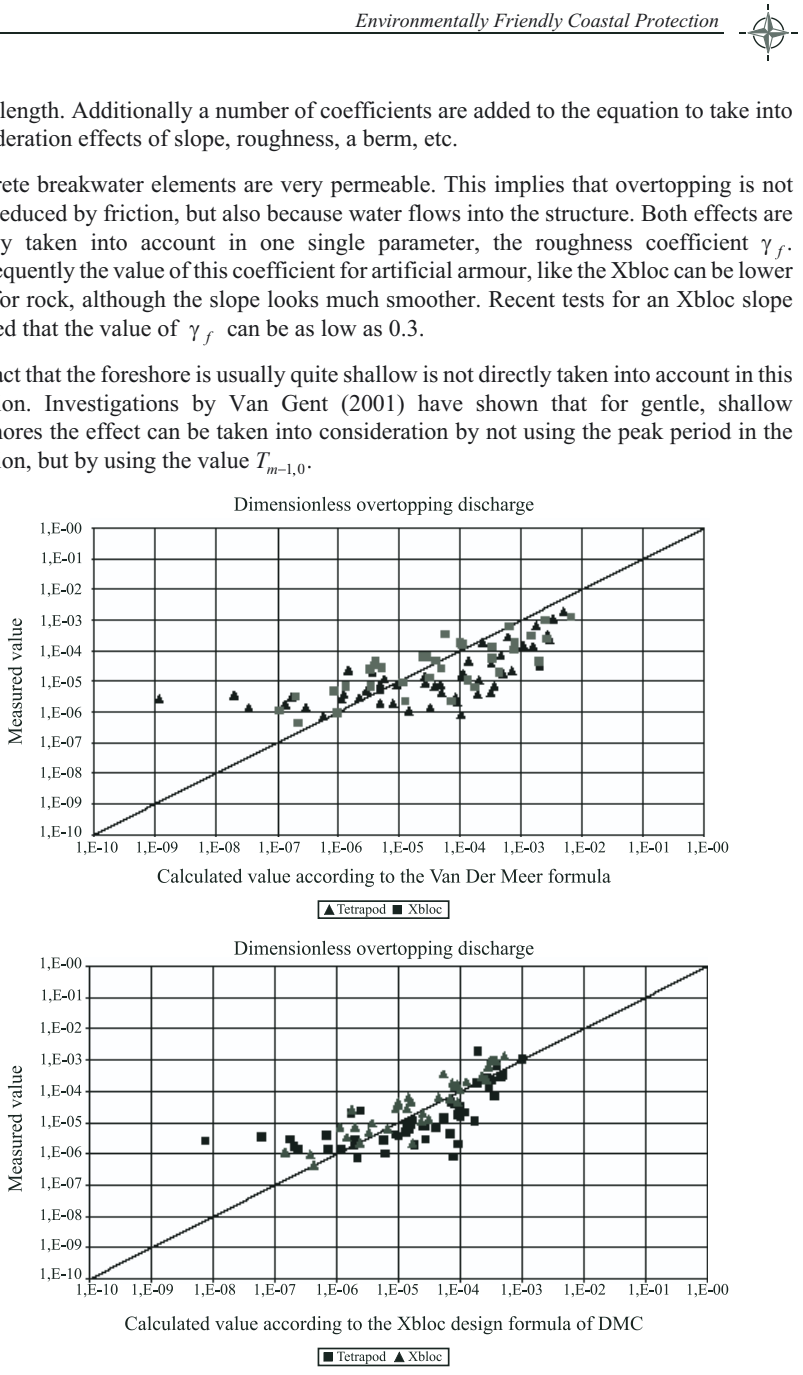

wave length. Additionally a number of coefficients are added to the equation to take into consideration effects of slope, roughness, a berm, etc.

Concrete breakwater elements are very permeable. This implies that overtopping is not only reduced by friction, but also because water flows into the structure. Both effects are usually taken into account in one single parameter, the roughness coefficient γ_f. Consequently the value of this coefficient for artificial armour, like the Xbloc can be lower than for rock, although the slope looks much smoother. Recent tests for an Xbloc slope showed that the value of γ_f can be as low as 0.3.

The fact that the foreshore is usually quite shallow is not directly taken into account in this equation. Investigations by Van Gent (2001) have shown that for gentle, shallow foreshores the effect can be taken into consideration by not using the peak period in the equation, but by using the value $T_{m-1,0}$.

Figure 5: Dimensionless overtopping according to Van Der Meer and Klabbers equation for Tetrapods and Xbloc (Cui, 2004)

As an alternative, Klabbers et al. (2003) has suggested not to use the Iribarren number [$Ir = \tan\alpha / \sqrt{(H / L)}$] as a basis for the overtopping equations, but the Ursell number [$U = (H / d) / (d / L)^2$]. Especially for concrete breakwater units, this leads to a more accurate prediction of the overtopping. Their equation is:

$$Q^* = aU.\exp\left(bR^*\right) \tag{2}$$

The fitted values for *a* and *b* are 0.01 and -3.58. In this equation the local wavelength at the toe of the structure should be used.

From the above figures it follows that especially for the Xbloc the formula of Klabbers et al. gives better results, but it can be seen that also in case of a Tetrapod slope, the results of this equation is at least as good as the Van der Meer formula. One should realise that in the formula of Klabbers et al., the slope of the structure is not included as a parameter. This effect has not been investigated, because slopes with concrete breakwater elements are usually constructed with a fixed slope of $1{:}1^{1/2}$.

4. The Use of Geofabrics

Geofabrics are used in many varieties in coastal protection. An important function of geofabrics is that they have filter properties, and may replace granular filters to prevent the washing out of fine particles. Another important function of geofabrics is that they can be used to construct containers with inexpensive aggregates, like sand, and in this way form large units to withstand the erosive forces of currents and waves. Thus, packed sand can become a substitute for rock and concrete elements. Three types of applications will be discussed in this paper.

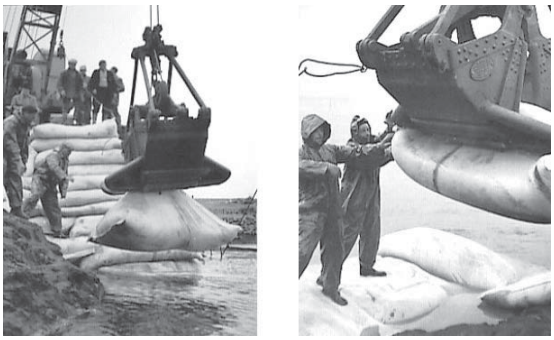

Figure 6: Nylon bags used for the closure of the Pluimpot, November 1957 (photo Cas Oorthuys, rvd)

5. Large Geotextile Bags

The use of simple sandbags is already quite old. For centuries, the sandbag has been used to combat flooding. However, as long as the sandbags have to be handled by hand, the size is limited. Sandbags should not weigh more than 50 kg; otherwise accurate placing by

hand is impossible (additionally European Labour Regulations limit the maximum weight of a bag to be handled by a single person to 25 kg. A 50 kg bag may only be handled by two persons). But by employing machines in the process, larger bags can be used. Already in 1957 tests with large nylon bags had been carried out during the closure of the Pluimpot estuary in the Netherlands. However, in subsequent years these bags have not been used frequently because of the high cost of the material in that time.

Figure 7: Emergency works at a dike breach in the Julianakanaal in the Netherlands, January 2004 (photo Michiel Wijnbergh/Hollandse Hoogte)

Currently, bags with a size of 1 m^3 are quite standard for transport and storage of bulk material in industry. These bags can also be used easily for emergency dikes; during the river floods in recent years these bags have been applied often. For waterboards it is an attractive option, because the bags are very cheap (they usually are bought second hand), readily available on the market, and easy to fill and handle with forklifts or cranes.

Figure 8: Deteriorating sandbags in Dubai, visual problems for local authorities (Weerakoon et al., 2003)

For permanent structures these types of bags are not often used. However, custom-made bags using strong non-woven material are used also for more permanent structures. Such bags are also marketed as Soft Rock (trademark of Naue Fasertechik, Germany). For

permanent structures it is very important to guarantee a sufficient degree of filling, otherwise the bags are not stable under wave conditions.

Usually the bags are applied as a “hidden protection”. In fact they form a layer of coastal protection, which only becomes active during storms, in order to prevent excessive cross-shore erosion. In case of erosion due to a gradient in longshore transport longshore protections are not effective. However, bags can be applied also to construct a groyne, although in most cases preference is given then to Geotubes.

As mentioned, longshore constructions are often executed as “hidden protection”. In this way the geotextile deteoriation due to UV-radiation is reduced, but also the geotextiles become less vulnerable to vandalism. Although damage by vandalism can be repaired (see also below when the Geotubes are discussed), this is costly and requires considerable management effort.

Because the bags are usually not fully stable, they will deform. A slight deformation is not a problem from a strength point of view, but gives a negative visual impact. Usually this is not acceptable for beaches with a tourist function.

One should realise that a longshore hidden protection can be executed easily, but it is not possible to construct groynes with sandbags as a hidden construction. They only way to hide sandbags in a groyne is to cover them with rock. However, in most cases this is not attractive economically.

6. Geocontainers

Geocontainers are relatively new engineering systems. Nicolon has developed the system and also copyrighted the name Geocontainer (Nicolon, 1988). Geocontainers are in fact large bags, filled in the hopper of a split barge and dumped by that barge in a selected position. Geocontainers have been applied at several places in recent years, mainly as fill units, shore protection and as breakwaters. The application depth is up to 30 meters. An overview of Geocontainer technology is given by Pilarczyk (2000).

The standard basic material of Geocontainers is the high grade Geolon PP with tensile strengths in both length and cross directions of 80- 100 and 200 kN/m. Geocontainers are always custom built to fit the hold of the split-bottom barge to be used with hull capacities vary from 200 m^3 to 300 m^3.

Figure 9: Placing a Geocontainer (Photos Rijkswaterstaat, DWW)

The procedure is that the empty Geocontainer is placed in the hull of the split barge, the container is filled with an appropriate material, and the container is closed by sewing. Then the barge sails to the right position where the container is dumped.

The advantages of the system include:

- containers can be filled with locally available soil; this can be from a land source or from nearby dredging activities;
- containers can be placed relatively accurately regardless of the weather conditions, current velocities, tides and waterdepths;
- contained material is not subject to erosion during or after placement;
- mobilization for container construction and placement can be relatively rapid.

This implies that Geocontainers will mainly be applied in situations where sand is abundantly available and rock is costly; where mild construction slopes are to be avoided and where erosion by currents and waves may be a problem.

The main design considerations include sufficient strength of the geotextile and appropriate filling. Because Geocontainers are applied under water, the effect of UV and vandalism are usually negligible.

Figure 10: Demo Geocontainer on a beach, Goldcoast, Australia

A Geocontainer will always contain a certain amount of air in the pores of the sand; the behaviour of this air determines largely the behaviour of the Geocontainer during sinking. Recently (de Groot et al., 2003) detailed research has defined the most relevant problems:

- the positioning of the Geocontainer during sinking;
- the geotechnical stability of the Geocontainers;
- the overload on the Geocontainer during dumping.

These tests resulted in the conclusions that in waterdepths of approximately 20 meters there was no problem to construct a 1:2 slope in still water and a 1:3 slope under conditions with waves and currents. The basis for this test was a 300 m^3 container. Placing the first container is the most difficult operation; the following containers can be placed more easily. In shallow water (less than 10 m) the placing accuracy is much better and slopes of 1:1.5 may be achieved.

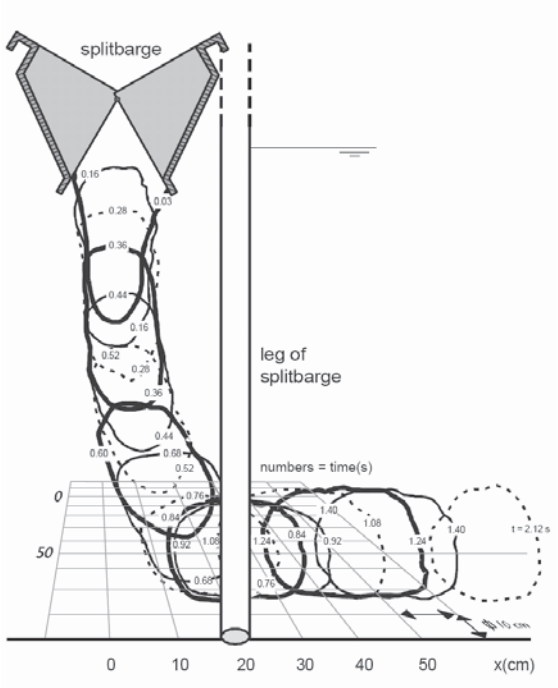

Figure 11: Falling pattern of a Geocontainer (De Groot et al., 2003)

Regarding the strength it was found that a nominal tensile strength of 120 kN/m for water depths up to 15 m did not cause any problems provided the sand had a low content of fines (less then 20% particles smaller than 63 μm). It is not expected that this conclusion will differ for larger waterdepths. Only for extremely shallow water the falling energy reduces considerably, which implies that that a tensile strength of 120 kN/m should be applied for all Geocontainers. Also it was found that using dry sand decreases the falling velocity and consequently the impact energy.

The geotechnical stability gave steeper critical slopes than the slopes which could be achieved by dumping; so geotechnical stability is not a criterion.

Geocontainers under wave attack are stable for values of $H_s / \Delta d$ up to 1. In this equation d is the height of the container after dumping. Practically it means that Geocontainers are stable up to waves of 3 m. The critical velocity for a pile of Geocontainers is given by $u / \sqrt{g \Delta d} < 0.5$ to 1. Liquefaction is no problem when the Geocontainer is filled with sand without fines (less than 20% silt fraction).

7. Geotubes

Geotubes are long woven polypropylene tubes; the name Geotube is a registered trademark from Nicolon, the Netherlands. Compared with the Geocontainer which is filled before placement, the Geotube is filled in place. This allows a longer structure. Geotubes are mainly used as core elements for dams and dikes, as groynes and as longshore protection. Recently in the Netherlands Geotubes have neen applied as core elements for guide dams near a lock and an aqueduct (Spelt, 2001). Experience in Dubai (Weerakoon et al., 2003) with unprotected Geotubes showed that with a qualified contractor the construction is no problem at all, but that because of wave action, some damage may occur to the tubes during minor storms. This damage causes leakage and loss of sand from the tube. The final result is some slumping of the tubes, and consequently the tube is no longer able to fulfil its function adequately (in this case the function of the tube was to protect an artificial beach).

Figure 12: Slumping of a Geotube after a small storm in Dubai (Weerakoon et al., 2003)

The exact cause of the damage is not fully understood. Probably it is a combination of rocking of the structure itself, causing a movement of sand inside the tube, in combination with some scouring under the tube. This may cause extreme tensions in the geotextile, leading to ruptures.

Figure 13: HDPE repair plates for a Geotube (Heilman & Hauske, 2003)

Geotubes, like other geotextile structures, are vulnerable to damage, both natural and man-induced. It is essential that damage be repaired as soon as possible. Recently a method has been developed by Heilman and Hauske (2003) to repair such structures,

using HDPE repair plates. Although this works very well technically, it requires good management of the structure. The structure must monitored very regularly, and repair must be done immediately after ascertaining the damage.

8. Simple Construction

The total costs (sum of construction costs and capitalized maintenance costs) of simple coastal structures, like groynes, can be decreased significantly by simplifying the structure (Crossman et al., 2003). Fewer layers and less prepared foundations make construction operations easier and more rapid. Reducing the depth of excavation, limiting geotextiles and reducing the number of rock gradings can achieve considerable savings. Also the volume of rock used in structures can be reduced as a result of less extensive foundations and improved understanding of performance requirements. Substitution of rock by alternatives (particularly waste) materials may also lead to savings.

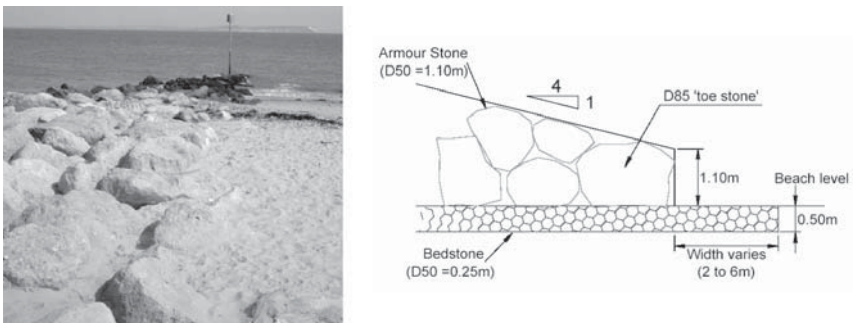

Figure 14: Simple groyne at the southern UK Coast, and toe detail (Crossman et al., 2003)

In a particular case in the southern UK, the use of a single armour grading with no under layer and the omission of a geotextile filter gave a saving of approximately 10% of the construction cost. Acceptance of regular minor damage enabled a smaller rock size, and consequently also a smaller rock volume. Of course, this lead to an increase in monitoring and maintenance costs. But altogether the total savings, assuming a discount rate of 4% and a 50 year assessment period gave savings in the order of 25% of the total cost of the scheme. Considering the damage factor in the stability formula for rock may reveal the optimum damage level. Sometimes a slightly thicker armour layer (e.g. 3 elements instead of 2) may reduce the size of the armour, and consequently also the total volume or rock required.

At the Bulgarian coastline, near Varna, some 15 years ago a number of breakwaters for marinas were constructed. Due to a number of reasons, the Tetrapods used for these marinas were of very poor material quality; accidentally they were also slightly over dimensioned. At present no serious damage has been observed. This shows that in case of a robust design, not so much money has to be spent to high quality materials. Also here, one has to find for a good balance between costs and material quality.

References

Bagheloe (1998) Breakwaters with a single layer. MSc Thesis, TU Delft, Hydraulic engineering Section

Crossman, M., Allsop, W., Segura Dominguez,S., Bradbury, A., A, Simm, J (2003) Economical rock groynes, *Proc. Coastal Structures 2003, Portland, USA*

Cui, J (2004) Experimental research of wave overtopping on a breakwater with concrete armour units. M.Sc.-thesis, TU Delft, Hydraulic Engineering Section (http://www.waterbouw.tudelft.nl/education//MScTheses/2004/2004Cui.pdf)

DeJong (2003) Experimental research on the stability of armour and secondary layer in a single layered Tetrapod breakwater. M.Sc.-thesis, TU Delft, Hydraulic Engineering Section.(http://www.waterbouw.tudelft.nl/education/MScTheses/2003/2003deJong.pdf)

Groot, M.B. de, Klein-Breteler, M, Bezuijen, A. (2003) Resultaten Geocontaineronderzoek (Results Geocontainer research), Delft Cluster Report DC1-321-11, (http://www.library.tudelft.nl/delftcluster/PDF-files/DC1-321-11.pdf)

Heilman, D.J., Hauske, G.J. (2003) Advances in geotextile tube technology, *proc. Coastal Structures, 2003, Portland, USA*

Klabbers, M, Muttray, M.O., Reedijk, J.S. (2003) Xbloc armour unit development: hydraulic performance of Xbloc armour units, 2D model tests at WL Delft, DMC report 210006-r-03, DMC, Gouda, The Netherlands (http://www.kennisbank-waterbouw.nl/SelfArchiving/archive/TPG1101261.pdf)

Melby, J.A., Turk, G.F. (1997) CORE-LOC concrete armor units.Technical Report CHL-97-4, US Army Engineer Research and Development Center, Vicksburg, MS (http://chl.wes.army.mil/library/publications/coreloc/trchl-97-4.pdf)

Nicolon (1988) Nicolon products; Geosystems, Geotubes and Geocontainers. *Company publication, TenCate/Nicolon, PO Box 236, Almelo, Netherlands*

Pianc-Marcom (2004) Catalogue of prefabricated elements, *Report of working group36*, PIANC, Brussels (http://www.pianc-aipcn.org/)

Pilarczyk K.W. (2000) Geosynthetics and geosystems in hydraulic and coastal engineering *Balkema, Rotterdam*, ISBN 90.5809.302.6, 913 pp

Reedijk, M., Klabbers. M., Vandenberge, A., Hakenberg, R. (2003) Development of the Xbloc breakwater armour unit, *2nd International Conference on Port & Maritime R&D and Technology, Singapore* (http://www.xbloc.com/documents/development of the xbloc breakwater armour unit.pdf)

Spelt, K (2001) Geotubes as the Core of Guide Dams for Naviduct at Enkhuizen, The Netherlands Terra & Aqua, nr 83 (IADC, The Hague, The Netherlands) (http://www.iadc-dredging.com/downloads/terra/terra-et-aqua_nr83_03.pdf)

Triemstra, R. (2000) The use of high density concrete in armour layers of breakwaters. M.Sc.-thesis, TU Delft, Hydraulic Engineering Section (http://www.waterbouw.tudelft.nl/education//MScTheses/2000/2000Triemstra.pdf)

Triemstra, R. (2001) Stability of high density concrete armour elements under wave attack *PIANC bulletin 108*

Vandenbosch, A, D'Angremond, K, Verhagen, H.J., Olthof, J (2002) Influence of the density of placement of armour layers on breakwaters, *proc . ICCE 2002, Cardiff, pp 1537-1549*
(http://www.waterbouw.tudelft.nl/public/verhagen/papers/icce2002-1.pdf)

Van Der Meer, J.W. (2002) Technical Report wave run-up and overtopping at dikes, *Technical Advisory Committee on Waterdefences, Delft, the Netherlands, 70 pp*
(http://www.tawinfo.nl/engels/downloads/TRRunupOvertopping.pdf)

Van Gent M.R.A., Spaan, G.B.H., Plate, S.E., Berendsen, E., Van Der Meer, J.W., d'Angremond, K.(1999) Single-layer rubble mound breakwaters, proc. Int. Conf. Coastal Structures, Santander, Spain

Van Gent, M.R.A.(2001) Wave run-up on dikes with shallow foreshores. *J. of Waterway, Port, Coastal and Ocean Engineering, ASCE, vol.127 (5), pp 264-272*

Verhagen, H.J., D'Angremond, K, Vandervliet, K. (2002) Positioning of cubes on a breakwater slope, *proc. ICCE2002, Cardiff, pp 1550-1560*
(http://www.waterbouw.tudelft.nl/public/verhagen/papers/icce2002-2.pdf)

Weerakoon, S, Mocke, G.P., Smit, F., Al Zahed, K. (2003) Cost effective coastal protection works using sand filled geotextile containers. proc. Copedec VI, Colombo, Sri Lanka

ON THE STABILITY OF ROCK SLOPES

Marcel R.A. VAN GENT
WL | Delft Hydraulics
Delft, The Netherlands

Abstract

The stability of rock slopes under wave attack is addressed in this paper. The research on this issue as presented in Van der Meer (1988) and in Van Gent, Smale and Kuiper (2003) forms the basis for the analysis presented here. In the latter paper new physical model tests were described and analysed to obtain information on how to apply design formulae for conditions that include situations in which wave breaking occurs on the foreshore. This paper resulted in recommendations to apply modifications to the formulae by Van der Meer (1988), mainly to enlarge the field of application to situations with shallow foreshores. In addition, a new simple formula with a comparable accuracy was presented. Here, the comparisons between stability formulae and data by Van Gent et al. (2003) are extended by including also data by Van der Meer (1988). The total data set applied here consists of about 800 test conditions.

1. Introduction

Many empirical methods for the prediction of the required size of rock material under wave attack have been proposed in the last 70 years; examples are the stability formulae by *a)* Iribarren (1938, 1953), *b)* Hudson (1953, 1959), *c)* Van der Meer (1988), *d)* a modification of the formulae by Van der Meer (1988) as proposed in Van Gent et al. (2003), and *e)* a formula by Van Gent et al. (2003).

The first three stability formulae (Iribarren, Hudson and Van der Meer) were mainly developed for relatively deep water wave conditions at the toe of the structure. However, in many practical circumstances coastal structures are positioned in relatively shallow water such that wave breaking occurs on the foreshore before the waves reach the structure. The latter two stability formulae (i.e., the modified formulae of Van der Meer, 1988, as proposed in Van Gent et al. 2003, and an alternative formula by Van Gent et al. 2003) were developed to extend the field of application of stability formulae such that they can be applied, not only for deep water at the toe, but also for shallow water at the toe of non-overtopped rubble mound structures.

Based on a relatively small amount of tests Van der Meer (1988) proposed to use the wave height $H_{2\%}$ (the wave height exceeded by 2% of the waves) so that the deviation from the Rayleigh wave height distribution, described by the factor $1.4/(H_{2\%} / H_s)$, was included in the formulae by Van der Meer (1988). Based on tests by Smith et al. (2002) and new tests, modifications to this method were proposed in Van Gent et al. (2003).

C. Zimmermann et al. (eds.), Environmentally Friendly Coastal Protection, 73-92.

In this paper the data used by Van der Meer (1988) and the data used by Van Gent et al. (2003) are compared to stability formulae in order to provide insight into their performance for deep-water wave conditions and shallow-water wave conditions at the toe of non-overtopped rock slopes.

2. Physical Model Tests

The main part of the physical model tests analysed by Van der Meer (1988) and the tests used by Van Gent et al. (2003) were performed in the Scheldt flume of Delft Hydraulics. This wave flume has a length of 55 m, a width of 1 m and a height of 1.2 m. The facility is equipped with a wave board for generating regular/monochromatic and irregular/random waves in relatively shallow water by a translatory wave board with Active Reflection Compensation (ARC). The latter test programme was carried out with a second-order wave generation technique. This means that the second order effects of the first higher and first lower harmonics of the wave field are taken into account in the wave board motion.

2.1 Van der Meer (1988) Test Conditions

The data set on which the formulae by Van der Meer (1988) are based can be characterised by the parameters given in Table 1. This data set covers wide ranges of several parameters such as the structure slope (1:1.5 to 1:6), the structure geometries (i.e. structures with an impermeable core, structures with a permeable core, and homogeneous structures), and the wave steepness ($s_m = 0.01 - 0.06$). Parameters that have not been varied significantly are the amount of wave breaking on the foreshore (most of the tests were with deep water at the toe), the spectral shape (for instance almost no double-peaked spectra), and grading (no very wide gradings).

The incident waves were obtained from the measured surface elevations (including reflected waves) near the toe of the structure by using a technique with two wave gauges in front of the structure.

For the analysis presented here the data on low-crested structures has been excluded from the data-set applied by Van der Meer (1988), such that only non-overtopped structures are included. This means that in total 579 test conditions were used here.

Table 1: Ranges of parameters in the data set used by Van der Meer (1988)

Parameter	Symbol	Range
Slope angle	$\cot\alpha$	1.5 – 6
Relative density	Δ	1 – 2.1
Number of waves	N	< 7500
Wave steepness based on mean wave period	s_m	0.01 - 0.06
Surf-similarity parameter using mean wave period	ξ_m	0.7 - 7
Permeability parameter	P	0.1 - 0.6
Grading armour material	D_{n85} / D_{n15}	< 2.5
Stability parameter	$H_s / \Delta D_{n50}$	1 - 4
Damage level	S	< 30

2.2 Van Gent et al. (2003) Test Conditions

The data set on which the formulae presented in Van Gent et al. (2003) are based can be characterised by the parameters given in Table 2. In contrast to the data set by Van der Meer (1988), in this data set the amount of wave breaking on the foreshore was varied significantly, i.e. from deep-water conditions to shallow water conditions. Also a large number of double-peaked wave energy spectra were used. Similar to the data set by Van der Meer (1988) no tests were performed with a very wide grading and the shape of the rock material was not varied; the tests were all performed with "standard rough angular rock". The data set contains 207 test conditions. This data set will be described in more detail here.

Table 2: Ranges of parameters in the data set used by Van Gent et al. (2003)

Parameter	Symbol	Range
Slope angle	$\cot\alpha$	2 – 4
Relative density	Δ	1.65 – 1.75
Number of waves	N	< 3000
Wave steepness based on mean wave period	s_m	0.01 - 0.06
Surf-similarity parameter using mean wave period	ξ_m	1 – 5
Surf-similarity parameter using spectral wave period	$\xi_{s,-1}$	1.3 – 15
Wave height ratio	$H_{2\%} / H_s$	1.2 - 1.4
Deep-water wave height over depth	H_{s-deep} / d_{toe}	0.2 - 2.7
Grading armour material	D_{n85} / D_{n15}	1.4 – 2.0
Core material	$D_{n50-core} / D_{n50}$	0 – 0.3
Stability parameter	$H_s / \Delta D_{n50}$	0.5 – 4.5
Damage level	S	< 62

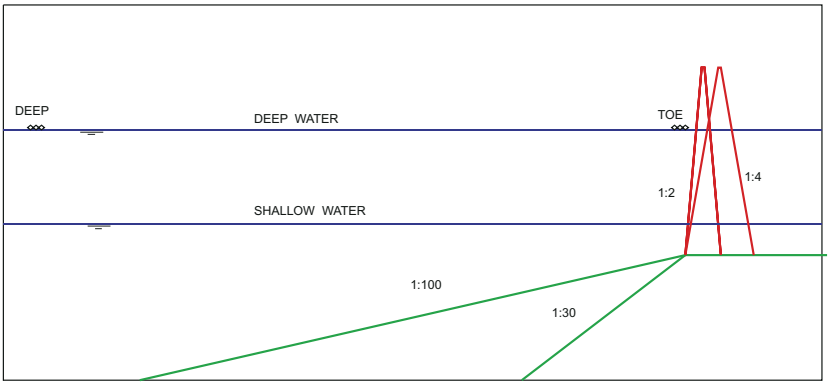

Figure 1: Foreshores and structure slopes

Figure 1 shows the model set-up for the tests analysed in Van Gent et al. (2003) with the two foreshores (1:30 and 1:100) and the two slopes (1:2 and 1:4) that were used. Many water levels were used, in the range between shallow water with severe wave breaking on

the foreshore to deep-water conditions with no wave breaking at all on the foreshore. Table 3 shows an overview of the tested structures. The first 3 series are obtained from Smith *et al* (2002). For all structures the crest was at a level such that no overtopping occurred. The type of rock material was "standard rough angular rock". Figure 2 shows a picture of the rock material (Series 4 - 7), used to provide an impression of the shape of the rock material. The density of the applied rock material was between 2650 kg/m^3 and 2750 kg/m^3. The aspect ratio of this material was 2.1 (see for instance the Rock Manual, 1995, for a definition of the aspect ratio).

Figure 2: Picture of rock material used in armour layer

Table 4 shows for each series of tests the ratio of $H_{2\%} / H_s$ at the toe of the structure (between 1.21 and 1.42), the ratio of the wave height and water depth at the toe (between 0.15 and 0.78), the ratio of the wave height at deep water and the water depth at the toe (between 0.18 and 2.7), and the ratio of the wave height at the toe and the wave height at deep water (between 0.17 and 1.1). This indicates that the test programme contains conditions with severe wave breaking but also conditions in which shoaling, but no wave breaking, occurs.

Table 3: Tested structures

	Description	Foreshore	Slope	$D_{n50-armour}$ (m)	$D_{n50-core}$ (m)
1	Permeable core	1:100	1:2	0.035	0.010
2	Permeable core	1:100	1:2	0.022	0.010
3	Permeable core	1:100	1:4	0.022	0.010
4	Permeable core	1:30	1:2	0.026	0.009
5	Permeable core	1:30	1:4	0.026	0.009
6	Impermeable core	1:30	1:2	0.026	0
7	Impermeable core	1:30	1:4	0.026	0

All above mentioned structures were tested with single and double-peaked wave energy spectra. In total 114 test conditions with single-peaked wave energy spectra were

performed (Jonswap or TMA-spectra) and 93 test conditions with double-peaked wave energy spectra. The double-peaked wave energy spectra were obtained by superposition of two single-peaked wave energy spectra of which the ratio of the peak wave periods was 0.65 or 0.4. Figure 3 shows a few examples of applied wave energy spectra.

Table 4: Range of parameters

	Number of tests	$H_{2\%-toe} / H_{s-toe}$	H_{s-toe} / d_{toe}	H_{s-deep} / d_{toe}	H_{s-toe} / H_{s-deep}
1	37	1.27-1.42	0.34-0.51	0.38-1.49	0.29-1.00
2	34	1.23-1.41	0.34-0.52	0.38-2.72	0.17-0.93
3	31	1.28-1.40	0.31-0.51	0.34-1.00	0.47-1.01
4	26	1.26-1.37	0.23-0.78	0.25-1.45	0.43-1.00
5	24	1.26-1.37	0.34-0.73	0.35-1.15	0.53-1.06
6	34	1.28-1.42	0.15-0.48	0.18-1.13	0.38-1.07
7	21	1.21-1.37	0.27-0.53	0.26-1.24	0.39-1.10

The wave conditions were measured by arrays of three gauges at deep water and at the location of the structure toe. The analysis was based on the time series of the incident waves at the toe. These incident waves, without reflected waves, were obtained using the method by Mansard and Funke (1980). Testing was performed initially with the structure in place. Once all stability tests were completed the executed, tests were repeated without the structure present in order to more accurately determine the incident wave height at the toe. Thereafter, a statistical and spectral analysis of the incident time series at the toe of the structure was performed. The significant wave height H_s ($H_s = H_{1/3}$), the wave height exceeded by 2% of the waves $H_{2\%}$, and the mean wave period T_m were obtained from time domain analysis. The spectral wave period $T_{m-1,0}$ ($T_{m-1,0} = m_{-1} / m_0$ with $m_n = \int_0^\infty f^n S(f)\,df$ with $n = -1$ or 0) was obtained from the measured wave energy spectra. For a standard Jonswap spectrum the relation between $T_{m-1,0}$ and T_p can be approximated by $T_p = 1.1\,T_{m-1,0}$.

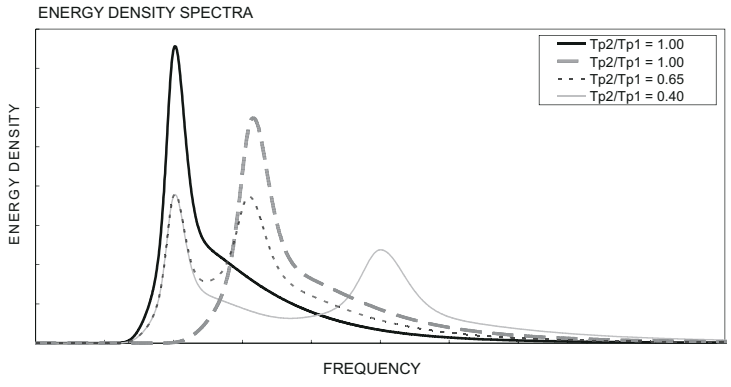

Figure 3: Examples of applied wave energy spectra

The slope of the structure was measured before and after each test run. The measurements of the profile were made with a surface profiler consisting of nine gauges at a spacing of 0.10 m across the flume width. The gauges were fastened to a computer-controlled carriage and each gauge measured the structure height every 0.040 m for the structures with a 1:4 slope and every 0.020 m for the structures with a 1:2 slope. With the profiles measured by each of the nine gauges an average erosion profile was computed and this average profile was used for further processing. Before each test a reference profile was measured. Then the profiles were measured after 1000 waves. Some tests were also performed with 3000 waves and for those tests a third profile measurement was made after 3000 waves. The armour layer was then reconstructed for the following test and the process was repeated. Thus, from each test run the eroded area A_e could be obtained from the average profile. This provided the required information on the damage level $S = A_e / D_{n50}^2$ for each test run. The damage levels obtained were between $S = 0$ and $S = 62$, although 95% of the tests resulted in damage levels smaller than $S = 30$. For armour layers with a thickness of about two diameters, "start of damage" can be described by $S = 2$. To describe "failure" $S = 8$ can be used for slopes of 1:2 or steeper, and $S = 17$ can be used for slopes of 1:4 or more gentle.

3. Stability Formulae

In the introduction five stability formulae were mentioned. Four of them are used here for comparison with the data used by Van der Meer (1988) and the data used by Van Gent et al. (2003); however, the by Iribarren formula (1938) has not been used here.

3.1 Formula Based on Hudson (1953, 1959)

The original Hudson formula (1953, 1959), developed based on tests with regular waves, can be re-written for applications with irregular waves into:

$$\frac{H_s}{\Delta D_{n50}} = \frac{\left(K_D \cot\alpha\right)^{1/3}}{1.27} \tag{1}$$

in which D_{n50} is the median nominal diameter: $D_{n50} = (M_{50} / \rho_a)^{1/3}$ (m), M_{50} is the mass that is exceeded by a mass percentage of the rocks of 50% (kg), K_D is a stability coefficient (-), α is the structure slope (-), H_s is the significant wave height of the incident waves at the toe of the structure (using SPM, 1984: $H_{Hudson} = H_{1/10} \approx 1.27\ H_s$) (m), $\Delta = \rho_a / \rho_w - 1$ is the relative buoyant density (-), ρ_a is the density of rock armour (kg/m^3) and ρ_w is the density of water (kg/m^3).

For design purposes it might be acceptable that 0-5% of the armour stones are displaced from the region between the crest and a level of one wave height below still water; the wave height to be used for this purpose could be the design wave height.

In the Shore Protection Manual of 1977 (SPM, 1977) the coefficient 1.27 in Equation 1 was set to 1.0 because the wave height $H_{Hudson} = H_s$ was used. In SPM (1977) the values given for K_D for rough, angular, randomly placed rocks in two layers on a breakwater trunk were $K_D = 3.5$ for "breaking waves on the foreshore", and $K_D = 4.0$ for

"non-breaking waves on the foreshore". "Breaking waves on the foreshore" refers to depth-induced wave breaking on the foreshore in front of the structure. It does not describe the type of breaking due to the slope of the structure itself.

In the Shore Protection Manual of 1984 (SPM, 1984) not only the coefficient 1.27 was introduced in Equation 1, but also the value of K_D for breaking waves was revised and decreased from 3.5 to 2.0 while for non-breaking waves it remained 4.0. This means that application of the formula by Hudson following SPM (1984) leads to a considerable larger stone diameter than if SPM (1977) is used. Here, the recommendations by SPM (1984) are used.

The use of Equation 1 is for situations with a fixed damage level, namely 0-5% of the armour stones displaced out of the region of primary wave attack. In order to apply this equation for damage levels described by the parameter $S = A_e / D_{n50}^2$ Van der Meer (1988) proposed the use of the following expression:

$$\frac{H_s}{\Delta D_{n50}} = 0.7\left(K_D \cot\alpha\right)^{1/3} S^{0.15} \tag{2}$$

Figure 4 shows the data used by Van der Meer (1988) and by Van Gent et al. (2003) compared to Equation 2. Two curves are shown, one for $K_D = 2$ and one for $K_D = 4$. This figure shows a very large amount of scatter. The use of $K_D = 4$ leads to a large number of test results for which the damage is larger than predicted; using $K_D = 2$ leads to considerably fewer test results for which the damage is larger than predicted.

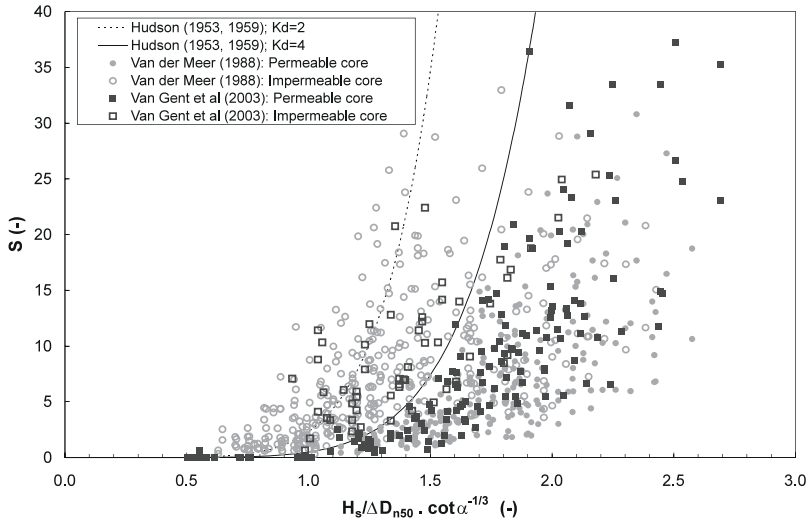

Figure 4: Data compared to formula based on Hudson (1953, 1959); structures with a permeable core and structures with an impermeable core

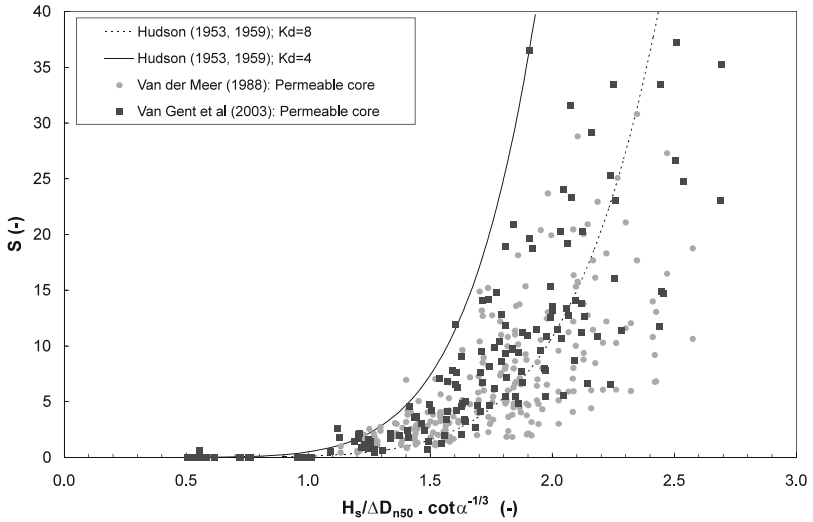

Figure 5: Data compared to formula based on Hudson (1953, 1959); structures with a permeable core only

Figure 5 shows the same data as in Figure 4 but now only the data for structures with a permeable core (about 400 test conditions). This figure shows that the use of $K_D = 4$ leads almost to no underpredictions. It can be concluded that the formula based on Hudson (1953, 1959), i.e. Equation 2, can be used for design purposes using $K_D = 4$ if the structure has a permeable core. Nevertheless, this approach may for specific conditions lead to stone diameters that are much larger than necessary.

In contrast to the SPM (1984), a value of $K_D = 4$ for the design of structures with a permeable core can be recommended, irrespective of whether or not the conditions are with breaking waves on the foreshore. The main trend through the data for structures with a permeable core can be described by using $K_D = 8$ but there is a (large) standard deviation between measured and predicted values for S: $s = 12$ (based on data used by Van Gent et al., 2003; this part of the data set is more uniformly distributed over the main parameters involved). This corresponds to a value of $\sigma = 0.37$ based on differences between measured and predicted values for values of $S / \sqrt{N}$. For the design of structures with an impermeable core a lower value is required for K_D; the use of $K_D = 2$ still leads to more than 25% of the test results for structures with an impermeable core for which the damage is underpredicted; the use of $K_D = 2$ leads to 5% of the test results on structures with an impermeable core for which the damage is underpredicted. This concerns both conditions with breaking waves on the foreshore and conditions without wave breaking on the foreshore. The main trend through the data for structures with an impermeable core can be described by using $K_D = 4$ but there is again a large standard deviation of differences between measured and predicted values for S: $s = 13$ (or $\sigma = 0.37$ based on values for $S / \sqrt{N}$).

3.2 Formulae Based on Van der Meer (1988)

The formulae by Van der Meer (1988) were based, amongst other work, on work by Thompson and Shuttler (1975) and a large amount of tests for which the majority were performed with relatively deep water at the toe. These formulae make use of a distinction between "plunging" and "surging" conditions:

Plunging conditions ($\xi_m < \xi_c$): $$\frac{H_s}{\Delta D_{n50}} = c_{plunging} P^{0.18} \xi_m^{-0.5} \left(\frac{H_{2\%}}{H_s} \right)^{-1} \left(\frac{S}{\sqrt{N}} \right)^{1/5} \quad (3)$$

Surging conditions ($\xi_m \geq \xi_c$): $$\frac{H_s}{\Delta D_{n50}} = c_{surging} \xi_m^P P^{-0.13} \tan\alpha^{-0.5} \left(\frac{H_{2\%}}{H_s} \right)^{-1} \left(\frac{S}{\sqrt{N}} \right)^{1/5} \quad (4)$$

in which H_s is the significant height of the incident waves at the toe, P is a parameter that takes the influence of the permeability of the structure into account, N is the number of incident waves, $\Delta = \rho_a / \rho_w - 1$ is the relative buoyant density, ξ_m is the surf-similarity parameter using the mean wave period T_m from time-domain analysis, and α is the structure slope. The transition from "plunging" conditions ($\xi_m < \xi_c$) to "surging" conditions ($\xi_m > \xi_c$) is given by the critical breaker parameter:

$$\xi_c = \left[\frac{c_{plunging}}{c_{surging}} P^{0.31} \sqrt{\tan\alpha} \right]^{\frac{1}{P+0.5}} \quad (5)$$

In the formulae by Van der Meer (1988) for relatively deep-water wave conditions at the toe, the ratio $H_{2\%} / H_s$ is replaced by the factor 1.4.

For slope angles more gentle than $\cot\alpha > 4$, Van der Meer recommended using Equation 3, irrespective of whether the surf-similarity parameter x_m is smaller or larger than the transition value ξ_c. For instance for slope angles of $\cot\alpha = 4$ the use of either Equation 3 or Equation 4 could lead to significant different results (discontinuity).

Van der Meer (1988) proposed $c_{plunging} = 8.68$ and $c_{surging} = 1.4$. Figure 6 shows the data used in Van der Meer (1988) and in Van Gent et al. (2003) for plunging waves, thus using the mean wave period T_m and the original coefficients. Also the original 5% exceedance curve is shown in Figure 6 (dashed). This figure shows that the data used in Van der Meer (1988), i.e. mainly deep-water conditions and single-peaked spectra, and the data used in Van Gent et al. (2003), i.e. including shallow-water conditions and other spectral shapes, lead together to a considerable scatter with the majority of the test results used in Van Gent et al. (2003) on the unsafe side (i.e., the formula leads to a smaller stone diameter than required). Some of the deviations exist for conditions with deep water at the toe of the structures and single-peaked spectra.

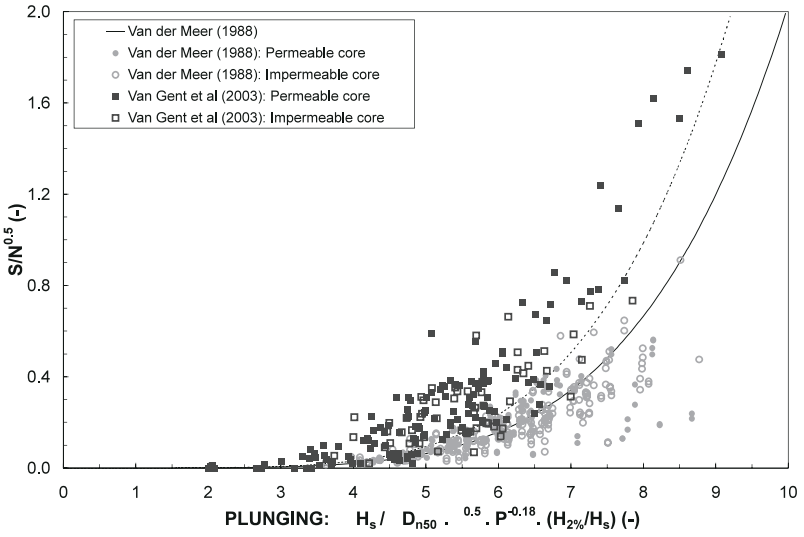

Figure 6: Data compared to formula by Van der Meer (1988) for plunging waves

Based on analysis of the stability of rock slopes for conditions including situations with shallow foreshores, Van Gent et al. (2003) proposed modifying the formulae of Van der Meer (1988) to extend its field of applications. The modified formulae are considered valid for both deep water and shallow water conditions. This concerns the following modifications:

- The spectral wave period $T_{m-1,0}$ instead of the mean wave period from time-domain analysis T_m is used to take the influence of the spectral shape into account;
- The coefficients are re-calibrated to $c_{plunging} = 8.4$ and $c_{surging} = 1.3$;
- The 5% exceedance levels are adapted; this will be discussed later.

The modified stability formulae are:

Plunging conditions ($\xi_{s,-1} < \xi_c$): $$\frac{H_s}{\Delta D_{n50}} = c_{plunging} P^{0.18} \xi_{s,-1}^{-0.5} \left(\frac{H_{2\%}}{H_s} \right)^{-1} \left(\frac{S}{\sqrt{N}} \right)^{1/5} \quad (6)$$

Surging conditions ($\xi_{s,-1} \geq \xi_c$): $$\frac{H_s}{\Delta D_{n50}} = c_{surging} \xi_{s,-1}^{P} P^{-0.13} \tan\alpha^{-0.5} \left(\frac{H_{2\%}}{H_s} \right)^{-1} \left(\frac{S}{\sqrt{N}} \right)^{1/5} \quad (7)$$

in which ξ_c can be obtained from Equation 5 with $c_{plunging} = 8.4$ and $c_{surging} = 1.3$. For slope angles more gentle than $\cot\alpha > 4$ Equation 6 needs to be used, irrespective of whether $\xi_{s,-1}$ is larger than ξ_c (see Equation 5) or not.

In Van Gent (1999, 2001) it was shown that the wave period $T_{m-1,0}$ is the optimal wave period to describe wave run-up and wave overtopping. The results by Smith et al. (2002) and Van Gent et al. (2003) show that this wave period is also the optimal wave period in

Equations 6 and 7. This is consistent with earlier work on the influence of wave energy spectra on processes on coastal structures.

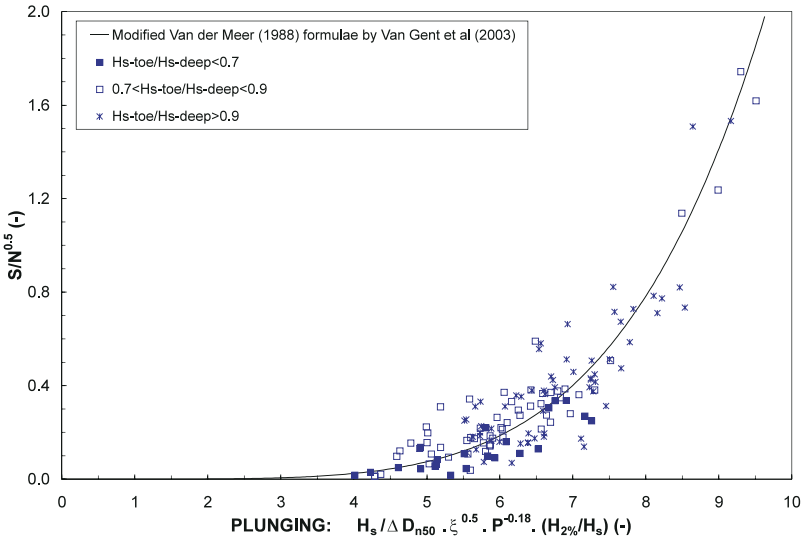

Figure 7: Data from Van Gent et al. (2003) compared to the modified formula by Van der Meer (1988) for plunging waves, for various ranges of the amount of wave breaking on the foreshore

Figure 7 shows the data from Van Gent et al. (2003) for various ranges of the amount of wave breaking on the foreshore. This figure shows that the proposed modifications lead to a formula where the conditions for relatively deep water ($H_{s-toe} / H_{s-deep} > 0.9$), conditions with more wave breaking ($0.7 < H_{s-toe} / H_{s-deep} < 0.9$), and conditions with a considerable amount of wave breaking ($H_{s-toe} / H_{s-deep} < 0.7$), are all described rather well irrespective of the amount of wave breaking.

In the data used by Van der Meer (1988) the values for the $T_{m-1,0}$ are not directly available. An assumption has been made to obtain values for the $T_{m-1,0}$ in the data used by Van der Meer (1988) for which the peak-wave period is available: $T_p = 1.07 * T_{m-1,0}$. This assumption is considered acceptable since almost all tests were performed with single-peaked spectra for which the ratio of these wave periods was likely to be within the range of $1.05 < T_p / T_{m-1,0} < 1.1$. Using this assumption, Figures 8 and 9 show the data compared to the modified formulae of Van der Meer (1988) for "plunging" and "surging" conditions. For "plunging" conditions, mainly for structures with an impermeable core and for a sub-set of data from structures with a permeable core, there are relatively large differences between data by Van der Meer (1988) and the formula for "plunging" conditions. Deviations were also present in Figure 6, nevertheless, it can be seen that the amount of scatter in Figure 8 is smaller than in Figure 6. For "plunging" conditions the damage measured in the tests used by Van der Meer (1988) is on average lower than the prediction based on the formula (i.e. about 7% in wave height). For "surging" conditions this is not the case. The reason for the mentioned differences (as illustrated in Figure 8)

could be caused by differences in wave generation (e.g. active wave absorption, second-order wave generation), model set-up (e.g. placement of stones on the slope, slope of the foreshores, shape of rock material) and analysis procedures (e.g. method of obtaining the values for S from the measured profiles, method of obtaining the incident waves at the toe, etc). The exact contribution of each of these aspects to the observed differences are not known and difficult, if not impossible, to trace exactly, but it is likely that such differences may cause some systematic differences and/or differences in the amount of spreading.

The main trend through the data can be described by using $c_{plunging} = 8.4$ and $c_{surging} = 1.3$ in Equations 6 and 7. The standard deviation of the differences between the measured and predicted values for $S / \sqrt{N}$ is $\sigma = 0.11$, based on data used in Van Gent et al. (2003). This standard deviation depends to some extent also on the type of structure. For structures with a permeable core the formulae are more accurate than for structures with an impermeable core: $\sigma = 0.10$ and $\sigma = 0.13$, respectively. If all data, including the data used by Van der Meer (1988) are taken into account, the above mentioned standard deviations of $\sigma = 0.11$, $\sigma = 0.10$ and $\sigma = 0.13$ become $\sigma = 0.15$, $\sigma = 0.15$ and $\sigma = 0.16$ respectively.

Besides probabilistic approaches using the standard deviation, one may use a more simple approach, not based on formulae that describe the main trend through the data, but on more conservative formulae with a low probability of exceeding the predicted damage. For instance formulae with a confidence level of 95% (i.e., 5% of the data leads to a higher amount of damage and 95% of the data leads to a lower amount of damage). For these formulae with a confidence level of 95% a curve of the shape: $S_{5\%} = S_0 + S'$ has been used. For S_0 the value 2 is used. This damage level corresponds to start of damage and is considered as acceptable for all types of rock slopes. S' is the damage obtained from Equations 6 and 7 in which the coefficients are replaced by $c_{plunging} = 7.25$ and $c_{surging} = 1.05$. In Figures 8 and 9 the curves for $S_{5\%}$ are shown (dashed curves).

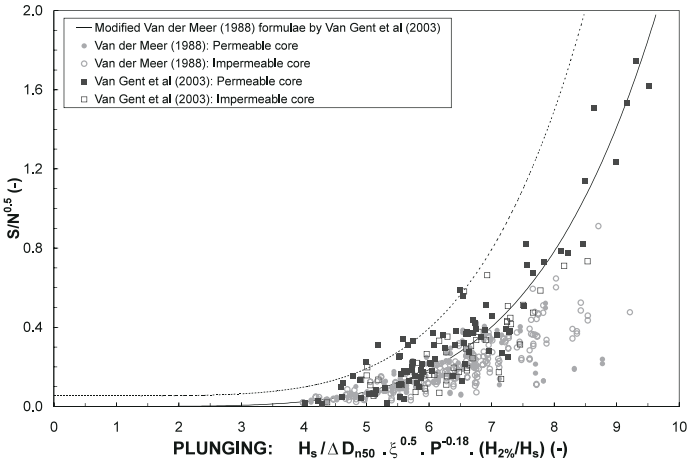

Figure 8: Data compared to modified formula by Van der Meer (1988), as proposed in Van Gent et al. (2003), for plunging waves

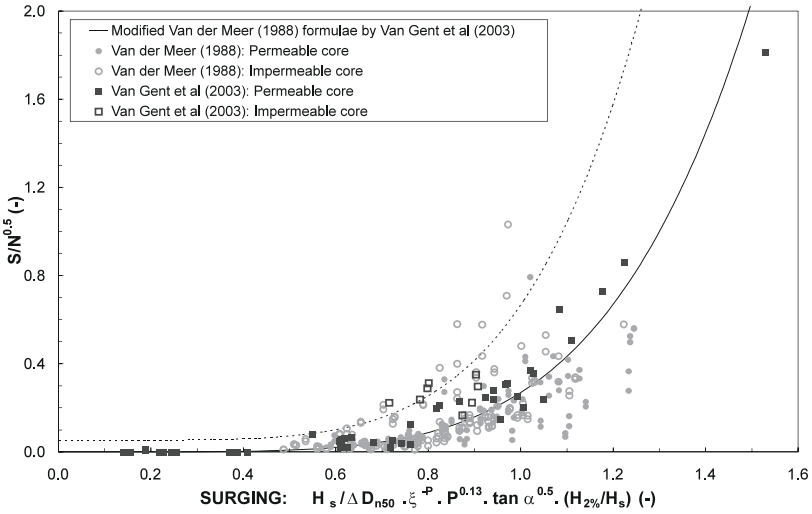

Figure 9: Data compared to modified formula by Van der Meer (1988), as proposed in Van Gent et al. (2003), for surging waves

3.3 Formula from Van Gent et al. (2003)

In Van Gent et al. (2003) a simple stability formula has been described. This stability formula is simpler than Equations 6 and 7 because of the following reasons:

- There is an influence of the wave period but this influence is considered small compared to the amount of scatter in the data due to other reasons. Therefore, the wave period is not used in this formula and there is no separation between "plunging" conditions and "surging" conditions;
- There is an influence of the ratio $H_{2\%} / H_s$ but this influence is considered small. Therefore, this ratio has been omitted;
- The influence of the permeability of the structure is incorporated in a direct way by using a structure parameter, i.e., the diameter of the core material.

The influence of the number of waves (N) is the same as found by Thompson and Shuttler (1975) and Van der Meer (1988). The influence of the parameter $H_s / \Delta D_{n50}$ is the same as found by Van der Meer (1988). The formula reads:

$$\frac{H_s}{\Delta D_{n50}} = 1.75 \cot\alpha^{0.5} \left(1 + D_{n50-core} / D_{n50}\right) \left(\frac{S}{\sqrt{N}}\right)^{1/5} \tag{8}$$

The influence of the permeability of the structure is incorporated by using the ratio between the diameter of the core and the diameter of the armour material: $D_{n50-core} / D_{n50}$. The influence of filters is not accounted for in this ratio.

Figure 10 shows the test results for structures with a permeable core compared to Equation 8. Figure 11 shows all test results, including those obtained with structures with

an impermeable core. It is clear from these figures that Equation 8 is rather accurate for structures with a permeable core but that the deviations are larger for structures with an impermeable core.

The standard deviation of the differences between measured values for $S/\sqrt{N}$ and Equation 8 is $\sigma = 0.11$. For structures with a permeable core the formula is more accurate than for structures with an impermeable core:$\sigma = 0.10$ and $\sigma = 0.12$ respectively (based on data used by Van Gent et al., 2003). The good performance for conditions with deep-water at the toe and for conditions with shallow water at the toe of permeable structures (Figure 10) indicates that the most important effects of shallow-water conditions are taken into account by using the H_s of the incident waves at the toe. This wave height is of course affected by processes on the shallow foreshore. For situations with shallow foreshores it is relatively complicated to obtain accurate values for H_s since it is affected by many processes on the foreshore, including effects of the (offshore) wave period and wave spectrum.

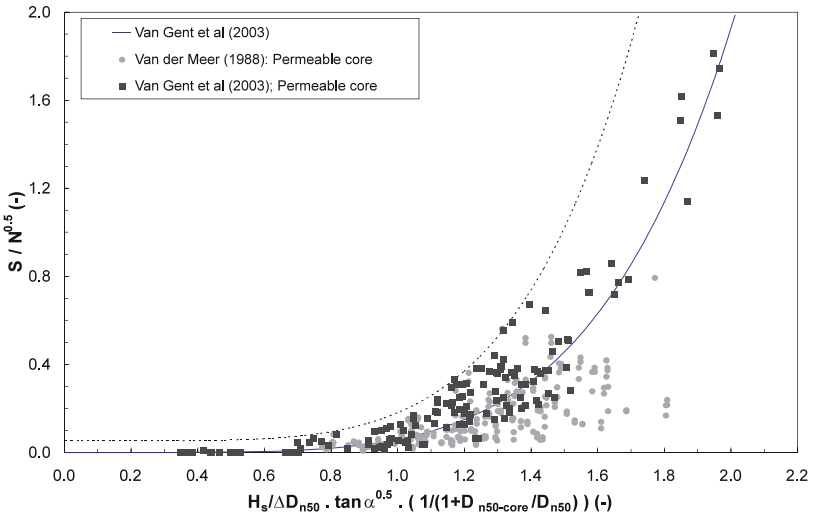

Figure 10: Data compared to the stability formula presented in Van Gent et al. (2003), for structures with a permeable core

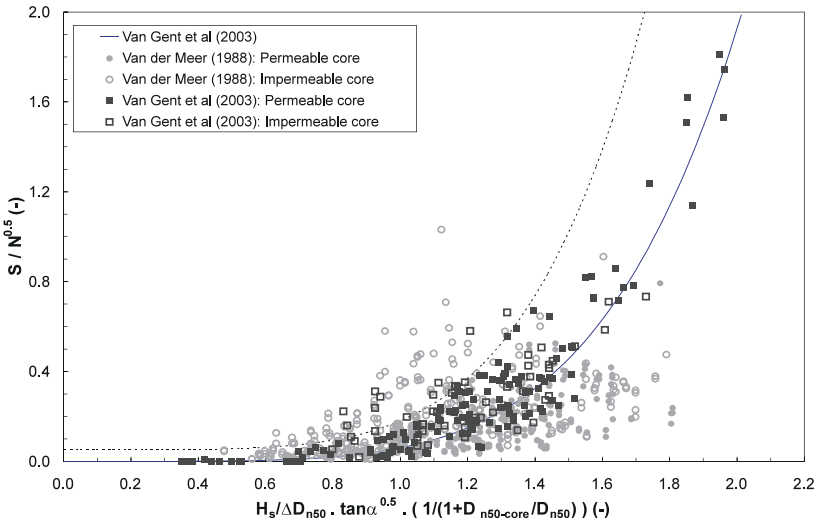

Figure 11: Data compared to the stability formula presented in Van Gent et al. (2003), for structures with a permeable core and structures with an impermeable core

Besides probabilistic approaches using the standard deviation, one may use a more simple approach, not based on the formula describing the main trend through the data, but a more conservative formula with a low probability of exceeding the predicted damage. For instance a formula with a confidence level of 95% (i.e., 5% of the data leads to a higher amount of damage and 95% of the data leads to a lower amount of damage). For these formulae with a confidence level of 95% a curve of the shape: $S_{5\%} = S_0 + S'$ has been used. For S_0 the value 2 is used. S' is the damage obtained from Equation 8 in which the coefficient 1.75 is replaced by 1.47 (based on data used by Van Gent et al., 2003). In Figures 10 and 11 the curves for $S_{5\%}$ are shown (dashed curves). The inclusion of the data by Van der Meer (1988) leads to only 1% of the tests with rock slopes with a permeable core being above this curve, but 20% of the tests with rock slopes with an impermeable core. Therefore, it is recommended using a lower value than 1.47 for structures with an impermeable core, namely 1.2, such that only 5% of all data on rock slopes with an impermeable core is above this curve.

3.4 Comparison of Performance of Stability Formulae

Table 5 provides an overview of standard deviations of differences between measured and predicted damage values for $S / \sqrt{N}$. For each stability formula and structure type two standard deviations are given; the standard deviations in the last column are based on the data used by Van Gent et al. (2003), the standard deviations (σ_{all}) in the last-but-one column are based on these data plus the data used by Van der Meer (1988).

Table 5: Standard deviations for three different stability formulae

Stability formula	Structure type	σ_{all}	σ
Hudson (1953, 1959)	Permeable core	0.5 ($K_D = 6.5$)	0.37 ($K_D = 8$)
Modified Van der Meer (1988)	Permeable core	0.15	0.10
Van Gent et al. (2003)	Permeable core	0.17	0.10
Hudson (1953, 1959)	Impermeable core	0.9 ($K_D = 2$)	0.37 ($K_D = 4$)
Modified Van der Meer (1988)	Impermeable core	0.16	0.13
Van Gent et al. (2003)	Impermeable core	0.18	0.12

The coefficients (K_D, $c_{plunging} = 8.4$, $c_{surging} = 1.3$, and 1.75 in Equation 8) from the three stability formulae are based on the data used by Van Gent et al. (2003). Taking also the data by Van der Meer (1988) into account may lead to different values for the standard deviations if these coefficients were adjusted. This is especially the case for the formula based on Hudson (1953, 1959), i.e. Equation 2. Table 5 shows standard deviations for this formula based on different 'optimal' values for K_D. For the other two stability formulae the standard deviations are not that sensitive to which data set is used for calibration. For instance, the coefficient 1.75 from the formula presented in Van Gent et al. (2003) leads to a standard deviation of $\sigma = 0.17$, based on all data on structures with a permeable core. If the coefficient in this stability formula would have been calibrated on all of these data instead of the data from Van Gent et al. (2003) only, the value would be 1.8, leading to a standard deviation of $\sigma = 0.15$. This difference is considered small. This illustrates that conclusions on the performance of stability formulae cannot be based on small differences between standard deviations. However, Table 5 shows that for the studied data set the predictions of the amount of damage using the formula based on Hudson (1953, 1959) are clearly less accurate than those based on the other two stability formulae. The differences in standard deviations for the modified formulae of Van der Meer (1988), as proposed in Van Gent et al. (2003), and the formula from Van Gent et al. (2003), are rather small; the performance of both stability formulae seems to be similar. This means that especially if no accurate information on the wave period $T_{m-1,0}$ and the ratio $H_{2\%} / H_s$ is available, Equation 8 is a good alternative for Equations 6 and 7.

To illustrate differences between the three stability formulae, Figures 12 and 13 show the predicted amount of damage as a function of $H_s / \Delta D_{n50}$. These examples are for the following conditions: $N = 1000$, $H_{2\%} / H_s = 1.4$, $P = 0.5$, $D_{n50-core} / D_{n50} = 0.25$, $K_D = 8$. Figure 12 shows results for $\cot\alpha = 2$ and Figure 13 is for $\cot\alpha = 6$. For the modified formulae of Van der Meer (1988) two different wave steepnesses are shown: $s_{m-1,0} = 0.02$ and $s_{m-1,0} = 0.04$.

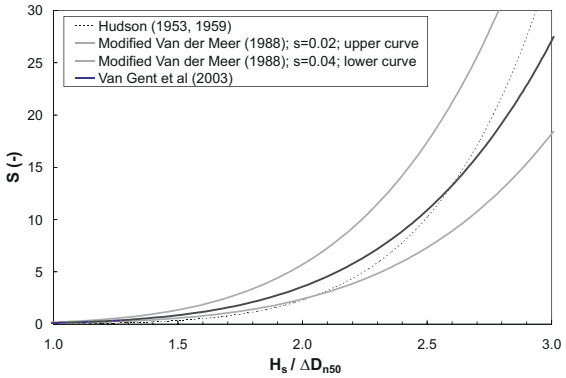

Figure 12: Predicted amount of damage by three different stability formulae; slope 1:2

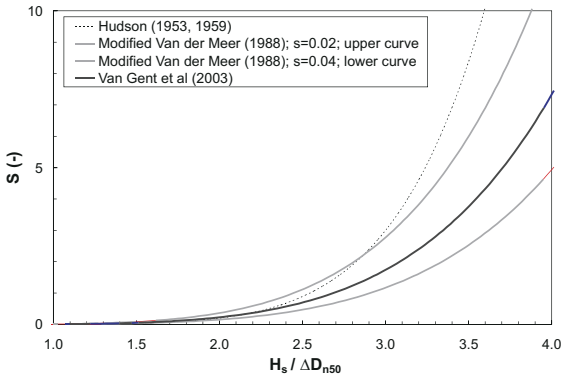

Figure 13: Predicted amount of damage by three different stability formulae; slope 1:6

Figure 12 shows that for the curves based on Hudson (1953, 1959) and Van Gent et al. (2003) are between the two curves (for two different wave steepnesses) based on the modified formula based on Van der Meer (1988). For more gentle slopes the damage predicted using Hudson (1953, 1959) is often higher, especially for higher values of $H_s / \Delta D_{n50}$. In these figures the conditions are all "plunging" conditions, thus Equation 6 is used.

Note that the curves in Figures 12 and 13 are predicted values; thus they do not contain any safety factor and do not take the observed scatter of test results around predictions into account.

4. Conclusions

The described study led to the following conclusions:

- Based on the data set studied here, it can be concluded that the stability formula based on Hudson (1953, 1959), i.e. Equation 2, can be applied for conditions with breaking waves on the foreshore and for conditions without breaking waves on the foreshore. The following values for K_D (i.e. "95% reliability values") are recommended:

  - Structures with an impermeable core: $K_D = 1$;

  - Structures with a permeable core: $K_D = 4$.

  The main trend through the test results can be described by using $K_D = 4$ and $K_D = 8$ respectively, however, with large deviations between the measured and predicted values of $S / \sqrt{N} : s = 0.37$ for both types of structures. More accurate stability formulae are summarised below.

- Based on the data set studied here, it can be concluded that the stability formulae by Van der Meer (1988) are suitable for conditions with deep water at the toe and for conditions with shallow water at the toe, with the modifications proposed by Van Gent et al. (2003), i.e. Equations 6 and 7. The modifications include:

  - using the spectral wave period $T_{m-1,0}$ instead of the mean wave period T_m from time-domain analysis;

  - re-calibrating the coefficients: $c_{plunging} = 8.4$ and $c_{surging} = 1.3$;

  - adapting the 95% reliability level.

  The standard deviations based on differences between measured and predicted values of $S / \sqrt{N}$ that can be used are $s = 0.10$ for rock slopes with a permeable core, and $s = 0.13$ for rock slopes with an impermeable core.

- Based on the data set studied here, it can be concluded that the stability formula described in Van Gent et al. (2003), i.e. Equation 8, is suitable for conditions with deep water at the toe and for conditions with shallow water at the toe.

  The standard deviations based on differences between measured and predicted values of $S / \sqrt{N}$ that can be used are $s = 0.10$ for rock slopes with a permeable core, and $s = 0.12$ for rock slopes with an impermeable core. Taking also the data of Van der Meer (1988) into account shows that this formula is relatively accurate for structures with a permeable core; for structures with an impermeable core there are test results that show relatively large differences. It is recommended to use this stability formula for the design of rock slopes with an impermeable core using an increased safety factor. In contrast to the modified Van der Meer (1988) formulae, i.e. Equations 6 and 7, this formula does not require information on the ratio $H_{2\%}/H_s$ and a wave period. This means that especially if no accurate information on the ratio $H_{2\%} / H_s$ or the wave period $T_{m-1,0}$ is available, Equation 8 is a good alternative for Equations 6 and 7.

For design purposes the deviations from the main trend should be taken into account using standard deviations or by taking the scatter into account in a deterministic way. For

structures with an impermeable core a relatively large amount of test results shows more damage than predicted by the three studied stability formulae. For designing rock slopes with an impermeable core one should take this aspect into account.

In the formulae by Van der Meer (1988) and the modifications to these formulae as proposed by Van Gent et al. (2003) there is a discontinuity close to slope angles of $\cot\alpha = 4$ for specific applications. Users of these formulae should be aware of this non-physical feature in these formulae.

It should be noted that the test conditions used in this paper cover a wide range of conditions, characterised by the ranges given in Table 1 and Table 2, but that the validity of the described empirical stability formulae are limited to these ranges.

The tests on which the performed analysis is based were limited to conditions with about 3000 waves, with some tests with 7500 waves. For practical applications for which the accumulation of damage due to a series of storms is relevant, it is desirable to know what is the dependency of the damage to a series of storms and to a larger numbers of waves. It is recommended to study these aspects, and to take the potential effects into account in the design of rock slopes.

Acknowledgements

Prof. Dr J.W. Kamphuis (Queen's University, Kingston, Canada) is acknowledged for his contribution to the discussion of the topic addressed in this paper. Mr. E.M. Coeveld, Mr. C. Kuiper and Ms. B. Pozueta of Delft Hydraulics are acknowledged for their contributions and reviews of a draft version of this paper.

References

Hudson R.Y. (1953), *Wave forces on breakwaters,* Transactions ASCE 118, pp 653-674, ASCE, New York, USA

Hudson R.Y. (1959), *Laboratory investigations of rubble mound breakwaters*, Proc. ASCE 85 WW 3, ASCE, New York USA

Iribarren Cavanilles, R. (1938), *Una formula para el calculo de los diques de escollera*, M. Bermejillo-Pasajes, Madrid, Spain

Iribarren Cavanilles, R. and C. Nogales y Olano (1953), *Nouvelles conceptions sur les diques a parois verticales et sur les ouvrages a talus,* XVIIIth Int. Navigation Congress, Rome, Italy

Mansard, E. and E. Funke (1980), *The measurement of incident and reflected spectra using a least-square method*, Proc. ICCE'80, ASCE, pp.154-172, Sydney

Rock Manual (1995), *Manual on the use of rock in Hydraulic Engineering*, CUR publication no.169, ISBN 9037600603

Smith, G.M., I. Wallast and M.R.A. van Gent (2002), *Rock slope stability with shallow foreshores*, ASCE, Proc. ICCE 2002, pp. 1524 - 1536

SPM (1973, 1984); *Shore Protection Manual*. Coastal Engineering Research Center. U.S. Army Corps of Engineers

Thompson, D.M. and R.M. Shutter (1975), *Riprap design for wind wave attack. A laboratory study in random waves*. HR Wallingford report EX 707, UK

Van der Meer, J.W. (1988), *Rock slopes and gravel beaches under wave attack*, Ph.D. thesis Delft University of Technology

Van Gent, M.R.A. (1999), *Physical model investigations on coastal structures with shallow foreshores; 2D model tests with single and double-peaked wave energy spectra*, WL | Delft hydraulics Report H3608

Van Gent, M.R.A. (2001), *Wave run-up on dikes with shallow foreshores*, ASCE, Journal of Waterway, Port, Coastal and Ocean Engineering, Vol.127, No.5, Sept/Oct 2001, pp.254-262

Van Gent, M.R.A., A.J. Smale and C. Kuiper (2003), *Stability of rock slopes with shallow foreshores*, ASCE, Proc. Coastal Structures 2003, Portland

INTEGRATED HYDRAULIC-ENVIRONMENTAL MODELLING

J.A. Roelvink
WL | Delft Hydraulics and Delft University of Technology
Delft, The Netherlands

1. Introduction

An increasing pressure on the coastal environment, due to population growth, climate change and sometimes bad management, has led to serious erosion problems and deterioration of water quality and ecological values. Increasingly, coastal managers are aware that single-issue approaches ('let's stop this hotel from falling into the water') often create more problems than they solve, and an integrated approach where the system as a whole is analysed and proposed solutions are evaluated for all their effects is needed.

In terms of modelling, this requires a clear understanding of the individual processes (waves, currents, morphological change, water quality, ecology) and their inter-dependencies. Each of the individual processes act on a range of space and length scales that require typical modelling approaches: for instance, the hydrodynamic schematisation (in time and space) in a water quality model is usually quite different from that in a morphodynamic model.

A typical approach in environmental impact assessments is to consider the 'effect chains' such as from hydrodynamics to water quality to primary production to higher trophic levels, or from hydrodynamics to morphological change to changing physiotopes to changes in species. A good example is the study into the effects of an airport island in the North Sea (www.flyland.nl). In such a study, the model set-up of individual models is governed not only by the physical phenomena that need to be represented with sufficient accuracy, but also by the data need of the 'clients' of each model. With clear definitions of the information stream from each model to the next model(s) such an approach can successfully integrate models and knowledge over various institutes. However, such a model typically assumes a one-way flow of information, from causes to effects. As soon as signficant feedback mechanisms occur, a more closely integrated approach is needed.

There is by now considerable experience in integrated modelling of waves, currents, sediment transport and morphology, to the extent that a merely morphological model is seen by others as mono-disciplinary, physical model. Still, the making of such model systems has brought together tools and skills that before were practiced in separate departments and organisations. Other separations, such as between coastal ('sandy') morphologists and estuarine ('mud') people are being removed as a good morphological model nowadays can handle combinations of sand and mud.

A logical next step is to include, where relevant, feedback-loops between morphological models and other models describing features that are influenced by morphology and themselves have an influence on morphology. First examples of such models include

C. Zimmermann et al. (eds.), Environmentally Friendly Coastal Protection, 93-105.

simple behaviour models of sea grass or salt marsh vegetation, where based on a set of rules considering morphology and hydrodynamics, vegetation maps are updated during a morphological run, and in turn the vegetation affects the resuspension of sediment, thereby stabilising the vegetated areas. Without pretending to represent the actual behaviour of salt marshes in detail, such model additions do give a more complete representation of the functioning of the system as a whole, as well as giving a first indication of the effect of measures on parameters such as salt marsh area.

The scheme below gives an indication of the processes that would be considered in a more or less complete model, where we would distinguish between detailed description of processes on an intra-tidal timescale and, after averaging or upscaling of the relevant parameters, the long-term evolution of the most important features of the system.

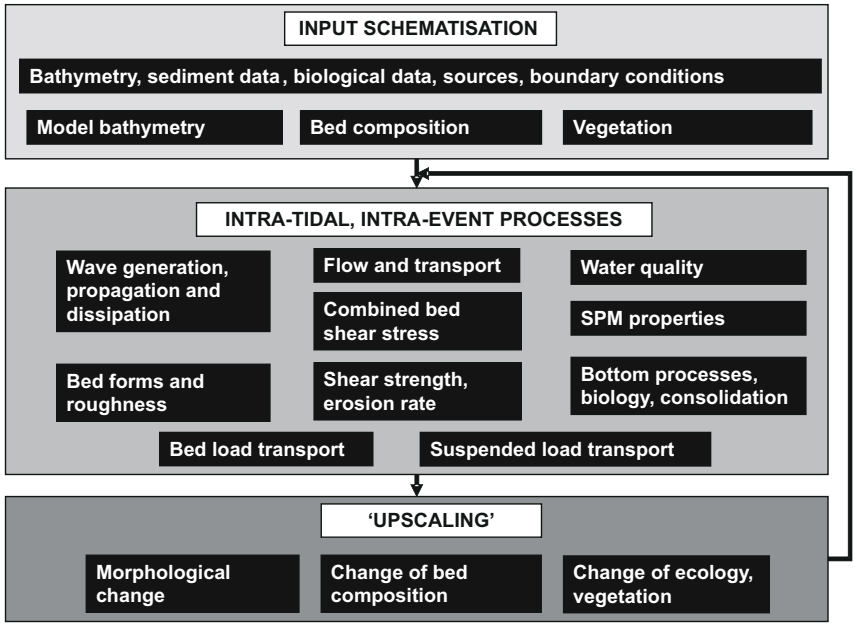

The development of such really integrated models requires a multidisciplinary approach where individual specialists may set up and calibrate their sub-models but at some stage have to let it go and interact with the other models. This puts high demands on the robustness of such sub-models and on their 'communication skills'.

The real challenge, however, will be to get to know and control the overall behaviour of such systems. This is a challenge that will probably keep modellers busy for quite a while.

In this paper we will discuss a number of different strategies of morphological updating, as an important component of integrated modelling.

2. Tide-Averaging Approach

This approach is based on the fact that morphological changes take place on far longer time-scales than changes in the hydrodynamics. Thus, morphological changes within a single tidal cycle are usually very small compared to the trends over a longer period, and such small changes do not affect the hydrodynamics or sediment transport patterns much. It is then acceptable to consider the bottom fixed during the computation of hydrodynamics and sediment transport over a tidal cycle. The rate of change of the bed level is computed from the gradients in the tidally averaged transport.

In the earlier morphological models, this rate of change or Initial Sedimentation and Erosion (ISE) was an end product; it could be applied to assess sedimentation rates in a navigation channel or it could be used to assess large-scale changes to a sediment budget.

In morphodynamic models however, the bed level is updated using some (usually explicit) scheme and fed back into the hydrodynamic and transport models. As the transport pattern now continuously adapts to bed changes, this allows bed patterns to migrate along with the mean transport direction.

In Figure 1 the flow scheme of the tide-averaging approach is shown. Starting from a given bathymetry, the wave-current interaction is solved over a tidal cycle, using the iterative approach as described in Chapter 2. The resulting flow and wave fields are then fed into a transport model, which computes bed load and suspended load transports over the tidal cycle. The averaged result is applied to compute bed changes. The updated bathymetry is looped back to the transport model through the 'continuity correction' (see next paragraph) or to the full hydrodynamics module. The same scheme is often applied to stationary situations, where the hydrodynamics and transport are made to converge at each full morphodynamic loop.

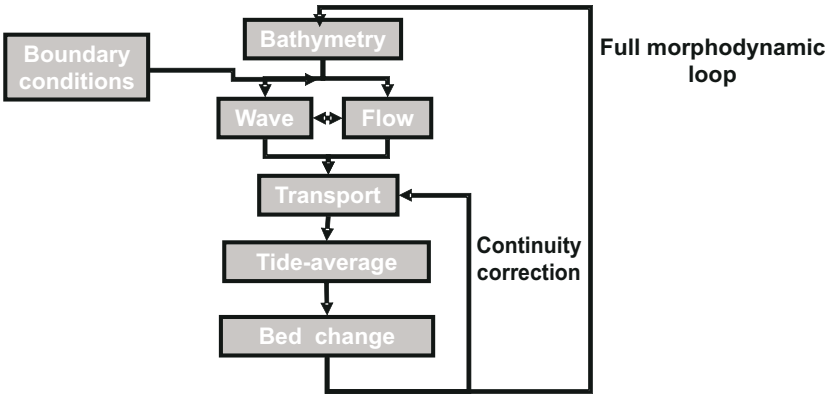

Figure 1: Flow diagram of tide-averaging morphodynamic model setup

The morphological time step is numerically restricted (for explicit schemes) by the bed Courant number:

$$CFL = \frac{c\,\Delta t}{\Delta s} \tag{1}$$

where the bed celerity c can be approximated by:

$$c = \frac{\partial S}{\partial z_b} \approx \frac{bS}{h} \tag{2}$$

Here b is the power of the transport relation, S is the tide-averaged transport in s-direction and h the tide-averaged water depth.

Apart from this numerical restriction the morphological time step is limited by the accuracy of the time-integration method. This can be estimated by the following:

The bed level change over a number n of tidal periods T is equal to:

$$\Delta z_b = \int_0^{nT} \frac{\partial z_b}{\partial t}\,dt = -\int_0^{nT} \left(\vec{\nabla}.\vec{S}\right) dt = -\vec{\nabla}\int_0^{nT} \vec{S}\,dt \tag{3}$$

Here the sediment transport vector changes both with time or phase of the tide and with the varying bed level. We may approximate the variation with bed level by a first-order Taylor expansion:

$$\vec{S}_{t,z_b} = \vec{S}_{t,z_b=0} + \frac{\partial \vec{S}_{t,z_b=0}}{\partial z_b}\Delta z_{b,t} + \mathrm{O}\left(\Delta z_b^2\right) \tag{4}$$

We can now time-integrate the transport vector, using the approximation in equation and assuming an approximately linear increase or decrease of Δz_b per tidal cycle:

$$\begin{aligned}
\Delta z_{b,t+nT} &= -\vec{\nabla}.\int_t^{t+nT}\left(\vec{S}_{\tau,z_b=0} + \frac{\partial \vec{S}_{\tau,z_b=0}}{\partial z_b}.\Delta z_{b,t} + \mathrm{O}\left(\Delta z_b^2\right)\right) d\tau \approx \\
&\approx -nT - \vec{\nabla}.\frac{1}{T}\int_t^{t+T} \vec{S}_{\tau,z_b=0}\,d\tau - \vec{\nabla}.\int_t^{t+nT}\left(\frac{b\vec{S}_{\tau,z_b=0}}{h}\Delta z_{b,t}\right) d\tau + \mathrm{O}\left(\Delta z_b^2\right) \approx \\
&\approx -nT\left(1 + \frac{1}{2}\frac{b\,\Delta z_{b,t+nT}}{h}\right)\vec{\nabla} < \vec{S}_{z_b=0} > + \mathrm{O}\left(\Delta z_b^2\right)
\end{aligned} \tag{5}$$

Here, "< >" denote tide-averaging. Compared to a simple Euler scheme of updating, which will not reproduce the second term between the brackets, we find that the relative error is proportional to the ratio of bottom change over water depth and to the power b in the transport relation.

Because of these limitations on the morphological time step, it is necessary to update the transport regularly. In the next section we discuss the 'continuity correction', a cheap way of doing this in an approximate way.

3. Continuity Correction

The sediment transport field is generally a function of the velocity field and the orbital velocity:

$$\vec{S} = f(\vec{u}, u_{orb}, \ldots) \tag{6}$$

When the bathymetry changes, the flow field and orbital velocity change, and must be recomputed. The "continuity correction" is a frequently applied method to adjust the flow field after small changes in the bathymetry. The flow *pattern* is assumed not to vary for small bottom changes, and therefore the local flow rate q can be assumed to be constant:

$$\vec{q} \neq f(t_{mor}) \tag{7}$$

where t_{mor} is the morphological time,

$$\vec{q} = h\vec{u} \tag{8}$$

is the flow rate vector and h is the water depth. Similarly, the wave pattern: wave height, period and direction are kept constant, and only the orbital velocity is adapted for the local water depth:

$$H_{rms}, T_p \neq f(t_{mor}) \tag{9}$$

Since :

$$\vec{u} = \frac{\vec{q}}{h} \tag{10}$$

and :

$$u_{orb} = f(H_{rms}, T_p, h) \tag{11}$$

Adaptation of the sediment transport field is now simply a matter of adjusting the velocity and orbital velocity and recomputing the sediment transport using eq. (6).

In case of a tidal flow situation, a number of velocity and wave fields based on the original bathymetry are stored, and when the depth changes, the adapted transport field is computed for a number of time points in the tidal cycle and subsequently averaged. This averaged transport field is then used in the sediment balance.

The method still requires full transport computations through the tidal cycle, which can be time-consuming when suspended-load transport is to be accounted for. The morphological time step is often dominated by some shallow grid cells, which are usually not of interest. This means that typically after some 5-20 continuity correction steps, the full hydrodynamic model has to be run on the updated bathymetry.

The main limitation to the continuity correction is the assumption that the flow rate and pattern remains constant in time. In the case of a shallow area becoming shallower, the flow velocity will keep increasing under continuity correction, whereas in reality the flow will increasingly go around the shallow area.

4. RAM Approach

In practical consultancy projects there is often a need to interpret the outcome of initial transport computations without having to resort to full morphodynamic simulations. One way of doing this is looking at initial sedimentation/erosion rates, but this method is flawed in many respects. Initial disturbances of the bathymetry lead to a very scattered pattern, and, as De Vriend et al. (1993) point out, sedimentation/erosion patterns tend to migrate in the direction of transport, a behaviour which is not represented in the initial sedimentation/erosion patterns.

The Delft3D-RAM module (Rapid Assessment of Morphology) is a simple method that overcomes these disadvantages (Roelvink et al., 1998, 2001). If we assume that for small bed level changes the overall flow and wave patterns do not change (an assumption also used in the "continuity correction" of many morphological models), the tide-averaged transport rates are a function of flow and wave patterns which do not vary on the morphological time-scale, and the local depth, which does vary on this time-scale. In other words: given a certain set of currents and waves, the transport at a given location is only a function of the water depth.

If we can now approximate this function by some simple expression with coefficients which vary from place to place, we end up with a very simple set of two equations: the sediment balance which expresses bottom change in terms of sediment transport gradients:

$$\frac{\partial z_b}{\partial t} + \frac{\partial S_x}{\partial x} + \frac{\partial S_y}{\partial y} = 0 \tag{12}$$

where z_b is the bed level and S_x, S_y are the sediment transport components, and:

$$\vec{S} = \frac{\vec{S}_{t=0}}{\left|\vec{S}_{t=0}\right|} f(z_b) \tag{13}$$

This equation describes the response of sediment transport to bottom changes. The form of the function $f(z)$ can be estimated by considering that transport usually is proportional to the velocity to a power b:

$$\left|\vec{S}\right| \propto |u|^b \propto \left\{\frac{|\vec{q}|}{h}\right\}^b \propto |\vec{q}|^b h^{-b} \tag{14}$$

where $\vec{q}$ is the discharge per unit width. Since a similar relationship with the orbital velocity can be assumed, a suitable function is:

$$\left|\vec{S}\right| = A(x,y)\, h^{-b(x,y)} \tag{15}$$

where the water depth h is taken as $h = HW - z_b$ and HW is the high water level, which ensures that water depth is always positive.

As a further simplification b is assumed constant throughout the field. In this case, the value of A in each point can be derived directly from the local water depth and the initial transport rate, which may be computed using a sophisticated transport model.

The combination of equations and can be solved using the same bottom update scheme as in the full morphodynamic model and requires very little computational effort (in the order of minutes on a PC).

In dynamic areas, such as estuaries and outer deltas, the RAM method may still work well enough to be applied as a quick updating scheme. As soon as bottom changes become too large, a full simulation of the hydrodynamics and sediment transport is carried out for a number of input conditions. A weighted average sediment transport field is then determined, which is the basis for the next RAM computation over, say, a year of morphological time. The updated bathymetry is then fed back into the detailed hydrodynamic and transport model. An important point is that the (costly) computations to update wave, flow and transport fields can be carried out in parallel, using different processors. The simplified updating scheme and the parallel computation for various input conditions together lead to a reduction in simulation time in the order of a factor of 20. The flow diagram of this scheme is depicted in Figure 2.

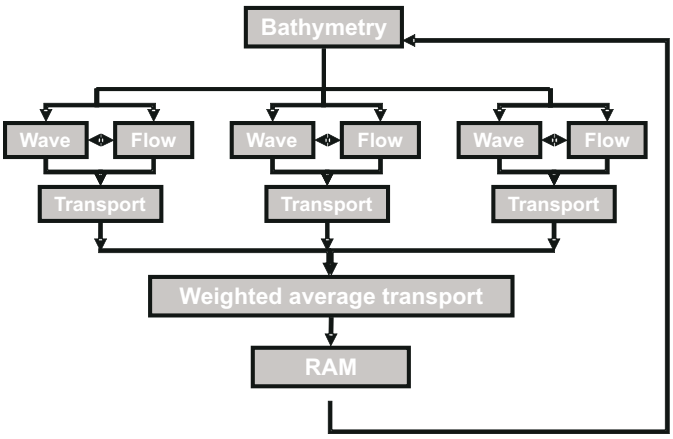

Figure 2: Flow diagram of RAM approach

5. Online Approach with Morphological Factor

The methods above have in common that the morphology is updated relatively infrequently compared to the number of flow time steps per tidal cycle (typically with less than one minute time steps) and the number of transport time steps per cycle (typically more than 20).

A completely different approach is to run flow, sediment transport and bottom updating all at the same small time steps. In case an advection-diffusion scheme is solved for the sediment transport this has to be done with comparable time steps as the flow solver anyway. The updating of the bottom only takes very little computation time. However, this brute force' method does not take into consideration the difference in time scales between the flow and morphology. Therefore a simple device is used, called the

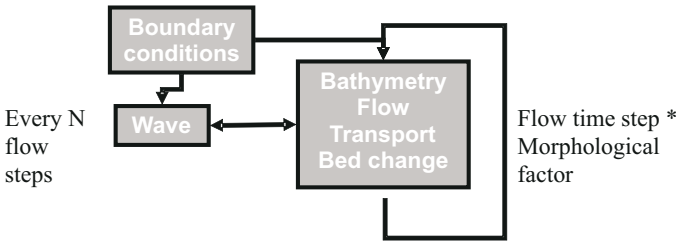

'morphological factor'. This factor *n* simply increases the depth change rates by a constant factor, so that after a simulation over one tidal cycle we have in fact modelled the morphological changes over *n* cycles. This is similar to the concept of the 'elongated tide' proposed by Latteux (1995). The idea is that nothing irreversible happens within an ebb or flood phase, even when all changes are multiplied by the factor *n*. The results obviously have to be evaluated after a whole number of tidal cycles.

Figure 3: Flow diagram of 'online' morphodynamic model setup

An important difference from the previous methods is that the bottom evolution is computed in much smaller time steps, even when relatively large values of *n* are used. If we use an *n* of 60, this means that after completing 12 tidal cycles we have covered approximately one year of morphological change. In a typical flow model we would apply a time step of 1 minute; even with this high morphological factor this means we still update the bathymetry every hour. In comparison, using a tide-averaging approach we would only need to take steps of a month in order to cover the same time period while calculating through the same number of tidal cycles. Even when applying 10 continuity steps in between each full morphological step this still means a 3-day time step; which then takes 10 times as many transport computations.

We can analyse the error made using this approach by time-integrating the transport vector multiplied by *n* as follows:

$$\Delta z_{b,t+nT} = -\vec{\nabla}.\int_{t}^{t+nT}\left(\vec{S}_{\tau,z_b=0}+\frac{\partial \vec{S}_{\tau,z_b=0}}{\partial z_b}.\Delta z_{b,t}+\mathrm{O}\left(\Delta z_b^2\right)\right)d\tau \approx$$

$$\approx -nT-\vec{\nabla}.\frac{1}{T}\int_{t}^{t+T}\vec{S}_{\tau,z_b=0}d\tau-\vec{\nabla}.\int_{t}^{t+nT}\left(\frac{b\vec{S}_{\tau,z_b=0}}{h}\Delta z_{b,t}\right)d\tau+\mathrm{O}\left(\Delta z_b^2\right)\approx \tag{16}$$

$$\approx -nT\left(1+\frac{1}{2}\frac{bn\,\Delta z_{b,t+nT}}{h}\right)\vec{\nabla}<\vec{S}_{z_b=0}>+\mathrm{O}\left(\Delta z_b^2\right)$$

Compared to the expression in equation we see that in the online approach with morphological factor, the second term between the brackets is not neglected as in the tide-averaging approach, but approximated by:

$$n\,\Delta z_{b,t+T} \approx \Delta z_{b,t+nT} \tag{17}$$

Tide-averaged approach vs. morphological factor

In order to make an objective comparison between the various methods we have devised a simple test case. Let us consider a tidal channel that is gradually widening over a typical length scale L. The flow diverges during flood (positive direction) and converges during ebb tide. A mean discharge is added. The transport gradient can then be approximated by the transport itself divided by a length scale L, so:

$$\frac{\partial z_b}{\partial t} = -\frac{\partial S_x}{\partial x} \approx -\frac{S_x}{L} \tag{18}$$

Let us now assume that the discharge per unit width through the channel has a mean component $\overline{q}$ and an oscillatory component at the M2 frequency, $\tilde{q}$. This discharge is not sensitive to the depth h, until the depth becomes so shallow that the flow chooses another channel and the discharge goes to zero. This effect is added by means of a smooth tapering function; the discharge including all effects is now described by:

$$q = \left(\overline{q} + \tilde{q}\cos(\omega t)\right).\left(1 - \exp\left(-\left(\frac{h}{h_{sh}}\right)^2\right)\right) \tag{19}$$

where h_{sh} is a depth scale that governs the tapering of the discharge to zero. We assume that the transport rate S_x is a simple function of the velocity and thus:

$$S_x = a\left(|u|\right)^{b-1}u = a\left(\left|\frac{q}{h}\right|\right)^{b-1}\frac{q}{h} \tag{20}$$

where u is the flow velocity, b the power in the transport formulation and a the transport scaling coefficient.

With this simple set of formulas, we can now test the various time integration schemes. We have done this by integrating equation numerically for each of the schemes. We have used the same factor n for the time step in the averaging approach (multiplied by the tidal period) and for the morphological factor; the value chosen in the example is $n = 70$. The intra-tide transport time step was equal to $T / 50$, which is approx. 15 minutes.

Figure 4 shows the evolution of the bed level in time. It is clear that with the ‘brute force’ integration, viz. the online approach with a morphological factor of 1, the intra-tidal bed changes are very small. The resulting bed change curve appears to be smooth. As the water depth decreases in the example, the transports increase and the rate of bed level change increases rapidly; as the depth becomes very shallow the tapering function starts to work and gradually nudges the water depth towards zero.

As long as the bed level change is small, both approximate methods do a reasonable job of following the ‘brute force’ line. The ‘morphological factor’ method wanders off within each (elongated) cycle, but returns very close to the correct value after each full tidal cycle. As the transport is updated much more frequently than in the case of the ’tide-averaging’ approach, this method is capable of following the curve even when the water depth becomes very shallow; it is also sensitive to the tapering of the transport for shallow depths. On the other hand, the ‘tide-averaging’ approach in this case misses the shallow part completely and shoots through the surface.

We can improve the 'tide-averaging' results without (in a realistic case) adding too much computational effort by using intermediate 'continuity correction' steps. If we keep the number of tidal cycles that we compute in a year constant (equal to 700/70 = 10) and use 10 continuity steps in between, we get the result as in Figure 5.

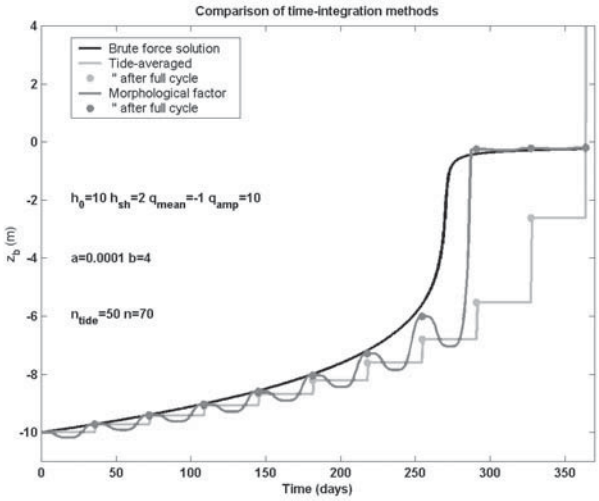

Figure 4: Comparison of time-integration methods: morphological factor vs. tide-averaged, equal number of tidal cycles

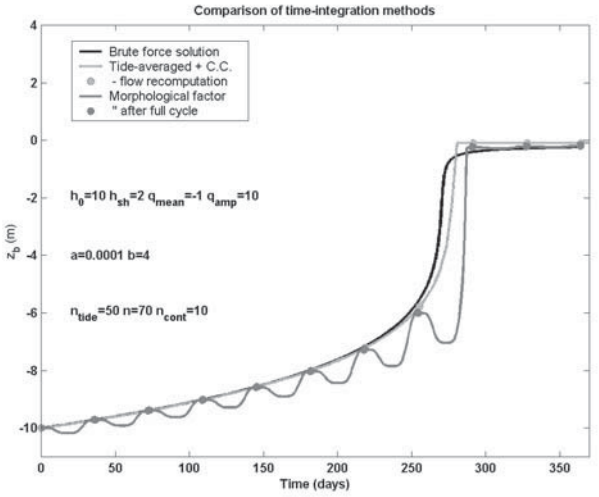

Figure 5: Comparison of time-integration methods, morphological factor vs. tide-averaging + continuity correction

6. Practical Examples

6.1 Humber Estuary and Western Scheldt

As part of the Humber Estuary Shoreline Management Plan – phase 2 a morphological study was carried out involving model runs over periods from one to 10 years (van Ormondt and Roelvink, 2004). The 'morphological factor' approach was applied and test runs were carried out to investigate the effect of the morphological factor on the predicted sedimentation and erosion. In Figs. 6 and 7 below, the results are shown for the predicted bed evolution in the inner estuary over one year, using a factor of 60 and 12, respectively. Although some small deviations occur, mainly in very shallow water, the overall picture is very similar. As the Humber inner estuary is extremely dynamic, it can be expected that even higher morphological factors can be used in less dynamic systems. An example of such a (somewhat) less dynamic system is the Western Scheldt, where in a recent study (van der Kaaij et al., 2004) it was found that comparison between simulations with a factor 24 and 120 showed no significant difference. The resulting sedimentation/erosion patterns over a 1 year simulation are shown in Figures 8 and 9, respectively.

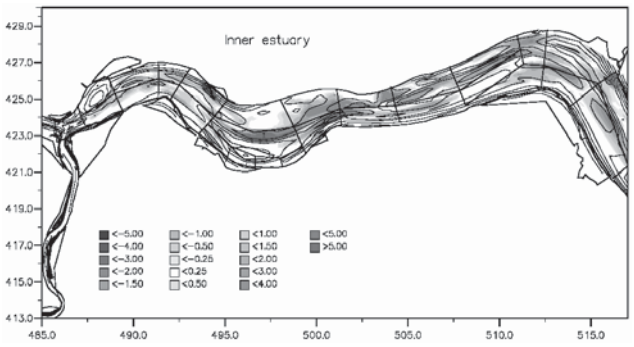

Figure 6: Morphological model of the Humber Estuary, simulated development 1997-1998 - sensitivity test with a morphological factor equal to 60

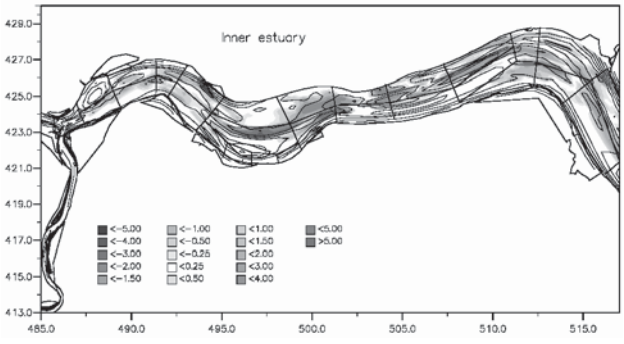

Figure 7: Morphological model of the Humber Estuary, simulated development 1997-1998 - sensitivity test with a morphological factor equal to 12

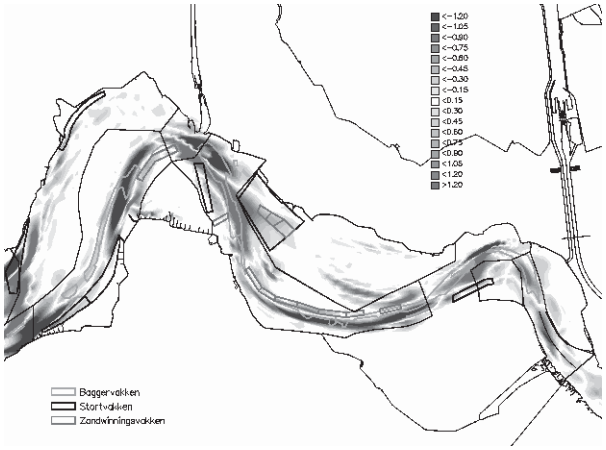

Figure 8: Western Scheldt morphological model; sedimentation/erosion 2000-2001, morphological tide, with a morphological factor equal to 24

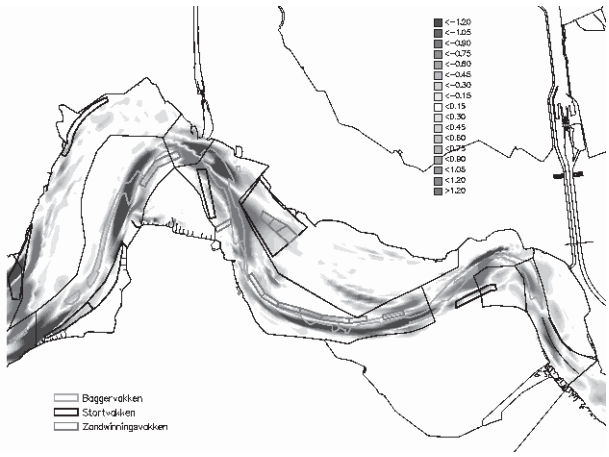

Figure 9: Western Scheldt morphological model; sedimentation/erosion 2000-2001, morphological tide, with a morphological factor equal to 120

7. Conclusions

Various strategies of morphodynamic updating have been discussed and reviewed and a simple test algorithm has been developed to compare the different methods. From a numerical point of view, the 'morphological factor' method has proven to be much more stable than the other updating methods, as the frequency of bed updating is much higher. This method is also relatively simple to implement as it allows a coupling of all processes at the flow time step level.

For very long simulations involving a large variety of input conditions, the RAM approach where many transport simulations for different conditions can be carried out in parallel, is a good alternative.

Acknowledgements

This work was carried out in the framework of the 'Estuary Processes' (EstProc) project funded by the UK DEFRA.

References

Latteux, B., 1995: Techniques for long-term morphological simulation under tidal action. *Marine Geology,* 126 (1995) 129-141

Roelvink, Dano, Alain Boutmy and Jean-Marie Stam. A simple method to predict long-term morphological changes. Proc. 26th Int. Conf. on Coastal Engineering, Copenhagen, 1998, ASCE, New York, pp. 3224-3237

Roelvink, J.A., Jeuken, M.C.J.L., van Holland, G., Aarninkhof, S.G.L. and Stam, J.M.T., Long-term, process-based modelling of complex areas. Proceedings 4th Coastal Dynamics Conference, Lund, Sweden

Van der Kaaij, Theo, Dano Roelvink and Kees Kuijper (2004). Morphological modelling of the Western Scheldt, intermediate report phase 2, Morphological model setup and calibration. Delft Hydraulics report Z3648

Van Ormondt, Maarten and Dano Roelvink (2004). Humber morphological model, Delft Hydraulics report Z3451

Vriend, H.J. de, Zyserman, J., Nicholson, J, Roelvink, J.A., Pechon, P., and Southgate, H.N. Medium-term 2DH coastal area modelling. *Coastal Engineering,* 21 (1993) pp. 193-224

INTERACTION OF WAVES AND REEF BREAKWATERS

Valeri Penchev
Coastal Hydraulics Division, Bulgarian Ship Hydrodynamics Centre
Varna, Bulgaria

Abstract

Reef breakwaters can provide shoreline protection with low environmental impact. They offer a sensitive engineering solution where a competent economical and functional design method needs the knowledge of relationships linking basic parameters such as freeboard, crest width, wave transmission and set-up behind the structure.

This paper aims to contribute to existing knowledge on hydrodynamic interaction of waves and submerged breakwaters, emphasizing results obtained by laboratory hydraulic model tests. Comparison of test data for various submerged structures versus existing design formulae, and available numerical models, is discussed in this paper. Results presented refer to: wave transmission; wave breaking; wave set-up; bed shear velocity; littoral currents and sediment transport. Conclusions on the application of various methods for studying and design of reef breakwaters are presented. Recommendations for further physical and numerical studies are proposed.

1. Introduction

Nowadays there is a strong negative public reaction to rock emplacement along the coast. This has led to uncertainty by decision-makers, regulators and local government authorities about how to treat shoreline erosion. One possible approach is the "planned retreat" where houses are simply removed and the coast is left to erode. However, planned retreat can be expensive, unnecessary and sometimes impossible, especially in highly modified environments. Reef breakwaters employed in conjunction with beach nourishment can provide an alternative shoreline protection solution with low environmental impact.

Reef breakwaters are permanently submerged breakwaters most often constructed as rubble mound structures (Fig.1). Alternative solutions, using special shaped blocks, reef balls, geotubes, and other are also successfully applied to create artificial reefs and submerged sills. A distinction between low-crested structures, reef breakwaters, and submerged sills can be made by noting their effects on waves and sediment transport. Breakwaters act to reduce waves; submerged sills act as barriers to shore-normal sediment motion. The primary characteristic that determine how a structure is classified is the structure's crest elevation. Low-crested structures have elevations high enough to significantly reduce the height of waves transmitted over them, while the effect of submerged sills on waves is relatively small because their crest elevations are significantly below the water level. The crests of low-crested structures may be exposed at low tide, or submerged at high water level. Reef breakwaters / artificial reefs are always submerged.

C. Zimmermann et al. (eds.), Environmentally Friendly Coastal Protection, 107-127.

The purpose of reef breakwaters is to reduce the hydraulic loading to a required level that maintains the dynamic equilibrium of the shoreline. The reef enhances wave breaking, and reduces wave action on the shore, providing shoreline stability, restricting coastal erosion, preserving existing or artificially nourished beaches. Reef breakwaters can provide water flow circulation (and thus avoid stagnant zones) by allowing currents to pass over their crest and between the reef and the shoreline.

Reef breakwaters are frequently employed in conjunction with beach nourishment. Most often they are used when:

- erosion control is needed in sensitive areas;
- a partial blockage to sand is required;
- hard-rock construction on the beach is not wanted or not suitable;
- natural character is to be preserved, or;
- improved recreational and environmental amenity values are required.

Owing to aesthetic requirements, low freeboards are usually preferred (freeboard below SWL). However, in tidal environments and when frequent storm surges occur these become less effective if designed as narrow-crested structures (Pilarczyk, 2003). This is also the reason why broad-crested submerged breakwaters (also called artificial reefs) became popular. However, broad-crested structures are much more expensive than narrow-crested ones and their use should be supported by proper cost-benefit studies.

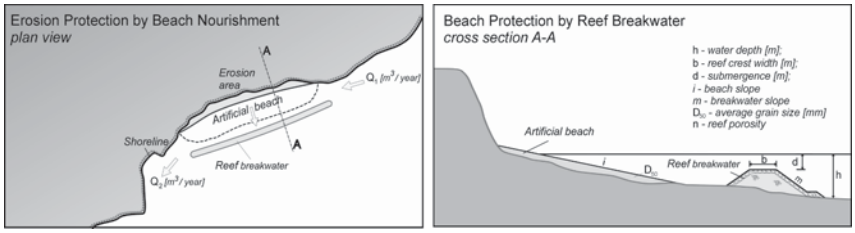

a) b)

Figure 1: Example sketch of application of reef breakwaters; a) plan view; b) cross-section

Offshore, submerged reefs respond to the growing demand for environmental-friendly solutions to coastal protection. They can achieve this by unifying coastal protection, environmental effect, and aesthetic advantages into a multi-faceted structure. Thus, they are needed because other coastal protection solutions do not offer the same overall value to the community.

However, it is worth noting that submerged breakwaters in general, may have serious disadvantages, with the most significant as follows:

- The low sill structure may not be high enough to significantly reduce wave action and may not reduce offshore losses (especially at tidal coasts);
- They may prevent beach recovery during beach-building wave conditions;
- Wave-pumping effect may increase long-shore currents and the shoreline erosion instead of reducing it;
- The placement of reef could create zones with high velocities (especially at the edges), and provoke scour;
- Submerged structures may pose a hazard to coastal navigation;

- The reef may be difficult to inspect since it is underwater;
- It may be difficult and expensive to build the reef because it is both offshore and submerged. Construction may require a floating plant and thus may be expensive.

Although both physical and numerical investigations have been performed, there has not been much experience with reefs/perched beaches; therefore, there are not much data upon which to base the functional design, and no reliable procedures are yet established. The roles played by structure permeability, crest width and water depth have not been fully clarified. Breaking wave processes are basically "qualitatively" understood and numerical models are crude.

2. Wave Transmission - Design Formulae

Reef breakwaters provide a sensitive engineering solution targeted to maintains the dynamic equilibrium of the shoreline. Improper design of reefs may provoke negative impacts, as presented above. For these reasons, a competent economical and functional design method requires the knowledge of relationships linking wave transmission and set-up behind the structure with freeboard, crest width, structure permeability, and other reef parameters. However, the roles played by these parameters have not been fully clarified.

Regarding wave transmission, a number of empirical formulae have been proposed. These formulae derive from data collected from different laboratories where is not certain that the same analysis procedures have been employed. Design formulae have indicated a variety of important variables associated with wave transmission over submerged breakwaters. The most important physical variables that reflect transmission coefficient $K_t = H_t / H_i$ have been identified as:

b - crest width of breakwater
d - freeboard
h - water depth (in front of the structure)
m - front slope (or other parameter for the shape) of the breakwater
n - permeability (or other parameter for permeability)
D_{50} - nominal material diameter of the cover layer
H_i - incident wave height (H_{si} or H_{moi})
L - wave length at local depth (or T_p - peak period)

Ahrens (1987) presented an empirical formula for submerged breakwaters, where most of the above parameters are included:

$$K_t = 1,0 \Big/ \left\{ 1,0 + \left(1 - \frac{d}{h} \right)^{1.188} \left(\frac{F}{h.L} \right)^{0.261} .\exp\left[0,529 \left(-\frac{d}{H_{si}} \right) + 0,00551 \left(\frac{F^{3/2}}{{D_{50}}^2 .L} \right) \right] \right\} \qquad (1)$$

where F - reef cross-section area. The formula is valid for a relative freeboard (submergence versus incident wave height) $d / H_{si} < 1$.

Van der Meer (1990) analyzed hydraulic model tests by Seelig (1980), Powell and Allsop (1985), Daemrich and Kahle (1985), Ahrens (1987), Van Der Meer (1988). A simple prediction formula has been derived where the transmission coefficient, K_t, decreases linearly with the relative freeboard, d / H_{si}:

$$K_t = 0,46 - 0,3\frac{d}{H_{si}} \tag{2}$$

K_t is limited between 0,8 and 0,1, respectively for $d / H_{si} < -1,13$, and $d / H_{si} > 1,2$. The formula does not directly take into account the effects of crest width, front slope, wave length, surface friction; therefore its application refers to some quite limited conditions.

A similar approach was used by Daemen (1991) who derived an empirical formula from data sets provided by various authors. The author introduced a different dimensionless freeboard including the size of the armour layer:

$$K_t = A\frac{d}{b} + B \tag{3}$$

where the angular coefficient A, is expressed as:

$$A = 0,031\frac{H_{si}}{D_{50}} - 0,24 \tag{3.a}$$

B represents the transmission coefficient for no freeboard structures ($d = 0$); and depends on relative wave height H_{si} / D_{50}, crest width b, and incident peak wave period, T_{pi}:

$$B = 5,24\lambda + 0,0323\frac{H_{si}}{D_{50}} - 0,0017\left(\frac{b}{D_{50}}\right)^{1.84} + 0,51 \tag{3.b}$$

where $\lambda = 2\pi H_{si} / gT_{pi}{}^2$ represents the wave steepness. The wave transmission coefficient is assumed to be not greater than 0,75 and not less than 0,075; the limits of the formula are: $1 < H_{si} / D_{50} < 6$, and $0,01 < \lambda < 0,05$.

Another wave transmission formula for emergent and submerged structures with relative crest submergence in the range $(-2,5 < d / H_{si} < 2,5)$ has been presented by d'Angremond, Van der Meer and de Jong (1996) based on experimental data analysis:

$$K_t = -0,4\left(\frac{d}{H_{si}}\right) + \left(\frac{b}{H_{si}}\right)^{-0,31}\left[1,0 - \exp(-0,5\xi)\right]c \tag{4}$$

$$\text{where: } \xi = \tan\alpha \Big/ \left[\frac{2\pi H_{si}}{gT_p{}^2}\right]^{0,5} \tag{4.a}$$

is the Iribarren parameter and c is a coefficient, $c = 0,8$ for impermeable structures, $c = 0,64$ for permeable ones.

Seabrook and Hall (1998) proposed for submerged breakwaters the following equation, gained on the basis of physical model tests using various freeboard, crest widths, water depths and incident wave conditions:

$$K_t = 1 - \left[\exp\left\{(-0,65)\left(\frac{d}{H_{si}}\right) - 1,09\left(\frac{H_{si}}{b}\right)\right\} + 0,047\left(\frac{b.d}{L.D_{50}}\right) - 0,067\left(\frac{d.H_{si}}{b.D_{50}}\right)\right] \tag{5}$$

The authors recommended application of the above formula within the ranges of:

$0 \le (b.d) / (L.D_{50}) \le 7,08$, and $0 \le (dH_{si}) / (bD_{50}) \le 2,14$.

Several new formulae have been suggested recently. Bleck and Oumeraci, (2002) investigated wave transmission over a submerged sill with rectangular cross section. Defining the most critical parameter d / H_{si} as "shallow water non linearity parameter", they proposed the following relationship for the wave transmission coefficient:

$$K_t = 1,0 - 0,83.\exp\left(-0,72\frac{d}{H_{si}}\right) \tag{6}$$

Friebel and Harris, (2003) developed a new empirical model as the "best fit" model from test data sets provided by Seelig (1980), Daemrich and Kahle (1985), Van der Meer (1988), Daemen (1991), Seabrook (1997). The study of Friebel and Harris confirmed that the transmission coefficient is highly dependent on the non dimensional freeboard parameter (d / H_{si}). Other non-dimensional variables in the formula of Friebel & Harris are relative crest width (b / L or b / h), relative structure emergence above seabed ($1 - d / h$), as well as freeboard to crest width parameter (d / b). The proposed formula is:

$$K_t = -0,4969\exp\left(\frac{d}{H_{si}}\right) - 0,0292\left(\frac{b}{h}\right) - 0,4257\left(1-\frac{d}{h}\right) - 0,0696.\log\left(\frac{b}{L}\right) + \\ +0,1359\left(\frac{d}{b}\right) + 1,0905 \tag{7}$$

Another prediction formula was developed using statistical analysis methods (Siladharma & Hall, 2003) based on a 3-D experimental study on wave transmission over submerged breakwaters carried out at Queen's University, Kingston, Canada (in order to compare with 2-D experimental data, the diffraction term of the formula is excluded):

$$K_t = -0,869\exp\left(-\frac{d}{H_{si}}\right) + 1,049.\exp\left(-0,003\frac{b}{H_{si}}\right) - 0,026\frac{H_{si}}{b}.\frac{d}{D_{50}} - 0,005\frac{b^2}{L.D_{50}} \tag{8}$$

One can see in Eq. (8) that the relative freeboard d / H_{si} is again the leading parameter. Other parameters included are the relative crest width b / H_{si}, the surface friction (roughness) parameter d / D_{50}, as well as the "internal flow parameter" $b^2 / (L.D_{50})$ taking in account for the wave length.

A modified version of the Daemen's formula, Eq.(3), combined with some parameters used in the formula of d'Angremond at all, Eq.(6) for shallow waters was suggested by Calabrese, Vicinanza and Buccino (2003), based on experimental test done in "Grosse Wellen Kanal", Hanover, Germany. Large-scale experimental data have been analyzed and following functional relationship for parameters A and B as defined in Eq.(3) was set:

$$A = \beta\exp\left(0,2568\frac{b}{H_{si}}\right); B = \alpha\exp\left(-0,0845-\frac{b}{H_{si}}\right) \tag{9}$$

where

$$\alpha = 1 - 0,562\exp(-0,0507\xi); \beta = 0,6957\frac{H_{si}}{h} - 0,7021 \quad (9.a)$$

For the intercept B, an exponential formula was suggested instead of the power function in Eq.(3). The angular coefficient A, is expressed as a function of the relative crest width, b / H_{moi} . The influence of the water depth at the structure is included in the scale parameter β; Calibration ranges of Eq.(9) are: $-0,4 \le d / b \le 0,3$; $1,06 \le b / H_{moi} \le 8,13$; $0,31 \le H_{moi} / h \le 0,61$; $3 \le \xi \le 5,20$.

Research results on wave transmission formulae are presented also by Sawaragi at all (1989), Kawai at all. (1996), Pilarczyk (2003), and other authors. Data from field measurements of wave transmission over submerged broad-crested reefs can be found in papers of Hamaguchi at all (1991), and Ohnaka and Yoshizwa (1994).

Some of the above presented formulae were compared with test data from a laboratory study of a broad crested trapezoidal reef breakwater $b / h = 3,6$, $b / L > 0,25$ (as described further in this paper). Formulae given in Eq. (2, 3, 6, and 9) have been excluded from this study as they refer to some restricted areas of application, and do not seem suitable for the case of a broad crested permanently submerged reef. Results are illustrated in Fig. 2.

Some basic conclusions follow from the review of the formulae presented above and the comparison with the test data for a broad-crested submerged rubble-mound reef:

- Obviously, different formulae refer to different conditions (fully submerged or emerging, short or broad-crested structure, breaking or non-breaking waves, etc.). Therefore, their application should be restricted to the ranges suggested by the authors. An additional check based on experimental tests is suggested always when possible;
- A major parameter that influences wave transmission (and that is present in most of the formulae) is the relative freeboard d / H_{si}. However, another important parameter that is of crucial importance is the relative crest width (expressed by b / L_i). For equal d / H_{si} a broad crested reef breakwater (compared to a narrow one) can cause breaking of wave, and therefore, can provide significantly different wave transmission coefficients. Other essential parameters that should be included are water depth (expressed most often by d / h), breakwater slope (expressed by the Irribaren parameter ξ), surface friction (expressed by d / D_{50}), and permeability (n).

For the case of the broad crested reef breakwater tested, the best fit refers to formulae suggested by Seabrook & Hall (1998), and Friebel & Harris (2003).

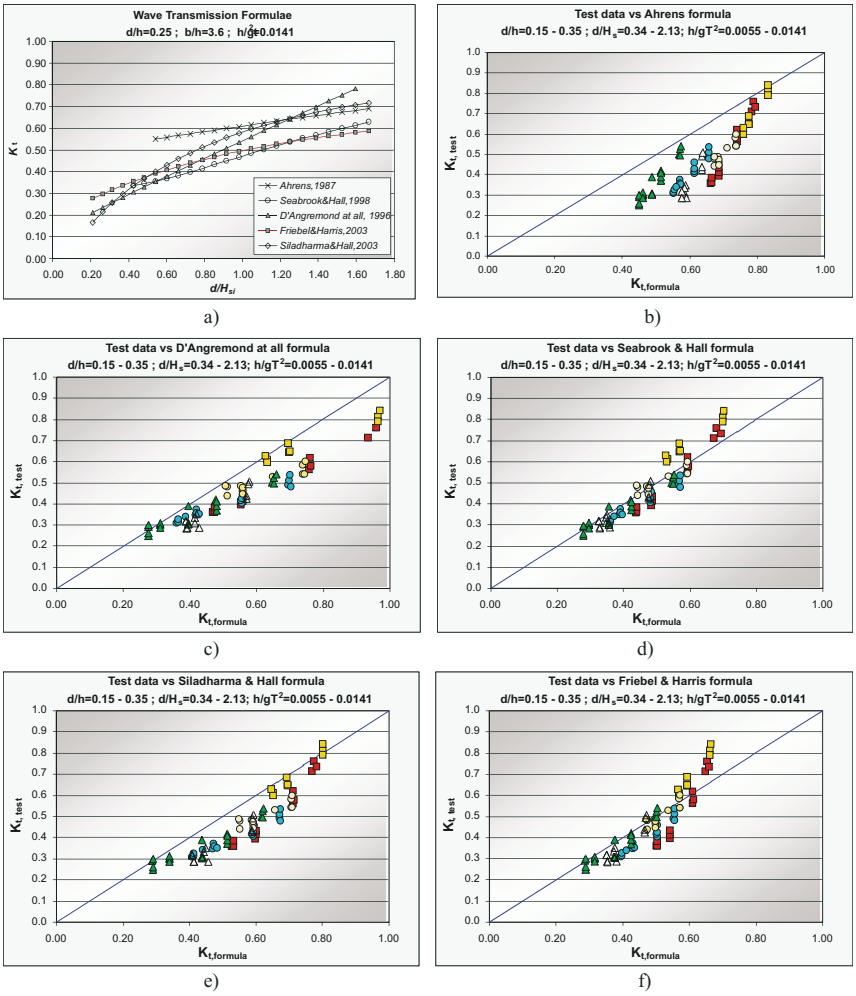

Figure 2: Comparison of wave transmission formulae: a) calculated formulae results for some fixed initial parameters; b) to f) comparison with test data for a broad-crested reef breakwater

3. Physical Model Studies - Case Studies

Although modern numerical models and computational techniques provide a good possibility to simulate nearly all the processes and to compute hydrodynamic behaviour in detail, physical model studies are still a powerful tool to improve the knowledge on the processes of interaction of waves with engineering structures. Besides, the experimental test data are used for calibration and validation of numerical models, which later can be exploited to generate different cases and to investigate various engineering options.

A number of physical model studies of submerged breakwaters have been carried out in the last 2 decades. Most of these studies concern wave transmission and stability. The main tendencies in implementation of physical model studies of reef breakwaters include:

- Use of (as much as possible) large scales;
- Precise analysis and evaluation of scale effects and model imperfections;
- Combination of physical tests with modern numerical model simulations.

In this paper some case studies of various submerged breakwaters are presented.

3.1 Submerged Obstacles with Various Geometry

A physical model study was carried out to test wave transmission over impermeable submerged obstacles with various geometry. The following submerged bodies were studied:

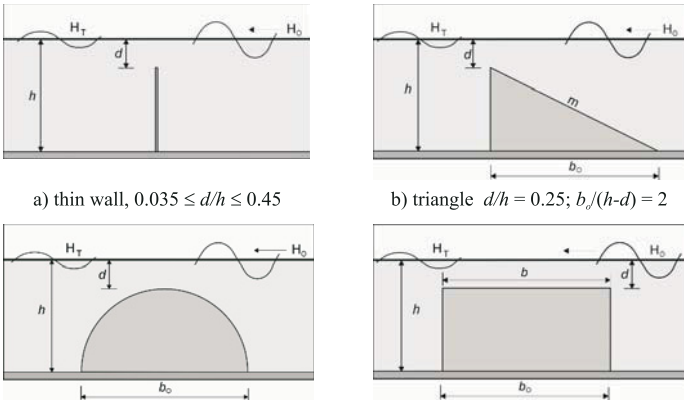

a) thin wall, $0.035 \le d/h \le 0.45$ b) triangle $d/h = 0.25$; $b_o/(h\text{-}d) = 2$

c) semi-cylinder, $d/h = 0.25$; $b_o/(h\text{-}d) = 2$ d) rectangle, $d/h = 0.25$; $b/(h\text{-}d) = 2$

Figure 3: Submerged obstacles tested

Experimental test study has been carried out at the Wave flume of BSHC – Varna (30,0 x 0,80 x 0,80) m. Tests have been done mostly in regular waves corresponding to available wind/wave data for Bulgarian Black Sea coast. Water level variations have been measured by 6 wave-meters, located in front of, over and behind the obstacle. Regular waves have been reproduced for three different wave periods, each including three different wave heights. The emphasis has been put on measurement of the transmitted and reflected wave heights. A three-probes laboratory method for separating incident and reflected waves has been applied. Tests have been carried out in different geometrical scales in order to analyze and evaluate scale effects, primarily related to wave breaking. Some selected results on the wave transmission coefficient obtained from the tests of the presented submerged obstacles are presented in Fig. 4 to Fig. 7. More results are presented in (Penchev, 1988).

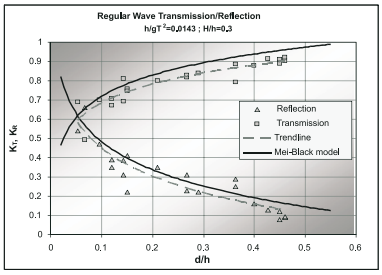

a) example wave transmission/reflection

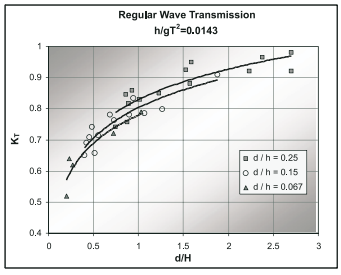

b) wave transmission for varying freeboard

Figure 4: Example wave transmission/reflection for a submerged thin wall

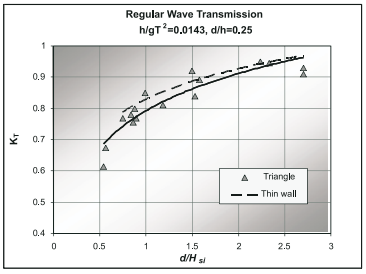

Figure 5: Example wave transmission over a submerged triangle breakwater

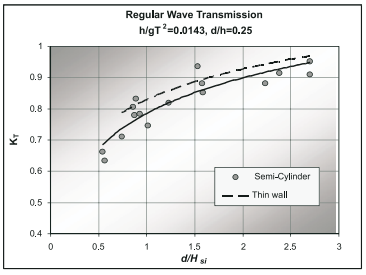

Figure 6: Example wave transmission over a submerged semi-cylinder breakwater

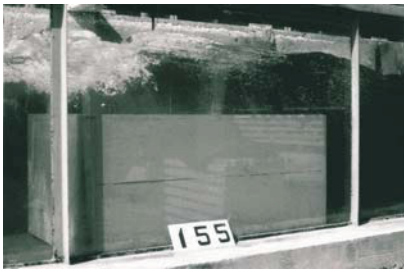

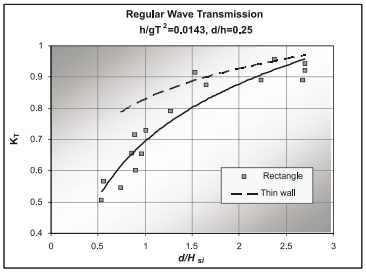

Figure 7: Example wave transmission over a submerged rectangular breakwater

A basic conclusion follows from the tests carried out on submerged obstacles with various geometries: The crest width of the submerged body is of essential importance for the wave transmission, as can be seen from Fig.7 where a rectangular shaped body is compared to a thin wall. Relative crest width (which can be expressed as b / L), together with the relative freeboard (d / H), are the most important parameters defining wave transmission coefficient of submerged obstacles.

3.2 Submerged Sill Protecting a Sand Fill

A physical model of a submerged sill protecting a sand fill (artificial beach) has been tested in the Wave flume of BSHC – Varna. The main objective was to study wave transmission behind the sill, and investigate local scour, and beach stability. Tests have been done in regular waves corresponding to wave climate data for Bulgarian Black Sea coast. Different types of materials have been used to simulate cross-shore sediment transport. Materials used were: sand ($\gamma_s = 2.63\,\mathrm{g/cm^3}, D_{50} = 0.16\,\mathrm{mm}$), polyvinyl-chloride (PVC, $\gamma_s = 1.44\ \mathrm{g/cm^3}$, $D_{50} = 0.46$ mm), and bakelite ($\gamma_s = 1.55\ \mathrm{g/cm^3}$, $D_{50} = 0.20$ mm). This required building of various scale models (including distorted horizontal and vertical scale models). Standard wave measuring techniques and software have been applied to measure wave transmission. A bottom profile meter which did not contact the bottom was used to measure local scour and beach profile evolution.

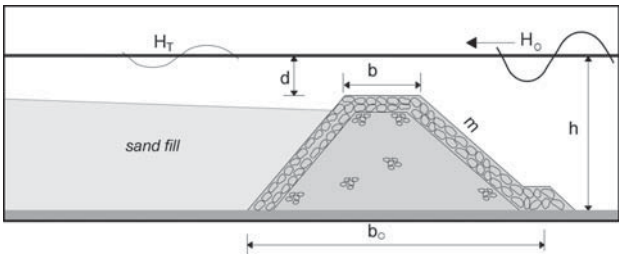

Figure 8: Model set-up of the submerged sill protecting a sand fill

A scheme of the model set-up is presented in Fig. 8. Some results of the study are illustrated in Fig. 9 to Fig. 11. Breaking of waves just behind the sill (the active scour zone) is illustrated on Fig. 9. Fig.10 shows local scour and equilibrium beach profile reached after a certain period of action of waves for the different movable bed models. Fig.11 illustrates evolution of the scour depth z_s until reaching equilibrium condition. More results are presented in (Penchev at all, 1986).

Figure 9: Breaking of waves behind the sill

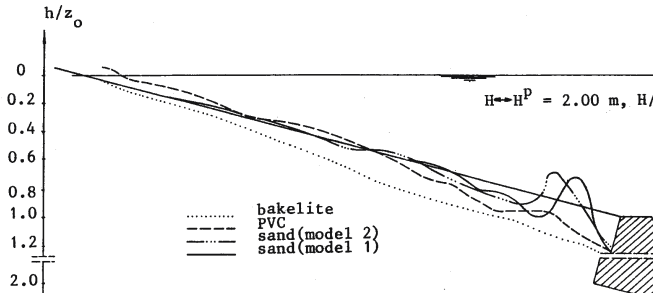

Figure 10: Equilibriums beach profile

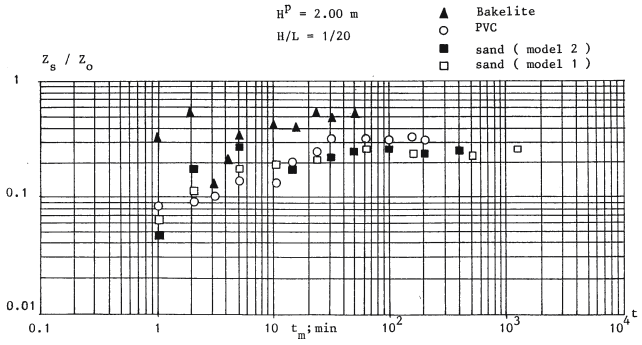

Figure 11: Scour depth evolution

Tests have proven that the combination of a sand fill protected with a submerged sill could provide a suitable engineering solution for coastal protection, providing a beach slope less than the natural one, and significantly shifting the closure depth toward the shore.

It should be noted however, that the geometry of the submerged sill is of primary importance for the intensity of the scour process: a short-crested sill will cause breaking of waves over the sand fill that means a serious scour and loss of sand will occur. Therefore, a broad-crested reef is recommended to provide scour protection, and reduce the possibility of appearance of strong long-shore currents in the area behind the sill.

3.3 Broad-Crested Rubble-Mound Reef Breakwater

Following the recommendations of the above studies, a detailed investigation on a broad-crested rubble-mound submerged breakwater (artificial reef) has been carried out. This test study has been accomplished at the WKS Wave flume of Franzius Institute, University of Hannover, Germany (120 x 2.2 x 2.0) m at water depth of 1.0 m, and a geometrical scale of 1:5. Tests have been done in both regular and irregular wave conditions, corresponding to available data for the Bulgarian Black Sea coast. Water level variations have been measured by 6 GHM-type wave-meters, located in front of, over, and behind the reef. Tests in irregular waves comprised of three different wave spectra (Jonswap type) corresponding to available field data observations. Tests in regular waves have been carried out for three different wave periods, each

including 3 ÷ 6 different wave heights. A three-probe laboratory method and corresponding software for wave records processing have been applied to separate incident and reflected waves. Three different heights of the reef have been tested, providing submergence factors "d / h" of 0.35, 0.25 and 0.15. The model revetment layer was constructed from stones (2÷8) kg. A cross-section of the reef is shown on Fig.12. The experimental setup is illustrated on Fig.13.

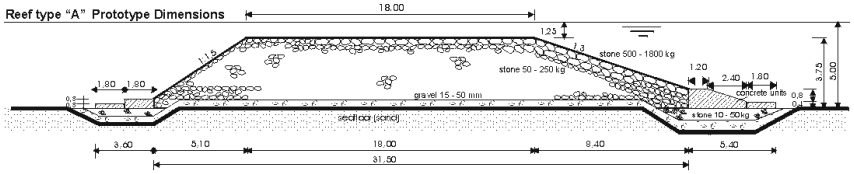

Figure 12: Cross-section of the reef breakwater

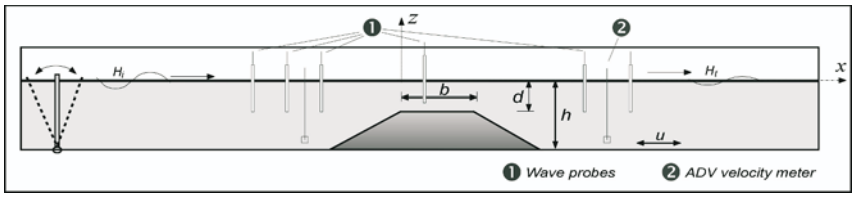

Figure 13: Experimental set-up

Wave transmission

An essential part of the tests was targeted to provide results of measurement of the transmitted wave height, and the wave energy dissipation factor. Wave spectra transformations behind the reef are illustrated in Fig.14. Results on the variation of the transmitted wave height dependence on incident wave parameters and relative freeboard are illustrated in Fig. 15 (regular wave tests).

The tests under irregular waves have proven that, for the given reef construction, and a relative submergence of d / h = 0.15 the most part of the wave energy dissipates during the wave-structures interaction process, mainly due to the wave breaking.

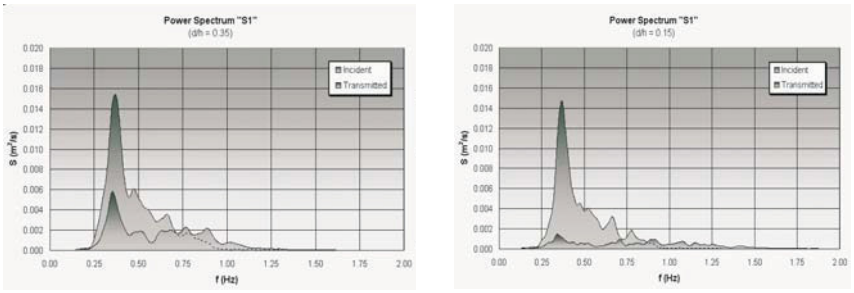

a) b)

Figure 14: Transmission of Jonswap spectra at two different freeboards of the reef breakwater

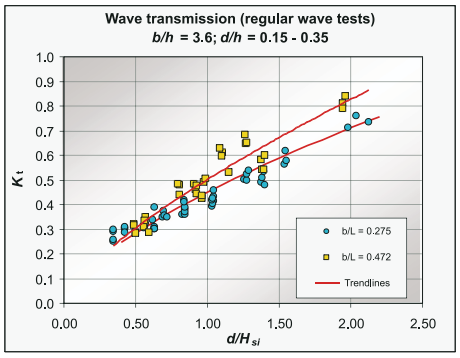

Figure 15: Wave transmission over a broad-crested reef breakwater

Regular wave test results have shown that a broad crested submerged reef could provide essential reduction of transmitted wave height (K_t values of up to 0.25 for highest waves), and respectively - on the wave energy acting on the beach. It should be noted that the relatively low freeboard, and relatively wide crest of the reef ($b / L_i > 0.25$) provided conditions for wave breaking for most of the waves tested (excluding the smallest ones that pass over the reef). The basic parameter that influences the wave transmission is the relative freeboard related to the wave height d / H_{si}. However, the relative crest width b / L is also an essential parameter, especially for values of the relative freeboard $d / H_{si} > 1$, as can be seen from Fig.15.

Wave breaking

It has been stressed previously that submerged breakwaters can cause breaking of waves at a distance from the beaches, and thus reduce wave energy flux. Breaking of waves is of primary importance for dissipation of wave energy. During the tests an attempt has been made to estimate characteristics of waves breaking over the reef, by means of measuring breaking parameters (wave height, distance of breaking, as well as wave envelopes). Results on measurements of the distance where waves break over the reef are illustrated in Fig. 16. Example wave envelopes for varying incident wave heights at a relative submergence of $d / h = 0.25$ are illustrated on Fig.17.

The main parameters that influence the wave breaking are the relative freeboard d / H_{si} and relative crest width b / L. As one can expect, wave breaking depends also on wave steepness, roughness of the structure, and other parameters. However, according to test results, the influence on these parameters is significantly lower.

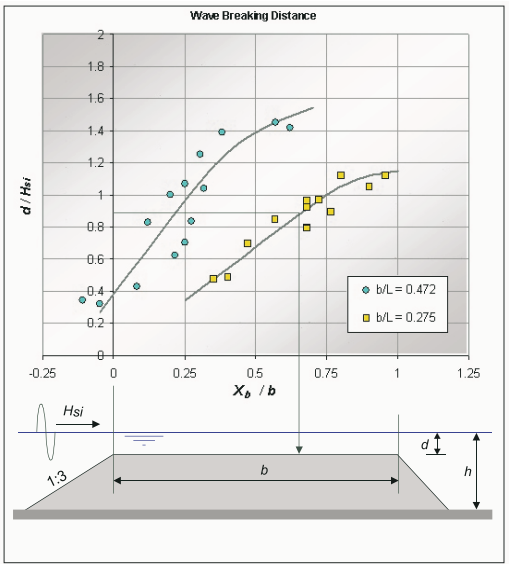

Figure 16: Average wave breaking distance

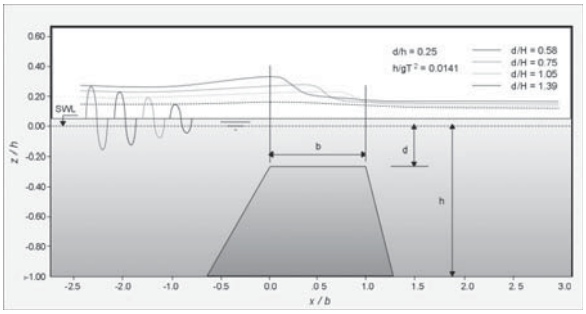

Figure 17: Wave envelopes for varying incident wave heights

One can see from Fig. 16 that breaking of waves can not be reached for a large freeboard and/or relatively long waves (for instance $d / H_{si} = 1.4$ and $b / L = 0.275$). This confirms again the conclusion regarding the importance of the crest width on the wave breaking and on the wave transmission. Fig. 14 - 17 gives some indications that can be used to make a preliminary selection of the freeboard and the crest width (and the dependence of wave climate data) for preliminary design. It should be stressed however that the above figures apply for the case of a permanently submerged reef, and relate the case of a tide-less sea (Black Sea) where no significant variations of water level exists (except wind-wave set-up). These figures are subject of further research to clarify influence of the relative crest width, the front slope of the reef, and other parameters.

Wave set-up

Wave-induced set-up has been observed for an essential part of the tests. It was mentioned previously that set-up could create both cross-shore and long-shore currents. The appearance of a cross-shore seaward bottom current behind the reef breakwater has been detected during physical model tests in the wave flume. The nature of this current could be explained by the increased water level, which is caused by the pumping effect behind the reef. In fact, this current causes a difference between the maximal offshore and onshore orbital velocities, with the offshore velocities being greater than those onshore. The velocity of this current depends on the incident wave parameters, and in general increases proportionally to the wave height and wave steepness. An accumulation of sediments could be expected just at the back toe, while some local scour could happen at some distance of (1,0 ÷ 1,5).*b* behind the reef.

An attempt was made to measure and determine wave-induced set-up during the tests. However, it was concluded that because of the 1D arrangements and numerous model effects in the wave flume this measurement is unreliable. More research is needed to quantify wave-induced set-up. This research should involve 3D physical model studies, as well as application of relevant numerical models. An example of application of numerical modeling for that purpose will be presented later.

Orbital velocity. Bed-shear velocity

A part of the experimental study was dedicated to investigate wave induced bottom velocities in the reef area. Wave orbital velocities have been measured by an ADV velocity meter at two sections behind the reef, respectively at distances of 1.5*b* and 2*b* from the back toe, as well as in one section in front of the reef at a distance of 1.5*b* from the front toe. Each of the sections included 4 measuring points, evenly distributed from the surface to the bottom. Tests have been carried out with regular and irregular waves. Emphasis has been put on the results of the measurement of the near-bottom wave orbital velocity and its relation to maximal shear velocity for waves transmitted over the reef without breaking. Typical velocity time series for irregular wave tests is illustrated in Fig.18. Results on the measurements of orbital bottom velocity in front of the reef (u_b^0) and behind the reef (u_b) as a function of incident wave parameters are illustrated in Fig. 19.

A significant reduction of the values of the bottom velocities behind the reef (compared to those in front of the reef) has been observed. The decrease of the average maximum velocity varies between $(25 \div 50)\%$ for $d / h = 0.35$, and between $(35 \div 75)\%$ for $d / h = 0.15$.

A comparison has been made between maximum wave shear velocities, calculated according to the eddy viscosity model (Grant & Madsen), and critical shear velocity (modified Shields diagram approach) for entrainment of sediment with $D_{50} = 0.2$ to 0.5 mm, at a bottom slope of $i = 0.03$, Fig. 20. One can see that the wave tested shear velocities are usually below the critical velocities for a sand with $D_{50} = 0.5$ mm.

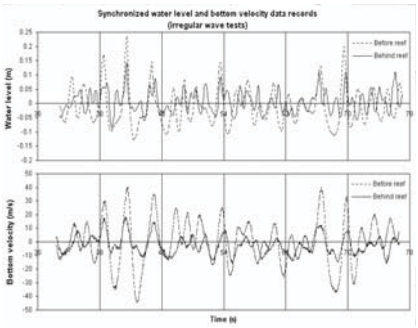

Figure 18: Typical water level and orbital velocity time series (irregular wave test)

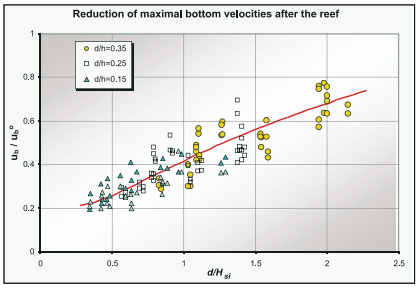

Figure 19: Reduction of average maximal orbital bottom velocity behind the reef

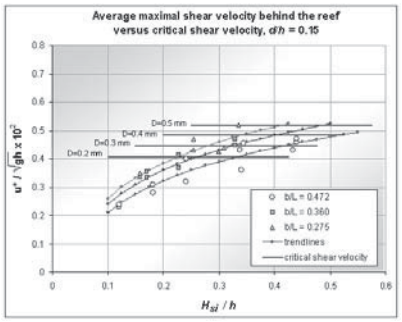

Figure 20: Maximum shear velocities behind the reef versus critical shear velocity

Results presented in Fig. 20 give an idea on selection of sand parameters, and bottom slope, in case of establishment of an artificial beach behind the reef.

4. Numerical Approach

It was stressed that reef breakwaters are applied to reduce wave energy flux by causing breaking of waves at a distance from the beaches. Breaking of waves in the nearshore results in changes of the wave-induced momentum that drive nearshore currents and pressure gradients, and in general results in an essential distribution of wave energy. Therefore, development of numerical models of wave-structure interaction for the case of submerged structures relates primarily to simulation of wave-breaking phenomena. However, breaking waves, bottom boundary layers, and associated turbulence are not understood well. Research performed so far on the mechanism of breaking of waves passing a submerged obstacle is incomplete.

Wave breaking and wave transmission

The effect of breaking on the transformation of waves propagating across the surf zone has been modeled by including heuristic dissipation terms in both time- and

frequency-domain Boussinesq models (Schaffer at all, 1993; Kaihatu and Kirby, 1995). With suitably tuned parameters that control the dissipation rate, Boussinesq-type models predict satisfactorily the wave height decay and shape changes of near-normally incident waves propagating across the surf zone, and 2-D waves breaking around circular shoals (Kennedy at all, 1999). Models have also been developed that incorporate the effect of the wave roller, the turbulent wedge of white water on the bore face that is advected shoreward at the wave phase speed. The above models can provide adequate prediction of wave propagation (including influence of wave breaking), but do not describe small-scale breaking wave dynamics (i.e. shape, type of breaking, aeration, etc). Breaking wave processes are basically "qualitatively" understood and models are crude. Turbulent wave boundary layers are just starting to be measured in the field using instrumentation with improved spatial and temporal resolution. There is a need for more comprehensive knowledge on mechanisms of wave breaking, in order to develop related numerical simulation models, and provide cost effective, functional, and environmentally sound engineering solutions.

Ongoing work is directed toward integrating small-scale breaking wave dynamics into Boussinesq and roller models that predict the evolution of wave height and shape across the surf zone. Numerical models that solve the unsteady Navier-Stokes equations are being used to simulate spilling and plunging waves over a sloping bed using VOF (volume of fluid) technique to track the discontinuous free surface (Lin and Liu, 1998; Liu at all 2000). However, extrapolating existing surf zone models to the case of sudden change of bottom topography (such as breakwaters) has proven to be problematic and further research in this area is recommended (Water Waves Euro Conference, 2001). Main challenges in developing such models include:

- Boundary conditions, at offshore boundary (incident waves, velocity field), and coast boundary (reflection);
- Turbulence model selection (high turbulence, vorticity, air entrainment);
- High-resolution grid to be applied;
- Calibration/Verification of the numerical model versus field and laboratory test data.

Wave induced set-up, littoral currents and sediment transport

It was noted that together with wave damping capability, performances of reef breakwaters are significantly affected by the phenomenon of wave set-up. The presence of the barrier, in fact, generates a hydraulic head surplus behind the structure driving large long-shore currents in the protected area. This may increase the shoreline erosion instead of reducing it. Studies on this topic should involve application of 2D and 3D numerical models. Once the transmission properties of the reef are known, such numerical models can be applied to study set-up, littoral currents and sediment transport in the reef area.

An attempt has been made to use SWAN (Simulating Waves Nearshore, TU-Delft), and MIKE'21 (DHI) Hydrodynamic and Sediment modules to simulate waves, radiation stresses, littoral currents and sediment transport in the area of an artificial coastal reef, (Penchev at all, 2001). A line of the above numerical models were set up and calibrated against selected field data and physical model tests. The SWAN model was used to

simulate wave climate and radiation stresses. A local model with fine resolution ($\Delta x = \Delta y = 10$ m, 2 km x 2,8 km) was nested in a wave model of the Bulgarian Black Sea ($\Delta x = \Delta y = 400$ m, 122 km x 198 km). For the reef breakwater selected, calibration was made using data of physical model tests. Fig. 21 presents an example of a single 1-D SWAN simulation and the correlation of wave transmission coefficients measured respectively calculated for all sets of boundary conditions of irregular waves.

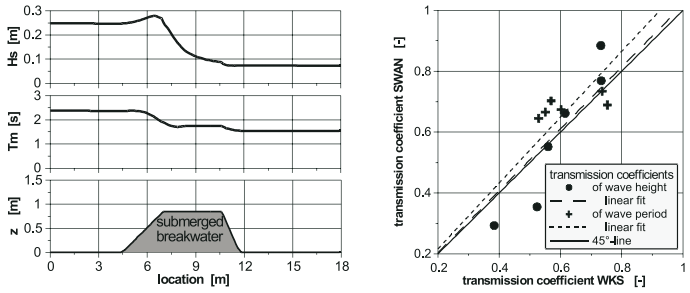

Figure 21: Wave propagation over a submerged breakwater calculated with SWAN (left), and correlation of transmission coefficients calculated with SWAN (right)

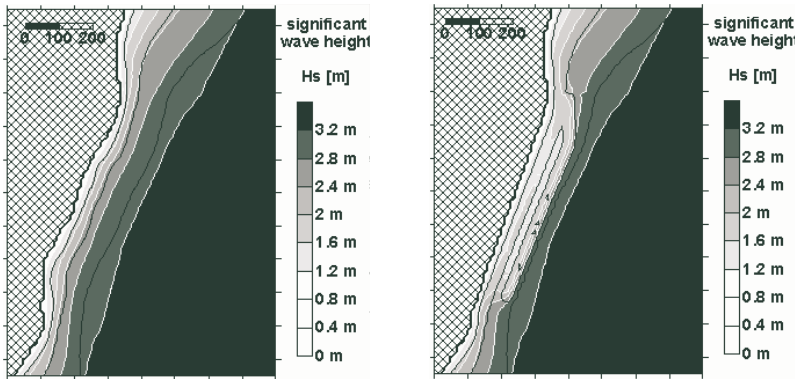

Figure 22: View of the significant wave height in study area without (left) and with (right) an artificial reef for a water-level of 1 m a. MSL and eastern wind of 28 m/s

Furthermore, wave spectra transformation was simulated by SWAN, and wave height distribution in the study area was calculated (Fig. 22), as well as distribution of radiation stresses was obtained. Radiation stresses calculated by SWAN wave model were used as input for the MIKE'21 HD (Hydrodynamic) module. HD module was used to simulate water levels and littoral currents (Fig. 23). Grid resolution and dimensions for all MIKE'21 models were the same as for the SWAN model. An interface was developed to transfer output files from SWAN to MIKE'21 HD-module and vice versa. Finally, MIKE'21 HD results (i.e. water levels, wave current velocities) were applied to simulate sediment transport using MIKE'21 ST (Sediment Transport) module.

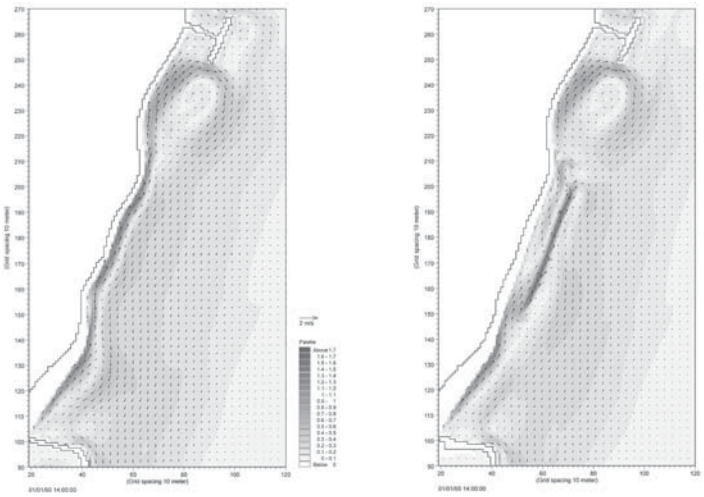

Figure 23: Currents in study area for scenarios without (left), and with (right) artificial reef

Results obtained to date are encouraging for further application of the suggested approach for numerical study of wave induced set-up, littoral currents and sediment transport in the area behind the reef.

5. Conclusions

This paper presents results on investigation on hydrodynamic interaction of waves with reef breakwaters. Based on available experience, as well as on comparison of test data for various submerged structures versus existing design formulae, and available numerical models, some general conclusions are suggested here below.

Results obtained confirm that properly designed reef breakwaters can reduce the hydraulic loading to a required level that maintains the dynamic equilibrium of the shoreline. Combined in conjunction with beach nourishment they can provide a suitable engineering solution unifying coastal protection, environmental effect, and aesthetic advantages.

However, design of the reef breakwater is more sophisticated than that required for traditional coastal protection structures. Existing knowledge is still incomplete.

Research should be carried out in the following areas:

- study on mechanism of wave breaking (intensity, turbulence, mass flux, vorticity, air entrapment), using both physical and numerical models;
- development of unsteady Navier-Stokes numerical models to simulate spilling and plunging waves over reef breakwater using VOF (volume of fluid) technique to track the discontinuous free surface;
- physical and numerical studies on wave set-up and long-shore currents generated behind the reef, and their effect on the sediment transport.

Acknowledgments

A part of this study related to modelling of a broad-crested artificial reef breakwater has been carried out with the support of the 5th Framework Program of the European Community, within the project "Fundamental Hydraulic Research for Coastal Areas by using Large-Scale Facilities of the Hydro-Lab-Cluster North Germany". The author expresses his acknowledgments to the European Commission, as well as to Franzius-Institut for Waterways, Hydraulic and Coastal Engineering, Hannover, Germany, for providing support and assistance in carrying out the research.

References

Ahrens, J.P., 1987, Characteristics of Reef Breakwaters, Technical Report CERC-87-17, U.S. Army Corps of Engineers, Waterways Experiment Station, Vicksburg, MS, pp. 62

Bleck, M., Oumeraci H., 2002, Hydraulic Performance of Artificial Reefs: Global and Local Description, Proceedings of 28th Int. Conference on Coastal Engineering, Cardiff, UK

Calabrese, M., D. Vicinanza and M. Buccino, 2003, Low-crested and Submerged Breakwaters in Presence of Broken Waves, HydroLab II "Towards a Balanced Methodology in European Hydraulic Research", Budapest, pp. 8/1-8/23

d'Angremond, K., Van der Meer J.W., and de Jong, R.J., Wave Transmission at Low-crested Structures, Proc. of 25th Int. Conf. on Coastal Engineering, Orlando, Florida, 1996, pp. 2418-2426

Daemen, I.F.R., 1991. Wave Transmission at Low-Crested Structures, M.Sc. Thesis Delft University of Technology, Delft Hydraulics Report H462

Daemrich, K. and Kahle, W., 1985, Schutzwirkung von Unterwasser Wellen brechern unter dem Einfluss unregelmassiger seegangswellen. Technical Report, Franzius-Instituts fur Wasserbau und Kusteningenieurswesen, Report Heft 61 (in German)

Friebel, H. C., L. E. Harris, 2003, Re-evaluation of Wave Transmission Coefficient Formulae from Submerged Breakwater Physical Models, (http:\\ocean.marine.fit.edu/papers/FriebelHarris.pdf)

Hamaguchi, T., Uda T., Inoue Ch., and Igarashi A., 1991, Field Experiment on wave-Dissipating Effect of Artificial Reefs on the Niigata Coast, Coastal Engineering in Japan, JSCE, Vol. 34, No. 1, June

Kaihatu, J.M. and J. Kirby, 1995, Nonlinear Transformation of Waves in Finite Water Depth. *Phys. Fluids* 7 (8), 1903-1914

Kawai H., Kudoh T., Masumoto T., Hiraish T., Uehara I., 1996, Laboratory Simulation and Application of Numerical Model on Wave and Current around Submerged Breakwater, Proc. Of Tecno-Ocean '96 Int'l Symposium-Proceedings II, Kobe, Japan

Kennedy, A.B., Q. Chen, J.T. Kirby, and R.A. Dalrymple, 1999, Boussinesq Modeling of Wave Transformation, Breaking, and Runup. J. Waterway, Port, Coastal and Ocean Engineering, 126 (1), 39-47

Lin, P. and P. L.-F. Liu, 1998, A Numerical Study of Breaking Waves in the Surf Zone, J. *Fluid Mech.,* 359, 239-264

Liu, P.L.-F., Hsu, T.J., Lin, P.-Z., Losada, I.J., Vidal, C., Sakakiyama T., 2000, The Cornell Breaking Wave and Structure (COBRAS) Model, Proc. Coastal Structures '99, ISBN 90-5809-092-2, Volume 1, pp. 169-174

MIKE'21, 1998, User Guide and Reference Manual, Release 2.7, Danish Hydraulic Institute, Denmark

Ohnaka S. and Yoshizwa T., 1994, Field Observation on Wave Dissipation and Reflection by an Artificial Reef with Varying Crown Width; Hydro-Port'94, Yokosuka, Japan

Penchev V., Dragancheva D., Matheja A., Mai S., Geils J., 2001, Combined Physical and Numerical Modelling of an Artificial Coastal Reef, Proc. of 22nd HADMAR 2001 Euro-Conference, Vol.2, Varna, Bulgaria

Penchev V., Sotkova M., Dragancheva D., 1986, Comparative Model Investigations of the Evolution of Artifficial Beach, Proc. of the IAHR Symp. on Modelling of Sediment Transport Phenomena, Toronto, Canada

Penchev V., 1987, Physical Model Study of Wave Interaction with Submerged Bodies, BSHC Internal Report TP-85.06.03/P-2.2.1, Varna, Bulgaria (in Bulgarian)

Pilarczyk K. W., 2003, Design of Low-Crested (Submerged) Structures – an Overview, 6th International Conference on Coastal and Port Engineering in Developing Countries, Colombo, Sri Lanka

Powell, K.A. and Allsop, N.W.H., 1985, Low-Crested Breakwaters, Hydraulic Performance and Stability. Technical Report, HR Wallingford, Report SR57

Sawaragi,T., Y. Okahara and I. Deguchi, 1989, Study on Reduction of Wave Energy by Submerged Breakwater with Wide Crown Width and its Scale Effect, Proc. 36th Japanese Conf. on Coastal Eng., JSCE, (in Japanese)

Schaffer, H., Madsen P., and Deigaard R., 1993, A Boussinesq Model for Waves Breaking in Shallow Water, *J. of Coastal Eng.,* 20, 185-202

Seabrook, S.R., 1997. Investigation of the Performance of Submerged Rubblemound Breakwaters, M.Sc. Thesis, Queen's University, Ontario, Canada, 200 pp.

Seabrook, S.R. and Hall, K.R., 1998, Wave Transmission at Submerged Rubble Mound Breakwaters, Proc. of 26th Int. Conference of Coastal Engineering, ASCE, 2000-2013

Seelig, W.N., 1980, Two Dimensional Tests of Wave Transmission and Reflection Characteristics of Laboratory Breakwaters, Technical report 80-1, Coastal Engineering Research Center, U.S. Army Corps of Engineers Waterways Experiment Station, Vicksburg, MS, 187 pp.

Siladharma, I.G.B., K. Hall, 2003, Diffraction Effect on Wave Transmission at Submerged Breakwaters, Index paper, Internet version

SWAN (Simulating WAves Nearshore), 2000, User Manual, Cycle III version 40.11, TU – Delft, The Netherlands

Theory of Water Waves, Special Euro-Conference, 2001, Two and Three Dimensional Water Waves, Conclusions, University of Cambridge, August 2001, (http://www.newton.cam.ac.uk/reports)

Van der Meer, J.W., 1990, Data on Wave Transmission due to Overtopping, Technical Report, Delft Hydraulic, Report n. H986

Van der Meer, J.W., 1988, Rock Slopes and Gravel Beaches under Wave Attack. Ph.D. thesis, Delft University of Technology, Delft Hydraulics Report 396

COASTAL PROTECTION AND ASSOCIATED IMPACTS - ENVIRONMENT FRIENDLY APPROACH

Grzegorz Różyński, Zbigniew Pruszak and Marek Szmytkiewicz
Dept. Coastal Dynamics&Engng., Inst. of Hydroengineering, PAS
Gdańsk, Poland

Abstract

The paper highlights coastal protection as a component of integrated coastal zone management (ICZM). ICZM particularly emphasizes environmental aspects of all activities in coastal areas, combining research results from natural and social sciences. In this context it particularly favors solutions avoiding undesired disturbances to coastal (eco) systems, including unnatural coastal morphology, poor water quality and impaired biodiversity. Simultaneously, it supports schemes being flexible enough to cope with the global climate change on a longer time perspective. Thus, in the ICZM view, the best measures incorporate soft coastal protection techniques, i.e. artificially initiated natural dunes and beach fills, permeable groins and submerged breakwaters, discussed extensively herein.

1. Introduction - Key ICZM Concepts

Modern approaches to coastal protection must take account of much broader perspectives, reflecting both natural and social impacts exerted on coastal zones. Any coastal protection scheme is thus a real challenge, because of the resulting profound consequences, related to the change of local sea-land interactions regime, subsequent impacts on the neighboring land and marine areas, the existing ecosystems with their biodiversity as well as the influence on the socio-economic side of the coastal segment to be protected. For these reasons, it is evident that coastal protection must be analyzed in connection with a variety of other issues and processes. This understanding paves the way for the definition of integrated coastal zone management.

In brief, ICZM is perceived as a 'continuous process with the general aim of implementing sustainable use in coastal zones and maintaining their overall diversity', Document 5/3, 2003. Hence, coastal protection no more remains a purely engineering discipline, in addition to remedying erosion it also requires assessment of various environmental impacts, such as pollution prevention and control, biodiversity, changes in salinity or water and sediment quality, plus social issues related to spatial planning, population development, job loss/creation, tourism, etc. Achieving that involves complex integration within and among various fields of activity. First of all, geographical integration highlights the functioning of sea-land and land-sea connections and interactions in vast areas of land-ocean continuum. Horizontal integration of the usually separately analyzed sectors of economy (agriculture, trade, fishery, forestry, industry, military, mining, natural reservations, urban development, tourism, transport, etc.) is intended to reveal their

C. Zimmermann et al. (eds.), Environmentally Friendly Coastal Protection, 129-145.

interactions that may be conflicting, synergistic, harmonious or neutral and whose joint influences produce substantial impacts on ICZM strategies. Vertical integration of governmental agencies and institutions from local up to (inter)national level is anticipated to generate consistent policies, recommendations and regulations matching long term ICZM objectives. Finally, interdisciplinary integration is assumed to identify cause-effect chains shaping coastal zones and to predict the resulting effects. This task is extremely difficult, because it requires huge amounts of information to be processed and requires top expertise and commitment from natural and social scientists, coastal planners and managers and (local) authorities. To be successful this type of integration must be supported by information provided by all users of coastal resources, which is not possible without their awareness and concern.

ICZM is a permanent process. Therefore, both the planning and management should be combined. It means that the results of adopted solutions, be it artificial beach fill, new regulation or administrative decision, should be monitored and the feedback should provide grounds for improved measures. Coastal protection is no exception to this rule. However, the desired sustainability outlines preferences for the measures that avoid irreversible and undesired effects on coastal (eco)systems, such as unnatural nearshore morphology, loss of biodiversity or impaired water quality. They also focus on the reduction of adverse developments to (local) economy. Therefore, ICZM opts for soft solutions with high adaptation abilities to current and future needs (wide beach), potential uses (tourism) and imminent physical processes, such as climate change, including sea level rise and increasing frequency of storms, Orviku et al., 2003. They are all environment friendly, as they minimize the use of hard materials (steel, concrete) in favor of natural materials (sand, gravel and wood) and their design concepts curb adverse side effects (scour, beach loss, unnatural landscape). Importantly, their combined applications often have a synergistic effect, so their overall protection efficiency is greater than the combined efficiency of individual solutions. The major groups of ICZM oriented coastal protection techniques include artificial dunes and beach nourishment, permeable groin fields, submerged breakwaters and reconstruction of beaches in front of seawalls. They are all discussed extensively in this paper.

2. Environmental ICZM Indicators - Coastal Protection Impact

Usually, the best indicator of environmental protection of coasts, apart from stability of shoreline and beaches, is water and sediment quality, expressed with suitably chosen key parameters. Their satisfactory values guarantee that biodiversity of various aqueous ecosystems will remain sustainable. By permanent monitoring of these parameters the current condition of a coastal system can be traced, indicating the progress achieved and the tasks remaining to attain the desired sustainability. Moreover, these parameters allow for comparisons of environmental situations at different sites or countries. This is very important, because the awareness of well informed general public is usually one of the strongest incentives towards sustainable ecosystems. Several major target quality parameters of coastal waters in Poland are presented in Table 1, Statute Book 116, item 503, 1991. These provisions define bathing safety for humans and are fully consistent with similar EU regulations. By targeting bathing safety they secure economic development related to recreation and tourism in coastal zones, based on the principles of sustainability.

Table 1: Major target water quality parameters

Biological Oxygen Demand BOD_5	8mg O_2/l
Chemical Oxygen Demand COD	70mg O_2/l
Total nitrogen N	10mg N/l
Total phosphorus P	0.25mg P/l
E Coliform bacteria	100/100ml

Coastal waters abound with marine flora and fauna, so they are particularly vulnerable to pollution. At the same time, they receive substantial amounts of contaminants from land as a result of natural and predominantly man induced processes. The latter include substances released in agricultural practices (overdosing of fertilizers) and insufficiently treated municipal and industrial waste waters, all discharged to marine ecosystems through river mouths. The exposure of coastal ecosystems to pollution is enhanced by complex shoreline and seabed configurations in forms of lagoons, gulfs, deep areas or shoals that impede water exchange, which results in accumulation of both organic and inorganic pollutants, bacteria, etc. Similar effects may appear in case of physical protection of a coastal segment or its artificial rearrangement with disregard for environmental impacts. The impact is sometimes so profound that huge areas can be affected; e.g. the creation of artificial islands between Denmark and Sweden as part of rail and road connection between those countries affected the entire Baltic Sea and required painstaking efforts before a satisfactory island location was reached, *cf*. Mangor et al. 1996. The scale of this problem is demonstrated in Fig. 1. Although most coastal protection schemes have only a local impact, they deserve similarly meticulous environmental impact assessment. Fortunately, coastal protection with soft measures, together with other environment friendly means of adaptation toglobal change, have a built-in environmental friendliness, so undesired side effects related to water and sediment quality can be easily minimized to the acceptable levels.

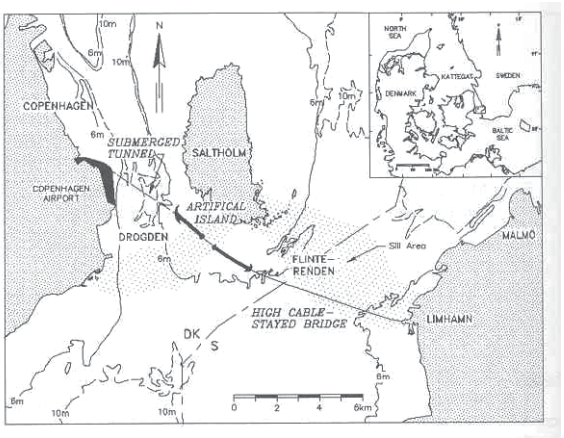

Figure 1: Øresund Link with artificial island placement, Mangor et al. 1996

3. ICZM Oriented Coastal Protection

Considering any measure of coastal protection requires assessment of value of a segment to be protected using the ICZM methodology that includes the principles of sustainability. Thus, the segment in question will typically fall into one of three categories that determine protection strategy:

1. low current and future value usually corresponds to a retreat approach, i.e. giving up the idea of any coastal protection. This is almost impossible in most European countries or the USA due to the general trend of growing property values, pressures from growing tourism and urban development in coastal areas;
2. medium current and future value: soft protection in line with ICZM suggestions including artificially initiated natural dunes and beach fills, fields of permeable and/or submerged groins and submerged/low crested breakwaters as well as reconstruction of beaches in front of seawalls; it is the most viable and environment friendly option in most cases with high adaptation capabilities to future developments, concerted actions consisting of more than one options applied jointly additionally highlight adaptation flexibility and point to a synergy of such complex solutions;
3. high and very high future value: hard protection with detached breakwaters, seawalls or revetments, possible only for relatively small coastal segments due to high costs and adverse side effects (beach loss, scour, damaged water quality), the existing hard structures can be combined with soft measures though, providing their environment friendly management is in line with ICZM recommendations.

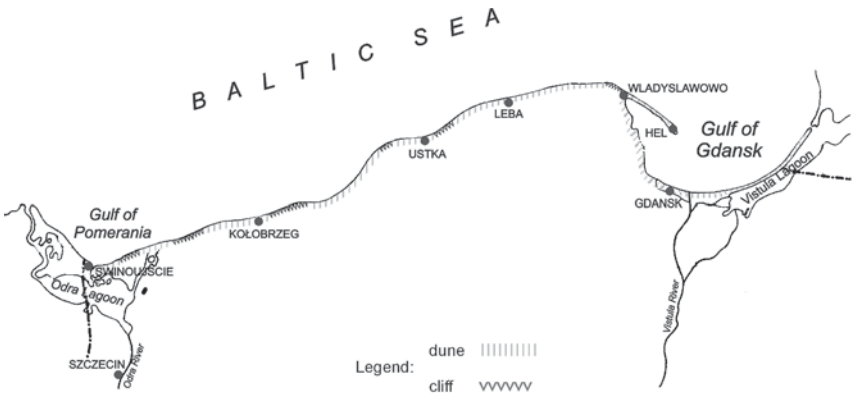

Figure 2: Schematic view of Polish coast

The versatility of the 2nd group, the desired sustainability and the growing numbers of coastal segments that need protection results in high popularity of soft protection techniques. It is worth noting that the entire Polish coast is an ideal entity for implementation of soft protection schemes. Sandy beaches, dunes and postglacial cliffs,

made of sand and loam layers, offer natural conditions that can respond particularly well to properly designed and executed soft coastal protection projects. The impacts of climate change, particularly the imminent threat of growing storminess on the one hand, and the growing pressure from tourism and recreation on the other, resulted in relative expansion of soft protection strategies over the last decades in Poland. For example, artificial beach nourishment was introduced in the late 1970's and now it protects about 60 km out of 500 km of the Polish open sea coastline. Fig. 2 presents a schematic view of the Polish coast. Of particular interest is the Hel Peninsula and its root, where vast tourism activities along 30 km of its length are confronted with continuous exposure to enhanced erosion from the open sea. Therefore, it has become a training area for coastal engineers and managers, who try to hold back the erosion with various soft measures. As a result a great deal of practical experience and theoretical knowledge has been accumulated. This paper can also be viewed in the context of these experiences.

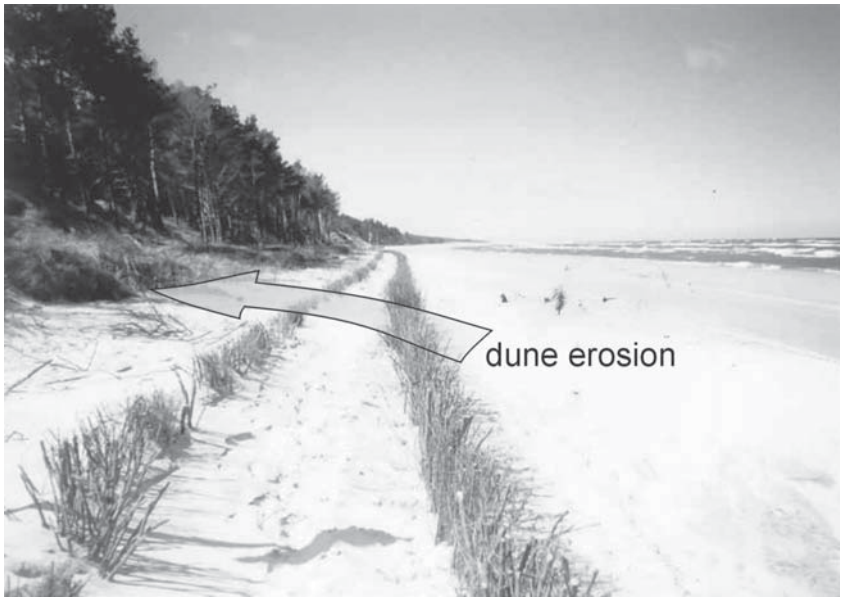

Figure 3: Coastal protection with artificially initiated natural dunes, South Baltic Coast, Poland

3.1 Artificially Initiated Natural Dunes

The cheapest and frequently the most suitable soft coastal protection are natural dunes, initiated by fences that trap dry sand, blown by the wind. The dunes form barriers situated in backshore beach regions and serve as sediment reservoirs that prevent intrusion of stormy waves during storm surges into the hinterland and feed the beach during extreme storms. Hence, they can provide sufficient shore protection to rare although very powerful events, after which they have enough time for their recovery. This type of coastal protection can thus be recommended in situations where sufficient volumes of sand are available, aeolian transport has adequate intensity and the beach to be protected is not

exposed to permanent erosion. The concept of formation of such dunes is to initiate natural aeolian accumulation of sand and then to stabilize the emerged dunes with grass and later shrubs. Such a gentle human intervention involves minimum costs and little disturbance to the natural evolution of the system. As a result, a virtually natural barrier against storms can be re-established. Dunes can be initiated with single or multiple, permeable, shore parallel fences extending 0.7-1m above beach level. They are usually made of wooden posts, sticks, fascine or reeds driven or dug 0.3-0.4m into the sand. The optimum fence permeability is between 40-50% and the distance between elements should not exceed 5cm, Basiński et al. 1993. If the beach is wide enough and aeolian processes are strong, multiple fences are usually built, see Fig. 3. Once the dune emerges, it is stabilized with site-specific grass that can endure severe conditions of dry and moving sand. When it takes root, the dune can be further reinforced by planting shrubs and then trees. Simultaneously, more fences can be added in order to further increase the dune volume.

Artificially initiated natural dunes are widely used in Poland, where dune sandy coasts predominate and large volumes of fine sand are available. Fig. 3 presents a two row fence trapping sand in the vicinity of IBW PAN Coastal Research Station at Lubiatowo. On the left hand side of this picture dunes destroyed during heavy winter storms can be seen.

3.2 Artificial Beach Nourishment

This approach is intended to prevent beach erosion with almost no disturbances to natural processes. Although this type of coastal protection can be expensive, it is one of the most common techniques currently encountered in engineering practice. Usually, artificial beach fills are targeted towards:

- beach protection, when abrasion of beach/dune by waves and currents requires artificial re-establishment of original beach/dune morphology;
- recreation, when a wide beach is needed for local economy (tourism);
- restoration, when damages occur as a result of disturbances in natural sediment budget due to hard coastal structures or river (over)regulation, decreasing sediment sources near river mouths;
- unfavorable changes in shoreline configuration due to climate change.

The fill placement is directly linked to its key function. Therefore, typical fill locations include:

- dunes; like artificially initiated natural dunes, this type of protection is designed to prevent intrusion of waves during extreme events, usually the fill stays on the beach for a long time, such nourishment is applied when aeolian processes are too slow to rebuild a dune before the next storms;
- shoreline and emerged beach; this scheme is typical in situations where a wide beach is a primary goal;
- submerged beach; the fill is intended to behave like an artificial nearshore bar; being exposed to permanent wave and current action it undergoes rapid disintegration.

The required volume of sediment strongly depends on nearshore hydrodynamics, cross-shore profile characteristics in the area to be filled and the associated features of native sediment. When the fill is placed on a dune or emerged beach, the required volume

can be calculated based on profile measurements of the nourished site and designed beach/dune configuration. Submerged fills are not so straightforward, because the most crucial factor that determines geometry and cost of a fill in this case is the relationship between representative grain diameters of the native sediment D_N and the fill diameter D_z. Fig. 4, (Pruszak 2003), demonstrates two classical situations; one when $D_z > D_N$ (top) and the other when $D_z \approx D_N$ (bottom). In the 1st instance the resulting cross-shore profile will be steeper than the native beach slope and the beach fill volume per unit shoreline length can be computed, using quantities from Fig. 4 as:

$$V = L_0.B_0 + \int_0^{x_*} \left[A_N x^{2/3} - A_z (x - L_0)^{2/3} \right] dx \tag{1}$$

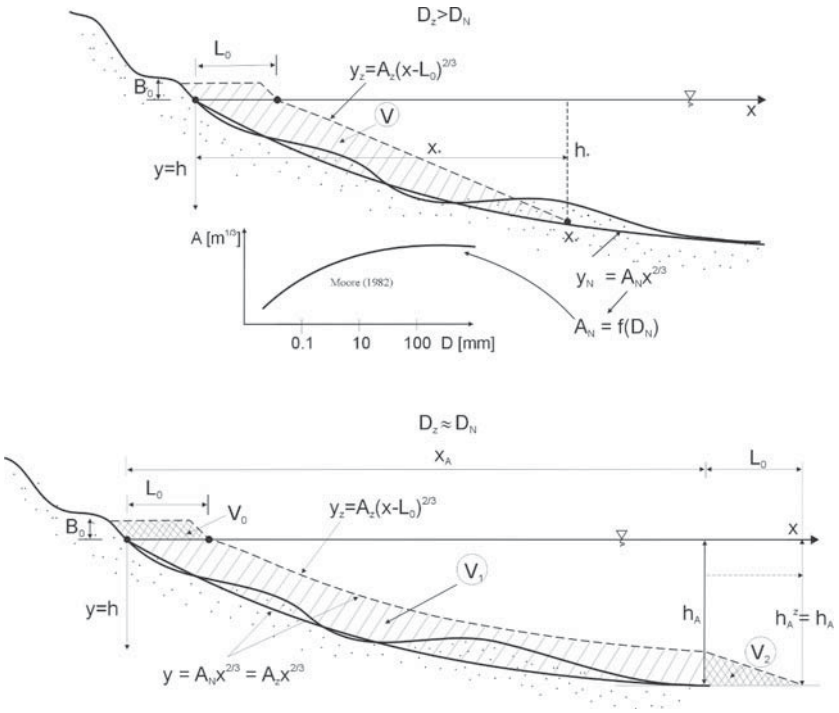

Figure 4: Classical beach nourishment schemes $D_z > D_N$ (top) and $D_z \approx D_N$ (bottom)

When both sediments have similar characteristics, the volume required is greater and is equal to:

$$V = L_0.B_0 + \int_0^{x_A} \left[A_N x^{2/3} - A_z (x - L_0)^{2/3} \right] dx + \frac{1}{2} A_z L_0^{5/3} \tag{2}$$

In these equations the coefficients A_N and A_z are Dean equilibrium profile parameters, of the native and fill sediment respectively. They describe beach slope steepness and can be

obtained from sediment characteristics, Moore 1982. The associated power function of the type $A.x^{2/3}$ determines the equilibrium profiles, from which beach fill volume can be calculated with Equations (1) or (2). If the fill is coarser than the native sand, the offshore fill range h_* can be found at a point where the steeper equilibrium profile of the fill intersects with a milder native profile. When both sediments have similar characteristics, the depth h_A must be found from wave statistics, from which the annual depth of closure can be deduced, (Hallermeier, 1977). The maximum fill depth should not exceed this value. In Poland most fills have been executed along the Hel Peninsula since the early 1980's. The experience gathered during these operations generally confirms long term engineering practice and monitoring results of various other fills, providing practical guidance for artificial beach nourishment execution:

- avoid fine sediment; using material with grains finer than the native beach results in rapid fill disintegration due to existing hydrodynamic regimes;
- place at least as much material as the calculated annual longshore littoral drift, otherwise the fill has little impact on evolution of the protected area;
- avoid contaminated materials dredged from harbor basins, it violates ICZM principles of sustainability;
- avoid destruction of the seabed where the fill material is dredged; deep holes in sea floor accumulate contaminants and retain high H_2S concentrations, originating from benthos degradation; this may kill the entire marine life in such areas;
- monitor changes in the nourished area and observe the dynamics at the site if possible (waves, currents, etc.); it will indicate the time by which the fill is operational; re-nourishment done just before this time will provide ongoing protection with minimum costs;
- increase the calculated fill volume by 50-70%;
- apply the fill over an area 50% greater than the protected segment to avoid end effects;
- repeat the fill before the lifetime of previous fill is over to ensure ongoing safety of the protected segment, usually re-nourishment is necessary every several years;
- make sure enough sediment for fills is available now and in the future; lack of sand may result in choosing another type of coastal protection.

There are several beach fill techniques. In the case of predominant littoral drift, sediment bypassing of harbors with a fixed pipeline is a routine practice. Fig. 5 shows the harbor in Wladysławowo at the root of Hel Peninsula with clearly visible accretion on the left, up-drift side. This harbor does not possess a permanent bypassing pipeline. Instead, the sand is dredged from the up-drift side and navigational channel. Then the dredger is attached to a pipeline on the lee side 370 m offshore and the sediment is pumped onto the beach. Such a solution, i.e. dredging of sediment with a sea-going vessel and its deposition on the lee side with a pipeline, built inside or outside a harbor, is a typical scheme in smaller ports in Poland, where there is a predominant west to east littoral drift, causing lee side erosion due to blocking of this drift by harbor breakwaters. To visualize the scale of the problem, the amount of sediment dredged near Władysławowo between 1989 and 1998 amounted to 8.8 million m^3, which cost about $10 million.

Figure 5: Władysławowo harbor: artificial nourishment on lee (right) side

Fig. 6 presents another widely known solution; a dredger throws the mixture of sand and water into air to place the fill in shallow area, where direct access of a sea-going vessel is not possible. It demonstrates the nourishment in the Danish west coast. This technique is known as the 'rainbow method' and requires powerful and specialized equipment. It is also widely employed to nourish portions of the Hel Peninsula towards its tip. Other methods of artificial beach nourishment are less popular in Poland. They involve fills placed in deeper areas of the nearshore region with dump barges that bring the material dredged elsewhere and release it to build artificial submerged barriers. For very large and systematic nourishment schemes, floating pipelines may even be viable. They can deliver the fill dredged offshore onto the nourished segment. In cases the sand can be mined in large amounts on the land but not far from the sea, it can be delivered with belt conveyors directly onto the beach.

Artificial beach fills are widely believed to be the most versatile type of modern coastal protection. This is because it can be easily adapted to various coastal systems (reflective and dissipative shores tidal and non-tidal environments, natural and man-made segments, etc.). Moreover, it is often applied in connection with other methods of ICZM oriented coastal defense, most commonly with permeable groins and submerged breakwaters. Their role as maintenance of existing hard structures is also well recognized. It should be realized though that choosing this type of coastal protection requires re-nourishments and that enough sediment must be available now and especially in future.

Figure 6: Artificial nourishment of Danish west coast with rainbow method (Viking R dredger)

3.3 Permeable Groin Fields

This approach represents another soft measure of current coastal protection techniques. They are build for systems with stable littoral drift and sediment abundance. They largely curtail the well known side effects related to the functioning of traditional groins, shown in Fig. 7.

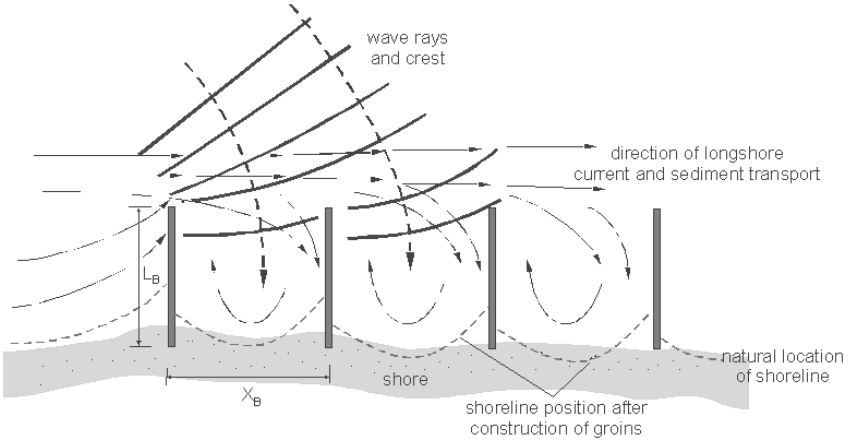

Figure 7: Undesired effects of groin; longshore current concentration and rip cell formation

First of all, such groins tend to push the longshore current just outside their tips. The resultant currents are concentrated, so their velocity is unnaturally high, prompting scour just beyond the tips. Moreover, favorable conditions for the generation of artificial rip current circulation cells are induced, so especially during periods of shore normal wave approach the sediment is carried offshore intensively. Unlike solid shore normal structures permeable groins do not fully block longshore sediment transport through their elements. Furthermore, they are less likely to activate rip currents. Over the years,

engineering experience and theoretical modeling allowed for formulation of design guides for optimum performance of permeable groin fields. It was possible, because in Poland hard solid groins were never used due to scarcity of cheap rock near the coast. Therefore, a typical permeable groin along the Baltic Sea coasts is a permeable palisade made of a single row of pine-tree trunks with clearance of two consecutive trunks between 1-2 trunk diameters. Observing the performance of such groins confirmed that the groin length L_B and their span X_B are interrelated. Moreover, the functioning of groins depends on surf zone width and angle of wave incidence. Upon these premises the ratio between usually varies between 1 and 4 for lengths ranging between 40 and 160m. For such provisions the groins occupy not more than 40-50% of the surf zone width during a storm. The elevation of groins over the sea level varies depending on the instantaneous wave climate, so sometimes they work as emergent and at other times as submerged structures. Normally, the designed elevation ranges between 0.5-1m above beach and mean sea level. Groins that are too high are impracticable, because they cause wave reflection producing scour. Interestingly, the latest Italian experience with permeable groins tends to highlight better performance of permanently submerged groins. Italian engineers argue that although the longshore sediment transport can be initially reduced by accumulation on the up-drift side, when the bottom rises up to the top of (submerged) groins the disturbance is quite negligible, Aminti 2003. Therefore, such groins acting as shoreline stabilization structures have very limited lee side effects. Another valuable factor is that submerged groins cause very little visual disturbance to coastal morphology.

Observations of more than 50 years of the behavior of groin fields on the lee side of the Władysławowo harbor or the Hel Peninsula proper suggest they alone are not sufficient for the protection of these areas. Similar developments were also observed for other small ports in Poland, where the western, lee side always suffered rapid erosion. It also corresponds to more general observations of the Polish coast, spanning 104 years between 1875 and 1979, which concluded that long term erosion of the adjacent down-drift shore near groin fields and lee sides of harbors was 4 times as fast as the average retreat during that period. Still, the performance of groin fields can be considerably enhanced in connection with other measures, particularly artificial beach nourishment and submerged breakwaters. Thus, the groin fields are now perceived to be an auxiliary measure of coastal protection, provided their use is economically justified. Fig. 8 shows the groin field on the lee side of Władysławowo harbor. A relatively wide beach was attained as the combined effect of groins and artificial sediment deposition.

Figure 8: Combined effect of groin field and artificial beach fill, lee side, Władysławowo harbor (Poland)

3.4 Submerged Breakwaters

Submerged breakwaters offer yet another solution that has gained popularity in modern coastal engineering. Generally, they are shore parallel structures in the form of underwater offshore breakwaters. Normally, they are built at depths where wave breaking commonly occurs, hence their predominant role is to force breakers and dissipate wave energy in this way. Thus, they are often regarded as artificial nearshore bars. Their second, yet equally important goal is to retard offshore sediment migration. Observations and experiments have shown submerged structures work particularly well in the conditions of (almost) shore normal wave incidence. In such instances longshore sediment transport has only secondary effects and the system is dominated by cross-shore phenomena. That is also why a synergistic effect is observed for submerged breakwaters combined with artificial beach fills.

Submerged barriers are becoming common in countries with long traditions of coastal protection with offshore emergent structures, (Aminti, 2003, Sánchez-Arcilla et al., 2003). In Italy or Spain, conventional detached mound breakwaters, made of inexpensive rock, have an established position as coastal defenses. However, observation of their long term performance also revealed clear disadvantages, such as scour and unnatural nearshore morphology in connection with unpleasant visual impressions. Furthermore, the growing economy, especially tourism, exposed perhaps the most acute drawback, i.e. emergent structures prevented natural water exchange in the protected areas. As a result, those areas became increasingly polluted due to the stagnant water, despite the growing efforts and expenses to curb discharges of untreated waste waters. To remedy all those

problems submerged alternatives of conventional coastal defenses were gradually developed, hoping adverse environmental impacts would be averted. The evolution of emergent structures to submerged breakwaters was a natural process, because the expertise accumulated during execution of traditional structures was readily available. Thus, submerged barriers in Italy and Spain stem from the same design concept as the emergent ones; they are made as mound constructions. Importantly, they can still be treated as environment friendly measures, despite using hard material for their construction, because rock abounds in most of Mediterranean coasts, being a natural component of the coastal (eco)systems there. Mound structures are also permeable, so they can dissipate more energy than purely solid structures and the reflection they generate can be reduced in this way.

The application of submerged breakwaters on sandy coasts requires additional considerations regarding their costs and environmental friendliness. Usually, submerged barriers are friendlier than traditional offshore breakwaters, because they are less likely to form areas of stagnant, dirty water between them and the shore. The use of rock is hardly possible due to potentially high costs, so the only alternative is prefabrication of suitably designed, predominantly concrete elements. They are usually positioned at depths between 2-5 m and their extension over the seabed usually falls between 0.5-1 m. A classical cross-section of a prefabricated element is a trapezoid with arbitrary crest width. The optimum width is usually dictated by trade-off between costs and expected protection effects. The offshore slope of such submerged breakwaters is about 1:4 in most cases, whereas the onshore slope is steeper and normally equals 1:2. Fig. 9 shows how such structures work; zones 1 and 5 remain unaffected, circulation cells develop in zones 2 and 4 and strong return current is produced due to the breaking waves. It demonstrates that scour and soil liquefaction can still be expected, so the resulting uneven settlement of individual elements should be anticipated. This poses a major concern related to the maintenance of submerged breakwaters. It is worth noting though, that in comparison with conventional emerged structures, the building and maintenance costs of submerged barriers are always lower.

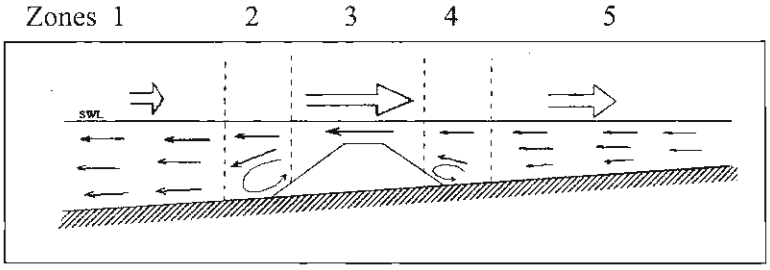

Figure 9: Impact zones of a classical submerged breakwater (after Sanchez-Arcilla et al., 2003)

In Poland submerged breakwaters have not been used yet. It is believed such schemes may become necessary to protect soft cliffs, whose erosion has been intensified during the last decades as a result of growing storminess due to global climatic changes. It is anticipated

that submerged barriers will be implemented in connection with artificial beach fills. In the most severe cases groins may become necessary as additional supplementary measure.

3.5 Reconstruction of Lost Beaches

Many coasts have lost their beaches as a result of hard protection measures. Such situation are most typical in front of seawalls and on adjacent shorelines. Although beach loss impairs local economy, until recently it was only viewed as a sad necessity. However, potential income from the recreation industry is so attractive nowadays that soft repair measures have become a seriously considered option, despite the fairly high costs. The most promising solution is formation of an artificial beach. In other words, the beach can be reconstructed with a huge artificial beach fill. Due to unnatural shape of the nearshore zone in front of a seawall such fills can require very large volumes of sediment. When gravel is used the required volume can be minimized. Gravel beaches turn out to be quite stable, but produce steep slopes. Despite this fact, the reflection they generate is much smaller that one might anticipate, due to the permeability and porosity of gravel fills. Thus, the water can infiltrate during the wave run-up and return in the form of sub-surface flow instead of the classical run-down that carries away sediment. This favors settling of grains carried by onshore fluxes and contributes to the formation of high berms, Orford & Carter, 1985. The recreational use of gravel beaches requires additional maintenance, e.g. annual re-nourishment of a beach surface with a thin layer of fine sand. Gravel beaches are becoming popular in Italy now. Fig. 10 shows the beach in Marina di Pisa, Tuscany, situated adjacent to hard structures, protecting the city and its harbor. The beach itself is designed to protect a road running along the coast. On the left hand side we can see a destroyed beach, on the right hand side the beach has been repaired.

Figure 10: Gravel beach in Marina di Pisa

The construction of this gravel beach is an interesting case study. Currently, its functioning has been monitored to observe long-term evolution of the repaired beach. The most important question the monitoring should address is whether reduction in beach permeability due to clogging of the gravel pores with finer grains can result in premature beach degradation. If the long term response of this gravel beach is satisfactory it will give grounds for substantial economic gains, because the construction of gravel beach is always cheaper than erection of hard structures. Since many roads in Italy are located on the coast, successful functioning of gravel beaches may significantly reduce their protection costs.

The other Italian site is the beach at Calagonone on Sardinia island. A degraded and repaired beach is shown in Fig. 11. The native beach was composed of mixed sediment and initially was nourished with gravel originating from crushed hard rock. Interestingly, this material, originally placed as a platform 0.3m below sea level, was moved shoreward rapidly. It was pushed to its original location three times with the same effect. The situation was improved when the fill was cleaned of its silty fraction and when the grains were rounded off mechanically, (Aminti & Capietti, 2004). Another aspect to be studied in more detail is alongshore gravel migration on fine sand beaches. This phenomenon was observed at another gravel beach in Marina di Cecina, Tuscany, where gravel and boulders were found 15 km south of the fill. In such cases submerged groins could be used to restrain such alongshore migration. These two facts show that engineering practice in dealing with gravel beaches is in the process of development and this type of soft protection calls for further research.

Figure 11: Calagonone beach (Sardinia) before (left) and after repair (right)

4. Conclusions

All techniques of soft coastal protection presented above are friendly from the environmental point of view, which can be summarized as follows.

Unlike traditional hard structures, soft coastal protection has a built-in mechanism of minimizing unfavorable side effects, such as scour, soil liquefaction or beach loss, which mainly stem from wave reflection from solid structures. Therefore, if the adopted measure is not tolerated by nature, it is rejected with little adverse effects on the environment and another type of soft solution must be developed. Such friendliness mainly originates from the fact that soft measures use mostly natural materials (sand, gravel, rock, timber, reed, etc.), so they can more easily adapt to local conditions. In this way they can respond in the most natural way to hydro- litho- and morphodynamic phenomena at the protected areas. Even if artificial material, such as concrete, has to be used, the designed elements emulate natural behavior.

The use of soft measures preserves landscapes, so ordinary people may be even unaware that they are in an engineered environment. This aspect is important for the economic side of ICZM, because coastal protection can peacefully coexist with tourism and recreation, providing a positive contribution to local economy.

Soft techniques do not impede free water exchange between nearshore regions and the main water body the way traditional detached breakwaters often do. In this way they take account of the needs of marine life, so coastal protection has no negative influence on biodiversity. This is directly related with the principles of sustainability that underline the whole ICZM methodology.

Soft measures are excellent approaches to the maintenance of existing hard structures. Suitably executed they can reduce such well known problems as the edge effects of groin fields or seawalls and scour between elements of detached breakwaters.

Soft techniques are less expensive than hard measures in most cases. Simultaneously, they require monitoring of their performance in order to establish their longevity as coastal protection. This provides perfect opportunities for coastal engineers to gain more insight into the nature of coastal processes, which in turn helps develop more refined soft solutions.

They are very flexible in a sense they can be tuned to site specific key morphodynamic phenomena, be it wave action, predominant littoral drift, sediment characteristics, etc. On the one hand this minimizes protection costs, on the other it can produce top performance.

The flexibility of soft techniques will become a crucial factor in the near future in the prospect of global climate change. The expected growth of storminess and sea level rise will have to be faced in an adaptive manner and soft techniques are capable of doing so.

The use of more than one technique can produce a synergistic effect. In this context, artificial beach nourishment appears to be the most versatile, because its efficiency is enhanced in combination with permeable groins and submerged breakwaters. Beach fills are also most commonly used for the maintenance of hard structures. Thus, this technique is believed to be the most universal.

Sustainability of coastal areas is the key target of ICZM efforts. It should be realized though the success of ICZM needs concerted actions in many fields, embracing all countries. For example, in Poland, which is believed to be a typical emerging economy, the improvement of quality of inland fresh waters is seen as a primary goal, which will need actions in the entire country before it can be accomplished. Since pollutants, discharged to rivers, always end up in coastal waters, coastal zones always indicate the country's overall environmental condition. This in turn demonstrates that sustainability of coastal zones means in fact sustainability of the whole economy. As there is a long way to go before it is feasible, coastal protection is a critical element now, because it can play a paramount role both in environmental degradation or improvement of coastal zones.

References

Aminti, P., Capietti, L., 2005, Rehabilitation of beaches intensively protected using environmental .friendly structures, Proceedings of NATO Advanced Research Workshop, Varna 25th-28th May 2004, Springer The Netherlands, this volume.

Basiński, T., Pruszak, Z., Tarnowska, M., Zeidler, R., 1993, Ochrona Brzegów morskich (*Coastal Protection*), IBW PAN Publishers, Gdańsk, 1-536, *in Polish*

Hallermeier, R.J., 1997, Calculating a yearly limit depth of the active beach profile, Tech. Pap. U.S. Army Corps of Engineers, Coastal Engineering Research Center, Fort Belvoir VA

HELCOM HABITAT 5/2003, Document 5/3, submitted by EUCC, A common approach to the implementation of ICZM in the Baltic Region: the principles underlying such an approach. A document prepared for Coastal Planning and Management in the Baltic Sea Region, as part of the fifth HELCOM-HABITAT meeting, Finland

Mangor, K., Driscoll, A.M., Brøker, I., Skou, A., 1996, Morphological impact assessment of artificial islands for the Øresund Link between Denmark and Sweden, Proc. Coastal Dynamics'95 Conference, ASCE, 939-950

Moore, B., 1982, Beach evolution in response to changes in water level and wave height. M.Sc. Thesis, Dept. Civil Eng., Univ. of Delaware, Newark DE

Orford, J.D., Carter, R.W.G., 1985, Storm generated dune armouring on a sand gravel barrier system, Southeastern Ireland, *Sed. Geol.*. 42, 65-82

Orviku, K., Jaagus, J., Kont, A., Ratas, U., Rivis, R., 2003, Increasing activity of coastal processes associated with climate change in Estonia, *Journal of Coastal Res.,* Vol.19, No.2, 364-375

Pruszak, Z., 2003, Akweny morskie. Zarys procesów fizycznych i inżynierii środowiska. *(Marine Basins. Outline of physical processes and environmental engineering)*, IBW PAN Publishers, Gdańsk, 1-272, *in Polish*

Sánchez-Arcilla, A., Alsina, J.M., Gironella, X., Cáceres, I., González, D., 2003, The role of low crested detached breakwaters in coastal engineering, Proc. Summer School-Workshop Coastal Zone '03, Lubiatowo, POLAND Aug. 25-31, 265-281

Statute Book of the Republic of Poland 116, item 503, 1991, Decree of the Ministry of Environmental Protection, Natural Resources and Forestry of 5th Nov. 1991 on water classification and waste water parameters, discharged into waters or soil *(in Polish)*

Chapter 2

Selected Participant Presentations

NUMERICAL SIMULATIONS IN COASTAL HYDRAULICS AND SEDIMENT TRANSPORT

Stephan Mai, Oliver Stoschek, Jan Geils, Andreas Matheja
Franzius-Institut for Hydraulic, Waterways and Coastal Engineering,
University of Hannover
Hannover, Germany

Abstract

Numerical simulations become more and more important within the analysis of coastal hydraulics and sediment transport. Sediment transport requires the knowledge of the flow profile related to tidal hydrodynamics and wave propagation. The basic sets of equations used in numerical modelling of the mentioned sub-processes as well as concepts of coupled numerical models are discussed within this paper. Additionally, the limits of different modelling concepts are discussed, e.g. three dimensional simulations are favourable in brackish estuarine waters because of the large density gradients caused by the difference in salinity of sea and fresh water. All different modelling concepts are applied to analyse tidal flow, wave propagation and sediment transport within the German estuaries of Jade and Weser. Special focus is placed on the analysis of the effect of climate change on coastal hydraulics.

1. Introduction

As a consequence of the improvement of computer technology, the capabilities of numerical simulations in coastal hydraulics and sediment transport have significantly increased since 1990.

Figure 1: Overview over the estuaries Jade and Weser (1)

C. Zimmermann et al. (eds.), Environmentally Friendly Coastal Protection, 149-162.

In relation to this improvement more and more problems in coastal hydraulics and sediment transport are now solved not by physical modelling but by numerical modelling, for example, in Germany, studies on the reduction of sediment entrainment into harbours were based on physical modelling until 1992 (Schwarze et al., 1995) and since then have been supplemented by (Ohle et al., 2000) or completely based on (Stoscheck and Matheja 2003) numerical modelling.

While in the beginning of numerical modelling the simulation of water levels and currents, of waves and of sediment transport were treated separately, modelling of the different aspects becomes more integrated nowadays. Nevertheless they are outlined separately in the following chapters. Besides a brief summary of the basic equations, examples of the application of different modelling approaches are given focussing on the estuaries Jade and Weser at the German North Sea. An overview of these estuaries is given in Figure 1.

2. Modelling of Water Levels and Currents

Modelling of water levels and currents is based on the equations of conservation of mass and momentum assuming water as an incompressible fluid. Simulating processes in the coastal zone, two-dimensional depth-averaged models and three dimensional models are distinguished. In 2D the basic equations are

$$\frac{1}{d}\frac{\partial \zeta}{\partial t} + \sum_{j=1}^{2}\frac{\partial u_j}{\partial x_j} = S_{QQ} \tag{1}$$

$$\frac{\partial u_i}{\partial t} + \sum_{j=1}^{2}\left(\frac{\partial (u_i u_j)}{\partial x_j} + 2\Omega_{ij} u_j \right) = -\frac{g}{d}\frac{\partial \zeta}{\partial x_i} + F_{wind,i} - F_{bottom,i} + F_{turb.,i} \tag{2}$$

with the depth-averaged flow velocity u, the water level ζ, the sinks and sources of water S_{QQ}, the acceleration of gravity g, the water depth d, the Coriolis parameter Ω, the wind forcing F_{wind}, bottom friction F_{bottom} and turbulent dissipation $F_{turb.}$.

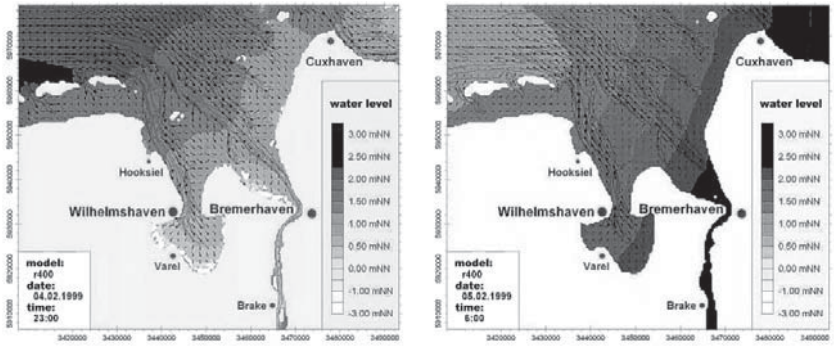

Figure 2: Tidal flow in the estuaries Jade and Weser during a storm surge in 1999, flood current (left) and ebb current (right)

In case of horizontal gradients in temperature and salinity the following conservation equations have to be considered also

$$\frac{\partial S}{\partial t} + \sum_{j=1}^{2} \frac{\partial}{\partial x_j}(S u_j) = \sum_{j=1}^{2} \frac{\partial}{\partial x_j}\left(D_S \frac{\partial S}{\partial x_j} \right) + S_{SS} \tag{3}$$

$$\frac{\partial T}{\partial t} + \sum_{j=1}^{2} \frac{\partial}{\partial x_j}(T u_j) = \sum_{j=1}^{2} \frac{\partial}{\partial x_j}\left(D_T \frac{\partial T}{\partial x_j} \right) + S_{TT} \tag{4}$$

with the depth-average temperature T, the depth-averaged salinity S, the turbulent diffusivities D_S and D_T and the sources or sinks of heat or salinity S_{TT} and S_{SS}.

An example of water levels and depth averaged flow velocities during a storm surge in 1999 calculated by numerical simulation is given for the estuaries of Jade and Weser in Figure 2 revealing a concentration of tidal flow in the fairways. The model is driven by prescription of water levels along the northern and western boundaries, of discharge of the river Weser and of the wind field over the model area. Figure 3 exemplifies the time series of boundary conditions at the north-western corner of the model area.

This model set-up is used to analyze the effect of climate change by altering the boundary conditions (Figure 3). The change in boundary conditions causes a change in the hydrodynamics of the entire coastal zone (Grabemann et al., 2004). For two locations in the fairway (P1+P3) and over the tidal flats (P4+P6) the changes in water levels and flow velocities are displayed in Figures 4 and 5.

In addition to the application of 2D numerical modelling in climate impact assessments the model can also be used to assess the effects of training works within estuaries. Figure 7 presents an example of the effect of the deepening of a fairway (Figure 6) on water levels and flow velocities. While the larger changes in flow velocity are restricted to the direct vicinity of the dredging works, changes in water level occur over much larger areas.

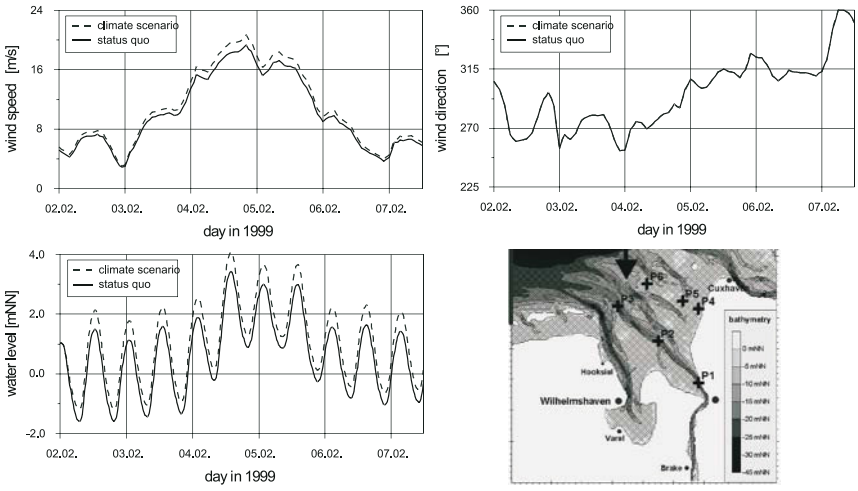

Figure 3: Bathymetry of the model area (bottom right) and scenarios of boundary conditions to analyse the effect of climate change wind speed (top left), wind direction (top right) and water level (bottom left)

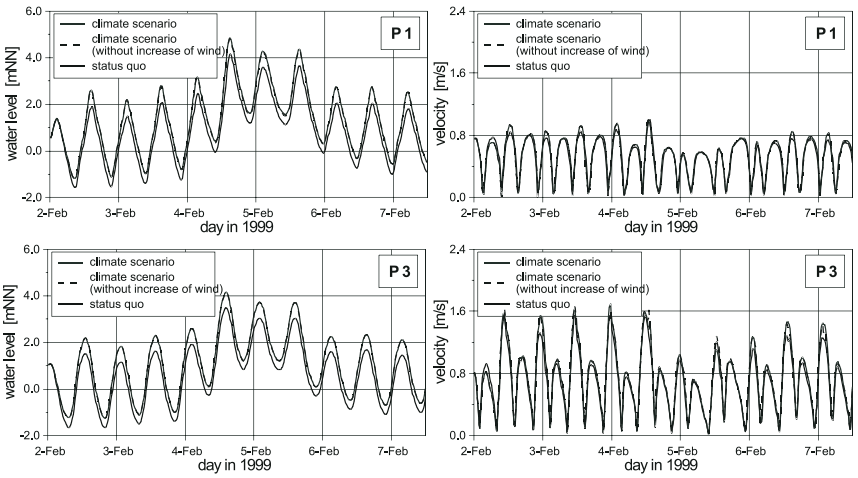

Figure 4: Effect of climate change on water level (right) and flow velocity (left) in the fairway

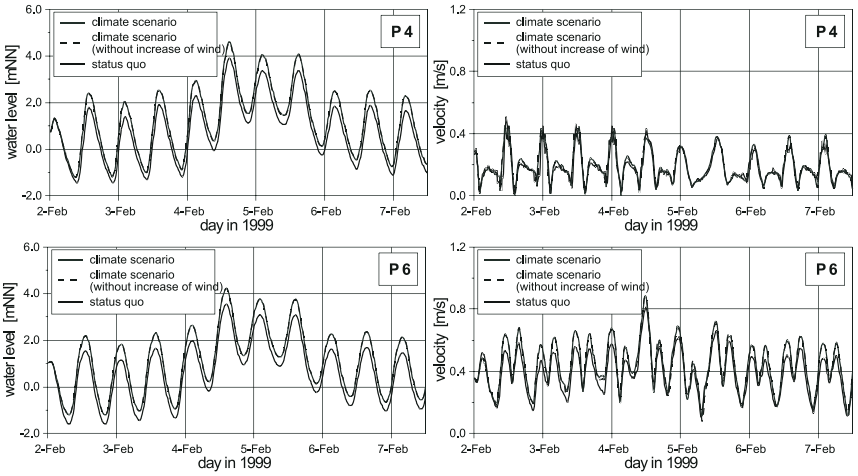

Figure 5: Effect of climate change on water level (right) and flow velocity (left) over the tidal flats

Although depth-averaged modelling gives a first impression of coastal hydraulics it is not sufficient for detailed analysis. This relates to the fact that large vertical gradients in salinity, and therefore in density, are found in coastal waters causing a significant change in the flow profile. A schematization of the flow profile with and without vertical density gradients is given in Figure 8. For this reason the vertical component is introduced into the conservation equations (1) to (4), i.e. the summation is carried out for $i = 1$ to 3. An example of vertical gradients in density or salinity respectively is given in Figure 9 displaying the contours of salinity during ebb and flood current along a cross section

outside of the harbour of Bremerhaven located on the river Weser. Fresh water is found at the surface while saline water is found at the sea floor.

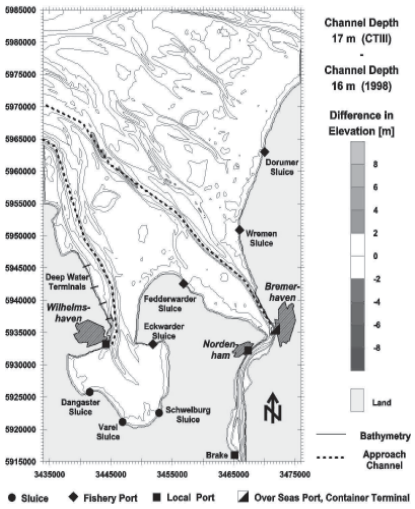

Figure 6: Dredging works within the fairway of the river Weser

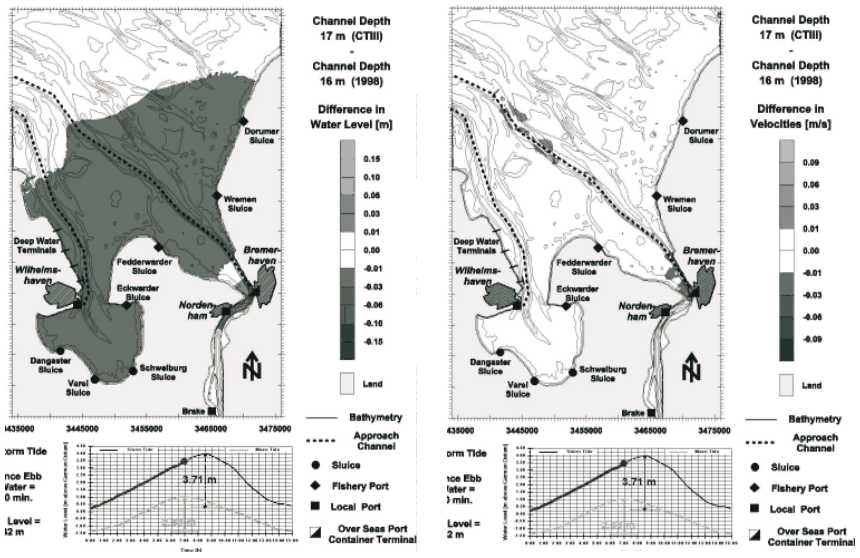

Figure 7: Effect of dredging works in the river changes in water levels (left) and flow velocities (right)

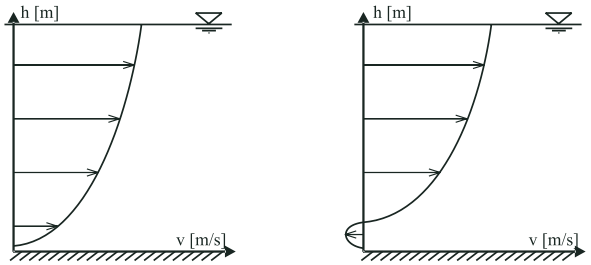

Figure 8: Flow profile with (right) and without (left) vertical gradients in density (Matheja et al., 2003)

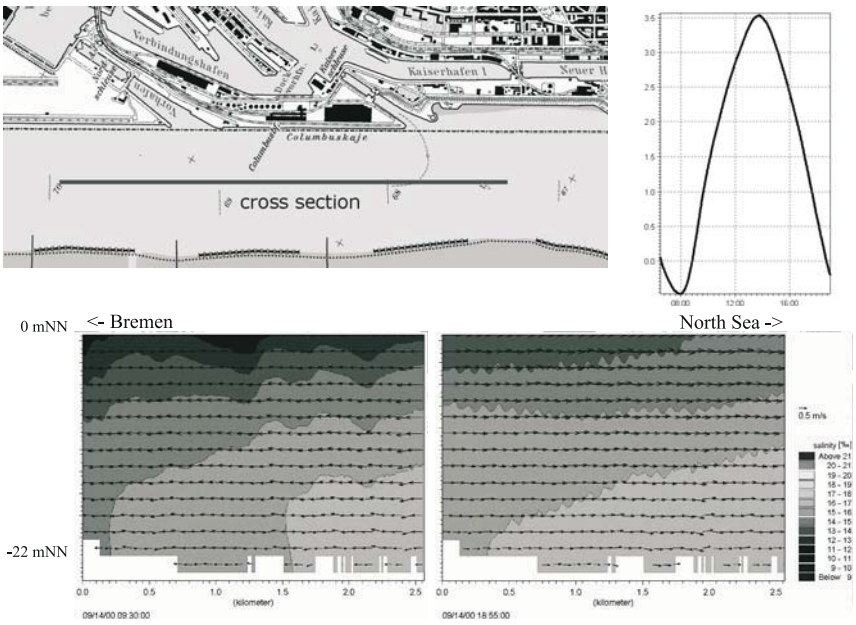

Figure 9: Cross section of the salinity in front of the harbour entrance (top) of Bremerhaven during maximum flood current (bottom left) and ebb current (bottom right)

This stratification can lead to opposite flow directions at surface and sea floor especially in harbour entrances (Figure 8 right). Figure 10 exemplifies this by showing the flow pattern in the harbour entrance called “Vorhafen” during flood current. At the bottom, the maximum inflow of saline water into the harbour is found while fresh water outflow occurs at the surface.

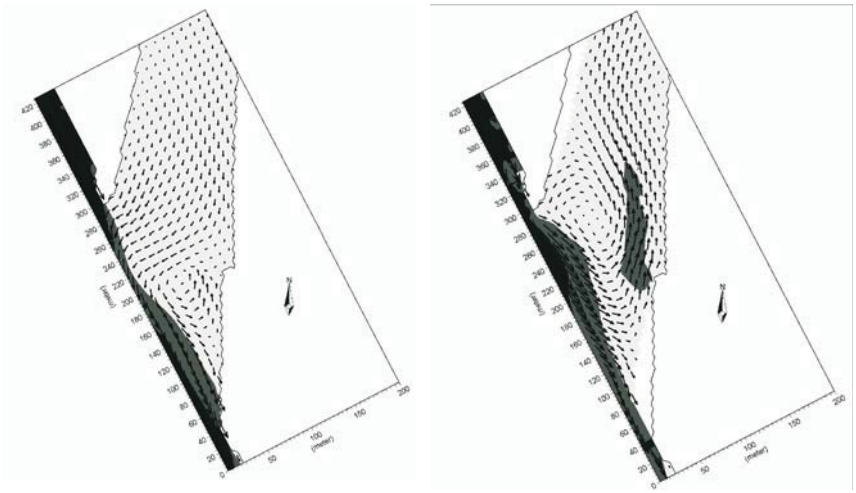

Figure 10: Flow in an entrance of the harbour of Bremerhaven during flood current, surface current (left) and bottom current (right) (Stoschek et al., 2003)

3. Modelling of Sediment Transport

The knowledge of the vertical profile of flow velocity is essential for the modelling of sediment transport due to the strong vertical gradient in sediment concentration as indicated in Figure 11. The basis to model sediment transport is a conservation equation similar to Eq. (3) and (4). However the settling velocity w_s must be introduced

$$\frac{\partial c}{\partial t} + \frac{\partial}{\partial x_j}\left(c(u_j - w_{s,j})\right) = \frac{\partial}{\partial x_j}\left(D_c \frac{\partial c}{\partial x_j}\right) + D + E \tag{5}$$

with the deposition rate D and the erosion rate E. The sub-processes of deposition and erosion are given in Figure 12.

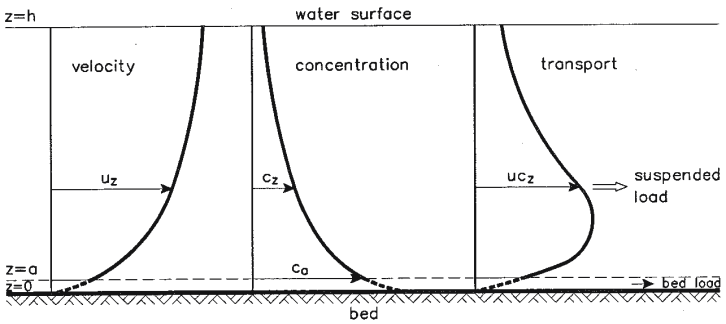

Figure 11: Profile of flow velocity, sediment concentration and sediment transport (Rijn, 1993)

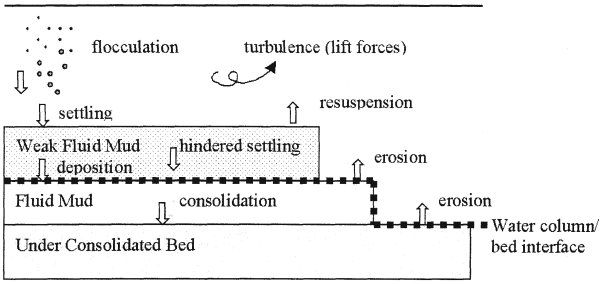

Figure 12: Processes of erosion and sedimentation (Mike3, 2000)

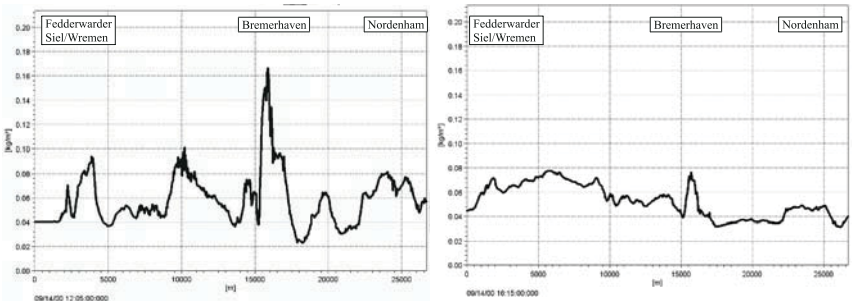

Figure 13: Sediment concentration in the estuary Weser during flood current (left) and ebb current (right)

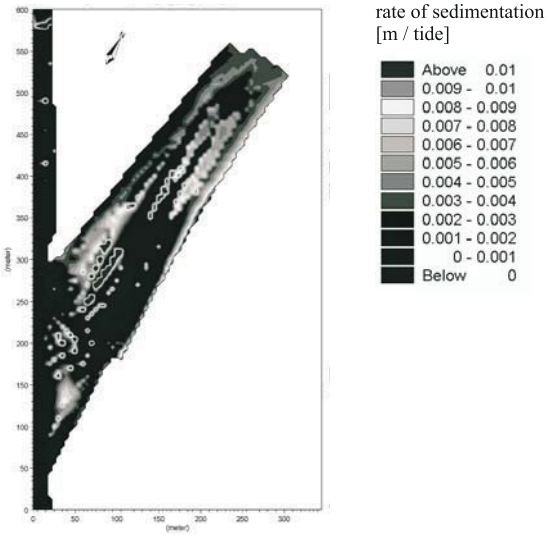

Figure 14: Rate of sedimentation within the harbour entrance of Bremerhaven (Stoschek et al., 2003)

Within the coastal zone, erosion and sedimentation undergo a strong tidal cycle and sediment concentration does as well. In Figure 13 an example of depth-averaged sediment concentration is given along the cross-section. In brackish coastal waters, sediment concentration reaches its maximum during flood current. Integrating the erosion and sedimentation over an entire tidal cycle results in the bathymetric changes to be expected over each tidal cycle. Figure 14 gives an example of this bathymetric change in the entrance to the harbour of Bremerhaven for average tidal conditions. Integrating the change over time will give the equilibrium state of the bathymetry. Changes of tidal conditions as presented in Figure 3 will cause a long-term bathymetric change. For the estuaries of Jade and Weser the bathymetric change relating to a scenario of climate change is given in Figure 15.

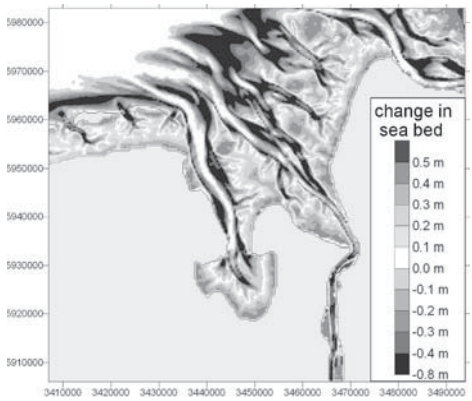

Figure 15: Long-term bathymetric changes as a consequence of climate change

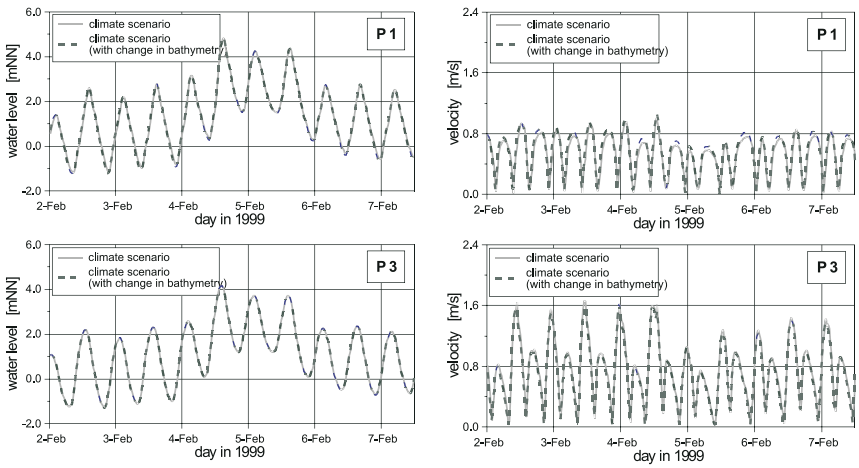

Figure 16: Effect of bathymetric changes on water level and flow velocity in the fairway

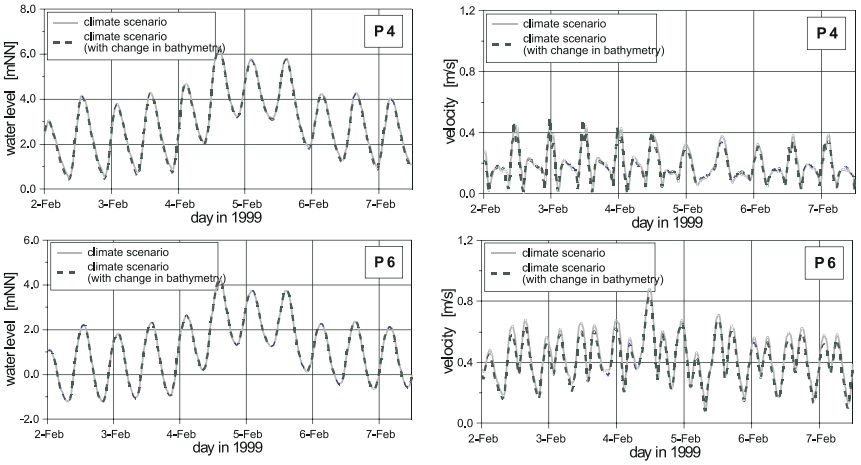

Figure 17: Effect of bathymetric changes on water level and flow velocity over the tidal flats

With the change of bathymetry the coastal hydraulics, i.e. water levels and flow velocities, change significantly. These changes are exemplified in Figure 16 and 17 for two locations in the fairway and over the tidal flats for a scenario of the storm surge of 1999.

4. Modelling of Wave Propagation

Besides of the influence of vertical density gradients, waves also alter the flow profile. The superposition of wave orbital motion and current velocity is exemplified in Figure 18. In addition to the orbital motion, additional wave induced currents also occur. The driving forces of these currents are typically calculated with phase-average numerical models, like SWAN (9, 10), based on the action balance equation

$$\frac{\partial}{\partial t}N(x,y,\sigma,\theta,t)+\frac{\partial}{\partial x}\left(c_{g,x}+u_x\right)N(x,y,\sigma,\theta,t)+\ldots+\frac{\partial}{\partial y}\left(c_{g,y}+u_y\right)N(x,y,\sigma,\theta,t)+$$
$$+\frac{\partial}{\partial\sigma}c_\sigma N(x,y,\sigma,\theta,t)+\frac{\partial}{\partial\theta}c_\theta N(x,y,\sigma,\theta,t)=\frac{S(x,y,\sigma,\theta,t)}{\sigma} \quad (6)$$

with the action density N, the current velocity u_x and u_y, the group velocity c_g, the velocities in the spectral domain c_σ and c_θ, the wave direction θ, the relative frequency σ as well as sources and sinks of wave energy, S.

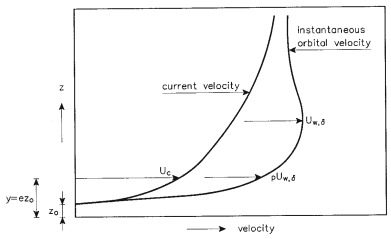

Figure 18: Effects of waves on the profile of flow velocity (Rijn, 1993)

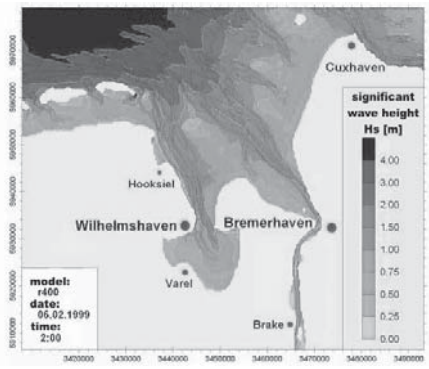

Figure 19: Wave propagation (significant wave height) in the estuaries Jade and Weser during a storm surge in 1999 (Mai and Zimmermann, 2004)

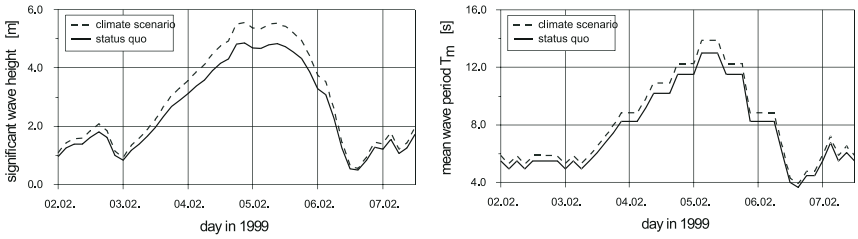

Figure 20: Scenarios of boundary conditions to analyse the effect of climate change in terms of significant wave height (left) and mean wave period (right) of the incoming wave field (Mai and Zimmermann, 2004)

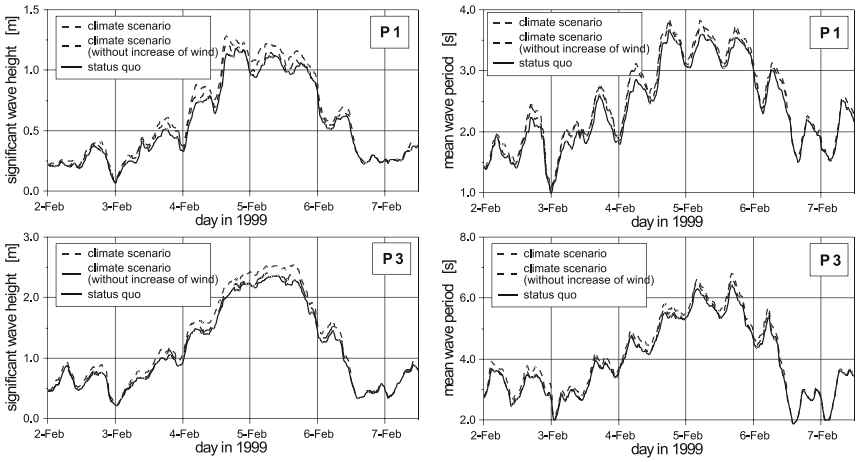

Figure 21: Effect of climate change on significant wave height (left) and mean wave period (right) in the fairway (Mai and Zimmermann, 2004)

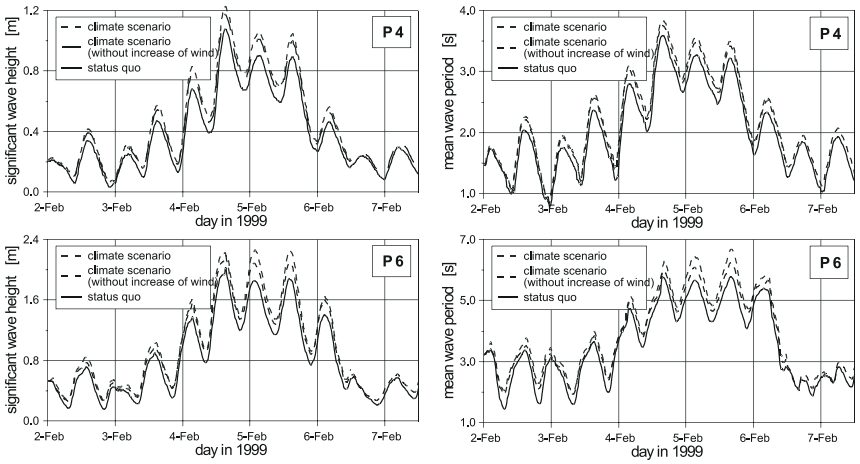

Figure 22: Effect of climate change on significant wave height (left) and mean wave period (right) over the tidal flats (Mai and Zimmermann, 2004)

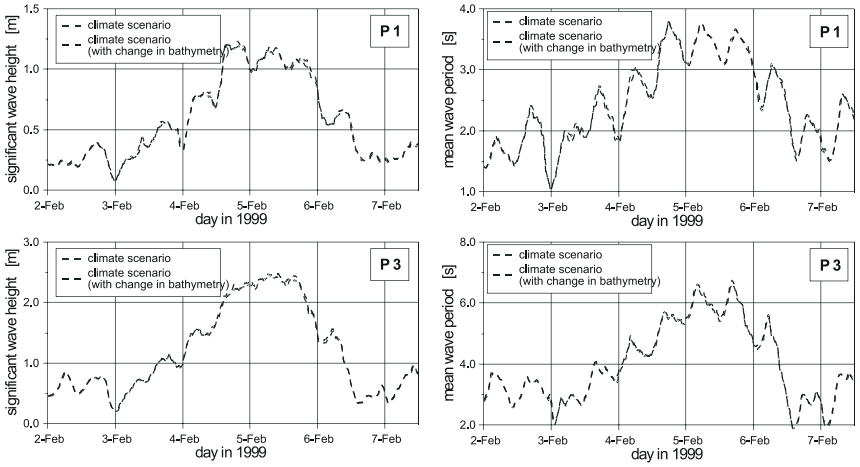

Figure 23: Effect of bathymetric changes on significant wave height (left) and mean wave period (right) in the fairway

Figure 19 presents an example of the wave field within the estuary of Jade and Weser during a storm surge in the year 1999, already given in Figure 3. In addition to the tidal water levels and flow conditions, as given in Figure 2, the incoming wave field was prescribed. The time-series of significant wave height and mean wave period are given in Figure 20. In addition to assumed climate changes, a possible scenario of the boundary conditions is also included to the status-quo. With the change in boundary conditions the wave parameters in the fairway and over the tidal flats also change, as indicated in Figure 21 and 22. The relative change over the tidal flats is approximately twice as great as in the

fairways. In the case of the long-term bathymetric changes given in Figure 15, the increase in wave height and wave period is partly compensated. Figure 23 and 24 prove this.

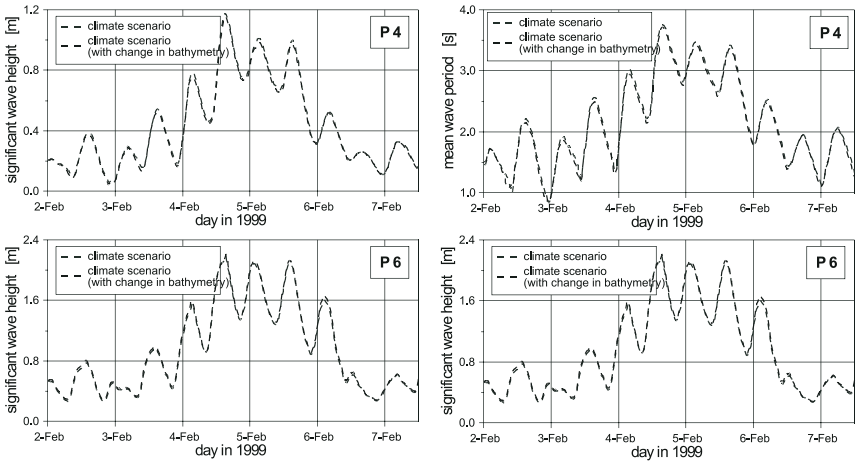

Figure 24: Effect of bathymetric changes on significant wave height (left) and mean wave period (right) over the tidal flats

5. Summary/Conclusion

The basic concepts of modelling in coastal hydraulics have been illustrated. In these models, the correct representation of the velocity profile, is essential for the correctness of sediment transport modelling. Therefore three-dimensional modelling is needed in brackish coastal waters. In addition to the 3D treatment of tidal flow, the inclusion of wave induced currents as well as wave orbital motion lead to further improvement of the results.

Acknowledgments

This work is based on the research projects “Climate Change and Preventive Risk and Coastal Protection Management on the German North Sea Coast” and “Measures for Minimization of Sedimentation in Harbour Entrances”. These were funded under Grant 01 LD 0014 by the German Federal Ministry for Education, Research and Science (BMBF) and under Grant 03 KIS 020 by the German Coastal Engineering Research Council (KFKI) respectively gratefully acknowledged by the authors.

References

Booij, N., Ris, R.C. Holthuijsen, L.H.A., 1999, “Third-Generation Wave Model for Coastal Regions, 1. Model Description and Validation”, JGR, 104, Washington, USA, 7649-7666

DHI, “Mike3 Estuarine and Coastal Hydraulics and Oceanography, Mud Transport Module, 2000, Scientific Documentation“, Horsholm, Dänemark

Grabemann, H.-J., Grabemann, I., Eppel, D. P., 2004, "Climate Change and Hydrodynamic Impact in the Jade-Weser Area: Case Study", Coastline Reports, 1, Warnemünde, Germany, 83-92

Mai, S., Zimmermann, C., 2004, "Impact of Climate Change on the Wave Conditions in Estuaries of Jade and Weser", Coastline Reports, 1, Warnemünde, Germany, 93-100

Matheja, A., Stoschek, O., Geils, J., Zimmermann, C., 2003, "Effects of a Current Deflection Wall in a Tidal Harbour Entrance", Proc. of the 6th Int. Conf. on Coastal & Port Engineering in Development Countries, Colombo, Sri Lanka

Ohle, N., Mai, S., Zimmermann, C., 2000, "Comparison of Physical and Numerical Simulations of Currents", Proc. of the 4th Int. Conf. on Hydroinformatics, Iowa, USA

Rijn, L.C., 1993, "Principles of sediment transport in rivers, estuaries and coastal seas", Aqua Publications, Amsterdam, The Netherlands

Ris, R.C., Holthuijsen, L.H., Booij, N., 1999, "Third-Generation Wave Model for Coastal Regions, 2. Verification", JGR, 104, Washington, USA, 7667-7681

Schwarze, H., Streich, G., Zimmermann, C., 1995, "Reduction of sedimentation in harbour entrances on tidal rivers by modifications of the entrance geometry and installation of stream guiding structures", Proc. of the 4th Int. Conf. on Coastal & Port Engineering in Developing Countries, Rio de Janeiro, Brasil, 1652-1662

Stoschek, O., Matheja, A., 2003, "Underwater structures against sedimentation at a ship berth in a tidal river", 6th Int. Conf. on Coastal and Port Engineering in Developing Countries, Proceedings, Colombo, Sri Lanka

Stoschek, O., Matheja, A., Geils, J., Zimmermann, C., 2003, "Dredging alternatives - The current deflection wall minimizing dredging activities in harbours", CEDA Dredging Days 2003, Amsterdam RAI, Netherlands

REHABILITATION OF HIGHLY PROTECTED BEACHES BY USING ENVIRONMENT-FRIENDLY STRUCTURES

L. Cappietti, P. L. Aminti
DIC – Department of Civil Engineering, University of Florence
Florence, Italy

Abstract

In the last few years, environmental impact has been one of the most discussed topics in Coastal Engineering. Actually, conferences on subjects like "soft shore protection" or "environment friendly-structures" have been held all over the world. However, there is still not a general agreement on what environment-friendly means for a coastal protection structure. In this work we try to give a better clarification of this subject by showing some relatively new coastal protection structures that can be considered environment-friendly. Results from laboratory experiments, numerical simulations and field experiments are reported. Concerning Low-Crested Structures (LCSs), laboratory experiments on the piling-up phenomenon are presented. Numerical simulations of flow field around a submerged groin and the morphodynamics measured by field monitoring are discussed. Finally, two case studies of gravel nourishment and their effectiveness are described.

1. Introduction

Beach erosion, which started affecting Italian coasts during the second half of the 19th century, has been controlled mainly by means of rubble-mound structures like breakwaters and groins. Starting from the first pioneering realizations (Franco, 1996), the coastal engineering community has monitored many such structures so that the knowledge of their effectiveness has been increased. This background should constitute the cultural base when a new type of shore defence structures is proposed. Nowadays, coastal managers focus their attention on the so-called "soft shore protection" or "Environment-Friendly Protection Structures" (in the following EFPS) although there is not any general agreement on what environment-friendly means. Actually, there are many different environmental aspects that need a "friendly structure", but coastal managers should be warned that in any case the goal remains the protection of the coast. In this perspective[1], any structure based on coastal engineering experience and optimised in order to preserve its positive behaviour and decrease its specific environmental impact can be considered an EFPS.

Conventional breakwater and groins have shown some effects that are negative for the coastal environment i.e. they are environment-unfriendly. Actually, long-term monitoring surveys show that detached breakwaters are able in general to control shoreline retreat, but

1 Concerning this point of view authors appreciated very much the discussion with Dr. Joan Pope during the Nato ARW, Varna, Bulgaria.

C. Zimmermann et al. (eds.), Environmentally Friendly Coastal Protection, 163-175.

they cannot control the offshore submerged beach deepening. Moreover, large values of wave induced current velocities at the gaps have been measured and scour channels often occur around the gaps (Aminti and Cappietti, 2003). Offshore submerged beach deepening and scour at gaps may cause frequent structure failures and heavy maintenance work is required to complete reconstruction of the barriers.

Groins have been used in Italy mainly in the last 50 years, although they are less popular than segmented breakwaters. Impermeable groins may concentrate rip currents on the up-drift side or interrupt sediment transport. When the groin spacing is small, they produce concentrations in velocity field seaward of the groin heads, with consequent scour and bottom deepening.

Considering this environment-unfriendly phenomenon related to the conventional coastal protection structures, changes were proposed to increase their efficiency. In the following chapter Low-Crested Structures (LCSs), submerged groins and gravel nourishment are discussed.

2. Piling-up Phenomenon in Presence of Low-Crested Structures

In recent years, interest in Low Crested Structures (LCSs) has been growing. They have become popular in beach defence in Italy and Europe although the understanding of their functionality and their project criteria were really poor. With respect to emergent breakwaters, they are less efficient in reducing the incident wave height, but their functionality in protecting beach nourishments has been widely recognised in the past few years. However, after wave breaking by the barrier the mass of water that passes over the barrier generates the piling-up. The phenomenon consists of a gradual increase of MWL behind the barrier. It is to be remarked that when submerged barriers show their highest efficiency in reducing transmitted waves there is also a maximum piling-up. This phenomena does not occur in conventional structures and can induce negative long term evolution of shoreline and coastal profile; moreover overtopping for LCSs, is potentially abundant so that its underestimation and therefore underestimation of the return flow have been the primary cause of failure of LCSs.

Italian experiences of recently built LCSs can be seen at Pellestrina, Venice, Lido di Dante, Ravenna and Ostia Lido (Lamberti and Mancinelli, 1996). Sometimes conventional breakwaters have been converted to LCSs in order to reduce their impact on the landscape. During the last four years, thematic projects for studying LCSs were conducted, such as the Italian PRIN 2001 *"Idrodinamica e morfodinamica di spiagge protette da opere tracimabili"* or the European DELOS providing an improved understanding of many aspects related to these structures and some guidelines for their design. However, piling-up, which is a crucial aspect of LCSs, has not been completely understood yet. References concerning this subject are very limited, most notably Diskin (1970), Lovless, (1998), Drei and Lamberti (1999), Ruol (2002).

A new set of experiments are in progress at the University of Florence in order to study the relation between piling-up and overtopping for low crested structures. Some of the experiments were conducted within the above mentioned Italian project and further tests are still in progress in a wave-current flume facility. The flume is 47.0 m long, 0 :8 m wide,

0.8 m high and is equipped with a recirculation system that may provide a maximum discharge of 0.025 m^3/s controlled by a magneto-electric flow meter with 0.15% accuracy. The depth decreases monotonically starting from the wave paddle towards the end of the flume. Starting from the wave generator the bottom is composed by a horizontal plane for 8.0 m; constant slope 1:100 for 30.0 m; horizontal plane for 2.4 m, over which the structure is placed; constant slope 1:20 (providing wave absorption) until the shore. Water depth in front of the wave paddle was for all tests equal to 50 cm, which results in 20 cm at the structure.

Two different kinds of trapezoidal LCSs formed by stones with nominal diameters in the range 4 to 8 *c*m, were tested. The structure *AE* is characterized by freeboard *Rc* = +5 cm, berm width of 20 cm and side slopes of 1:2 whereas the structure *D*0 is characterized by null *Rc*, berm width of 40 cm and lateral slope of 1:2. Measurements have been carried out using 15 wave gauges (*WGs*), of which 1 is placed in front of the wave-maker, for checking the generated waves; 4 are in front and 3 behind the structure for measuring reflection, transmission and piling-up; 7 are inside the structure, for analysing overtopped wave evolution; 2 three-dimensional Acoustic Doppler Velocity meters (*ADVs*), of which 1 is placed in front and one inside the structure, for measuring filtration; 1 propeller just over the structure, for obtaining overtopped wave celerity; 8 piezometers connected at the two edges of the structure, for measuring piling-up; the piezometers are pipes with small diameter, so that surface oscillations are naturally filtered out. The layout of the experimental apparatus is reported in Figure 1.

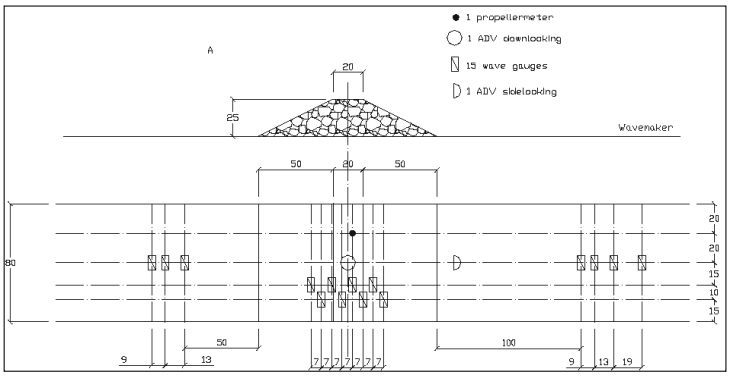

Figure 1: Cross section of the tested structure AE (up) and plan view of the flume (down), with instruments placement

A summary of the reproduced wave conditions are reported in Table 1. Whereas, the results of reflection analysis, carried out using the method proposed by Goda and Suzuki (1976) are reported in Table 2. Irregular waves were generated by an hydraulic piston-type wave-maker driven by a signal obtained using the Deterministic Spectral Amplitude method, according to Hughes (1995). A target JONSWAP spectrum was generated with peak enhancement factor $\gamma = 3.3$.

Table 1: Target wave parameters

Code	*H*mo (cm)	*T*p (s)	*S*op = *H*mo = *L*op
0510J	5	1.0	0.030
1015J	10	1.5	0.030
1518J	15	1.8	0.030
1525J	15	2.5	0.015
1515J	15	1.5	0.045

Table 2: Results of the reflection analysis

Test	H_i (cm)	k_r (%)	k_t (%)
0510JAE	1.1	19	4
1015JAE	3.9	27	8
1518JAE	8.1	34	9
1525JAE	8.5	39	13
1515JAE	7.7	33	8
0510JAE	1.0	15	9
1015JAE	7.9	25	15
1518JAE	8.0	29	15
1525JAE	8.5	32	21
1515JAE	6.9	25	15

Every test included 6 runs, characterised by a different recirculation discharge, starting from a null value and increasing gradually until a null or negative piling-up was measured. Runs were 20 min long in order to approach stationary conditions and included more than 600 waves. Data analysis was carried out on the last 5 minutes acquisition of each run of 20 minutes. The tests suggest that a return flow is driven through the permeable structure, resulting in turbulent conditions, with discharge directly proportional to piling-up. Furthermore, the overtopping discharge in totally confined conditions appears proportional to piling-up even for different wave conditions.

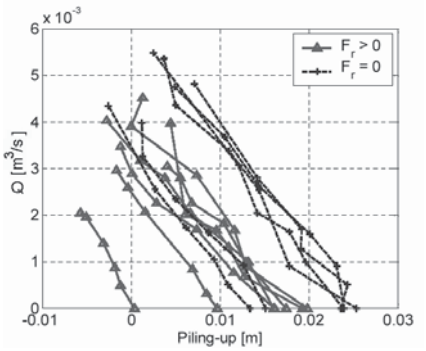

Figure 2: Recirculation discharge vs piling-up. Each curve represents a single test and is formed by 6 points, corresponding to each run

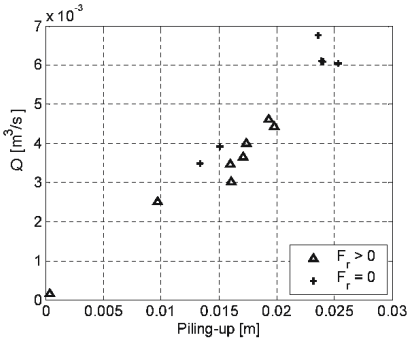

Figure. 3: Overtopping discharge for null piling-up vs piling-up for null recirculation

Overtopping for null piling-up is a function of the incident wave conditions and of the structure geometry. A clear relation has not been found yet, but Fig. 3 shows that, for the different tests, the discharge flowing over the structure is roughly proportional to piling-up in confined conditions. This observation suggests that the dependency on incident wave parameters and structure geometry of both variables must be similar. Fig. 3 confirms the results obtained by Ruol and Faedo (2002); the slope of the hypothetical line fitting the data is also similar. It should be stressed that the target structure geometry is equal to Roul's and is formed by stones of the same size, so that permeability is also

similar. Analysing each test, which is characterised by a given wave load and different recirculation degrees, the relation between recirculation discharge and piling-up appears to be inversely proportional (Fig.2). Discharge Q and piling-up p in intermediate conditions of confinement can be found by a simple proportionality law on the basis of the two extreme conditions, piling-up for null recirculation and discharge for null piling-up. A simple interpretation of this behaviour is based on the assumption that inshore-directed overtopping Q does not depend on piling-up and is constant during the test. The recirculation discharge increases for each run, affecting filtration and piling-up. According to Lamberti et al. (2003), a linear relationship between piling-up and filtration can be assumed. In totally confined conditions, i.e. in absence of recirculation, the overtopping and filtration are in equilibrium for a given value of piling-up. When the recirculation is artificially forced, the piling-up, and therefore the filtration, is reduced. For any value of piling-up, filtration is given by the difference between overtopping Q and the actual recirculation discharge. In other words, Q can be measured by means of the recirculation system when the filtration is null, i.e. when the observed piling-up is null. Moreover the direct proportionality between piling-up and filtration results in an inverse proportionality between piling-up and recirculation for same test conditions. This relation explains the trend shown in Fig. 3.

3. Submerged Groins

Groins are another example of traditional shore defence structures widely used all around the world. At the state of the art there are still many discussions about their effectiveness (see for instance *J.* Coast. Research, Special Issue, Winter 2004). Groins should be employed in presence of substantial long-shore sediment transport in order to act as a trap for the sand. They are often criticized by coastal managers since sometimes they have shown scarce efficiency in shore protection and induced unexpected long term shoreline evolution. Indeed, their impediment to sediment transport leads to beach deposition up-drift, but on the other hand may cause problems down-drift if there is a beach that still needs to be preserved. Moreover, they can induce the formation of rip currents up-drift, with consequent seaward loss of sediments, and stationary macro-vortex down-drift. Because of these environmental unfriendly effects, changes to the shape of conventional groins have been proposed in order to preserve their positive features and minimise the negative one. Increasing the sand bypassing with respect to conventional groins is one of the main goals that has been studied. Many different modified groins have been proposed, one of which - where tidal range is low - could be represented by submerged or partially submerged groins as shown in Figure 4. In principle, a submerged groin can reduce the long-shore current velocity and sediment mobility with respect to the unprotected beach. They have been recently used as protection structures to beach nourishments in different protection designs along Italian coasts (Berriolo, 1993); their effectiveness is at present under study but in many cases initial results have been encouraging.

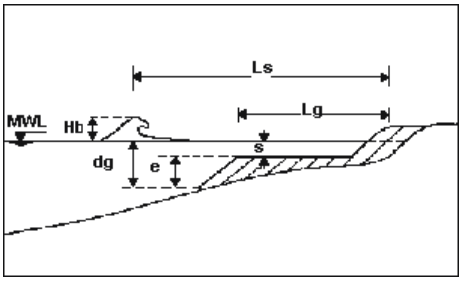

Figure 4: Typical shape of a submerged groin and its characteristic functional parameters

Numerical simulations of an ideal case and field experiments were performed. The coast was assumed to be infinitely long with straight and parallel bathymetry. Its profile was schematised as a plane with slope of 2% from water depth of 0 to –6 m and 1% from –6 m to deep water. Groin lengths ranged from 150 m to 250 m and the submergence from 0.5 m to 1.5 m. The simulated waves were characterised by $H = 2$ m, $T = 6.8$ s and direction ranging from 5° to 15°. Results show that the formation of the rip current up-stream is avoided. Moreover, the stationary macro-vortex downstream is minimized due to the reduced long-shore gradient of the wave set-up respect to the emerging type (see Fig. 7 and Fig. 8).

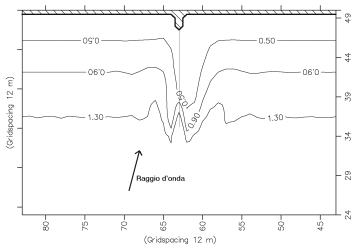

Figure 5: Contours of simulated wave height field around a submerged groins

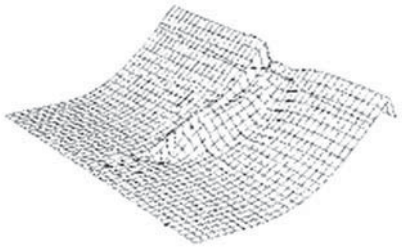

Figure 6: Long-shore variations of wave set-up around a submerged groins

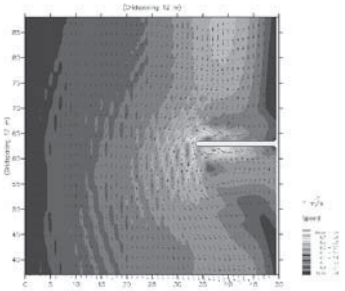

Figure 7: Simulated wave-generated currents in presence of a conventional groin

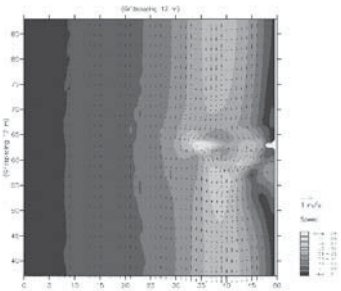

Figure 8: Simulated wave-generated currents in presence of a submerged groin

However, wave-structure interaction leads to a local focusing of refraction processes at the groin tip resulting in anomalous wave heights. In fact once the wave propagates from water depth in front of the groin tip up to the submerged part of it, its wave energy cannot be dissipated instantaneously so that wave height increases drastically. Such discontinuity produces violent breaking from which a strong radiation stress gradient results that is able to induce large shoreward currents (see Fig. 5 and Fig. 6).

Results from numerical simulations were analysed. A plot of dimensionless wave height at groin tip (H_g / H_b) versus dimensionless groin elevation (e / d_g) is reported in Fig. 9 whereas a plot of dimensionless maximum velocity at groin tip ($V_{\max} / \sqrt{g.H_b}$) versus dimensionless groin elevation (e / d_g) is reported in Fig. 10. It is evident that once the submergence approaches zero (i.e. e / d_g tends to one) the interaction between the waves and the groins leads to a local increase in wave height and the generation of strong currents. On one hand, both effects can induce a remarkable morphodynamics around the groins tip. On the other hand, they may represent a danger for the safety of bathers.

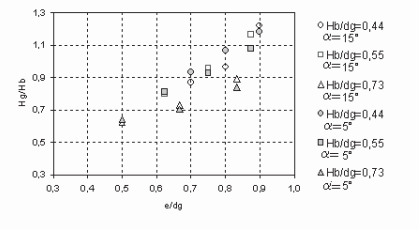

Figure 9: Dimensionless wave height at groin tip VS dimensionless groin elevation, for different wave conditions

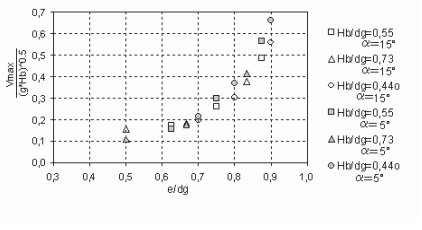

Figure 10: Dimensionless maximum velocity at groin tip VS dimensionless groin elevation, for different wave conditions

A field study is in progress on the beaches of Marina di Ronchi (Tuscany, Italy) where 4 submerged groins were built in the last 3 years. A picture taken during the construction is reported in Figure 11.The impacts of the groin are mostly in the subaqueous profile. The visual impact of the structure is negligible because the groin is completely covered by sand on the backshore and in the nearshore, and there are no conspicuous morphological changes on the upper beach. A detailed survey was performed for the first groin including evaluation of beach morphology and sediment characteristics. Correlation with wave data, measured morphodynamics, sediment budget calculations and numerical simulations are reported in Aminti et al., (2004).

Figure 11: Submerged groins construction at Marina di Ronchi (Tuscany, Italy)

In summary, the first year field study suggested that the submerged groin can interact with nearshore dynamic contributing to the elevation changes caused by the seasonal cross-shore displacement of bar-trough system, although it may not change the overall character of the system. Actually its performances are related to its length compared to the surf-zone width. Moreover, the longshore sediment transport may be initially reduced down-drift by the accumulation on the up-drift side, but when the bottom surface rises up the top of the structures the disturbance is quite negligible. In fact, long term shoreline evolution does not shows the unnatural behaviour induced by an emergent groin. However, the groin as constructed did not fully cross the bar system and strong currents were concentrated at its tip, resulting in deep scouring that could lead to the damage of the head of the structure.

Numerical simulations of this field prototype were performed in order to simulate wave-structure interaction, the resulting wave-induced current velocity and the short-term morphological evolutions. Simulations indicated that the short-term morphodynamics were consistent with the observed long-term scour formation since scour processes at the tip of the groins occurred in the simulations, also. The numerical model showed that this scour is due to a meandering longshore current moving between the bars and surrounding the tip of the groin. This agreement between simulated and measured morphological evolution justified the performance of new simulations to investigate how the changes in the geometrical properties of the groins were able to eliminate this environment-unfriendly effect. Results showed that the lengthening of the groins beyond the bar system eliminates the problem (see Fig. 12).

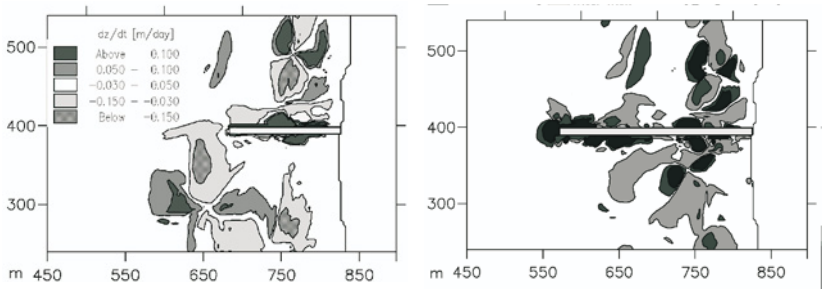

Figure 12: Numerical simulations of the short term morphodynamics induced by groins of different lengths. On the left, the simulation of prototype realization at Marina di Ronchi where long term large scour at the seaward end of the groin was measured. On the right the simulations of the lengthening of the groins beyond the bar system are presented

The structure is still being monitored and the complete results are not available, but a generalized bottom elevation and a shoreline stabilization observed in a coast affected by chronic erosion could be considered as an encouraging result.

4. Converting Sea-Walls into Artificial Beaches Using Gravel Nourishment

Gravel beach fills can provide an alternative solution for a coastal protection substituting an existing seawall and restoring a more natural system. In fact in many cases beaches have been completely lost in front of seawalls. In case a seawall is present, a large quantity of sand is required due to the unnatural shape of submerged beach profile, but it will be quite expensive. Gravel beaches are more stable, but their resultant profile is very steep. This induces problems in management for leisure use and maintenance. This section discusses results based on several years of monitoring of two experimental beaches in Tuscany and Sardinia.

Marina di Pisa is a seaside resort on the Southern side of the Arno River delta (central Tuscany, Fig. 13) which dates back to the early decades of the 19th century. The changes in land use inside the catchment and river bed quarrying, together with dam construction, reduced the river sediment load from the estimated value of 5x10^6 m^3/yr during the 17th century to about one fifth of this value in recent years. Strong erosion started in mid 19th century at the delta apex and gradually expanded to the lateral beaches. Detached breakwaters and seawalls were built after the World War II and gradually expanded southwards, following the erosion but being themselves co-causes of this phenomenon. The coastline is now defended for 2.5 kilometres by a continuous seawall and 10 breakwaters; in addition, a few groins divide the protected coast into five cells of different size. As a result, more than 5 km of hard structures defend 2.5 km of coastline. Toe scouring and breakwater collapse call for frequent maintenance, performed by adding boulders on the top of the same breakwaters. Those structures are no longer sustainable.

Figure 13: Marina di Pisa: aerial view

A new project is based on razing the detached breakwaters to the sea level and absorbing the overtopping waves with a gravel beach placed in front of the present seawall. The transmitted waves in the seaward zone can be efficiently absorbed by coarse sediments, which proved to be very stable both in nature and in artificially nourished beaches, thanks not only to their size, but also to their permeability and porosity (Pacini et al., 1999). These characteristics allow the water to infiltrate during the *uprush*, and the same water goes back to the sea through a sub-surface flow, which does not give rise to those tractive forces acting during the backwash and responsible of the grain removal from the swash-zone. In order to test the effectiveness of the project, a physical model of the Marina di Pisa coast was performed, in a two-dimensional model at the scale of 1:25, at the Civil Engineering Department of the University of Florence. The main results can be summarized as follows. Significant wave height ($H_{1/3}$) at the beach base is related to the transmission coefficient of the breakwater and by the reflection index of the work near the beach. The former is strictly determined by the height of the breakwater above the sea level (van der Meer, 1992). When a low reflectivity beach is present, the mean wave height increase produced by the breakwater lowering is only partially balanced by the reduction in the wave reflection by the nearshore structures, and wave height in the protected zone is significantly increased. Setup values behind the detached breakwater increased when low emergent breakwaters were converted to submerged structures with a gravel beach behind. Run up values were significantly reduced by a gravel beach.

Moreover, at the Southern limit of the stretch defended by detached breakwaters and seawalls, a gravel beach was built to protect the street along the coast. The main function of the beach is to protect the road but it can also create a waterfront between the city and the sea (see Fig. 14). The new beach can be used for recreational purposes. This new beach represents a link between the sandy southern beaches and the urban waterfront, protected by seawall. The beach profile shows a characteristic crest and a very steep seaward slope. Under storm wave attack, the crest moves landward. The protection is efficient only if the volume of gravel is sufficient to allow a retreat maintaining a protection of the seawall by the direct wave attack.

Figure 14: Marina di Pisa beach before nourishment (left) and after nourishment (right)

The construction of this gravel beach represents an interesting case study because in Italy there are hundreds of kilometres of coastal roads affected by erosion processes requiring protection. The gravel beaches can be quickly built and their cost is relatively low compared to seawalls and breakwaters. The behaviour of this beach and its evolution when permeability is reduced by trapping of sand, is under monitoring.

The tendency of gravel to move onshore on mixed sediment beaches was also observed during recent beach nourishment performed in Sardinia at Calagonone (Pacini et al., 1999); here, fill material – gravel produced from hard rock cracking – was pushed offshore for three times, forming a platform at 30 cm below the sea level; each time waves brought it back immediately to the shore (Fig. 15). This facilitated the cleaning of the material from the silty fraction and a preliminary rounding of the grains.

Figure 15: Calagonone beach before nourishment (left) and after nourishment (right)

Another aspect to be studied in detail is the high mobility characterising gravel on fine sand beaches. In the case of Marina di Cecina (Tuscany), four years after the gravel nourishment, the material was found 15 kilometres southwards. Similar results have been observed at Lido di Policoro (Matera) (Aminti and Pranzini, 2002), where gravel and boulders discharged without any protection on the shore have spoiled a downdrift fine sand beach. All this suggests that the offshore dispersion of the filling is very limited, but strong lateral fluxes are to be taken into account. In our project this flux is reduced by short groins connected to the underwater parallel structure with a submerged connection.

Acknowledgements

The support of MIUR (Ministero Università e Ricerca), under PRIN 2001 *"Idrodinamica e morfodinamica di spiagge protette da opere tracimabili*", Prot. 2001082247, is gratefully acknowledged.

References

Aminti P.L., Cappietti L., 2003, Sea bottom scour near gaps in coastal protection structures. In Int. Conf. Medcoast

Aminti P.L., Cappietti L., Cammelli C., Norstom K., Pranzini E., 2004, Evaluation of beach response to submerged groin construction at Marina di Ronchi, Italy, using field data and numerical model simulation, *Journal of Coastal Research*

Aminti P., Pranzini E., 2002, Spiagge artificiali in ghiaia per la difesa e l'utilizzazione turistica del litorale, atti del convegno Riqualificazione e salvaguardia dei litorali: idee, proposte e confronti tra esperienze mediterranee. Bernalda

Berriolo G., 1993, Interventi di riequilibrio delle spiagge della provincia di Latina. Conv. Naz. La difesa dei litorali in Italia, Cecina. pp.153 -174

Diskin, 1970, Piling-up behind low and submerged permeable breakwaters. Journal of the Waterway and Harbour division - ASCE

Drei E., Lamberti A., 1999, Wave pumping effect of a submerged barrier. In Proc. Coastal Structures'99, Santander, Balkema, pages 667–673

Environment Friendly Coastal Protection Structures, Advanced Research Workshop NATO, 25-27 May 2004, Varna Bulgaria

Franco, L., 1996, History of Coastal Engineering in Italy, in History and Heritage of Coastal Engineering, Edited by Nicholas C. Kraus, ASCEE

Goda and Suzuki, 1976, Estimation of incident and reflected waves in random wave experiments", Proc. 15th Int.Conf. Coastal Engrg. Hawaii, pp. 828-845

Lamberti A., Mancinelli A., 1996, Italian experience on submerged breakwaters as beach defence structures. In ASCE, Billy Edge, Editor, Int Conf. of Coastal Engineering, pages 2353 –2365

Lamberti, A., Zanuttigh B. and Kramer, M., 2003, Waves and current flow around low-crested structures, Proc. Coastal Structures 2003, Oregon

Loveless J., Debski D., and MacLeod A., 1998. Sea level set-up behind detached breakwaters. In ASCE, editor, Proc. Int. Conf. Coastal Eng., pages 1665–1678

Pacini M. et al.,1999, La ricostruzione della spiaggia di Cala Gonone, Studi costieri 1

Raudkivi, A.J., 1996, Permeable pile groins. *Journal of Waterway, Port Coastal and Ocean Engineering* Vol. 122 No. 6., pp. 267-272

Ruol, P. and Faedo, A., 2002, Physical model study on low-crested structures under breaking wave conditions, Proc. Medcoast 2002, 83-96

Soft shore protection against coastal erosion, First international conference, 18-21 October, Patras, Greece

Trampenau T.G.F., Raudkivi A.J., 1996, Permeable pile groins. Coastal Engineering, pp 2353-2365

Van der Meer J., 1992, Conceptual design of rubble mound breakwaters, Design and Reliability of Coastal Structures", Venice, pp. 447-510

Weggel J.R e J.C. Escadillos, 1987, A comparison of the performances of three types of groins Int Conf. Of Coastal Eng, in Dev. Countr, Pekino, pp 371 - 384

Weggel J.R. Vitale P., 1985, Sand transport over weir jetties and low groins. Physical Modelling in Coastal Engineering, Dalrymple R.A., pp. 163-197

LOW-CRESTED STRUCTURES: BOUSSINESQ MODELING OF WAVES PROPAGATION

P. Prinos, I. Avgeris, Th. Karambas
Hydraulics Lab., Dept. of Civil Engineering, Aristotle University of Thessaloniki
Thessaloniki, Greece

Abstract

In the last few decades, low-crested structures have been extensively used in costal zones for shoreline protection and to prevent beach erosion. Their presence results primarily in wave energy dissipation through the physical mechanisms of wave breaking and friction. In most of the cases these structures are rubble mound permeable breakwaters whose design is based on empirical rules.

In this study wave evolution over porous submerged breakwaters is investigated with the use of a 2DH-Boussinesq-type model, following a procedure similar to that of Cruz et al. (1997). A higher-order Boussinesq-type model, with improved linear dispersion characteristics is used to describe wave motion in the regions upstream and downstream of the breakwater (Karambas and Koutitas, (2002)). In the region of the breakwater, the model is used in conjunction with a depth-averaged Darcy-Forchheimer (momentum) model describing the flow inside the porous medium. Above the breakwater the model incorporates two extra terms accounting for the interaction between the waves over the structure and the flow within the porous structure, one in the continuity equation and one in the momentum equation respectively.

Computed results are compared with experimental measurements in a wave flume and a wave basin, provided by Vidal et al. (2002) and Zanuttigh and Lamberti (2003) respectively, as part of a research carried out for the European Research project DELOS-(http://www.delos.unibo.it).

1. Introduction

Submerged breakwaters are commonly used for coastal protection on many eroding coasts. A desirable feature of submerged breakwaters (and low crested structures, in general) is that they do not interrupt the clear view of the sea from the beach. This aesthetic feature is important for maintaining the touristic value of many beaches and it is usually one of the considerations in using such structures for shoreline protection.

The basic idea in the use of submerged structures is to reduce the wave energy reaching the beach, by triggering wave energy dissipation over the structure, and thus reduce sediment transport and the potential for coastal erosion. A proper understanding of the effect of submerged breakwaters on nearshore waves and currents is necessary for the calculation of sediment transport and morphological evolution in the vicinity of such structures. This

C. Zimmermann et al. (eds.), Environmentally Friendly Coastal Protection, 177-189.

is important in order to achieve a good functional design of the submerged structure for coastal protection.

Several researchers have presented a number of models addressing this problem. Sollitt and Cross ((1972), (1976)) in their pioneering work presented an analytical approach having as a starting point the unsteady equations for flow in the pores of a coarse granular media. Madsen (1977) also included inertia and resistance forces, due to the presence of a rectangular porous structure, in his linear wave model. Wave propagation over porous seabeds was investigated theoretically and experimentally by Gu and Wang (1991), extending the analysis of Sollitt and Cross (1972). Losada et al. (1995), examined experimentally the validity of the theory of Sollitt and Cross (1972), while Losada et al. (1996) presented a numerical model in order to describe regular wave interaction with submerged breakwaters. In his dissertation, van Gent (1995) simulated wave interaction with permeable coastal structures by developing a one-dimensional model based on the non-linear shallow-water wave equations and a two-dimensional (2DV) model based on the Reynolds-averaged Navier-Stokes equations. As part of his work porous media flow was studied both theoretically and experimentally with emphasis on the resistance of porous media to oscillatory wave motion.

Incorporation of porous flow equations into Boussinesq-type models was recently achieved by Cruz et al. (1997) and Liu and Wen (1997). Cruz et al. (1997), derived a set of 2D- Boussinesq equations over a porous bed of arbitrary thickness and tested their applicability on a plane porous slope and for refraction, diffraction and reflection around a submerged porous breakwater with an opening. Recently, Hsiao et al. (2002) presented a fully non-linear 2D-Boussinesq-type model for waves propagating over a permeable bed and compared model results with experimental data for the case of regular waves passing over a porous submerged breakwater.

In this study, wave evolution over permeable submerged breakwaters is investigated with the use of a 2DH-Boussinesq-type model, following a procedure similar to that of Cruz et al. (1997). A higher-order Boussinesq-type model, with improved linear dispersion characteristics is used to describe wave motion in the regions upstream and downstream of the breakwater (Karambas and Koutitas, (2002)). Initially, 1D model results were evaluated using data collected during the experiments that took place in the wave and current flume of the Coastal Laboratory of the University of Cantabria (UCA), Spain as part of a research carried out for the European Research project DELOS (http://www.delos.unibo.it). The experimental set-up is described in detail by Vidal et al. (2002). Several data sets corresponding to different regular and irregular wave conditions were used for model verification. In this work the comparison of model results with the experimental data of one regular test and one irregular test is presented. For the former the target wave characteristics were: $H = 0.10$ m, $T = 1.6$ sec, while for the latter $H_s = 0.04$ m and $T_p = 1.6$ sec.

The 2D version of the model is tested against the 3D hydrodynamic experiments carried out at the 9.7 x 12.5 basin of Aalborg University, Denmark (Zanuttigh and Lamberti (2003)) for the same European project. Two different layouts were considered during these experimental tests. The first one was a symmetrical layout, composed by two detached porous breakwaters forming a rip channel in the middle. The second layout

consisted of a single breakwater inclined at 30° with respect to the beach. The numerical results of a single regular wave test corresponding to the symmetrical layout with narrow crest structures are presented. For this test the target wave characteristics were: $H = 0.1026$ m, $T = 1.81$ sec.

2. Description of the Model

2.1 Governing Equations - Numerical Procedure

A higher-order Boussinesq-type model, with improved linear dispersion characteristics is used to describe wave motion in the regions upstream and downstream of the breakwater (Karambas and Koutitas, (2002)). Above the breakwater the model incorporates two extra terms accounting for the interaction between the waves over the structure and the flow within the porous structure, one in the continuity equation and one in the momentum equation respectively, following the approach of Cruz et al. (1997). In two-dimensional depth-averaged form the governing equations (continuity and momentum equations) are:

$$\eta_t + \nabla\left[(h+\eta)u\right] + \varphi\nabla(h_s u_s) = 0 \tag{1}$$

$$\begin{aligned} u_t + u\nabla u + g\nabla\eta = {} & \left(\frac{h^2+2h\eta}{3}\right)\nabla^2 u_t + \nabla h\nabla^2 u_t + \nabla h_x u_t + \\ & + \frac{h^2}{3}(u\nabla^3 u - \nabla u\nabla^2 u) + (h\nabla\eta\nabla u_t + h\nabla hu\nabla^2 u) + \\ & + Bh^2\left[\nabla^2 u_t + \nabla^3\eta + \nabla^2(u\nabla u)\right] + 2Bh\nabla h(\nabla u_t + \nabla^2\eta) + \\ & + \frac{\varphi}{2}h\nabla^2\left(h_s u_{S_t}\right) \end{aligned} \tag{2}$$

where u = depth-averaged, horizontal velocity vector, η = surface elevation, h = water depth, B = dispersion coefficient, u_s = depth-averaged, seepage (fluid) velocity vector inside the porous medium, h_s = porous medium thickness and φ = porosity. The above variables are shown in Figure 1.

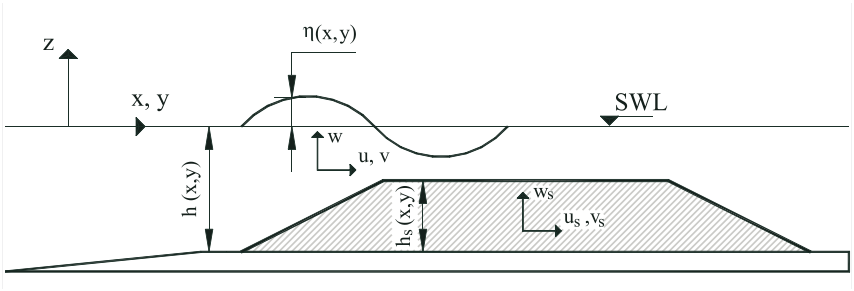

Figure 1: Definition of variables

The additional dispersion terms proportional to B extend the applicability of the model into a wider range of depths. As suggested by Madsen and Sørensen (14), B is set equal to 1/15, value that gives the closest match to linear theory dispersion relation for h / L_0 as large as 0.5.

Equations (1) and (2) are solved in the region of the breakwater in conjunction with a depth-averaged Darcy-Forchheimer (momentum) equation describing the flow inside the porous medium. Assuming that $O\left[(h_s / L)^2\right] << 1$ the two-dimensional, depth-averaged momentum equation written in terms of the fluid velocity u_s ($u_D = u_s$, u_D = Darcy velocity) reduces to (Cruz et al., (1997))

$$c_r u_{S_t} + u_s \nabla u_s = -g\nabla\eta + \varphi\,\alpha_1 u_s + +\varphi^2 \alpha_2 u_s |u_s| \tag{3}$$

which is refered as the non-linear long wave equation for porous medium. The fourth term in equation (3) is the Darcy term, while the fifth term is the Forchheimer term accounting for viscous and inertia forces respectively. In equation (3), c_r= inertial coefficient, given by (van Gent, (1995))

$$c_r = \frac{1 + c_m}{\varphi} = \frac{1 + \dfrac{1-\varphi}{\varphi}}{\varphi} \tag{4}$$

where c_m = added mass coefficient and γ = empirical coefficient that accounts for the added mass.

The porous resistance coefficients α_1 and α_2, are estimated from the following relationships (Ward, (1964), Sollitt & Cross, (1972), Losada et al., (1995), Cruz et al.,(1997))

$$\alpha_1 = \frac{v}{K}, \qquad \alpha_2 = \frac{C_f}{\sqrt{K}} \tag{5}$$

where v = kinematic viscosity ($1.0 \cdot 10^{-6}$ m^2/sec), C_f = dimensionless parameter and K = intrinsic permeability (m^2). The latter may be calculated from the following experessions given by van Gent, (1995), Burcharth and Andersen, (1995), Engelund (1953)

$$K = \frac{{d_{50}}^2 . \varphi^3}{\alpha (1-\varphi)^2}, \qquad K = \frac{{d_{50}}^2 . \varphi^2}{\alpha (1-\varphi)^3} \tag{6}$$

where α = empirical coefficient and d_{50}= the mean size of the porous material.

According to Ward (1964), the parameter C_f is a constant, equal to 0.55, however, van Gent (1995) proposes the following expression for calculating C_f

$$C_f = \beta \frac{1-\varphi}{\varphi} \frac{\sqrt{K}}{d_{50}} \tag{7}$$

where β = empirical coefficient.

An alternative expression for the coefficient α_2 is (van Gent, (1995))

$$\alpha_2 = \beta\left(1 + \frac{7.5}{KC}\right)\frac{(1-\varphi)}{d_{50}.\varphi^3} \tag{8}$$

where KC = (ÛT) /($d_{50}.\varphi^3$) is a Keulegan-Carpenter number for porous media flow (Û = the maximum velocity in the porous medium).

A number of studies (Madsen, (1977), Vidal et al., (1988), van Gent, (1995)) propose values for the non-dimensional coefficients α, β and γ depending on the material type and the length scale of the solid particles. For the present model the value of 1000, 1.1 and 0.34 is chosen for α, β and γ respectively, as recommended by van Gent (1995). The corresponding values of K, C_f, α_1, α_2 and c_r assuming that $\varphi = 0.5$, are calculated from equations (6), (8), (5) and (4) and are equal to $0.0005.d_{50}^{\ 2}$, 0.0246, $0.002 / d_{50}^{\ 2}$, $1.1001 / d_{50}$ and 2.68 respectively.

The governing equations are finite-differenced utilizing a high-order predictor-corrector scheme that employs a third-order explicit Adams-Bashforth predictor step and a fourth-order implicit Adams-Moulton corrector step (Wei and Kirby, (1995)). The corrector step is iterated until the desirable convergence is achieved. First order spatial derivatives are discretized to fourth-order accuracy.

2.2 Wave Generation

Wave generation is implemented inside the computational domain using the source function method as described by Wei et al. (1999). This method employs a mass source term in the continuity Equation (1) that acts on a limited 'source region' while it is combined with wave damping sponge layers at the boundaries. The method is adapted to be consistent with the Karambas and Koutitas (2002) equations, used in the present work, instead of the Nwogu type of equations, used by Wei et al. (1999).

2.3 Wave Breaking

An eddy viscosity formulation is adopted in order to simulate wave breaking (Kennedy et al., (2000)) by introducing an eddy viscosity term in the right-hand-side of the momentum equation (2)

$$u_t + \ldots = \left(\frac{h^2 + 2h\eta}{3}\right)\nabla^2 u_t + \ldots + E_b \tag{9}$$

This term is analysed (subscripts of x, y and t denote spatial and temporal differentiation respectively) as

$$E_{b_x} = \frac{1}{h+\eta}\left\{\left(v_e[(h+\eta)u]_x\right)_x + \frac{1}{2}\left(v_e[(h+\eta)u]_y + [(h+\eta)v]_x\right)_y\right\} \tag{10}$$

$$E_{b_y} = \frac{1}{h+\eta}\left\{\left(v_e[(h+\eta)v]_y\right)_y + \frac{1}{2}\left(v_e[(h+\eta)v]_x + [(h+\eta)u]_y\right)_x\right\} \tag{11}$$

The eddy viscosity v_e, is a function of both space and time and is given by

$$v_e = B_b \delta_b{}^2 (h + \eta)\, \eta_t \tag{12}$$

where δ_b = mixing length coefficient equal to 1.2. The quantity B_b controls the occurrence of breaking and varies from 0 to 1 as follows

$$B_b = \begin{cases} 1, & \eta_t \geq 2\eta_t^* \\ \dfrac{\eta_t}{\eta_t^*} - 1, & \eta_t^* < \eta_t \geq 2\eta_t^* \\ 0, & \eta_t \leq \eta_t^* \end{cases} \tag{13}$$

The parameter η_t^* determines the onset and cessation of breaking and is defined as

$$\eta_t^* = \begin{cases} \eta_t^{(F)}, & t \geq T^* \\ \eta_t^{(I)} + \dfrac{t - t_0}{T^*} \left(\eta_t^{(F)} - \eta_t^{(I)} \right), & 0 < t - t_0 \geq T^* \end{cases} \tag{14}$$

where T^* = transition time ($= 5\sqrt{h/g}$), t_0 = time that breaking was initiated ($\eta_t \geq \eta_t^{(I)}$), and thus $t - t_0$ = age of the breaking event. The values of $\eta_t^{(I)}$ and $\eta_t^{(F)}$ are $0.35\sqrt{gh}$ and $0.15\sqrt{gh}$ respectively.

3. Analysis of Results

3.1 1D Model

Initially, model results were evaluated using data collected during the experiments that took place in the wave and current flume of the Coastal Laboratory of the University of Cantabria (UCA), Spain (Vidal et al. (2002)). The wave and current flume of the UCA Coastal Laboratory is 24 m long, 0.60 m wide and 0.80 m high. The piston–type wavemaker has two attached free surface wave gauges integrated in a wave absorption system that allows the absorption of reflected waves from the experimental model.

Wave propagation over a rubble mound breakwater on a sloping beach was tested. The breakwater had a trapezoidal shape, while its crest width ranged between 0.25 and 1.0 m. Crest elevation from the bottom (0.25 m), front and back slope angles (1:2) and rubble characteristics were maintained constant. The model had two-layer armour of selected gravel and a gravel core.

The rubble mound breakwater was built over a horizontal false bottom, 0.10 m over the bottom of the flume. In the frontal foot of the rubble, a Plexiglas ramp with 1:20 slope connected the false bottom with the bottom of the flume. In the rear end, another 8 m 1:20 Plexiglas ramp simulated the rear beach. During the experiments water depth at the paddle was either 0.30 m, or 0.35 m, or 0.4 m resulting in a freeboard of 0.05 m, 0.00 and –0.05 m respectively. To assess free surface evolution and run-up on the beach, 15 resistive free surface gauges were installed along the flume. Three free surface gauges were installed in the slope in front of the breakwater to separate incident and reflected waves. Another two

free surface gauges were located over the front slope of the structure. Six free surface gauges measured transmitted waves over the crest and in the flat bottom behind the structure.

Evaluation of the numerical model was performed for the case of the submerged breakwater (freeboard = –5 cm) with 1 m crest width. There were several data sets available, involving regular and irregular waves, respective to this layout. In this work the comparison of model results with the experimental data of one regular test and one irregular test is presented. For the former the target wave characteristics were: $H = 0.10$ m, $T = 1.6$ sec, while for the latter $H_s = 0.04$ m and $T_p = 1.6$ sec.

For the regular wave test, the location of the wavemaker was defined as the centre of the source function. On the other hand, in the case of irregular waves the centre of the source function coincided with gauge 1 in order to use the free surface time series at this gauge as an input for the derivation of the source function record. The time step used was either $\Delta t = 0.0025$ sec (regular waves) or $\Delta t = 0.002083$ sec (irregular waves) and the grid size $\Delta x = 0.05$ m. The layout of the computational domain is depicted in Figure 2. In this figure, the numbered vertical lines indicate the location of the wave gauges for which computed results are compared with experimental measurements.

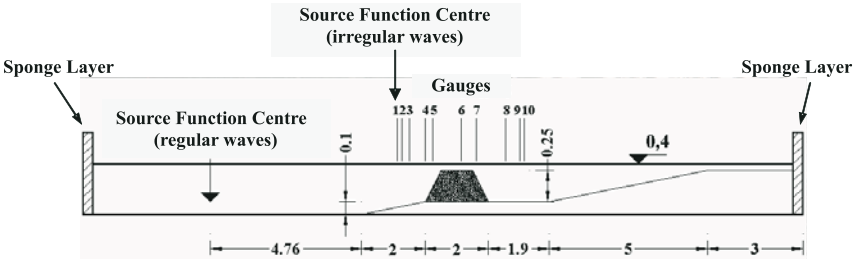

Figure 2: Layout of the computational domain

The porosity of the rubble mound was set equal to 0.5 while the characteristic diameter d_{50} of the gravel was set equal to 2 cm, resulting in a permeability K equal to $2 \cdot 10^{-7}$ m^2 (Equation 6). Hence, the respective values of α_1 and α_2 are 5.0 and 55.0.

For the regular wave case considered, incident wave height was calculated by employing the Funke and Mansard incident-reflection analysis method, using the free surface elevation time series of wave gauges 1, 2 and 3.

Figure 3 presents comparatively, computed and recorded free surface elevation time series at wave gauges 4 – 8 for the irregular waves case. In Figure 4 comparison between computed water surface elevation and experimental data is shown for regular waves with $H = 0.10$ m and $T = 1.6$ sec. Figure 5 illustrates comparatively the computed and experimental incident and transmitted spectra respectively for the same case.

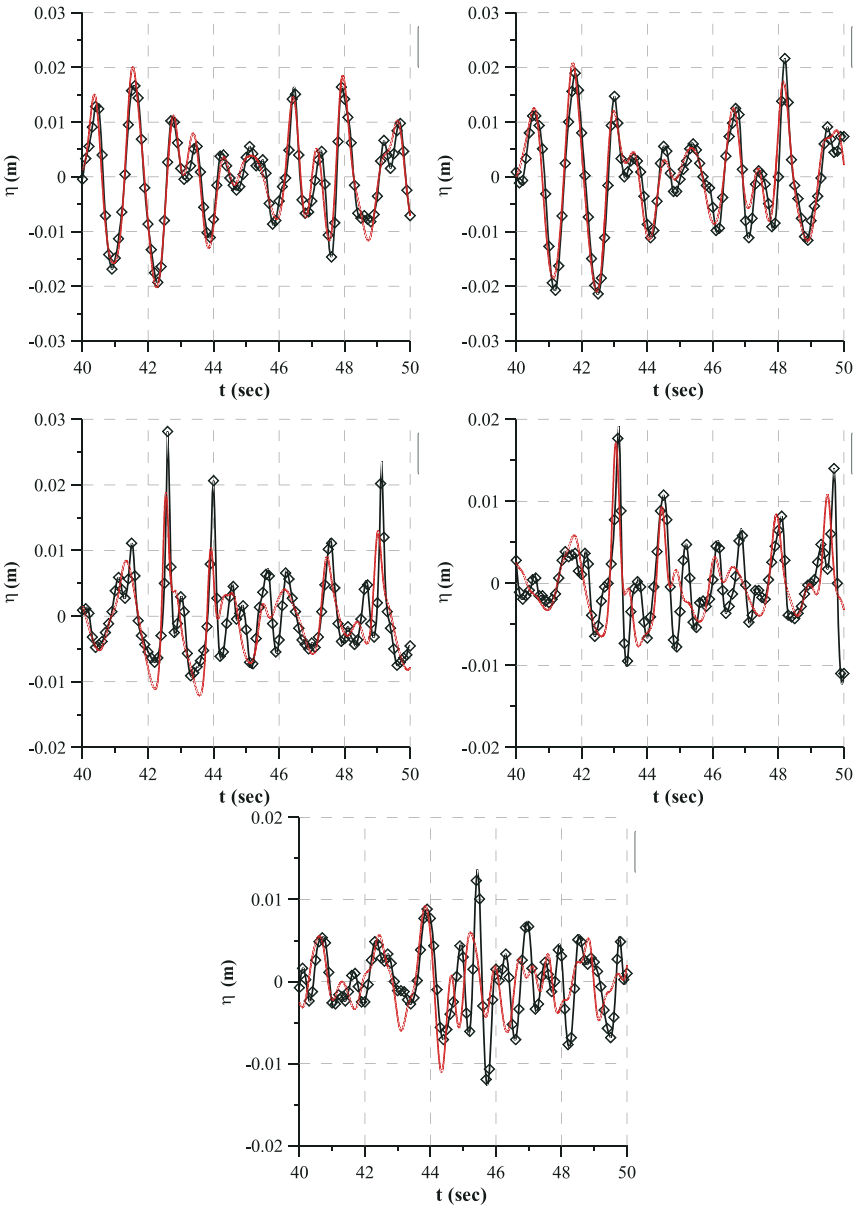

Figure 3: Computed and experimental free surface elevation at gauges 4, 5, 6, 7 and 8 respectively (UCA, $H_s = 0.04$ m, $T = 1.6$ sec, model —, experiment —◇—)

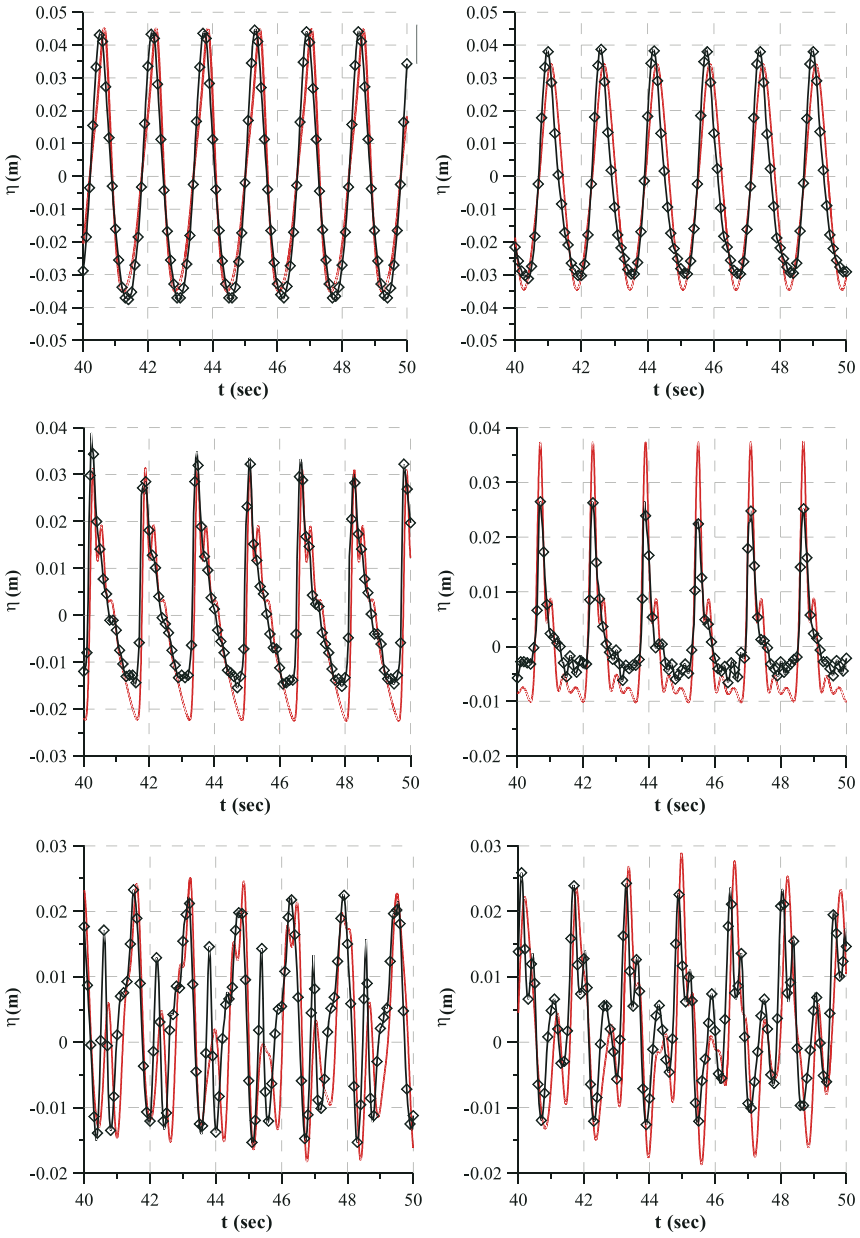

Figure 4: Computed and experimental free surface elevation at gauges 2, 4, 6, 7, 8 and 9 respectively (UCA, $H = 0.10$ m, $T = 1.6$ sec, model —, experiment —◇—)

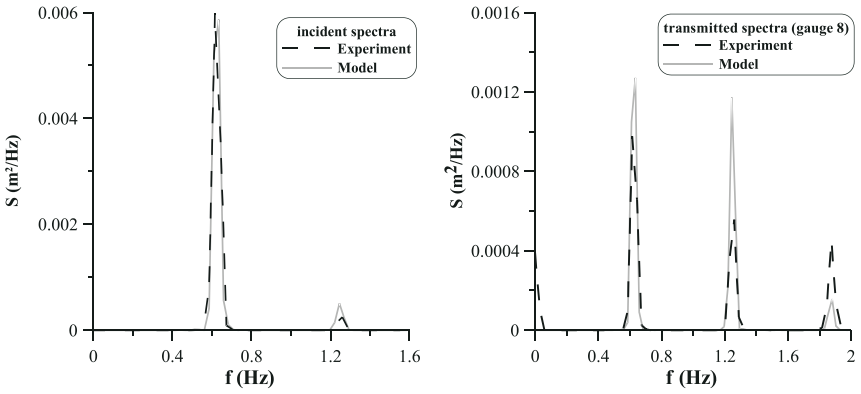

Figure 5: Computed and experimental incident and transmitted spectra (UCA, $H = 0.10$ m, $T = 1.6$ sec)

3.2 2D Model

Further, preliminary tests of the present model against the 3D hydrodynamic experiments carried out under the framework of the DELOS project at the 9.7 x 12.5 basin of Aalborg University, Denmark were performed. Detailed description of the experimental layouts and the characteristics of the tests is provided by Zannutigh and Lamberti (2003). Two different layouts were considered during these experimental tests. The first one was a symmetrical layout, composed by two detached porous breakwaters forming a rip channel in the middle. The second layout consisted of a single breakwater inclined at 30° with respect to the beach. Here, the numerical results of a single regular wave test (test 19) corresponding to the symmetrical layout with the submerged (freeboard = –0.07m) narrow crest structures are presented. A plan view of this layout is shown in Figure 6. For this test the target wave characteristics were: $H = 0.1026$ m, $T = 1.81$ sec. In the model, the porosity of the rubble mound was set equal to 0.5 while the characteristic diameter d_{50} of the gravel was set equal to 3.5 cm.

Figure 7 presents a comparison of surface elevation time series between model results and experimental data at 2 wave gauges, seaward of the breakwater, over the horizontal bed (gauge 11) and behind the breakwater (gauge 19) respectively. Finally, figure 8 shows the wave-induced current field, averaged over two wave periods for this test. The onshore flow over the submerged breakwater and the offshore flow at the rip channel can also be recognized.

The comparisons indicate that the model simulates quite well wave evolution at the regions before and over the breakwater. Behind the breakwater the decomposition of the leading wave component into higher frequency waves is predicted with less accuracy.

A deficiency of the model affecting the results is that the linear dispersion relationship is not accurate, although improved. However, it should be emphasised that in the present study the model was tested for rather extreme geometrical conditions as far as the ratios of wave height and water depth to freeboard of the submerged breakwater are concerned.

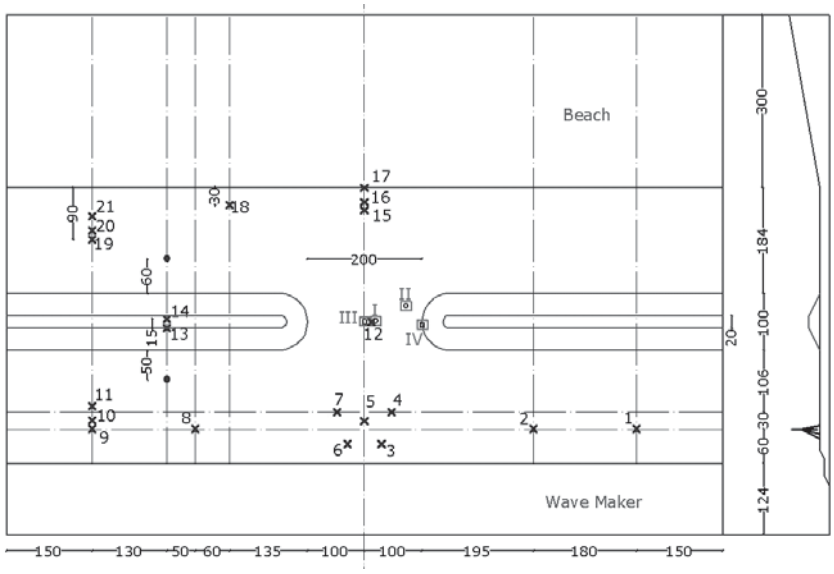

Figure 6: Plan view of Aalborg experimental layout 1 (narrow crest structures). ('X' marks WGs, 'o' marks the 2D ADVs (F and B, in front and behind the structure), '□' marks ADVPs (I and II) and 3D ADVs (III and IV))

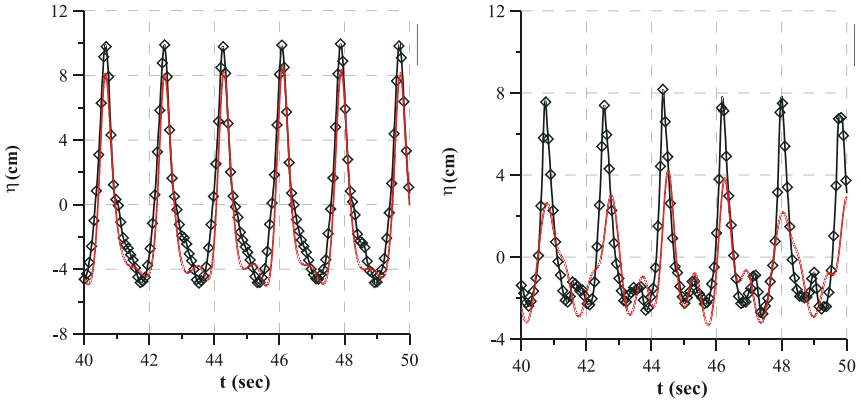

Figure 7: Computed and experimental free surface elevation at gauges 11 and 19 respectively (UCA, $H = 0.1026$, $T = 1.81$, model —, experiment —◇—)

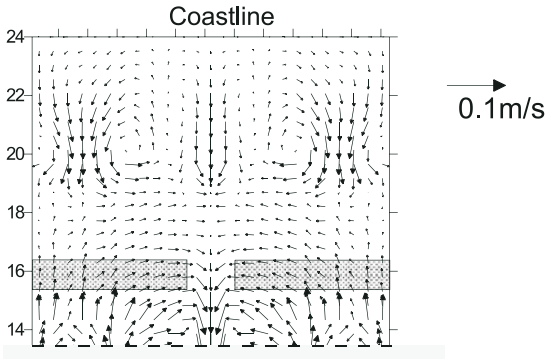

Figure 8: Computed wave-induced current field

4. Conclusions

A 2DH-Boussinesq-type model combined with a depth-averaged Darcy-Forchheimer equation is applied in this study for simulating wave propagation over submerged porous breakwaters. The model was tested against experimental measurements for the case of a rubble mound trapezoidal breakwater on a sloping beach. Both regular and irregular wave cases were used in order to assess model performance. The comparative analysis demonstrates that the model predicts quite accurately the wave pattern over and behind the structure. Additional higher order non-linear terms improve the ability of the model to describe the process of non-linear harmonic generation behind the structure.

References

Burcharth H.F., Andersen O. H., 1995, "On the one-dimensional steady and unsteady porous flow equations", *Coastal Engineering,* 24, pp. 233-257

Cruz E.C., Isobe M., 1997, Watanabe A., "Boussinesq equations for wave transformation on porous beds", *Coastal Engineering,* 30, pp. 125-156

Engelund F. A., 1953, "On the laminar and turbulent flows of ground water *through* homogeneous sand", Danish Academy of Technical Sciences

Gu Z., Wang H., 1991, "Gravity waves over porous bottoms", *Coastal Engineering,* 15, pp. 497-524

Hsiao S.-C., Liu P.L.-F., Chen Y., 2002, "Nonlinear water waves over a permeable bed", . Proceedings R. Soc. Lond. A , 458, pp. 1291-1322

Karambas Th.V., Koutitas C., 2002, "Surf and Swash Zone Morphology Evolution Induced by Nonlinear Waves", *Journal of Waterway, Port, Coastal and Ocean Engineering, ASCE,* 128 (3), pp. 102-113

Kennedy A.B., Chen Q., Kirby J.T., Darlymple R.A., 2000, "Boussinesq modeling of wave transformation, breaking, and runup. I: 1D", *Journal of Waterway, Port, Coastal and Ocean Engineering, ASCE,* 121 (5), pp. 251-261

Liu P.L.-F., Wen J., 1997, "Nonlinear diffusive surface waves in porous media", *Journal of Fluid Mechanics,* 347, 26, pp.119-139

Losada I. J., Losada M.A., Martín A., 1995, "Experimental study of wave-induced flow in a porous structure", *Coastal Engineering,* 26, pp.77-98

Losada I. J., Silva R., Losada M. A., 1996, "3-D non-breaking regular wave interaction with submerged breakwaters", *Coastal Engineering,* 28, pp. 229-248

Madsen O.S., 1977, "Wave transmission through porous structures", *Journal of Waterway, Harbour, Coastal and Ocean Engineering, Div., ASCE,* 100 (3), pp. 169-188

Madsen P.A., Sørensen O.R., 1992, "A new form of the Boussinesq equations with improved linear dispersion characteristics. Part 2: A slowly varying bathymetry", *Coastal Engineering,* 18, 183-204

Sollitt C.K., Cross R.H., 1972, "Wave transmission through permeable breakwaters", Proc. of 13th International Conference on Coastal Engineering, ASCE, New York, pp. 1827-1846

Sollitt C.K., Cross R.H., 1976, "Wave reflection and transmission at permeable breakwaters", Technical Paper No. 76-8, CERC

Van Gent M. R. A., 1995, "Wave interaction with permeable coastal structures", PhD Thesis, Delft University, Delft, The Netherlands

Vidal C., Lomonaco P., Migoya L., Archetti R., Turchetti M., Sorci M., Sassi G., 2002, "Laboratory experiments on flow around and inside LCS structures. Description of tests and data base", DELOS Project Internal Report, pp. 19

Vidal C., Losada M. A., Medina R., Rubio J., 1988, "Solitary wave transmission through porous breakwaters", Proc. of 21st International Conference on Coastal Engineering, ASCE, New York, pp. 1073-1083

Ward J. C., 1964, "Turbulent flow in porous media", *Journal of Hydraulic Division, ASCE,* 90 (HY5), pp. 1-12

Wei G., Kirby J.T., 1995, "Time-dependent numerical code for extended Boussinesq equations", *Journal of Waterway, Port, Coastal and Ocean Engineering, ASCE,* 121 (5), pp. 251-261

Wei G., Kirby J.T., Sinha A., 1999, "Generation of waves in Boussinesq models using a source function method", *Coastal Engineering,* 36, pp. 271-299

Zanuttigh B., Lamberti A., 2003, "Wave basin experiment final form: 3D Hydrodynamic tests at Aalborg University, DK", DELOS Project Deliverable D 31, pp. 76

FLOW MEASUREMENTS AND NUMERICAL SIMULATION ON LOW-CRESTED STRUCTURES FOR COASTAL PROTECTION

Pedro Lomonaco, Cesar Vidal, Iñigo J. Losada, Nicolas Garcia and Javier L. Lara
Ocean & Coastal Research Group, University of Cantabria
Santander, Spain

Abstract

A series of laboratory and prototype experiments have been performed to measure and model the flow around and inside low-crested structures and submerged breakwaters. The results of the tests are used to improve the understanding of the wave-structure interaction and its effect on the near-shore dynamics. The database become the core to develop an empirical model to determine dynamic pressure and velocity profiles for design purposes, and to assess the laboratory scale effects on coastal structures. Finally, the large amount of measured information is used to calibrate and validate COBRAS, a 2DV, VOF-type, RANS numerical model, proven to be a powerful tool for the functional and structural design of low-crested and submerged breakwaters, as well as a numerical wave flume to increase the applicability of empirical models.

1. Introduction

Low-crested structures and submerged breakwaters have been used for coastal protection for many years, and application examples can be found in several locations worldwide. Since they are infrastructure works meant to preserve and improve the environment, in their design it is required to warrantee a certain level of stability in its lifetime, and also is necessary to know, beforehand, the morphodynamic effect produced by the structure.

Examples of low-crested structures are groins and detached breakwaters, aimed to protect and to stabilize a beach; tidal inlet groins (jetties), intended to stabilize the entrance channel and to reduce maintenance dredging costs; and, finally, sea outfalls, where the pipeline protection is a long submarine rubble mound.

Low-crested and submerged breakwater's stability depend on the flux properties, acting around and inside the structure, as well as the characteristics of the structure itself, i.e. stone size, permeability and structure geometry, including the structure's angle with the flow direction (Vidal, et al., 1999). The flux is found to be characterised by the instantaneous velocity and pressure field around the structure (Lomonaco, et al., 2002).

From the morphodynamic point of view, the presence of the structure will modify the wave and current patterns. Therefore, the sediment motion and, moreover, the corresponding morphology will be affected accordingly.

Hence, during the design stage, it is necessary to understand and predict the structure's response under wave and currents, and vice versa, i.e. the effect of the structure on the

C. Zimmermann et al. (eds.), Environmentally Friendly Coastal Protection, 191-210.

wave and current field. Nowadays, the wave-structure interaction is studied and predicted by performing laboratory and prototype tests, as well as with numerical models.

The Ocean & Coastal Research Group, at the University of Cantabria, has been involved in a series of research projects aimed at improving our knowledge of the stability and behaviour of low-crested structures, and their interaction with the flow dynamics. The aim of this paper is to illustrate the most recent findings in these projects, including a description of the measurements in a series of laboratory and prototype tests performed, as well as the implementation of a non-linear, turbulent, VOF-type, numerical model.

2. Prototype Tests

The prototype experiment was designed to take place over the Santander sea outfall, a 1.6 m diameter high-density polyethylene (HDPE) pipeline, laid over a rocky bottom, 6 km north of the city (Figure 1). Santander is located on the northern coast of Spain, where the mean tidal range is around 3,5 m (max. up to 5 m) and subject to very high wave energy. In deep water, a typical storm of $H_s = 5-6$ m, $T_p = 15-18$ s can be observed every year, and a storm of $H_s = 7$ m, $T_p = 16$ s occurs on average every 5 years. Longitudinally, the pipeline is placed from the shoreline in an excavated trench and covered by concrete along 580 m. From this point (10 m water depth), a rubble mound, formed by a core, a filter layer and a 3-ton main layer, protects the pipeline. The typical cross-section of the pipeline rubble mound protection is depicted in Figure 2. The total length of the outfall is 2430 m, reaching up to 43 m water depth (LLW), it is designed for a maximum waste water discharge of 4.5 m^3/s and to withstand a 200 year return period storm (at the outfall, $H_s = 9.44$ m, $T_p = 18$ s).

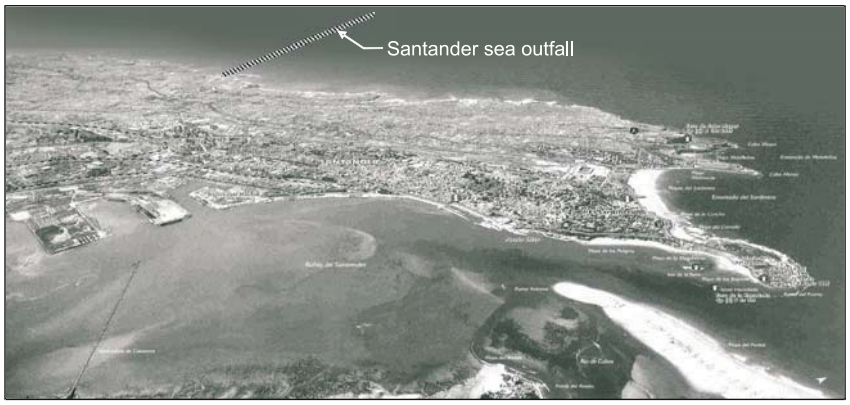

Figure 1: Santander and location of the outfall

The prototype tests included stability assessment and flow measurements. The stability tests consisted of building three sections, 20 m in length, on top of the original rubble mound, approximately 1000 m from the shoreline, at a water depth ranging from 15 to 20 m (LLW). In Figure 3 the stability sections over the outfall are presented schematically,

where the corresponding stone sizes are indicated. The stability of the tested sections was evaluated by very fine bathymetry measurements spanning three years. Preliminary results of the stability prototype tests can be found in (Vidal, et al., 2002).

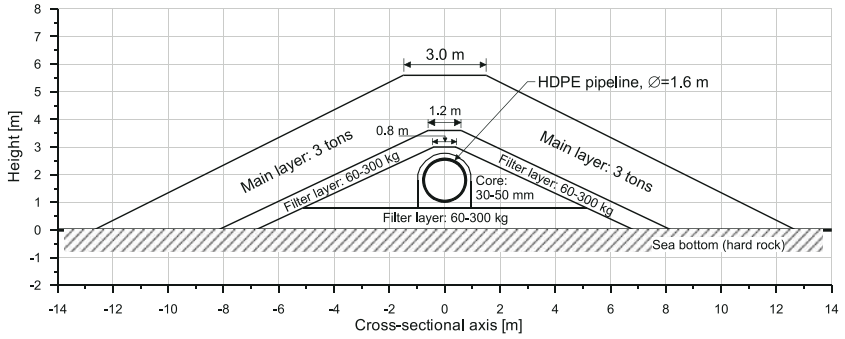

Figure 2: Typical cross-section geometry of the Santander sea outfall

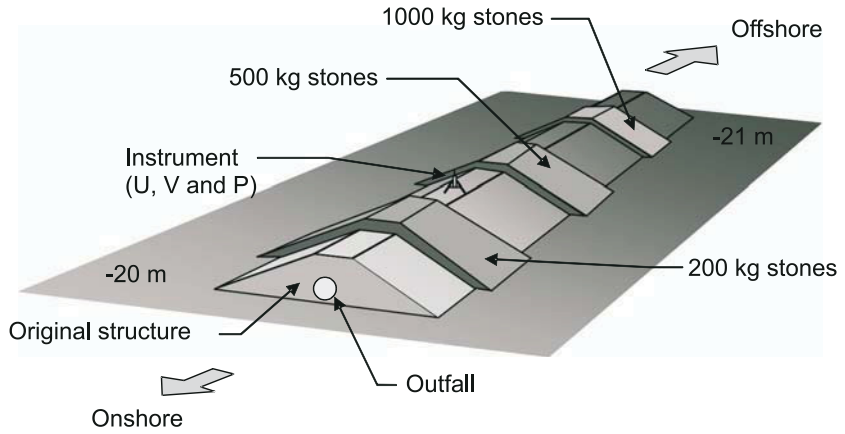

Figure 3: Schematisation of the test sections over the rubble mound of Santander's outfall

Figure 4 shows one example of average profiles measured in two field surveys on the test section of 200 kg stones. After two years of wave attack, total destruction of the first layer of these stones was reached (the second layer was less prone to damage due to its location over the 3-tons rocks of the main armour layer). The damage on the 500 kg section was lower, but affected wide areas of the first layer of the armour. Finally, the damage on the 1000 kg section was small, not perceptible by the measuring technique used. It should be noted that the divers reported the movement of some of these stones as well as some of the stones of the main armour of 3-tons near the location of the deployed instrument.

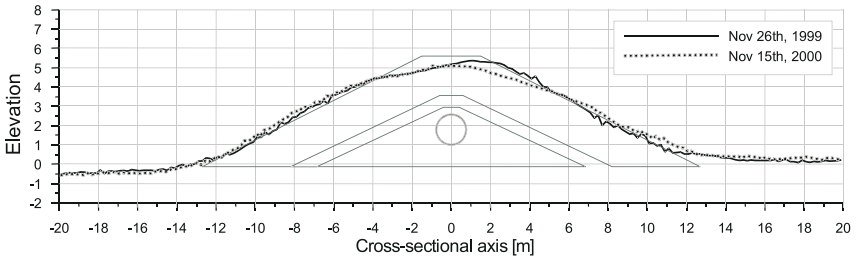

Figure 4: Comparison between average profiles of November 1999 and November 2000 at the 200 kg test section of the Santander sea outfall

As part of the stability tests, 2D horizontal velocities and pressures were measured at the crest of the structure. One data sample each second was recorded on 30-minute bursts every 2 hours from January 20th through March 22nd, 2000, and 20-minute bursts every 3 hours from February 22nd through March 18th, 2001. Several storms were recorded and the damage produced to the test sections can be related to the registered wave-induced velocity, pressure and computed wave height. The incident wave height was also obtained from wave buoys placed in near-by ports. For each burst, the free surface time series and, thus, the entire set of wave statistics can be obtained by applying a frequency domain, linear transfer function to the pressure energy spectra. In Figure 5 the significant wave height time history is presented. In the same graph, a time series sample of the pressure and horizontal velocity is shown for the burst measured on February 27th, 2001 at 22:00 ($H_s = 6.09$ m, $T_p = 14.22$ s).

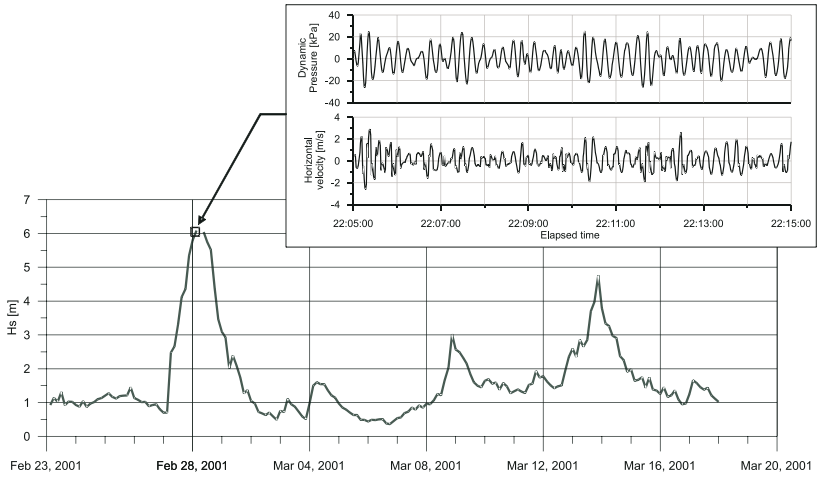

Figure 5: Significant wave height time history and time series sample of measured horizontal velocity and computed free surface elevation at the crest of Santander sea outfall

Figure 6.a shows the comparison between the distribution of measured wave heights (obtained from the pressure record) and the theoretical Rayleigh distribution. Figure 6.b shows the comparison between the distribution of measured velocity amplitudes and the theoretical Rayleigh distribution. From the figures it can be seen that the velocities follow the Rayleigh distribution better than the wave heights in the upper end of the distribution. This difference is due to the perturbation of the velocities produced by the presence of the protection, which increased the wave velocity in the crest of the protection.

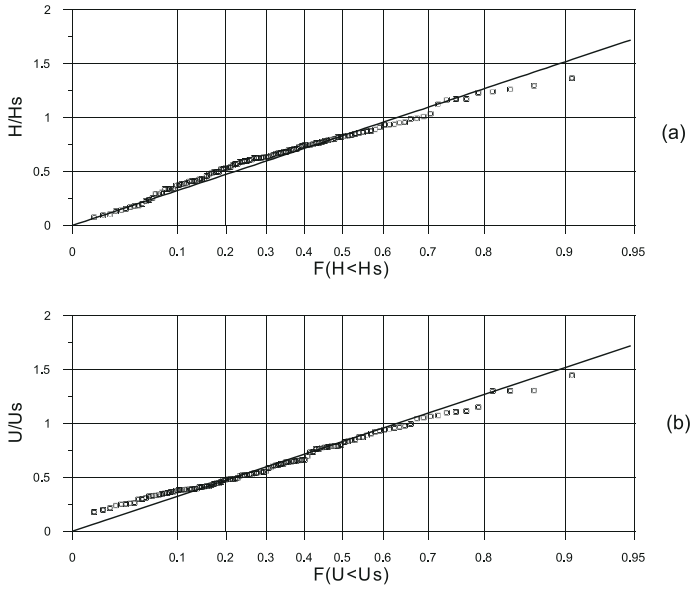

Figures 6: Comparison with Rayleigh distribution: (a) zero-upcrossing wave height and (b) measured velocity amplitudes

This velocity enhancement on the crest, also known as *overshooting*, was observed previously by (Lomonaco & Klomp, 1997) and described in (Lomonaco, et al., 2002), and can also be seen in Figure 7, where the modulus of the velocity obtained from the pressure gauge and a linear transfer function is compared with the velocity obtained directly from the UV sensor. From Figure 7 it can be seen that the velocity modulus obtained from the UV sensor is always greater than the velocity obtained from the pressure sensor and linear theory.

For each burst, the measured horizontal velocity component in the direction of the wave propagation can be plotted versus the relative wave number. In Figure 8 the peak measured horizontal velocity is plotted in dimensionless form versus the relative wave number. Applying linear wave theory, the velocity can be computed at the crest elevation for each relative wave number. In Figure 8, the linear theory approximation is also presented for comparison, indicating the corresponding formulation and a definition diagram.

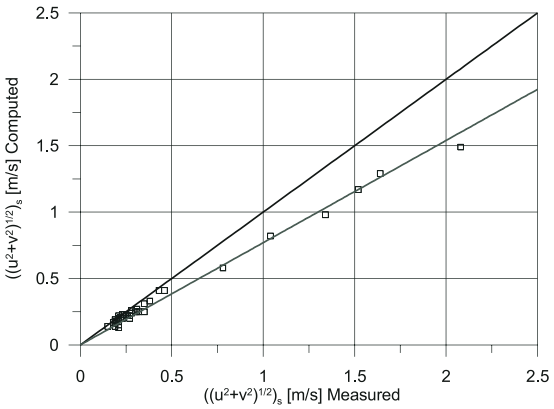

Figure 7: Comparison of velocity modulus obtained from the pressure gauge with a linear transfer function and that obtained from the UV sensor

In Figure 8, u_s is the measured significant horizontal velocity in the direction of wave propagation, H_s is the significant wave height (computed by applying the linear transfer function to the measured pressure at the crest of the structure), T_p is the peak period of each burst, $k_p = 2\pi / L_p$ is the wave number related to the peak period of each burst, L_p is the wave length related to the peak period of each burst, h is the total water depth and h_c is the crest water depth.

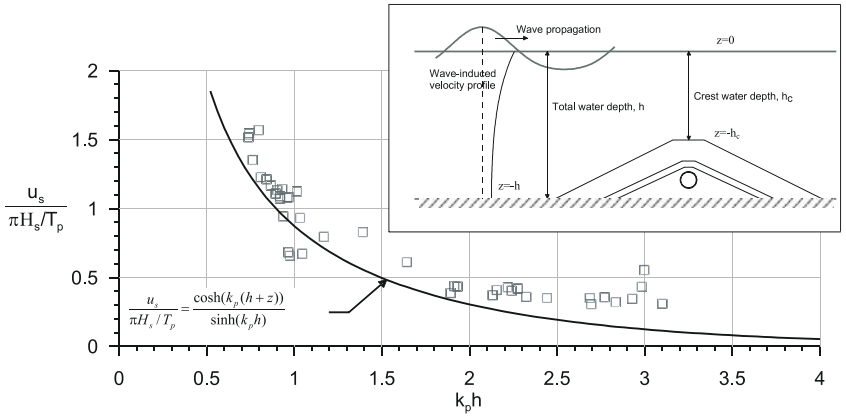

Figure 8: Dimensionless wave-induced horizontal velocity at the crest of the Santander sea outfall

As can be seen in Figure 8, the measured velocity is larger than that predicted by linear wave theory. On average, the predicted velocity underestimates the measured velocity by 16% (correlation coefficient, $r_{xy} = 87.8\%$). In the linear theory application, the structure geometry has no effect on the velocity profile, thus the freeboard effect has not been included. As a first approach, following previous findings related to the stability of

submerged rubble mounds, the relative local wave number ($k_{p,c}$) is applied to improve the empirical model correlation. As a result, the linear approximation presents a much better fit to the measured data, as shown in Figure 9, where the dimensionless measured velocity is again plotted, but now versus the relative local wave number. In this case, the predicted velocity is on average only 0.4% smaller than the measured one (r_{xy} = 88.8%). As shown in the definition sketch inserted in Figure 9, the velocity profile is enhanced by assuming the actual water depth as h_c, i.e. at the crest of the rubble mound. The role of $k_{p,c}\ h_c$ is to include in the measured data the water depth reduction and its effect on wave celerity.

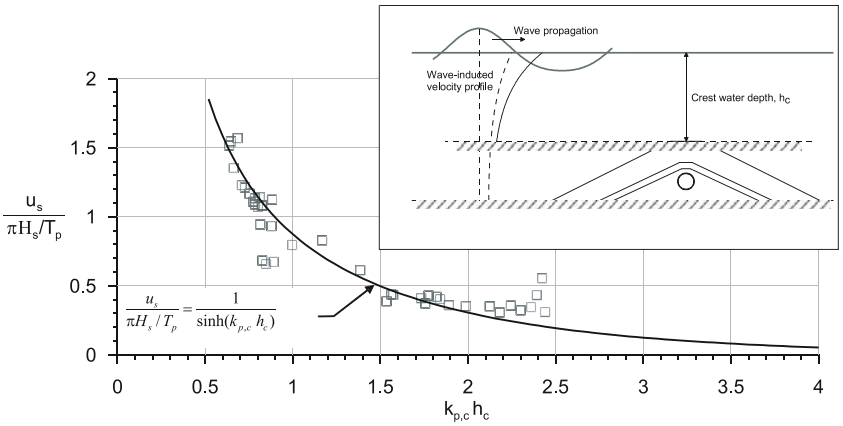

Figure 9: Dimensionless wave-induced horizontal velocity at the crest of the Santander sea outfall. Correlation improved by the effect of the relative local wave number on the velocity profile

Note that, whenever the individual wave height statistics are Rayleigh distributed, and also for the velocity distribution, then the dimensionless wave-induced velocity is independent of the statistical parameters (H_s, $H_{1/10}$, H_{rms}, $H_{\max}$, etc.) being used, given that the same parameter is employed for the velocity as well as for the wave height.

3. Laboratory Tests

A long series of laboratory tests has been conducted for several research projects related to low-crested structures and submerged breakwaters. Both, stability and flow measurements have been measured for a broad variety of wave conditions, water depths, model scales, stone sizes and structure's cross-section geometry. On one hand, detailed damage profiles were measured with a high-resolution laser profiler, as well as manually, when applicable, for freeboards ranging from an emerged low-crested reef breakwater to a deep submerged rubble mound. On the other hand, flow measurements included surface elevation evolution, dynamic pressure inside the structure, high resolution LDA around the structure and video imagery. Different scales and geometries were used, including crest width changes, filter layers and a geometrically similar cross-section of the Santander sea outfall.

4. The FEDER Flow Tests

As mentioned above, a series of laboratory tests was performed in one of the wave flumes at the University of Cantabria. Basically, the aims of the tests were to reproduce the flow conditions of the Santander sea outfall, in order to obtain a data set to develop an empirical model for velocity and pressure prediction, as well as to assess scale effects. The data set also will be used to calibrate a 2DV-RANS, VOF-type numerical model, so the number of test conditions can be increased, improving the empirical model applicability. The FEDER tests were conducted under the framework of the European Funds for Regional Development.

The wave flume used in this case is 60 m long, 2 m wide and 2.5 m deep. The wave paddle is a piston type board with a dynamic absorption system and is able to generate fifth-order regular and irregular waves up to 0.6 m. The Santander sea outfall model was placed on top of a horizontal platform, approximately 45 m from the wave paddle. A 12 m wave absorption ramp was placed behind the structure in order to minimize wave reflection.

During the tests, the surface elevation, velocity profiles and dynamic pressure were measured in several points simultaneously. Figure 10 depicts the test layout, showing the wave and pressure gauges positions, as well as the 2D Laser Doppler (LDA) and 3D Acoustic Doppler (ADV) velocity measurement arrangements. Three wave gauges were placed in front of the structure to evaluate incident and reflected waves; five more gauges were placed on top of the structure to analyse wave energy dissipation, shoaling and steepness. Moreover, the first four gauges on top of the structure coincide longitudinally with the LDA velocity profiles. The 3D ADV is placed at the second wave gauge (see Figure 10) to study co-located data for wave reflection analysis. Twenty-five points (regular waves) and ten points (irregular waves) were selected for 2DV velocity measurements with the LDA on top of the structure. Finally, eight pressure gauges were installed around a plastic, tailor-made, pipeline. In Figure 10 the theoretical 1:20 structure cross-section is shown, as well as the actual measured profile. As can be seen, the LDA measurement points were fixed to be as close as possible to the actual cross-section to identify the velocity that produces the stone instability. These velocity measurements also allow detecting flow separation and turbulence sources.

Figure 11 presents the pressure gauges disposition inside the pipeline, as well as the final structure configuration. As mentioned previously, the rubble mound is a geometrically similar 1:20 model of the Santander sea outfall, where the main layer, filter and core are scaled following the Froude criteria.

Overall, 28 tests were performed, with wave heights ranging from 5 to 40 cm, two water depths, three periods, and regular and irregular waves. The irregular wave tests were based on a narrow banded TMA spectrum (JONSWAP spectrum adapted for limited depth conditions). For each measured point, a zero up-crossing analysis was performed to check whether the measured parameter is Rayleigh distributed (Lomonaco, et al., 2003). Finally, the root-mean-squared amplitudes for the surface elevation, pressure and velocity were computed and included in a data set to develop an empirical model of velocity and pressure assessment for design purposes (Lomonaco, et al., 2002).

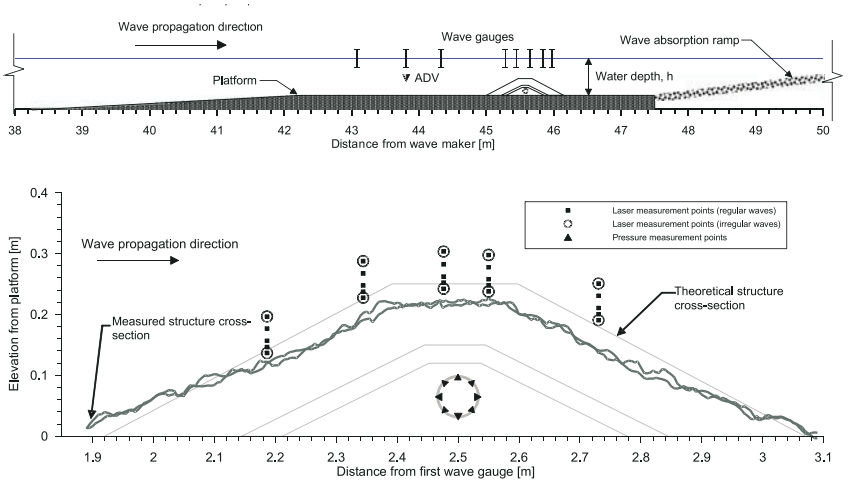

Figure 10: Laboratory tests layout. Setting of the wave gauges, ADV, LDA measurement points and pressure gauges around the pipeline

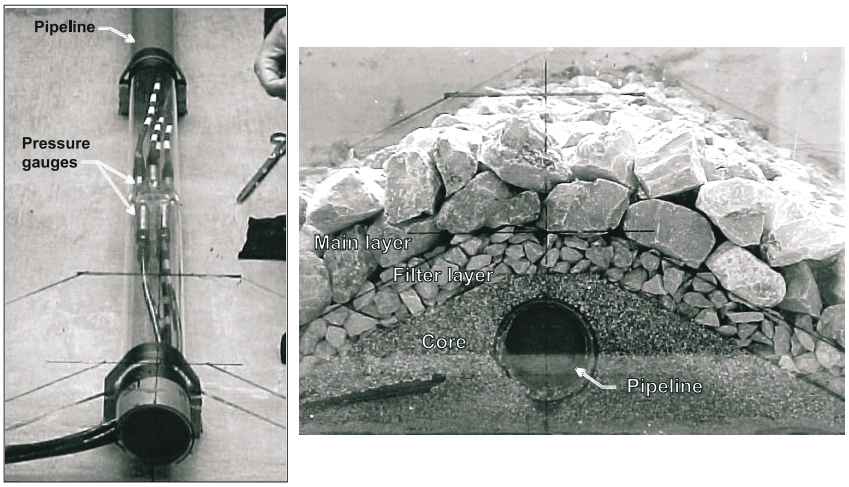

Figure 11: Pressure gauges disposition inside the pipeline and final configuration of the cross-section tested

In the regular wave tests, a phase-averaged procedure is applied to obtain a mean period response. Finally, from each phase-averaged time history, the positive and negative peak values were included in the data set of the empirical model. In Figure 12, the phase-averaged surface elevation, pressure and velocity are shown as an example for test № 9 ($H = 15\,\text{cm}$, $T = 2\,\text{s}$, $h = 59.4\,\text{cm}$, regular waves, 2000 s test duration), where a limited number of measured points are presented for clarity purposes.

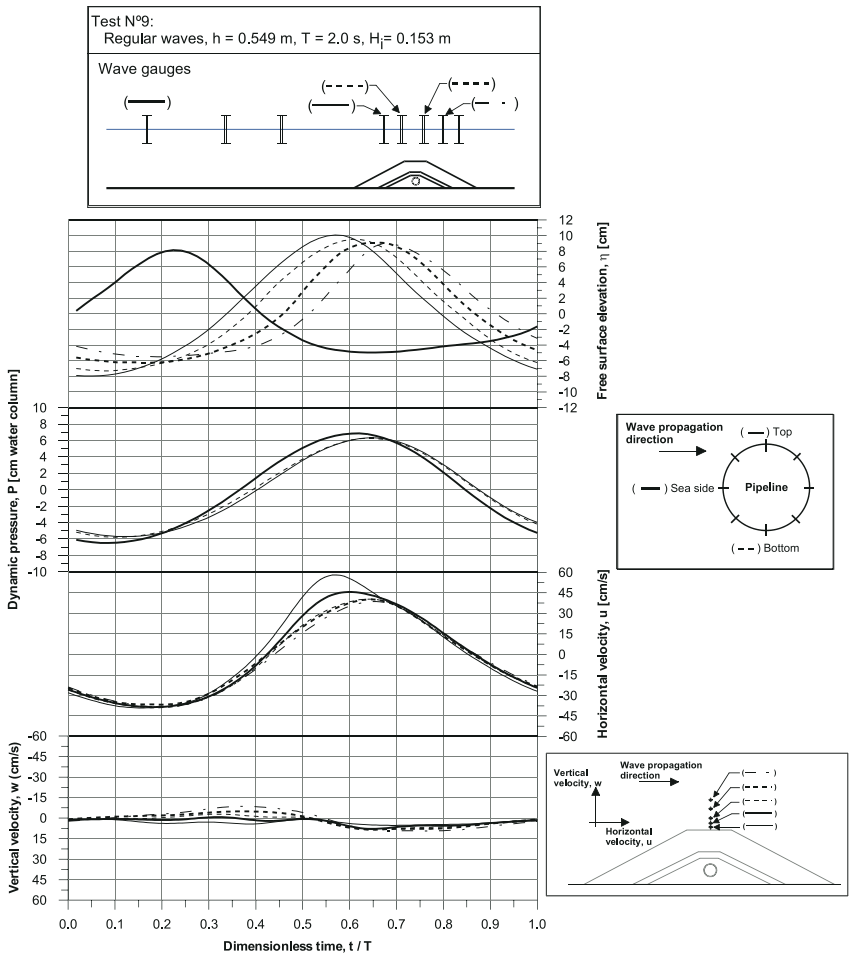

Figure 12: Example of phase-averaged measured surface elevation, pressure and velocity for Test № 9

From Figure 12, several comments are provided. The wave non-linearity can be observed from the surface elevation profile, which in turn induces an asymmetry on the pressure and velocity time histories. This leads to a separate treatment of the peak values. Observing the surface elevation envelope, the effect of the structure on energy dissipation and wave reflection can be assessed. For the performed tests, the surface envelope resembles a quasi-stationary wave system where the nodes and anti-nodes are clearly seen. Comparing the wave reflection coefficient with tests made without the structure, it was found that the wave energy dissipation due to the submerged rubble mound protection could be considered negligible, since the average structure reflection coefficient is around 5%. This is an important characteristic of a submerged structure compared with a low-crested or reef-type structure: the energy reflection is an image of the low influence of the structure

on the wave field, yielding a basis to identify the range of applicability of the different stability formulations found in the literature.

In general, the maximum and minimum pressure and velocity values are in-phase with the corresponding surface elevation. The velocity profile is almost vertically uniform but, in some cases, the horizontal velocity shows a larger peak value near the structure, which occurs slightly before the wave crest passes. This effect is, again, the overshooting and here is found to be related to the fluid advection and flow constriction due to the structure freeboard. The dynamic pressure can be assumed to be in-phase around the pipeline. As a first approximation, this can be considered true, given that the pipeline diameter is rather small compared with the wavelength. This is of outmost importance, since the rubble mound is acting as a low-pass filter of the dynamic pressure, avoiding vortex shedding, turbulence generation and pipeline interference. In other words, the flow remains laminar inside the core. Whether this behaviour is also present in the prototype or not is directly linked with the scale effects, as the Reynolds number may differ significantly.

5. The DELOS Flow Tests

The DELOS laboratory experiments described here are part of the research carried out for the European Project DELOS "Environmental DEsign of LOw Crested Coastal Defence Structures". The objective of these experiments is to provide calibration data for numerical and empirical models of flow and stability. The following description is summarized from the corresponding DELOS technical report by (Vidal et al., 2001) and from (Losada, et al., 2003).

The experiments were carried out in the wave and current flume of the Coastal Laboratory of the University of Cantabria. The wave flume is 24.05 m long, 0.60 m wide and 0.80 m high and is divided, as can be seen in Figure 13, in different zones. The piston–type wavemaker has two attached free surface wave gauges integrated in an Active Wave Absorption System (AWACS®) that allows the absorption of reflected waves. The current generation system is a reversible pumping system including two zones of flow injection or withdrawal through the bottom of the flume, two pumps, with a combined maximum discharge of 150 l/s, and a recirculation pipe. Bottom and sidewalls of the testing area are made of glass, allowing the use of laser velocimetry techniques.

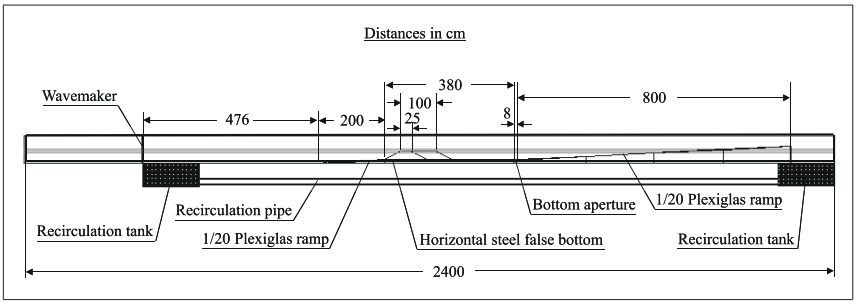

Figure 13: Definition sketch of the wave flume. Experimental set-up

Two rubble-mound low-crested structures of 0.25 m and 1.00 m crest width were tested. Crest elevation from the bottom (0.25 m), front and back slope angles (1V/2H) and rubble characteristics were maintained constant for both structures. The models had a two-layer armour of selected gravel and a gravel core.

During the tests, thirteen resistance wave gauges measured free surface evolution, three gauges were placed inside the structure core to assess pressure gradients as the wave propagates, twelve LDV measurement points were defined on the sea-side of the structure's slope, while a 3D ADV was located on the back slope. At the same time, four acoustic velocity profilers were installed at the crest of the structure and along the dissipation ramp and, finally, digital video imagery was taken during the test focusing on the wave impinging and overtopping the structure.

Three of the free surface gauges were installed on the slope in front of the structure to separate incident and reflected waves, Figure 14. Another two free surface gauges were located over the front slope of the structure at the same locations of two of the LDA measurement profiles. Two free surface gauges were placed over the structure crest and on the leeside slope. Four more were placed to measure transmitted waves along the flat bottom landward of the structure. Finally, one was installed on the final beach slope to measure run-up and set-up.

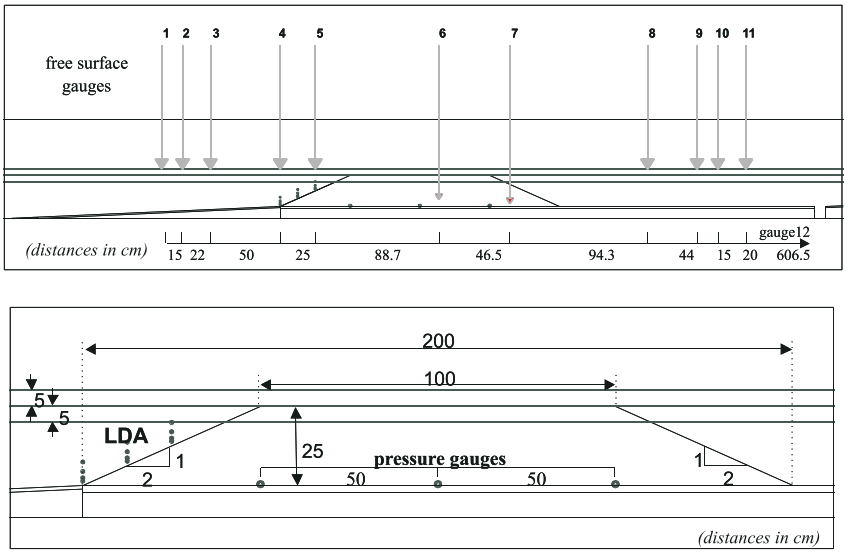

Figure 14: Instruments and measurement points around and inside the structure

Two different models (0.25 and 1.00 m crest width) were tested for three different water depths (0.30, 0.35 and 0.40 m) or three different freeboards (-0.05, 0 and 0.05 m). Regular and random waves were tested. The total number of different wave conditions was 54 for both regular and irregular waves for a total of 108.

Figure 15 presents the construction phase of the "short-crested" structure and LDA measurements during the tests.

Figure 15: The DELOS Project flow tests. Construction of the "short-crested" (0.25 m) structure and LDA measurements during the tests

6. Numerical Simulations

The laboratory and prototype tests are useful to improve our understanding of the processes involved in the stability of the structure, as well as its interaction with the wave field. Moreover, the data set led to a series of empirical formulations aimed at assessing the flow characteristics and the corresponding induced damage. However, the range of application is limited, in particular when the processes are highly non-linear or scale effects may be present. The current state-of-the-art allows computing the full flow field with numerical models. The experimental data is then used for calibration and validation, and later the model can be exploited to generate different cases, as a numerical wave flume. Furthermore, the model can be used to investigate magnitudes of interest, difficult or impossible to measure in the laboratory.

The numerical model used for the present analysis of wave interaction with low-crested structures is the COrnell BReaking waves And Structures (COBRAS). The original model, named RIPPLE and developed at Los Alamos National Laboratory (Kothe, et al., 1991) is a general program for two-dimensional, transient, free surface, incompressible

fluid dynamics model. It has been modified at Cornell University to deal specifically with coastal engineering issues, in particular breaking wave action and flow within porous media. During the last years, an intensive program has been carried out at the University of Cantabria to extend the applications of the model to different kinds of coastal structures and more specifically to Low Crested Structures (LCS).

The COBRAS model solves the 2DV Reynolds Averaged Navier-Stokes (RANS) equations, based on the decomposition of the instantaneous velocity and pressure fields into mean and turbulent components. Reynolds stresses are closed with an algebraic non-linear $k-\varepsilon$ turbulence model that can solve anisotropic eddy-viscosity turbulent flows. For the resolution of the flow inside the porous structure, the COBRAS model solves the Volume-Averaged Reynolds Averaged Navier-Stokes (VARANS) equations, obtained by integration of the RANS equations in a control volume larger than the pore structure but smaller than the characteristic length scale of the flow (Liu, et al., 2000). Another set of $k-\varepsilon$ equations similar to the previous one is used to model turbulence production-dissipation within the porous media. The COBRAS model includes several wave generation mechanisms, among which an internal wave-maker procedure that has been used for the present study. A sponge-layer method is used to absorb the waves that propagate in the direction opposite to the zone of interest. The computational domain in the COBRAS model is discretized in rectangular cells. The computing mesh can be divided into sub-mesh regions with a variable grid resolution. The free surface is tracked using the Volume Of Fluid (VOF) method that identifies the free surface location, tracking the density change in each cell. Besides, the model allows the definition of flow obstacles using a partial cell treatment. More details of the model can be found in the literature, e.g. (Liu, et al., 2000).

7. Model Calibration and Validation

As mentioned previously, one of the main goals of the laboratory experiments is to calibrate and validate COBRAS, since the model requires the definition of several parameters. The first step of the numerical analysis presented here consists of testing the model ability to reproduce the experimental results.

At this stage, calibration of COBRAS for the FEDER flow tests is still in progress. Nevertheless, preliminary results are available. In Figure 16, numerical results are shown of the velocity field and vorticity, for the wave flume without the structure. In order to perform reliable numerical simulations, it is necessary to include in the model all the geometric details of the flume, assuring that the flow behaviour will be only governed by the physical properties of the structure.

In Figure 17 preliminary results are shown of the submerged structure tested. As can be seen, the model includes the effect of the flow within the structure, as well as the breaking and dissipation processes. In the horizontal velocity panel, the velocity enhancement at the crest of the structure is distinguished, supporting the hydrodynamic source of the overshooting effect. The intensity of this velocity may be equal to the velocities found in the plunging jet of the breaking wave. The importance of this velocity enhancement on the armour layer stability is clear.

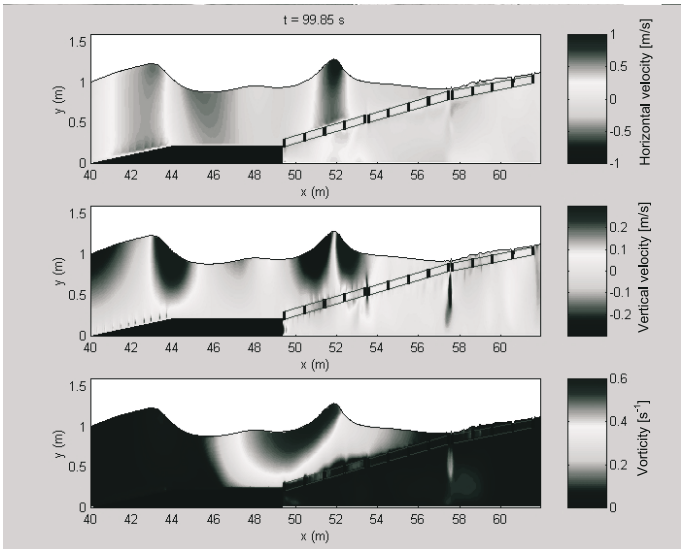

Figure 16: Preliminary results of the FEDER flow tests. Velocity and vorticity field for the wave flume without the structure ($H = 35$ cm, $T = 3.4$ s, $h = 100.5$ cm)

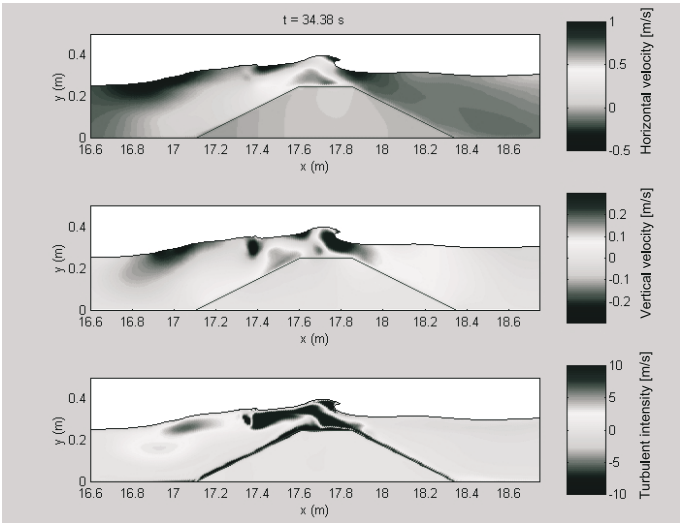

Figure 17: Preliminary results of the FEDER flow tests. Velocity and turbulent intensity field for the submerged structure ($H = 12$ cm, $T = 1.8$ s, $h = 30$ cm)

The DELOS flow tests have been analysed thoroughly during the project duration, since several numerical models were verified with this database. The computational domain for

the experimental layout is much more complicated, since the tests were rather ambitious in terms of the amount of data gathered. Figure 18 presents the computational mesh designed for this purpose. As can be seen on the figure, the general configuration of the laboratory experiments is reproduced. It includes the low-crested structure made of two porous media of different hydraulic properties, the false bottom supporting the breakwater and connected to the bottom of the flume by a 1/20 slope and the final dissipative 1/20 slope. The return flow system, forced by the difference of water level between the seaside and leeside parts of the flume, is also introduced, consisting of a pipe set under the flume and three apertures allowing the water to flow under the final ramp, then through the pipe and finally back to the flume. The mesh grid is non-uniform in the *x*-direction, with a higher resolution (cells of 1 cm x 1 cm) in the vicinity of the structure. The first sub-mesh region corresponds to the wave generation zone, using the internal wave-maker mode of generation, and consists of a two wavelength-wide sponge layer, the source region and a one wavelength-wide zone for flow regularization. Cells in the first sub-mesh region are 4 cm x 1 cm (Losada, et al., 2003).

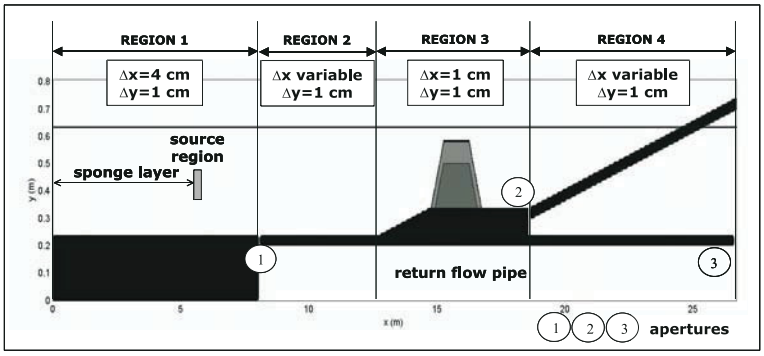

Figure 18: DELOS flow tests. Sketch of the computational mesh (axes not scaled)

Among the whole set of experimental magnitudes available, the calibration of the numerical model has been conducted comparing the measured and the computed values of free surface displacement in the case of the slightly submerged ($F = -0.05$ m) wide-crested ($b = 100$ cm) breakwater. The numerical parameters to be calibrated are the α and β parameters that govern the flow in the porous media. As the modelled breakwater is made of two different porous media, two pairs of porous flow parameters are to be calibrated. In the present study, the calibration of the numerical model led to the following values: $\alpha = 1000$, $\beta = 0.8$ for the armour layer; and $\alpha = 1000$, $\beta = 1.2$ for the core. The results obtained with these values were found to best fit the time series of free surface displacement recorded by the gauges placed all along the flume.

In Figure 19, the measured and computed ensemble-averaged surface elevation envelopes and mean water levels are shown for the "long-crested" structure during two different wave and water level conditions. The comparison shows satisfactory results and confirms the values of the porous media parameters resulting from the free surface calibration as the optima. As can be observed, the numerical model in both cases accurately captures the

wave height evolution pattern along the flume. The wave height decay resulting from energy dissipation by breaking over the breakwater and friction inside the porous structure is well reproduced. Wave height envelopes show a clear quasi-standing wave pattern seaward of the structure due to reflection at the sloping face of the breakwater.

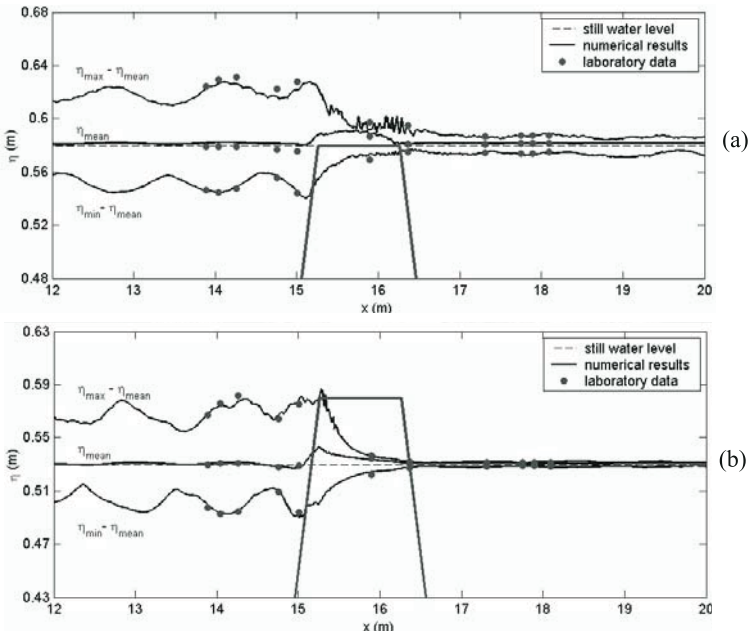

Figure 19: Measured and computed ensemble-averaged surface elevation envelopes and mean water levels for (a) $H = 3.6$ cm, $T = 1.6$ s, $h = 0.35$ m and (b) $H = 7$ cm, $T = 1.6$ s, $h = 0.35$ m

The evolution of the wave field along the flume can be observed in Figure 20, where the time series of the free surface displacement recorded by the gauges located in the vicinity of the structure are presented for the "long-crested" breakwater. The good level of agreement of the computed time series with the measurements should be noted in terms of amplitude and shape of the wave profile, for each one of the stations at the seaside, on the crest and at the leeside of the breakwater. Wave shoaling and the gradual loss of symmetry of the wave profile is correctly reproduced, as well as the broken wave profile. The complex wave field leeward of the crest, with the multiple crests associated with the higher harmonics released in the deeper waters of the transmission zone, is accurately simulated also.

Finally, the velocity field obtained numerically is validated using the measurements performed on the seaside slope of the structure, as presented in Figure 21. The first row displays the location of the measurements points, distributed in three profiles. The wave height envelopes and mean water level are also represented, the same way as in Figure 19. The second and third rows of the two figures show the maximum, mean and minimum

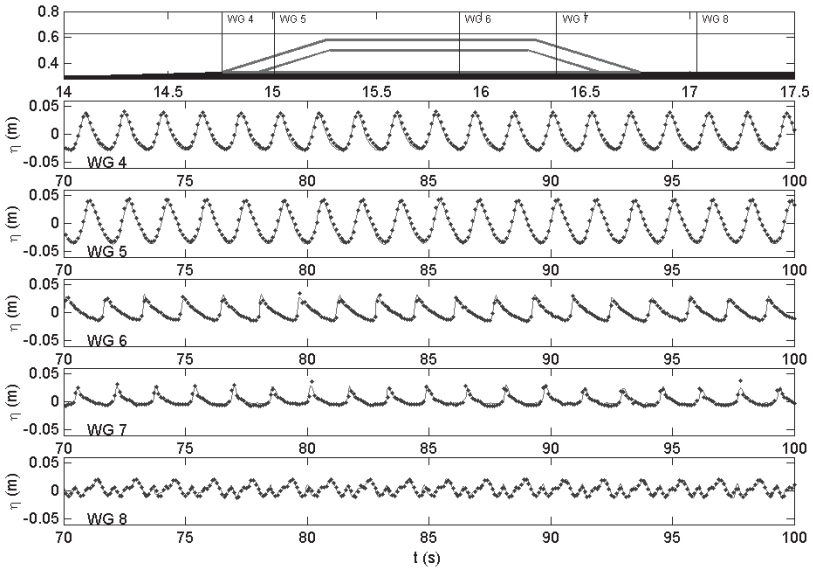

profiles of phase-averaged horizontal and vertical velocities, respectively. After the simulation has reached a quasi-steady state, results have been obtained based on a phase averaging of a significant number of waves. As can be seen on the figure, the agreement between experimental and numerical data is rather good.

Figure 20: Free surface time series for gauges WG4 to WG8. Target wave conditions: $h = 40$ cm, $T = 1.6$ s, $H = 10$ cm. Solid lines: experimental data. Dots: numerical results

An interesting feature of both the numerical and measured velocities is the aforementioned overshooting, i.e. a velocity enhancement near the structure. Nevertheless, it should be stressed the difference, sometimes difficult to distinguish, between the overshooting, associated with the wave advection and available freeboard, and the near-bed velocity enhancement due to the viscous boundary layer. Apparently, the overshooting can be identified when, for a fixed position, the peak velocity occurs slightly before the wave crest passes.

8. Concluding Remarks

A series of laboratory and prototype tests have been performed successfully to improve the understanding of the stability and behaviour of low-crested and submerged coastal structures. The free surface elevation was recorded in front and behind the structure, near bed velocity profiles were measured on the slopes and over the crest, and dynamic pressures were measured around the protected pipeline and within the breakwater. Among several objectives, the main purposes of the tests were: (1) to develop an empirical model to predict wave-induced pressure distribution around the pipeline for strain computations, velocity profiles over the structure for stone stability and damage assessment, and wave height

evolution, reflection, transmission and dissipation to indirectly assess the effect of the structure on the coastal sediment dynamics, (2) to assess the scale effects on laboratory experiments and (3) to calibrate and validate a 2DV non-linear numerical model to exploit as a numerical wave flume, increasing the validity and applicability of the empirical models.

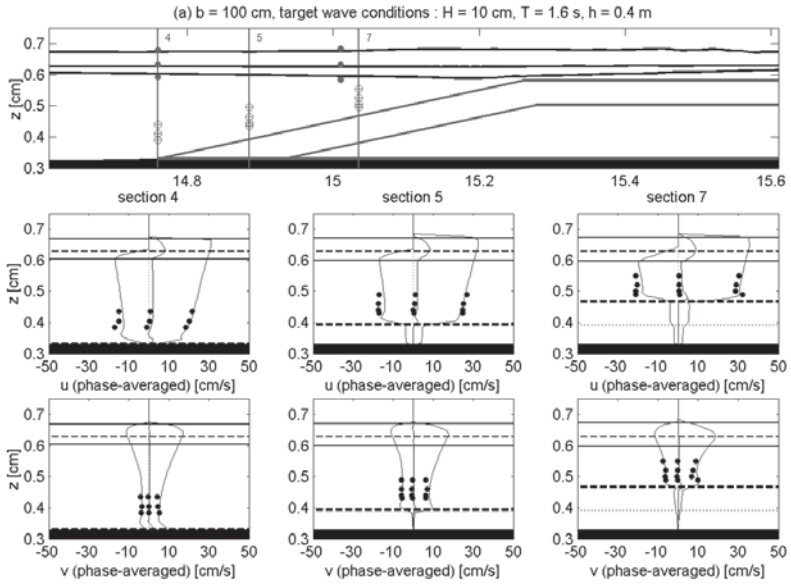

Figure 21: Measured and computed phase-averaged velocity profiles along the seaside slope of the long-crested structure

From the prototype tests, it was found that the significant horizontal velocity on top of the structure can be computed by applying linear wave theory, considering the water depth at the crest as the total depth, thus the structure freeboard and the wave steepening is taken into account. From the FEDER laboratory tests, it was found that the pressure around the pipeline and the velocity over the structure are, in general, in-phase with the water surface elevation. Near-structure velocity profiles are vertically uniform, but close to the structure and, in particular, over the crest, the velocity shows a larger peak that occurs slightly before the wave-crest passes. This velocity enhancement is called overshooting and is related to the fluid advection and flow constriction due to the structure freeboard. Hence, as the structure crest becomes relatively greater, the velocity overshooting should be vertically transported, modifying the whole velocity profile and, thus, the free surface.

COBRAS, a 2DV VOF-type RANS numerical model, have successfully reproduced the DELOS laboratory tests. The numerical model has been validated comparing the computational results with experimental information of free surface time series along the flume and mean velocity profiles at the offshore slope of the structure. The breaking and post-breaking wave transformation processes are shown to be adequately reproduced by

the model. Production/dissipation energy processes associated with wave breaking and internal porous flows are correctly simulated. The COBRAS model is then shown to be a powerful tool for the functional and structural design of low-crested rubble-mound breakwaters.

Acknowledgements

This study has been funded by the European Community in the framework of the European Funds for Regional Development (FEDER) and Environmental DEsign of LOw-crested coastal defence Structures (DELOS) under the research projects 1FD97-1500, 1FD97-0404 and EVK3-CT-2000-41. Additionally, the research program on submerged structures has been party funded by the Spanish Comisión Interministerial de Ciencia y Tecnología (CICYT) under the research project DIETER REN202-04662/MAR.

References

Kothe, D.B., Mjolness, R.C., Torrey, M.D. (1991). "RIPPLE: a computer program for incompressible flows with free surface." Los Alamos National Laboratory, LA-12007-MS

Liu, P.L.-F., Hsu, T.J., Lin, P.-Z., Losada, I.J., Vidal, C and Sakakiyama, T. (2000). *The Cornell Breaking Wave and Structure (COBRAS) model.* Proc. Coastal Structures '99. ISBN 90-5809-092-2, Volume 1, pp. 169-174

Lomonaco, P. and Klomp, W.H.G. (1997). *Rock cover damage assessment*. Proc. BOSS Conference. ISBN 0-08-042834-7, VOLUME I, 1997 (ISBN 0-08-042831-2). pp. 179-193

Lomónaco, P., Vidal, C., Losada, I.J. and Méndez, F.J. (2004). *Wave Height, Pressure and Velocity CDF's around Rubble Mound Protections for Submarine Outfalls*. Proc. Coastal Structures 2003 (in Press)

Lomónaco, P., Vidal, C., Revilla, J.A. and Losada, I.J. (2002). *Flow and pressure distribution around rubble mound protected pipelines.* Proc. 2nd International Conference on Marine Waste Water Discharges (MWWD 2002). Volume 2

Losada, I.J., Lara, J.L. and Garcia, N. (2004). *2-D Experimental and numerical analysis of wave interaction with low-crested breakwaters including breaking and flow recirculation*. Proc. Coastal Structures 2003 (in Press)

Vidal, C., Losada, I.J. and Martín, F.L. (1999). *Stability of near-bed rubble-mound structures.* Proc. 26th International Conference on Coastal Engineering (ICCE '98). ISBN 0-7844-0411-9, Volume 1, pp. 1730-1743

Vidal, C., Lomónaco, P., Migoya, L., Archetti, R., Turchetti, M., Sorci, M., Sassi, G. (2001). "Laboratory experiments on flow around and inside LCS structures. Description of tests and data base." DELOS European Project, technical report

Vidal, C., Lomónaco, P. and Martín, F.L. (2002). *Prototype analysis of stability of rubble mound protections for submarine outfalls.* Proc. 28th International Conference on Coastal Engineering (ICCE 2002). ISBN 981-238-238-0, pp. 1936-1948

PERFORMANCE OF SUBMERGED BREAKWATERS AS ENVIRONMENTAL FRIENDLY COASTAL STRUCTURES

Sevket Cokgor, M. Sedat Kapdasli
Istanbul Technical University, School of Civil Engineering, Division of Hydraulics, Maslak, Istanbul, Turkey

Abstract

An experimental study on the improvement for the problem of wave transmission in slightly submerged breakwaters is carried out in the present paper. The breakwater shape, effect of the porosity, water depth regarding the breakwater crest height and, dynamic stable deformed breakwater were examined as parameters. During the experiments, porosity was varied between 0.57-0.34, breakwater crest height to water depth ratio changed from 1 to 0.83. The similarity between a longshore bar and a dynamic stable submerged breakwater was also studied in one set of the experiments. Results indicated that a dynamic stable breakwater similar to a longshore bar resulted in better energy dissipation and the best transmission coefficient values determined between 0.3-0.1 in the mentioned condition.

1. Introduction

The purpose of installing a breakwater is to reduce the height of incident water waves on the leeward side to a level compatible with the intended use of the site to be protected. A submerged breakwater is a barrier with its crest at or slightly below the still water level. In situations where complete protection from waves is not required, submerged breakwaters offer a potentially economic solution. Submerged breakwaters have been effectively used to protect harbor entrances to reduce siltation in entrance channels, against beach erosion and, for creation of artificial fishing grounds.

The energy associated with storm waves is dissipated on beaches, moving sediment offshore and depositing in the near shore zone, forming a bar just after the storm events and causing shoreline recession on a coast with dominant cross-shore sediment transport (Fig.1). The bar gradually moves onshore under milder post-storm wave conditions, and eventually it emerges and is deposited on the beach as a berm. A typical sequence of such a beach change was illustrated in the beach stage model by Sunamura (1984). As wave and beach conditions change, therefore, longshore bars may or may not be present in the near shore zone (Rector (1954), Iwagaki and Noda (1962), Halis and Carr (1975), Miller (1976), Larson and Kraus (1992), Silvester (1974), Nadaoka et al. (1988)).

C. Zimmermann et al. (eds.), Environmentally Friendly Coastal Protection, 211-218.

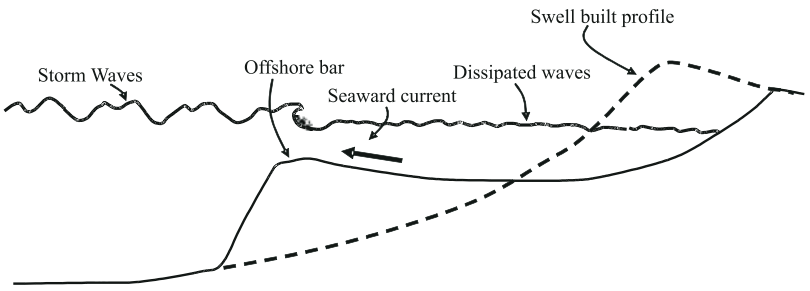

Figure 1: Profile of beach under the storm condition

Waves approaching the beach interact with the near shore morphology. When the inner bar exists in the nearshore zone, it acts as an effective filter for wave height. In the case of storm wave conditions, the inner bar affords considerable protection of the beach from erosion by acting as a submerged breakwater (Silvester (1974), Takeda et al. (1992), Dean (1973)). Moreover, if the inner bar has the effect of wave filtering and beach protection, the outer bar should also have same effects. Because the efficiency of wave filtering is affected by the water depth of bar crest which will change with the offshore distance and depth of bar, it can be considered that the degree of beach protection will vary according to the offshore distance of the bar. The condition for beach erosion depends on the situation of the bars i.e., presence or absence, offshore distance shore normal width, and probably the numbers of bars. When the bars act as an effective wave filter, the beach is not always eroded even by the large storm waves.

There are many papers published relating to submerged breakwater and their wave transmission performance. Twu et al. (2001) examined wave transmission over deep submerged breakwaters by using theoretical approximation with different porosities of the structure. Thickness of the body to depth ratio was 20 in their study and they found a reduction in the transmission coefficient to approximately 0.6. The work of Mendez et al (2001) was focused on wave induced mean water heights in permeable breakwater by using first and second order theory and they noticed that methods supplied reasonable results for determining mean magnitudes around/over the breakwater. The porosity effect of the submerged breakwater was studied by Ting et al. (2003). They examined the submerged breakwater for different porosities, between 0.421-0.912. They found energy loss decreases for porosities above 0.75. The work of Huang et al. (2003) also supported this previous study. Their numerical work found that transmission coefficients increase with porosity.

The aim of the present study is to simulate nearshore bar formation with a dynamically stable submerged breakwater. The best way to protect a shore may be to mimic the behavior of a stable beach profile under storm and normal conditions.

2. Experimental Set Up and Test Conditions

Experimental research has been carried out in order to investigate the similarity between a longshore bar and a dynamically stable submerged breakwater. Experiments were

performed in a wave flume of 22.5 m length, 1 m width and 0.5 m height, under regular waves generated by a flap type wave generator (Fig.2). A gravel wave absorber was placed behind the wave paddle and a 1/5 slope sandy beach was located behind the breakwater. Wave heights were measured by parallel wire resistance probes located 5 m offshore and on the shore sides of the structure and wave time series were recorded by the computer. A submerged breakwater was built with a trapezoidal crossection at different crest widths and slopes. Three different gravel materials were used for the breakwaters with $D_{50} = 2.85$ cm, $D_{50} = 1.3$ cm, $D_{50} = 0.85$ cm median diameters that supplied different porosities of 0.57, 0.43 and 0.34, respectively.

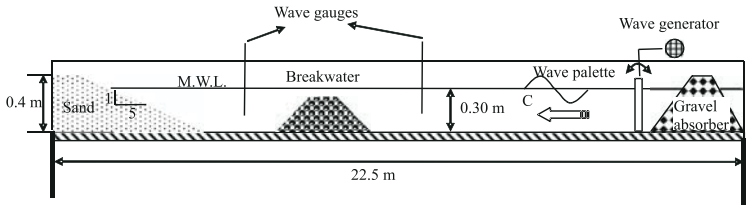

Figure 2: Wave flume

In the experiments, different conditions were tested including different slopes, grain sizes for various wave heights and lengths (more than ten for each set). During the experiments the breakwater slopes were varied 1/2 to 1/4, crest widths were 20 cm and 40 cm. Relative water depths over the submerged breakwater were also varied and crest height to water depth ratio varied between 1–0.83 during the experiments. Test conditions are summarized in the Table 1, where T is the wave period in seconds.

Table 1: Test Matrix

Test №	Slope of the breakwater		d_{50} (cm)	Crest Width (cm)	e	Water depth (cm)	*Hi* (cm)	*T* (s)
	Offshore side	Beach side						
1	1/2	1/2	2.85	20	0.57	30	8.0-1.4	1.06-0.54
2	1/2	1/2	2.85	40	0.57	30	7.8-1.9	1.08-0.54
3	1/4	1/2	2.85	20	0.57	30	8.5-1.0	0.96-0.58
4	1/2	1/2	2.85	20	0.57	28	8.0-1.25	0.98-0.58
5	1/2	1/2	2.85	20	0.57	25	7.2-2.1	0.85-0.56
6	1/2	1/2	1.30	20	0.43	30	8.2-2.55	0.88-0.60
7	1/2	1/2	0.85	20	0.34	30	7.4-1.15	0.92-0.57

3. Results and Discussions

The coarse gravel ($d_{50} = 2.85$ cm) trapezoidal breakwater with 0.25 m height, 0.20 m crest width was tested at 0.30 m still water depth in the first set of the experiments. Crest height to water depth ratio was 0.83. Test results are given in the Fig.3 as transmission

coefficient, (*Ht* / *Hi*), versus incident wave properties, (*Hi* / *L*). Transmission coefficient varies between 0.8-0.5 in this configuration.

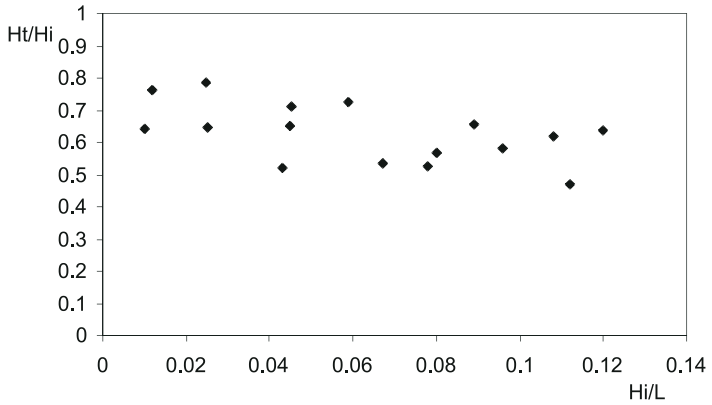

Figure 3: Variation of the *Ht* / *Hi* versus *Hi* / *L* for Test № 1

In the second test, the breakwater crest width was increased from 0.20 m to 0.40 m with all other parameters unchanged from Test № 1. The transmission coefficient versus incident wave properties are presented in Figure 4 for Test № 2.

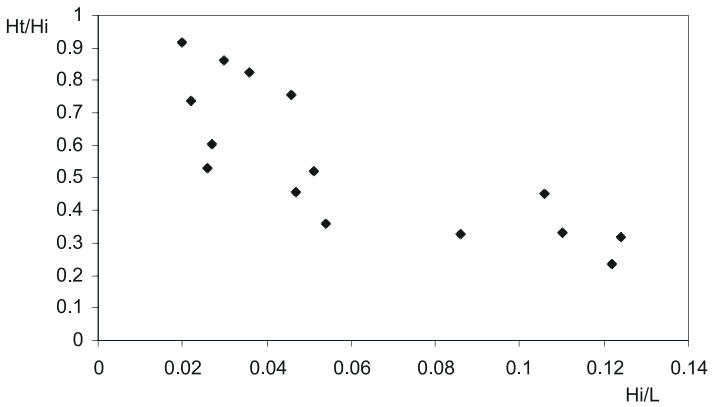

Figure 4: Variation of the *Ht* / *Hi* versus *Hi* / *L* for Test № 2

Two different characteristics are evident in the wave transmission coefficient results. First; large *Hi* / *Ht* ratios occur between 0-0.04 values of *Hi* / *L*. When the *Hi* / *L* is greater then the 0.04 wave transmission coefficient drops dramatically. In this zone (*Hi* / *L* > 0.04) waves were broken over the structure completely and they dissipate their energy over the structure. The ratio *Hi* / *Ht* varied between 0.4-0.2 in this zone. This results indicate the importance of the crest width of the breakwater. The incident wave steepness has an important influence on wave breaking phenomenon. Waves near the critical steepness

may be induced to break by the submerged breakwater and, since wave breaking process is always accompanied by energy looses, steeper waves are likely to be attenuated more than waves with milder steepness.

Test № 3 investigated the effect of breakwater slope with the offshore slope of the breakwater changed from 1/2 to 1/4. Results of the experiments are presented in Fig 5. The wave transmission coefficient is not affected significantly due to decreasing the slope. Only moderately large values of the ratio (*Ht* / *Hi*) were observed (0.9-0.5) in that series. The breakwater crest width 0.20 m and d_{50} were 2.85 cm in Test № 3.

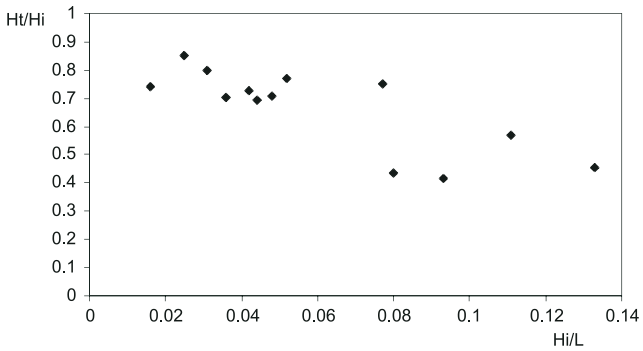

Figure 5: Variation of the *Ht* / *Hi* versus *Hi* / *L* for Test № 3

In Test № 4, the water depth was reduced from 0.3 m to 0.28 m. The shape and material of the breakwater were for Test № 1. The results of this series of experiments are presented in Fig.6. This figure shows that the transmission coefficient is reduced by decreasing the water depth over the breakwater and that the results are fairly close to those of the second set of experiments with a crest width of 0.40 m compared to a breakwater width of 0.20 m in this set. These results indicate the importance of the wave breaking phenomenon.

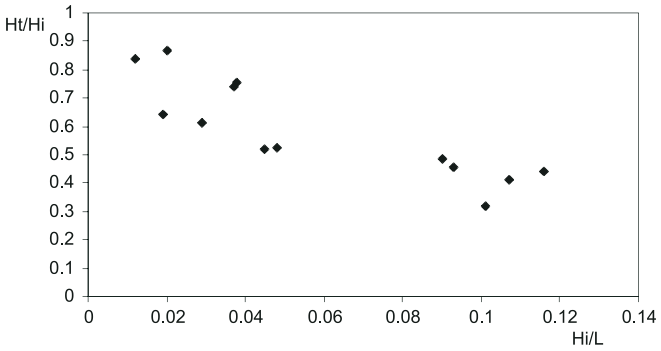

Figure 6: Variation of the *Ht* / *Hi* versus *Hi* / *L* for Test № 4

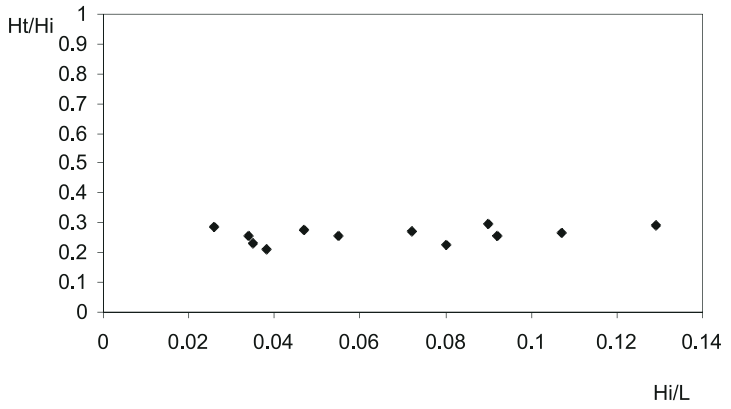

In the 5th set of experiments, the water level was equal to the breakwater crest elevation (Crest height to water depth ratio = 1). In this condition, the wave transmission is quite small as expected (Fig.7) and the incident wave characteristics are not significant. The *Ht* / *Hi* ratio is almost constant around 0.25.

Figure 7: Variation of the *Ht* / *Hi* versus *Hi* / *L* for Test № 5

The effect of the porosity was highlighted in the 6th test series by reducing the gravel size from 2.85 cm to 1.30 cm. The results are given in Fig. 8. The shape of the breakwater and water depth were the same as for Test № 1. The *Ht* / *Hi* coefficient decreased with increasing wave steepness compared to the Test № 1 results (Fig. 3). The performance of the breakwater was increased by reducing porosity.

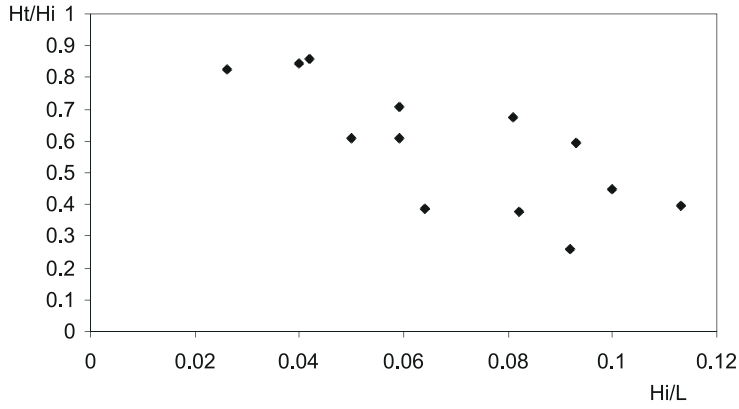

Figure 8: Variation of the *Ht* / *Hi* versus *Hi* / *L* for Test № 6

The 7th test series may be the most crucial test of the study. In this test, the shape of the breakwater tested was a dynamically stable breakwater after deformation by the storm

wave heights. Before recording the wave heights, the dynamically stable condition was generated. After that incident and transmitted waves were recorded. The deformation shape was also observedusing sand as a breakwater material too. In this set of the experiments, the initial shape of the breakwater and water depth were the same as for the initial test (Test № 1). The results of this set of the experiments are given in Fig. 9 and also deformation of the structure plotted.

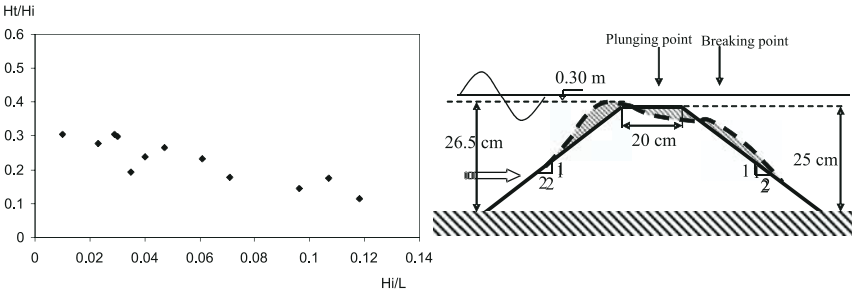

Figure 9: a) Variation of the *Ht* / *Hi* versus *Hi* / *L* Test № 7; b) Stable condition of the submerged breakwater ($d_{50} = 0.85$ cm)

The higher performance of the breakwater could be clearly seen from Fig. 9. The *Ht* / *Hi* values range between 0.3-0.1. Waves were observed to break over the dynamic profile of the structure and dissipate their energy over the structure.

4. Conclusions

The results of the experiments may be summarized as follows:

The porosity of the breakwater (grain size) is directly related to the performance of the structure.

Waves breaking over the structure and splashing over the crest were observed to reduce fluctuations behind the submerged structure.

During the storm waves conditions, deformation of the structure was observed. The structure eventually reached a stable condition. However, the structure was not totally destroyed and the breakwater continued to cause wave height reduction.

Dynamic stability (after deformation) of the breakwater results in wave plunging type breaking over the structure resulting in more energy dissipation.

After the dynamic stabilization of the breakwater, the shape of the breakwater has similar properties and shape as a natural longshore bar formation.

References

Dean, R.G., (1973), Heuristic models of sand transport in surf zone., conference on engineering dynamics in surf zone, Sydney, Australia

Halis, J., Carr, A., (1975), Nearshore sediment dynamics and sedimentation. Elsevier. NL

Huang, C., Chang, H., Hwung, H., (2003), Structural permeability effects on the interaction of a solitary wave and a submerged breakwater, *Coastal engineering,* Elsevier, Vol 49, 1-24

Iwagaki, Y., Noda, H., (1962), Laboratory study of scale Effects in two-dimensional beach processes, in Prooceed.8th Int. conf. On coast. Eng., Mexico, ASCE

Larson, M., Kraus, N.C, (1992), Dynamics of longshore bars, Proceeding of the 23rd Coastal Eng. Conf. ASCE

Mendez, F.J., Losada I.J., Losada M.A., (2001), Wave induced mean magnitudes in permeable submerged breakwaters. *J. of Waterway, Port and Ocean Eng.* Vol 127. No 1. 7-15

Miller, R.L., (1976), Role of vorticities in surf zone prediction: sedimentation and wave forces, beach and nearshore sedimentation. Edited by Davis Jr, R.A., Ethington, R.L., Society of economic paleontologists and mineralogists, Spec. Pub. No.24, pp. 92-114

Nadaoka, K., Uneo,S., Igarash, T., (1988), Sediment suspension due to large scale eddies in the surf zone, Int. Coastal Eng. Conf. Malaga, Spain

Rector, R.L., (1954), Laboratory study of equilibrium Profiles of beaches., B.E.B. Tech. Memo., 41,38 pp.

Silvester, R., (1974), coastal engineering I, II, Elsevier scientific publishing company, NL

Sunamura, T., (1984),Sandy beach geomorphology elucidated by laboratory modeling., Applications in coastal modeling., Edited by Lakhan, V.C., and, Trenhalie, A.S.,Elsevier Oceanography series NL

Takeda, I., Sunamura, K., Sunamura T., (1992), conditions for beach erosion on a barred beach, Z. Geomorphology, N.F. Berlin, Stuttgart

Ting, C., Lin, M., Cheng C., (2003), Porosity effects on non-breaking surface waves over permeable submerged breakwaters., *Coastal engineering,* Elsevier, Vol 50, 213-224

Twu, S., Liu, C., Hsu, W., (2001), Wave damping characteristics of deeply submerged breakwaters, *J. of Waterway, Port and Ocean Eng.* Vol 127. No 2. 97-105

SCOUR DEVELOPMENT IN FRONT OF COASTAL STRUCTURES AT INTERMEDIATE PHASES OF CONSTRUCTION

Tomasz Marcinkowski
Dept. Maritime Hydrotechnic, Maritime Institute, Gdańsk, Poland
Dept. Marine Civil Engineering, University of Technology
Gdańsk, Poland

Abstract

This paper aims at describing the erosive influence of structures on the sea bottom. It describes the threat that may appear during the construction of rubble mound breakwaters, massive breakwater heads of vertical walls and dumping structures made as cellular cofferdam or perforated walls. Measurements and observations made in nature are compared with existing recommendations while damages and failures, which took place during recently realized projects, are described.

Most observations presented in the paper concern the reconstruction of the West Breakwater in Łeba Harbour, Poland, and the modernization of the entrance to the Port of Kołobrzeg, Poland.

1. Introduction

Scour is the erosive force of moving water. This general definition of scour includes any erosion of sediment under any circumstances but with regard to the coastal structures a more precise definition is used: *Scour is removal by hydrodynamic forces, of granular bed material in the vicinity of coastal structures* (CEM, 2003). Any structure appearing in the wave field causes a change of the flow pattern in its neighbourhood. In the immediate neighbourhood of the structure the velocities of water particles caused by waves and current grow, increasing at the same time the movements in the sediments in those areas. As a result, erosion processes develop in the foreground and/or along the structure causing the lowering of the bottom. These processes, however, may also appear during natural reconstruction of the shore profile, so it is difficult to assess the amount of local erosion. Other factors, which, apart from hydrodynamic conditions, influence the degree of erosion, are also geotechnical properties and thickness of individual layers in the subsoil. As (Sumer et al., 2001) stated, the following phenomena may appear in the vicinity of structure: the contraction of flow; the formation of vortices in front of the structure (horseshoe) and behind the structure (lee-wake); the generation of turbulence; the occurrence of wave reflection, diffraction and breaking; and conditions leading to liquefaction. These changes, as mentioned above, usually cause an increase in the local sediment transport capacity and thus develop scour. Finally scour that occurs at the structure can lead to partial damage or complete failure of the whole or a part of the structure.

C. Zimmermann et al. (eds.), Environmentally Friendly Coastal Protection, 219-232.

2. Prediction of Scour

To study the risk of scour in the vicinity of costal structures, a 3-year research program (1997-2000), *Scour Around Coastal Structures* has been undertaken within the framework of the Marine Science and Technology program of the European Union. This subject has been extensively studied also in the United States and in Japan. Some studies focused on discovering the physical processes of scour, whereas other studies were directed at developing engineering methods for prediction the location and maximum depth of scour. Even if the hydrodynamic aspects of scour were fully understood, there remains the difficulty of coupling the hydrodynamics with sediment transport. Consequently, most scour prediction techniques consist of rules of thumb and fairly simplistic guidance developed from laboratory and field observations.

The scour process depends both on structural aspects such as geometry, location, physical characteristic (roughness, permeability, etc) and on structure-hydrodynamic interaction, and include following, (CEM, 2003):

- Localized increase in peak orbital wave velocities due to combined incident and reflected waves;
- Particular structure orientations or configurations that focus wave energy and increase wave velocity or initiate wave breaking;
- Structure orientations that direct currents along the structure or cause a flow acceleration near the structure;
- Flow constrictions that accelerate the fluid;
- Breaking wave forces that are directed downward toward the bed or that generate high levels of turbulence capable of mobilizing sediment;
- Pressure differentials in the soil that may produce liquefaction conditions allowing sediment to be transported away by currents;
- Flow separation and creation of secondary flows such as vortices.

The scour processes are even more complicated since the above mentioned factors may act individually or in combination.

Some engineering prediction methods for estimating scour for selected coastal structures and hydrodynamic conditions from the *Coastal Engineering Manual* are presented below.

2.1 Scour at Vertical Walls

Non-breaking waves. Close to the structure located in deeper water, incident and reflected waves superimpose creating standing a wave field with amplified horizontal particle velocities beneath the water surface nodes and minimal horizontal velocities beneath the antinodes. In regular, uniform waves for fine sand maximum scour nearest to the wall occurs at a distance $L / 4$ from the wall where L is the wavelength of the incident wave. Irregular waves produce a similar scour pattern with decayed tendency along with increasing distance from the wall. To estimate maximum scour the following empirically based equation is suggested for regular waves:

$$\frac{S_m}{H} = \frac{0.4}{[\sinh(k\,h)]^{1.35}} \tag{1}$$

where

S_m - maximum scour depth at node (L / 4) from wall,
H - incident regular wave height,
h - water depth,
k - incident regular wave number,
L - incident regular wavelength,

and for irregular waves:

$$\frac{S_m}{(u_{rms})_m T_p} = \frac{0.05}{[\sinh(k_p h)]^{0.35}} \tag{2}$$

where

T_p - wave period of the spectral peak,
k_p - wave number associated with the spectral peak by linear wave theory,
$(u_{rms})_m$ - root-mean-square of horizontal bottom velocity.

The value of was given by Hughes as:

$$\frac{(u_{rms})_m}{g\,k_p T_p H_{m0}} = \frac{\sqrt{2}}{4\pi\cosh(k_p h)}\left[0.54\cosh\left(\frac{1.5 - k_p h}{2.8}\right)\right] \tag{3}$$

where H_{m0} is the zeroth-moment wave height, and g is gravity. Eq. 3 is empirically based and should not be applied outside the range $0.05 < k_p h < 3.0$.

One should stress that scour predicted for irregular waves is smaller than scour predicted for regular waves. Obliquely incident non-breaking waves tend to scour more then equivalent normally incident waves. The addition of current running parallel to the vertical front structure also increases the process of scour. Unfortunately, no engineering methods are presently available to estimate scour in these more complicated conditions regarding non-breaking waves.

Breaking waves. Scour caused by normally incident breaking waves on vertical structures is generally greater than for non-breaking waves, and there is more likelihood of scour leading to structure damage. The physical mechanisms responsible for scour by breaking waves are not well understood, but it is generally thought that the breaking process creates strong downward directed flows that scour the bed at the base of wall. The prediction of scour depth of cohesionless sediment at vertical walls is based on rules of thumb. The maximum scour depth (S_m) is approximately equal to the non-breaking wave height ($H_{\max}$), which may roughly be estimated by the water depth (h) at the structure, i.e.,

$$S_m = H_{\max} \qquad \text{or} \qquad S_m \cong h \tag{4}$$

For estimating maximum scour of noncohesive sediment due to normally incident breaking irregular waves with a mild approach slope the following empirical equation was proposed by Fowler:

$$\frac{S_m}{(H_{m0})_0} = \sqrt{22.72\frac{h}{(L_p)_0} + 0.25} \tag{5}$$

where

S_m - maximum scour,

$(H_{m0})_0$ - zeroth-moment wave height in deep water,

H - pre-scour water depth at vertical wall,

$(L_p)_0$ - deepwater wavelength associated with the peak spectral wave period, T_p.

Application of this empirical equation is limited by the data to values of relative depth and relative steepness within the ranges:

$$0.011 < \frac{(H_{m0})_0}{(L_p)_0} < 0.040 \tag{6}$$

It is worth noting, that above methods assume no current along the vertical wall.

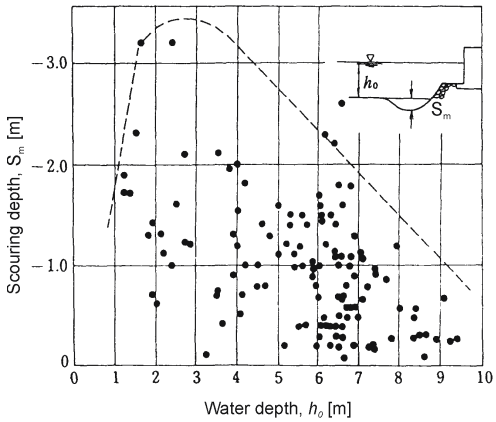

Figure 1: Field data on scour, (Horikawa, 1988)

Research at full scale concerning the development and dimensions of scour in front of the vertical wall structures and in front of rubble mound breakwaters have been conducted mostly in Japan. The results of measurements in nature presented in (Horikava, 1988) address also the quantitative assessment of the erosion processes. Fig. 1 presents the maximum scouring depth appearing in front of an obstacle with a vertical wall, depending on the depth of the structure foundation. The envelope of these measurements indicates the appearance of maximum depths in places with water depths up to approximately 3 m.

Model test results from several laboratories clearly support the thesis of the appearance of maximum scour in the area between the breaking point and the shoreline.

2.2 Scour at Sloping Structures

Scour at the toe of sloping-front structures depends on structure slope and porosity, incident wave and current conditions, water depth, and sediment grain-size. There are no generally accepted techniques for estimating maximum scour depth or 3-dimensional scour configurations. Simple rules of thumb are used as engineering guidelines for scour at sloping structures.

- The maximum scour at the toe of a sloping structure is expected to be somewhat less than the scour calculated for vertical wall under the same condition. Therefore a conservative estimation of scour depth is $S_m < H_{\max}$;
- The scour depth increases with increasing structure reflection coefficient;
- Scour depth is significantly increased when currents act in conjunction with waves along structure;
- Obliquely incident waves may cause greater scour then normally incident waves.

Some observations in nature indicate considerable dimensions of bottom erosion, depending on the hydrodynamic conditions, in front of rubble mound structures founded on small depths. Fig. 2 presents examples of measured scour in front of the toe of a detached breakwater with the outer layer of concrete blocks. The breakwater in the design was founded at a depth of 3 to 4 meters.

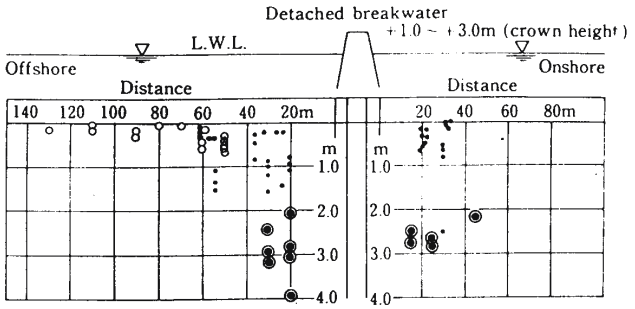

Figure 2: Field measurements of scour around a detached breakwater (Pilarczyk et al., 1996)

2.3 Scour at Piles

Scour at small vertical piles (pipe diameter, D, is less then one-tenth of the incident wavelength) is caused by three simultaneously acting mechanisms: formation of a horseshoe-shaped vortex wrapped around the front of the pile; vortex shedding in the lee of the pile; and local flow accelerations due to streamline convergence around the pile. The scour formation is governed by the following key parameters: current magnitude, orbital wave velocity, and pile diameter. A general, and somewhat conservative rule of thumb (even for combination of waves and currents) is: maximum depth of scour at a vertical pile is equal to twice the pile diameter. For the prediction of pile scour by waves at

a vertical pile under live bed condition (Sumer et al., 1992) established an empirical equation in which maximum scour depth (S_m) depends only on pile diameter (D) and Keulegan-Carpenter number (KC) by eq. 7.

$$\frac{S_m}{D} = 1.3\left[1 - e^{-0.03(KC-6)}\right] \tag{7}$$

From tests conducted by Mory at al., (2000), one observation should be stressed: the global scour associated with the pile group is more significant than the local scour.

3. Case Study

3.1 Modernization of the Entrance to the Łeba Harbour

A vital element of the modernization of the entrance to the Łeba harbour in Poland was the improvement of navigation conditions. The analysis of hydrodynamic and navigation conditions has led to the solution consisting of the lengthening of the existing structure of West Breakwater to the North, and then to the North-East direction. The extended part of the breakwater is of rubble mound construction with a 5.0 m wide concrete superstructure. The elevation of the crest is +2.50 m, while the elevation of the reflection wall of reinforced concrete at the seaside is +3.50 m. The cross section of the breakwater has been adjusted to the changing depth and loads (Fig. 3 presents the structure cross section at the depth of 4.0 m) by the use of the following materials:

- geotextile;
- a bedding layer of 3 ÷ 8 cm in size – as a load and protection layer for the geotextile;
- broken stone from nonweathered magma, 10 ÷ 30 cm fraction, as the breakwater core;
- irregular magma blocks of various weights according to the particular sections of the structure, as outer layer of the breakwater and as intermediate layers;
- tetrapods, weighing 20 and 50 kN.

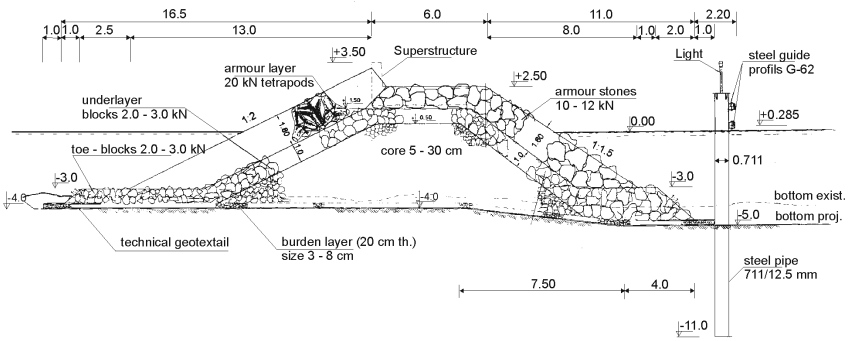

Figure 3: Breakwater cross section at the depth of 4.0 m

The breakwater head has been constructed inside a steel sheet pile cofferdam made of G-62 sheet piles (Fig. 4) as a vertical massive structure in the form of a concrete block, 9.0 m wide, and 27.50 m long. On the outside, blocks of rock and tetrapods also protect the breakwater head.

Further details on the Łeba project concerning: morphological background; breakwater, subsoil and marine environment interaction as well as technology used are given in (Marcinkowski, 2001).

During the reconstruction of West Breakwater in Łeba, scour problems occurred several times at intermediate phases of construction.

Case 1a

In the initial stage of construction work, was started on the vertical wall massive head with the use of floating equipment together with the work done from the shore.

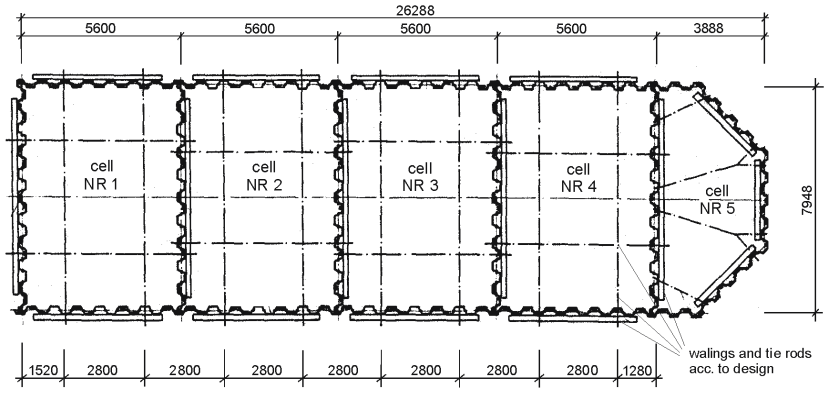

Figure 4: Plan of steel sheet pile cofferdam

Bathymetric measurements in the place where the sheet piles were driven showed depths of 3.5 to 4.5 m. The design assumed the –6.00 elevation for the calculated sea bottom for two parts of the cofferdam and –7.00 for the remaining three. The elevations of the sheet pile tip were assumed as –10.50 m and –11.50 m. After driving two walls of the first section the severe wind and hydrodynamic conditions made further work impossible. This was followed by an average storm with wind speeds of up to 14 m/s which caused damage to the driven sheet pile walls by overturning them seaward; however, the sheet piles themselves were not damaged. The damage mechanism can be described as the considerable scour in the vicinity of the structure and the loss of overall stability of the whole wall. The breakwater head would withstand this hydrodynamic load in its final design stage but collapsed at intermediate phase of construction.

The measured elevation of the depth after storm in the working area was about –8.50 m. It is likely, however, that the maximum depths of the scour were at times greater than

measured. The situation observed and measured in the Łeba region suggests larger depths of the erosion forms than those shown in Fig. 1. The maximum wave height (H_{max}) at the site did not exceed 2.5 m, while the initial water depth was 4.5 m. Having this in mind the predicted maximum scour depth for the extreme conditions should be estimated at the level of 4.5 m referring to recommendation (4) or almost 4 m referring to recommendation (5) (Fig. 5). It is worth noting that although the storm did not represent extreme conditions, the predicted maximum scour depth was measured.

The design guidelines recommended construction of the breakwater head in the summer season i.e. at the time when the probability of storm occurrence is least. Unfortunately there was a delay in construction works not caused by the contractor. For a bottom of considerable mobility it is suggested that one assume the most adverse of the observed bathymetric conditions in the place where the construction is to be performed, and to consider additionally the interactions between the structure and the seabed.

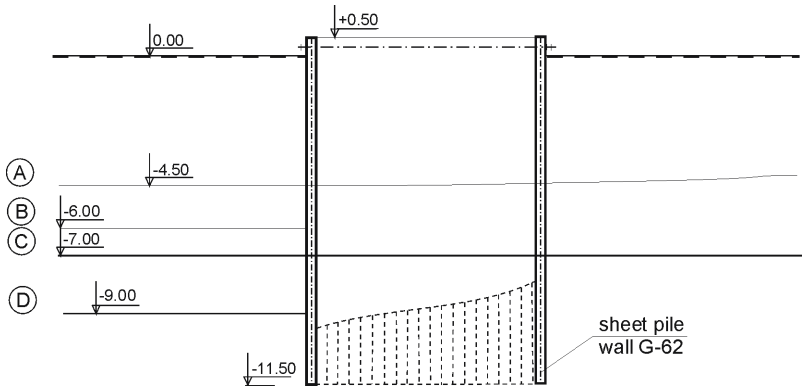

Figure 5: Considered levels at failure of sheet pile wall
A - initial bottom; B - scour assumed in design; C - scour recommended (CEM) for site conditions; D - scour as recommended for extreme conditions, scour measured

Case 1b

The body of the rubble mound breakwater, in compliance with the technology assumed, was first constructed from the landside. The front of rubble structure during its intermediate stages is formed of definitely much finer material than the protective armour layer designed for such conditions. The slope inclination of the front from the seaside is larger during construction (by 1:1 – 1:1.25) than the final inclination of the slope. The above parameters result in a structure with a higher wave reflection coefficient during construction. This influences the development of scour in front of the structure, which is intensified with increasing waves and currents.

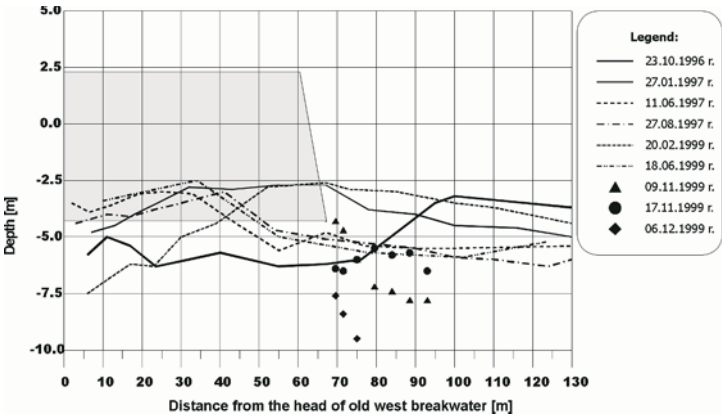

Figure 6: Scour in front of the structure under construction

Fig. 6 shows profiles measured before the construction was started, in the years 1996 –1999. They represent the part from the head of the existing West breakwater along the designed rubble mound breakwater. The picture shows the body of the breakwater for the stage when work was suspended for winter. Additionally, points show the depth measurements in the front of the structure performed in wintertime. The scour appearing during the storm on 03 – 04.12.1999 caused considerable adjustment of the breakwater slope. The depth of the scour, which was over 5.0 m in extreme conditions, was larger than those observed by Horikawa (Fig. 2) but also exceeded conservative estimation of scour depth regarding a sloping structure. The range of scour, as far as the distance from the front of breakwater is concerned, is also substantial when compared with the wavelength. Such changes in the bottom have a large influence on the changes of wave conditions in front of the structure. The incident wave approaching from the larger depth is getting steeper before breaking, yet propagating over the changed, deeper bottom it does not break, but impacts the sloping breakwater with even more energy. This effect was observed both for final stage and for intermediate phases of construction.

It is known from observations that the extreme scour is reduced after the peak of the storm, yet the sea bottom does not recover completely to prestorm elevations. Assuming that the interactions between the new established construction and a marine environment will lower the average elevation of the bottom by about 1 m, the necessity of the additional 35 m^3 of the construction material for one running meter of the described breakwater has to be assumed. It is evident that this change will cause a significant increase in construction costs and concern between the various parties. This negative effect of the scour should be taken into consideration during design, while estimating foundation level of the breakwater.

Case 1c

The analysis of conditions, presented in case 1a led to changes in the design, requiring about 4.0 m longer sheet piles for the head cofferdam. Also the technology of driving the sheet pile walls was changed – the works were performed from the finished part of the rubble mound

breakwater. During the construction of the third section, the quickly changing meteorological conditions did not allow the cofferdam to be filled with concrete, so the storm waves from the NE direction hit the sheet pile walls of the third section directly.

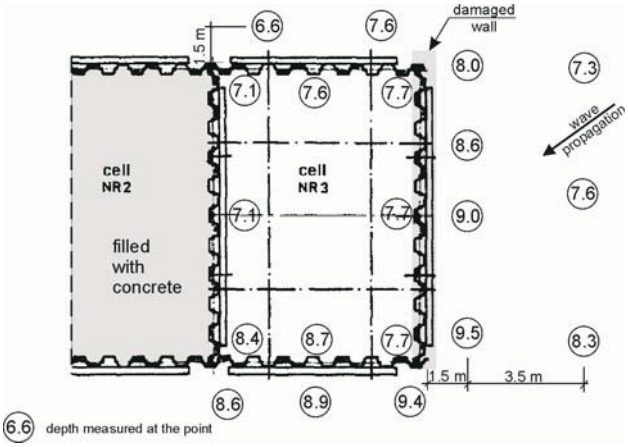

Figure 7: Measured depth in the vicinity of damaged cell

The sheet piles of the front wall broke at the elevations from – 9.50 to – 11.50 m. Fig. 7 presents depth conditions in the vicinity of the structure and Fig. 8 shows the broken sheet piles. In this case the damage mechanism was the result of exceeding stresses in the material. The problem should be analyzed in the dynamic mode. An approximate analysis indicates the important influence of dynamic loads in the changed conditions (scour at the bottom, cracking of corner elements or loosening of locks, dynamical load from waves).

Figure 8: Damaged sheet piles

The damage of sheet piles may indicate flaws in the material (tests are needed), yet it surely confirms the appropriateness of fixing them in the soil. The future solution of the

described situation should be sought in the emergency, quick closing of the capping slab of the section of cofferdam under construction.

3.2 Modernization of the Entrance to the Kołobrzeg Harbour

The development of the harbour in Kołobrzeg is in a great part limited by the narrow and dangerous entrance to the harbour. It does not allow larger vessels to enter and it limits the entrance of other vessels due to hazardous weather conditions. After the reconstruction, according to assumptions made by the harbour management, the harbour should be prepared for the access of larger vessels with maximal length 100 m, width 20 m and draught 6 ÷ 6.3 m. The reasonable design of the harbour entrance widening through the construction of a new western breakwater with the demolition of the existing one is in any case connected with the lengthening of the breakwaters. The western breakwater will be 155 m longer than previously. The eastern breakwater will be extended by about 150 m. The lengthening of the breakwaters as well as the construction of damping elements assures larger attenuation of the incoming waves. The layers of broken stones with adequate sizes will comprise the West rubble mound breakwater. The superstructure founded at elevationl +0.70 m was designed as a reinforced concrete structure erected partially from prefabricated elements and partially made as monolithic concrete on site. The global breakwater parameters are:

- inside water depth near the breakwater 7.5 m
- elevation of the pavement of the communication lane +2.50 m
- elevation of the top of the parapet +4.0 m
- seaward slope 1:2.8
- inside slope 1:2

The breakwater is placed on the geotextile layer with IV resistance class (DIN 5430) compound with following layers:

- filtration and protection layer made of gravel;
- core of broken stones (granite, syenite) with mass of 10 ÷ 50 kg;
- intermediate layer of stones with mass of 0.4 ÷ 0.8 t in places with extreme exposure, and of 0.2 ÷ 0.6 t from the harbour side;
- protection layer, similar to the above, of stones with mass of 4 ÷ 8 t and of 4 ÷ 6 t;
- layer of tetrapods with mass of 5 t at the structure head from the datum –3.0 m.

The whole structure consists also from dumping elements along the interior part of the breakwater. The dumping elements, which are near the breakwater head, are designed as cellular cofferdam limited by the palisade made of steel pipe piles of 612 mm diameter and wall thickness of 12.5 mm; steel 18G2. The cofferdams will be filled with broken stones, while their superstructures are assumed to be reinforced capping beam of the total width 4.3 m and height 2.3 m.

The construction technology of the breakwater in Kołobrzeg will be completely carried out with the help of the floating equipments which is different than the technology used in the Łeba breakwater. The problem of scour occurred while constructing the West breakwater. This structure is still under construction.

Case 2a

During the execution of the next to last dumping structure of the West breakwater, when all 70 piles were driven, the deterioration of the weather conditions made it impossible to finish the cofferdam and fill it with broken stones. The storm waves (the wind velocity was less then 15 m/s from NW direction and average sea elevation was 547 cm) approached obliquely the palisade made of the steel piles. The initial depth at the structure was varying from 7.5 to 8.0 m and elevations of the driven piles tips were -15.5 and -17.0 m. The maximal scour depth in the direct vicinity of the dumping structure (see Figure 9) reached 3.0 m. This scour depth value decidedly exceeds the value of

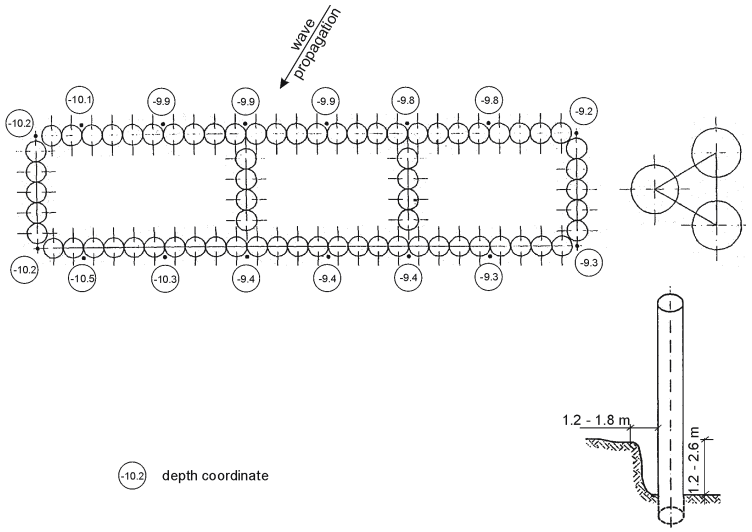

Figure 9: Depth and configuration measured after storm in the vicinity of dumping structure 8-OZ

a double pile diameter as for a pile group. On the other hand, under assumption of the vertical wall, the scour depth meets the case of maximum wave height, but exceeds the envelope obtained by (Horikawa, 1988) and presenting in Fig. 1. The measurement of the bathymetry just after the storm indicates a local character of the scour hole with a significant steepness. Such a form of scour differs from the ones observed for rigid structures having a vertical wall under breaking and non-breaking waves. This effect is probably associated with a more slender, driven structure submitted to cyclic loadings and local liquefaction of soil in the vicinity of the structure. Due to changes occurring in the subsoil during wave action, along with development of scour, the palisade lost overall stability and 65 of 70 piles became inclined, however, without a deformation of the piles.

After the failure of the structure, additional calculations, using PLAXIS numerical model (Brinkgreve, 2002), were performed to check the stability of the dumping structure, its deformations, and stress in the soil for some different scour depth that simulate phases of the project. Fig. 10 shows the initial conditions and scheme of the finite elements grid used in calculation. The most important results of the stress-strain analysis are presented in

Table 1. In all calculations the structure was treated as a quasi-static model. This assumption allows forcing the static system by instantaneous values of the maximal dynamic loads.

The simulations performed indicate a significant increase of the displacements of the upper and lower ends of pipe piles also for scour depth equal to 1.5 m that was assumed in the breakwater design in the phase when the cells were not filled with stones, but it does not lead to structure failure. During the fatal 20/21 of June 2003 the scour depth was about 3.0 m. The simulation confirms those extreme conditions led directly to the failure of the structure.

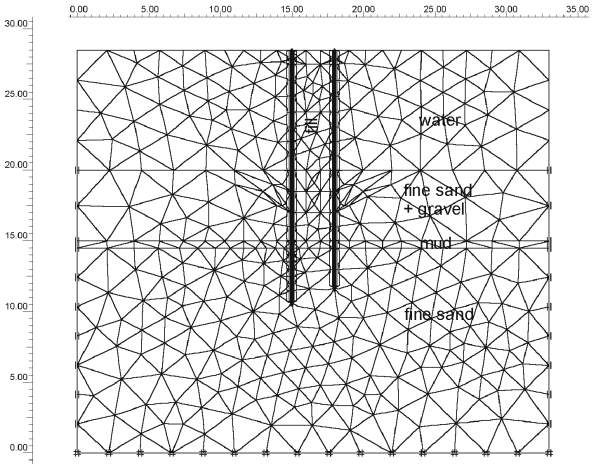

fine sand + gravel $\gamma = 20\ \text{kN/m}^3$, $\varphi = 32°$; mud $\gamma = 14\ \text{kN/m}^3$, $\varphi = 5°$, $c = 20\ \text{kPa}$
fine sand $\gamma = 19\ \text{kN/m}^3$, $\varphi = 31°$; fill $\gamma = 18\ \text{kN/m}^3$, $\varphi = 40°$

Figure 10: Scheme assumed for stress-strain analysis

Table 1: Results of calculation

Construction stage	Effective mean stresses in soil (kPa)	Displacement of the top (m)	Displacement of the tip (m)	Remarks
Without scour, the cell is empty	184	0.218	0.006	stable
Without scour, the cell is half filled	157	0.182	0.005	stable
Without scour the cell is totally filled	149	0.158	0.005	stable
Scour 1.5 m, the cell is empty	276	0.298	0.015	limit condition
Scour 1.5 m, the cell is half filled	221	0.242	0.009	stable
Scour 3.0 m, the cell is empty	307	0.980	0.087	failure

4. Conclusions

The observations taken during the construction of the breakwater indicate the necessity of considering the timetable of the construction in the design process. Any structures built in a marine environment have an instant influence on the wave field and flow pattern in its neighbourhood and as a consequence it has a significant influence on changes of the sea bottom configuration in the structure vicinity. These changes should be considered during the design phase, particularly in the case of rubble mound structures.

The actual scour in the neighbourhood of the structure can reach a magnitude more dangerous for its safety in relation to that recommended in the available professional literature. The majority of the formulas used to predict the scour are empirical or semi-empirical based on hydraulic model tests. The scale effects of the sediments transport, fluid dynamics and geometry of analyzed structure are usually the source of errors in the laboratory experiments therefore in-situ measurements are appropriate for the development and verification of empirical formulas.

The stability conditions in intermediate phases of breakwater erection, influenced among other by scour development, can be decidedly worse than those occurring for the final shape of the structure. Therefore the choice of the optimal structure design has to consider all construction phases that will occur during the construction timetable.

References

Brinkgreve R.B.J., 2002, “PLAXIS-Finite Element Code for Soil and Rock Analyses”, A.A. Balkema Publishers, The Netherlands

Horikawa K., 1988, “Nearshore Dynamics and Coastal Processes”, University Tokyo Press, Tokyo

Marcinkowski T., 2001, “Hydraulic Effects and Loads Occurring in Intermediate Phases of a Breakwater Construction”, Proceedings of the V-th International Seminar on Renovation and Improvements to Existing Quay Structures, Gdańsk, pp 63-72

Mory M., Larroudé Ph., Carreiras J., Seabra Santos F. J., 2000, “Scour around pile groups”, Proceedings of Coastal Structures 99, Santander, Spain, vol. 2. Balkema, Rotterdam, Netherlands, pp 773-781

Myrhaug D., Håvard R., 2003, ”Scour below pipelines and around vertical piles in random waves”, *Coastal Engineering,* Elsevier, Vol. 48, pp 227-242

Pilarczyk K. W., Zeidler R. B., 1996, ”Offshore Breakwaters and Shore Evolution Control” A.A. Balkema, Rotterdam, Brookfield

Sumer B. M., Fredsøe J., Christiansen N., 1992, “Scour Around Vertical Pile in Waves”, *Journal of Waterway, Port, Coastal, and Ocean Engineering Division,* American Society of Civil Engineers, Vol. 118, No. 1, pp 15-31

Sumer B. M., Whitehouse R. J., Tørum A., 2001, “Scour around coastal structures: a summary of recent research”, *Coastal Engineering,* Elsevier, Vol. 44, pp 153-190.

U.S. Army Coastal Engineering Research Center, 2003, “Coastal Engineering Manual”, Washington, DC 20314-1000

CLIFF EROSION – HOW MUCH DO WE REALLY KNOW ABOUT IT

Ping Dong
Division of Civil Engineering, Faculty of Engineering and Physical Sciences,
University of Dundee
Dundee, United Kingdom

Abstract

In this paper, the current state of art research on coastal cliff erosion is briefly reviewed. It is shown that apart from the mean erosion rate which is predictable at the sites where long-term erosion data are available, time-dependent erosion and erosion statistics are not yet predictable. The existing methods either do not address completely the problem or rely on parameterizations that are inadequate for describing beach-cliff system dynamics. Some alternative approaches are suggested and discussed.

1. Introduction

In many areas of the UK and other parts of the world marine cliffs are receding rapidly resulted in considerable losses of land and properties. Understanding why and how these cliffs are being eroded is therefore of considerable interest to coastal engineers and managers alike. Without such an understanding prediction of cliff recession cannot be made with the required degree of confidence on which cliff managements schemes could be based. The knowledge of cliff recession is also important from the point of view of large-scale coastal morphodynamics as the eroding cliffs could be the major sources of beach materials. The creation of many barrier beaches and fluctuations of longshore transport rates can be intimately linked with the locations, amount and timing of large cliff erosion episodes.

The cliff-top retreat is the result of coastal landslides which can take place in various forms. The most common types of cliff failure are rock-soil falls, slides and avalanches although topples and flows also occur (Schuster and Highland, 2003). Despite that cliff erosion rates are routinely predicted, our knowledge of the topic is grossly inadequate for such predictions to be evaluated rationally or relied upon. Many pertinent questions remain unanswered such as:

1. Could cliff erosion be understood/modelled in terms of the individual, physical properties of beach/cliff system?
2. Is cliff erosion a complex system with unknown predictability limits?
3. Under what conditions individual slips and rock falls are uncorrelated (Gaussian) or correlated (indicating nature works in its self-organised state by action and reaction)?

C. Zimmermann et al. (eds.), Environmentally Friendly Coastal Protection, 233-242.

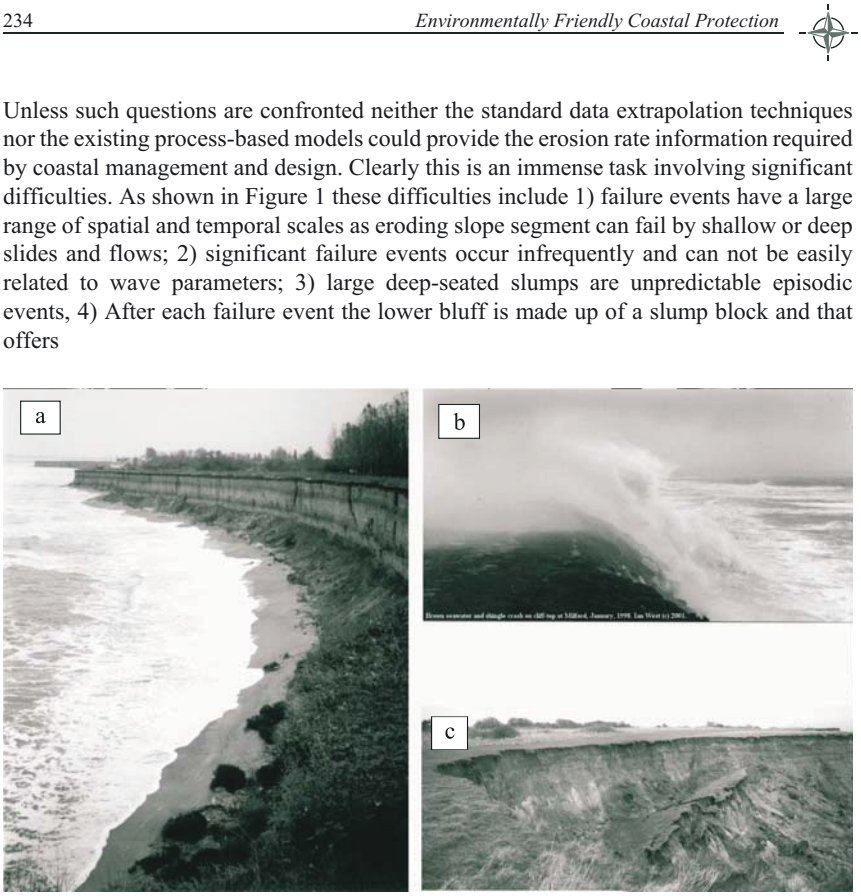

Unless such questions are confronted neither the standard data extrapolation techniques nor the existing process-based models could provide the erosion rate information required by coastal management and design. Clearly this is an immense task involving significant difficulties. As shown in Figure 1 these difficulties include 1) failure events have a large range of spatial and temporal scales as eroding slope segment can fail by shallow or deep slides and flows; 2) significant failure events occur infrequently and can not be easily related to wave parameters; 3) large deep-seated slumps are unpredictable episodic events, 4) After each failure event the lower bluff is made up of a slump block and that offers

Figure 1: a) Receding loess cliff at the Bulgarian Black Sea Coast near Krapets (courtesy Jesper Damgaard); b) Brown seawater and shingle crash on cliff-top at Milford, Wessex, England, January, 1998 (courtesy Ian West); c) Typical rotational failure at the Naze

temporary protection. No methods are currently available to predict how the slump block is eroded by waves. Therefore the rate of cliff erosion could be due to extreme water levels and waves as in case b; cumulative effects of sediment transport and beach erosion, case a; or weakening of the internal strength within the cliff by water pressure build-up or cracking, case c.

The purpose of this paper is to review briefly the current understanding on the subject and modeling approaches with emphasis on the knowledge gaps and uncertainties. It is shown that apart from the mean erosion rate which is predictable at the sites where long-term erosion data are available, time-dependent erosion and erosion statistics are not yet predictable. Possible alternative approaches are suggested and discussed.

2. Processes and Mechanisms

As illustrated in Figure 2 coastal cliffs can fail due to various mechanisms such as wave impact, foreshore erosion or pore pressure built-up due to intense rainfall.

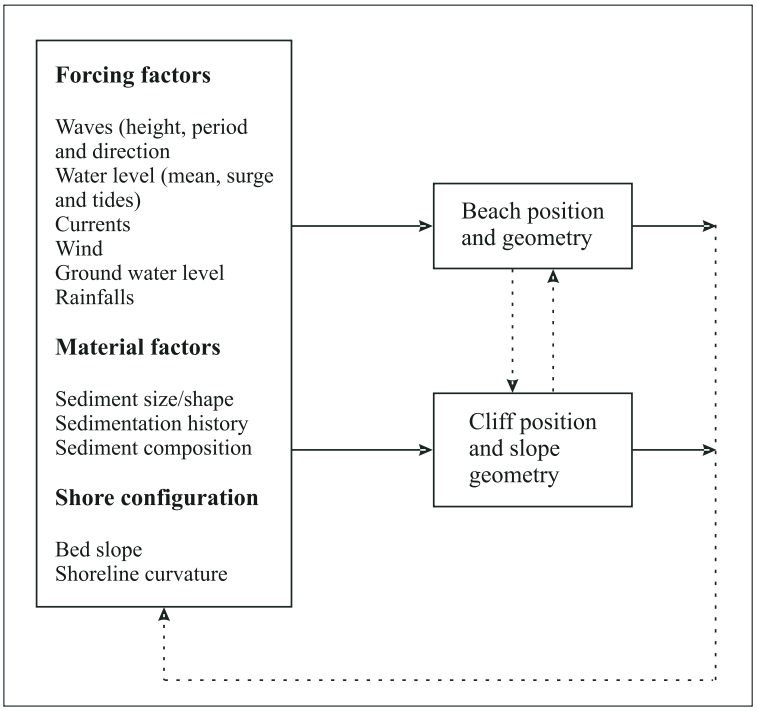

Figure 2: Conceptual process-response model of a beach-cliff system (adapted from (Pilkey and Cooper, 2002))

The failure triggering mechanism and subsequent slope recession are therefore controlled by both processes on the beach and on (and within) the cliff. There exist a multitude of interactions and feedback processes which could be random and intermittent and are almost always three-dimensional and time-dependent. For example, waves and water levels are random and it is not clear over what time scale the corresponding statistical parameters of these processes should be used to characterise the erosion statistics. Furthermore, erosion of failing debris is intermittent and is only reached by wave run-up. The erosion rate could vary considerably even for the same incoming waves as the position and geotechnical properties of the debris change with time. The influence of groundwater and rainfall is believed to be important but no measurements of such influence are currently available. Perhaps the most important difficult problem is the mismatch in time-scales, ie. the episodic nature of slumping and gradual/intermittent erosion of the toe and foreshore. This demand as well sets the limits of spatial and temporal aggregation of the cliff erosion data and models. As an aid for the subsequent discussions, a rough categorisation of the processes and mechanisms is given in Table 1.

Table 1: Cliff erosion process categorisation

Cliff types	Dominant processes	Mechanisms	The mode of cliff erosion	Attainment of equilibrium (under cross-shore actions only)
Hard cliff	Weathering	Wind/water actions	Quasi-Continuous	No
	Abrasion of shore platform	Wave actions	Quasi-Continuous	Yes
	Basal erosion/notch development	Wave impact	Quasi-periodic	Yes
Soft cliff	Foreshore erosion	Increased wave attack Increased cliff height/slope	Quasi-periodic	No
	Erosion of debris	Run-up and transport	Intermittent	No
	Residual pore water pressure build- up due to waves	Reduction of the effective strength	Episodic	Yes
	Rainfall	Develop seaward gradient of water table Pore pressure build up	Episodic	Yes

3. The Existing Methods

3.1 Data-Based Models

Many examples of coastal cliff retreat have been documented in the literature. The mean annual retreat values range from approximately zero to 2 meters as shown by Schuster and Highland (2003). Despite the fact that such mean retreat rates are inevitably affected by the sampling frequency and data length they remain the best indicator of future long-term erosion trend at any given site. However it must be recognised that the local episodic retreat could exceed many times of these mean values. Although these large retreat events are infrequent their impact on the morphological evolution of the cliff and the beach can be very significant over engineering time scale (years to tens of years). This is why, when establishing development setbacks from coastal cliffs, both long-term average retreat rate (deterministic and linear) and episodic slope failures (probabilistic and nonlinear) should be considered.

The data-based methods do have some severe limitations. Firstly the average recession rate is fixed so that it will not reflect any time dependent changes of hydrodynamic environment or the cliff properties. The obvious examples of such changes are the influences of sea level rise and engineering protection works (slope protection or beach recharge).

3.2 Semi-Theoretical Correlation

In order to overcome the limitation of purely data-based methods, various semi-theoretical models have been developed in recent years to predict cliff erosion rate by relating it to the forcing and resistant parameters of the waves and cliff. The historical cliff top positions

are used to calibrate the models. Most formulations focus on estimating the retreat rates of the cliff on the basis of a single dominant failure mechanism. For example, Komar et al (2002) proposed to correlate the cliff erosion rate with the average period when the cliff would be subject to wave attack. Kamphuis (1987) relates the average erosion rate of the Great Lake bluff with the rate of clay foreshore under-cutting. Mano and Suzuki (1999) examined the soft rock cliff at the Fukushima Coast and proposed a relationship between the mean erosion rate with the onshore component of wave energy flux at the breaking point, the Young's modulus and the cliff height.

Although these models are generally sound and easy to use they rely heavily on the coefficients that are calibrated using site-specific data. This limits their applicability to sites where such data are available. Furthermore as such type of models either assumes a single erosion mechanism or relies on limited wave parameters, actual erosion processes, particularly their temporal and spatial variability, have been completely ignored.

3.3 Slope Stability Analysis

Like any soil bank failure or landslides, the main failure modes of coastal soft cliffs are translational and rotational slips. The mechanisms by which cliff failure occurs differ depend on the nature and state of soil. Therefore, a more fundamental approach to the problem is based on the formulation of the slope failure mechanism and incorporating the failure mechanism in modeling of slope behavior. According to the basic soil stability concept, if the shear stress mobilized by the failing soil mass at its base is τ_{mob}, and the shear strength of soil is referred to as τ_f, then the factor of safety against shear failure of the cliff is simply defined as

$$FS = \frac{\tau_f}{\tau_{mob}} \tag{1}$$

According to Eq (1), failure occurs in theory when $FS \leq 1$. Due to the large uncertainties in the model parameters and time-dependent changes of these parameters, actual failure usually occurs when the calculated FS is greater than 1. For a natural slope the acceptable value of the FS is dependent on the degree of risk and uncertainty involved but typically greater than 1.3 (Chapman et al. 2002). Over the past decade, a number of slope stability models have been developed and their predictive capabilities evaluated among which the Bishop's method is often used because of its general applicability and simplicity. The Bishop's method is

$$FS = \frac{1}{\sum w \sin\alpha} \sum \left\{ [c'b + w(1 - r_u)\tan\phi'] \frac{1}{\cos\alpha + \frac{\sin\alpha \tan\phi'}{FS}} \right\} \tag{2}$$

where the summation is over all calculation elements, α is angle of inclination, c' is the apparent cohesion, ϕ' is the angle of friction, $b = 1\cos\alpha$, l is the base length of an element, $r_u = ub / w = u / \gamma h$, $u = z_w \gamma_w$ is pore water pressure, γ_w is the unit weight of water, z_w is the piezometric height of water.

Edil and his co-workers (Chapman et al., 2002, Edil and Schultz, 1983 and (Edil and Vallejo, 1983) have used this and several other methods to compare predicted and observed failures of Lake Michigan shoreline bluffs between a given time period (the late 1970's and the mid 1990's. The results were presented using the reliability index, which can be converted into a probability of failure. The comparison of the model results to observed slope failures demonstrated that it is necessary to adjust the failure criteria so that the statistics of the failing slopes could be more accurately predicted. An empirical calibration value of the probabilistic model was then developed to give the engineer a realistic probability of slope failure. As a result the model is highly site-specific and cannot be used at the sites where no erosion data are available.

Another deficiency of their approach is that the external erosion impact on the bluff was not modeled directly. Instead they assumed that the water and soil properties such as $\gamma_w c'$ and ϕ' are independent of the hydrodynamic conditions and include the effect of waves by varying the slope profile through the changes in α and h.

3.4 Cliff-Beach System Processes

Apart from the properties of the cliff itself, the effects of wave impact on the cliff face or its toe play an important role as it could either cause local failures around the point of impact or result in the erosion of the toe of the cliff. The latter will reduce the area of the shear surface and resistant shear force. Therefore a more complete process-based model of cliff evolution must include the following controlling mechanisms: 1) internal shear force balance along the slip surface; 2) the rate at which the falling debris is removed and 3) the rate of toe scour development. As the failure event is almost instantaneous, the time scale of cliff top retreat is then determined by the time scales of mechanisms 2) and 3) both of which are still poorly understood. Despite this, some attempts have recently been made in developing more sophisticated process-based numerical models. One of such models is cliffSCAPE (Soft Cliff And Platform Erosion) as reported by Walkden et al. (2002).

In this model the cliff was represented by a two-dimensional shore section with a deep vertical face and a sloping shore platform attached at the base of the cliff. Model time-steps are arbitrarily chosen as one tidal period or one hour. At every time-step, wave and tide data are sampled from files. A cross-shore distribution of longshore sediment transport is calculated using the breaker depth and assumed distribution under static conditions. A similar approach provides a cross-shore erosion distribution function. Potential sediment transport at each shore section is calculated using a CERC type equation. Slope stability is represented using a simple probabilistic model that calculates the probability and magnitude of slope failure from the angle of the cliff face. This angle is made more severe by the wave-induced erosion and reduced by the slope failure events. As it can be seen from the flow chart in Figure 3, the model includes several feedback loops to account for the influence of beach and clay profile changes on the future wave transformation and erosion patterns.

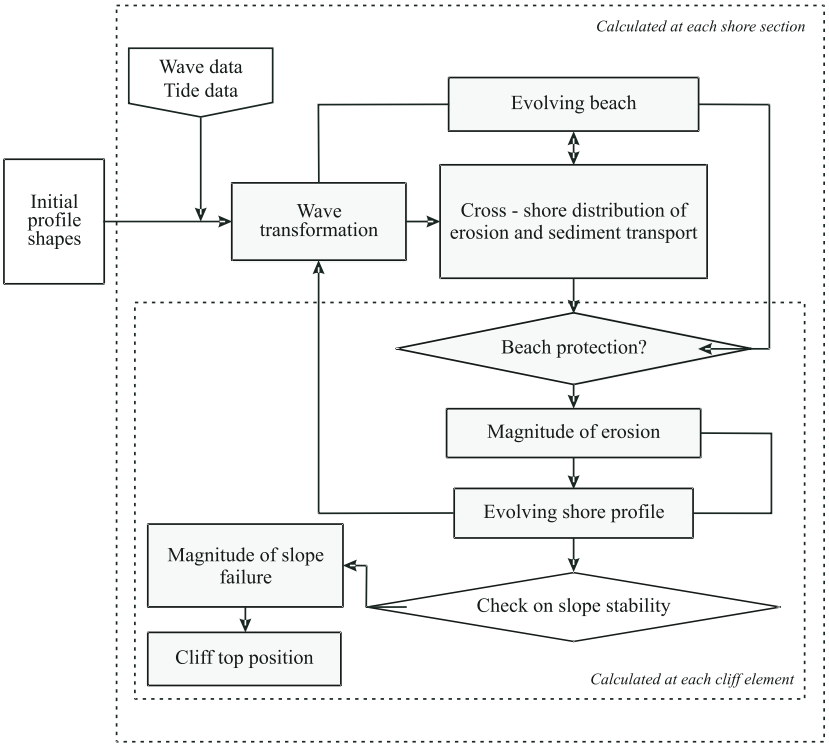

Figure 3: Flow-chart representation of cliffSCAPE (From Walkden et al., 2002)

Clearly the CliffSCAPE model contains all main ingredients of a complete model for the coast/cliff system including wave transformation, sediment transport, shore erosion and cliff stability. Although some elements of the model such as the use of CERC formula and the choice of time scale for model runs can be improved upon, it nevertheless represents a significant step towards the goal of developing a practicable as well as rational process-based model for predicting cliff retreat. It should be pointed out however that the model requires the calibration of one parameter against historic data. As the model predictions may vary with the chosen aggregation time scales, this calibration coefficient is implicitly dependent on the chosen time scale. Therefore, it should be interpreted more appropriately as a model parameter rather than the material strength coefficient as they have originally suggested. In addition, the model is still essentially two-dimensional, particularly within the cliff (a single model coefficient for all). This could be problematic as even when the relevant time scales have been worked out by trial and error or other means, there is yet little that is known about the spatial scales of cliff erosion. Large erosion events are well known to be highly non-uniform in space and such events may trigger or be correlated to smaller erosion events nearby. If this were true, the conventional two-dimensional approach would unlikely be able to address these fundamental processes adequately.

3.5 Size-Frequency Distributions

Compared with the deterministic approach with limited ability to consider uncertainties in the analysis, probabilistic approaches, either data based or model based, inherently contain uncertainties and allow a better quantification of risks (Emery and Kuhn, 1982). Hall and his co-workers (Hall et al., (2002), Lee et al., (2001) and Lee et al., (2002)) presented a range of probabilistic methods applicable to the erosion of soft cliffs including the extrapolation of historical records, event tree approaches, simulation of recession of episodically eroding cliffs through Monte Carlo techniques and process-based simulation. Regarding episodic erosion in particular, they considered the failure sizes to be log-normally distributed. This distribution was based on the data from a model cliff made from damp sand. Although the model is valuable in gaining insight into the effect of wave run-up on the toe erosion, it is restricted by the wave conditions simulated. Also as the model cliff is much easier to fail than that in the prototype, the distribution of failure size will be distorted by many unrealistic small failures. The frequency-size relation of real cliffs is expected to be quite different from that of log-normal distribution.

In order to find alternative distributions for the failure size, it is worth examining those processes which are similar to coastal cliff erosion such as landslides. The behaviour of landslides has been studied intensively over the past decades. For example, Dai and Lee (2001) investigated the magnitude-cumulative frequency relationship and relationship between rainfall and the occurrence of landslides. Their results show that landslides with a failure volume of not less than 4 m have a cumulative frequency-size distribution with a power-law dependence on volume of failure. Similarly Guzzetti et al. (2002) also studied the frequency-area statistics of landslides in central Italy. The non-cumulative frequency-area distribution of these landslides were found to correlate well with a power-law relation, exponent - 2.5 (which is equivalent to an exponent of -1.5 for the cumulative distribution). Perhaps the most convincing evidence was that presented by Pelletier et al. (1997). They found that the cumulative frequency-size distributions of landslides induced by precipitation in Japan and Bolivia as well as landslides triggered by the 1994 Northridge, California earthquake, despite being triggered by different mechanisms, have a cumulative frequency-size distribution with a power-law dependence on area with an exponent ranging from -1.5 to -2.

Based on the above observation and considering the similar episodic nature of the coastal soft cliff erosion, it is postulated that the frequency-size distribution of the cliff failures could also show a similar power-law dependence. To test this idea the field data of cliff erosion measured on two field sites have been obtained. The first data set is from 20-m high cliffs at Cliff End in East Essex on the south coast of England. The site characteristics and the data extraction methods used can be found in (Hall et al., 2002). The second data set used consists of measured annual erosion data taken from a cliff section at Hornsea/Rolston along the Holderness, England. Figures 4 show cliff size-frequency distributions of the cliffs obtained at these sites. Clearly the data can not be represented by a single known distribution. However the middle portion of both data sets can be fitted to power-law distributions. Further studies are currently under way to explore deeper in the data structure and uncover the underlying reasons for these distributions.

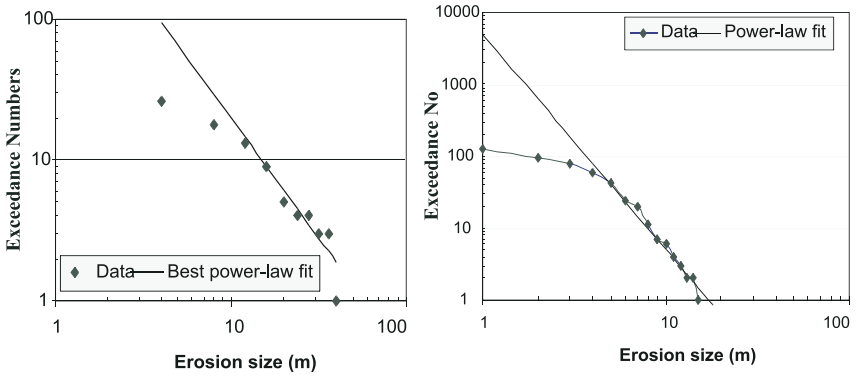

Figure 4: Failure size distributions a) Sussex and b) Hornsea/Rolston

4. Conclusions

Prediction of cliff erosion remains one of the most difficult challenges in coastal morphodynamics. The existing methods either do not address completely the problem or rely on parameterizations that are inadequate in representing beach-cliff system dynamics. The understanding of cliff processes is also hampered by the scarcity of field data, by the complexity and site-specific nature of the processes and by incomplete knowledge of the behaviour of coastal cliffs. In order to make further progress, it is essential to collect high resolution data and develop internally consistent prediction methodologies. This then allows the possible power-law behaviour of the failure size-frequency distribution to be evaluated fully and correctly interpreted in terms of the underlying physical processes. A complete model of erosion processes including rational treatment of uncertainties is feasible as long as the fundamental problems discussed in this paper are properly resolved.

Acknowledgement

The research is supported, in part, by a research grant from the Leverhulme Trust (Grant No.: F/00143/D).

References

Chapman J. A., Edil, T. B. and Mickelson D. M., 2002, Interpretation of probabilistic slope analyses for shoreline bluffs, Solutions to Coastal Disasters '02, ASCE, San Diego, CA, 2002, L. Ewing and L. Wallendorf, (editor), 640-651

Dai, F.C. and Lee, C.F., 2001, Frequency-volume relation and prediction of rainfall-induced landslides, *Engineering Geology,* 59 (3-4), 253-266

Edil, T and Schultz, M., 1983, Landslide Hazard Potential Determination Along a Shoreline Segment. *Engineering Geology,* 19, 159-177

Edil, T.B. and Vallejo, L.E., 1983, Shoreline erosion and landslides in the Great Lakes, Wisconsin Sea Grant Advisory Report 15, 7p; also in Proceedings 9th Int'l Conf Soil Mechs & Foundation Engrg, Tokyo, Japan, v.II, 51-57

Emery, K.O. and Kuhn, G.G., 1982, Sea cliffs: their processes, profiles, and classification. Geological Society of America Bulletin. 93, 644-654

Guzzetti, F., Malamud, B.D., Turcotte, D.L. and Reichenbach, P., 2002, Power-law correlations of landslide areas in central Italy, *Earth And Planetary Science Letters,* 195(3-4), 169-183

Hall, J.W., Meadowcroft, I.C., Lee, E.M. and Van Gelder, 2002, P.H.A.J.M., Stochastic simulation of episodic soft coastal cliff recession, *Coastal Engineering,* 46(3), 159-174

Kamphuis, J.W., 1987, Recession rate of glacial till bluffs, *ASCE Journal of Waterway, Port, Coastal, and Ocean Engineering* 113(1), 60 – 73

Komar, P. D., Marra, J. J. and Allen, J. C., 2002, Coastal erosion processes and assessments of setback distances. Solutions to Coastal Disasters'02, L. Ewing and L. Wallendorf, eds., ASCE, Reston, Virginia, 808-822

Lee, E.M., Hall, J.W. and Meadowcroft, I.C., 2001, Coastal cliff recession: The use of probabilistic prediction methods. *Geomorphology,* 40(3-4), 253-269

Lee, E.M., 2002, Meadowcroft, I.C., Hall, J.W. and Walkden, M.J.A., Coastal landslide activity: A probabilistic simulation model. *Bulletin of Engineering Geology and the Environment,* 61(4), 347-355

Pelletier, J.D., Malamud, B.D., Blodgett, T., Turcotte, D.L., 1997, Scale-invariance of soil moisture variability and its implications for the frequency-size distribution of landslides, *Engineering Geology,* 48 (3-4), 255-268

Pilkey, O.H. & Cooper, J.A.G., 2002, Longshore transport volumes: a critical view. *Journal of Coastal Research Special Issue,* 36, 572-580

Schuster, R. L. and Highland, L. M., 2003, Impact of Landslides and Innovative Landslide-Mitigation Measures on the Natural Environment, Geologic Hazards Team, U.S. Geological Survey, Denver, Colorado, USA

Walkden, M.J.A., Hall, J.W. And Lee, E.M., 2002, A modelling tool for predicting coastal cliff recession and analysing management options, in Instability Planning and Management, Ventnor, Isle of Wight, May 20-23, 2002, edited by R.G. McInnes and J. Jakeways. London: Thomas Telford, 415-422

ENVIRONMENTAL DESIGN AND MONITORING OF LARGE SUBMARINE OUTFALLS: AN INTEGRATED APPROACH FOR COASTAL PROTECTION

J.A. Juanes, J.A. Revilla, C. Alvarez, A. García, A. Puente
Submarine Outfall & Environmental Hydraulics Group;
Dept. of Water and Environment; University of Cantabria
Santander; Spain

K. Nikolov
North Basin Water Authority; Spanish Ministry of Environment
Santander, Spain

Abstract

In order to address the environmental impact produced for decades to the water bodies, the authorities of the major coastal municipalities and counties in North Spain (Gulf of Biskay) initiated, during the 90`s, the design and construction of new sanitation systems, according to the legal requirements imposed by the 91/271/EC Directive. Site planning, environmental risk assessment of discharges and objective-oriented monitoring were the three main tasks supporting the decision-making process related to the validation of the new sewerage projects. This process consists of four consecutive stages: 1) Design and selection of alternatives (strategic assessment), 2) Risk evaluation for different scenarios (impact assessment), 3) Verification of adverse effects (objective-oriented monitoring) and 4) Action plan for mitigation of registered impacts (management of pollution events).

Regarding impact assessment, mathematical and statistical studies for the selection of appropriate points of discharge of sewage outfalls have been an important time and labor-consuming task for the pre-commissioning stage, taking into account the random nature of the factors that influence the dispersion and reaction of different contaminants in the sea. Thus, depending on the stage of the analysis (planning vs. project design) and, consequently, the precision level needed to infer from the respective results, this procedure might support either the preliminary selection of alternatives (SEA) or the final design of the projected alternative (EIA). On the other hand, monitoring programs were based on modeling predictions and assumptions about likely responses of a great variety of environmental compartments to disturbances, through the implementation of a program of continuous measurements, that support both the definition of the specific objectives to be addressed and the more appropriate technical designs, in order to produce predefined management information useful for decision making.

1. Introduction

At the beginning of the current decade, a new conceptual approach for the design of sanitation systems was introduced in the European Union (EU), because of the legal requirements imposed by the 91/271/EC Directive on the treatment of urban wastewaters.

C. Zimmermann et al. (eds.), Environmentally Friendly Coastal Protection, 243-253.

Furthermore, the recent enforcement of both the Water Framework Directive (WFD, 2000/60/EC) and the Strategic Environmental Assessment Directive (SEA, 2001/42/EC) make up as the perfect complement for the implementation of an integrated management strategy for the protection, maintenance and/or restoration of all the aquatic ecosystems receiving urban and industrial discharges.

Traditional hydraulic and hydrological-based methods used for the validation of discharges in coastal areas have brought about important environmental problems. Thus, during the 90`s, the authorities of the major coastal municipalities and counties in North Spain (Gulf of Biskay) initiated the design and construction of new sanitation systems, in order to address the environmental impact produced for decades in the water bodies. For this purpose, the University of Cantabria and the North Basin Water Authority developed a methodology (Alvarez, 1996; CHN, 1995), which has already been applied to the "environmental design" of the sewerage of thirteen coastal communities, most of them with over two hundred thousand inhabitants (Figure 1). This methodology considered, five years in advance of the principles adopted by the WFD, the fulfillment of both the specific quality objectives tied to the water bodies receiving overflows and treated effluents and the environmental rehabilitation of the natural values of previously degraded areas (Revilla, et al., 2002).

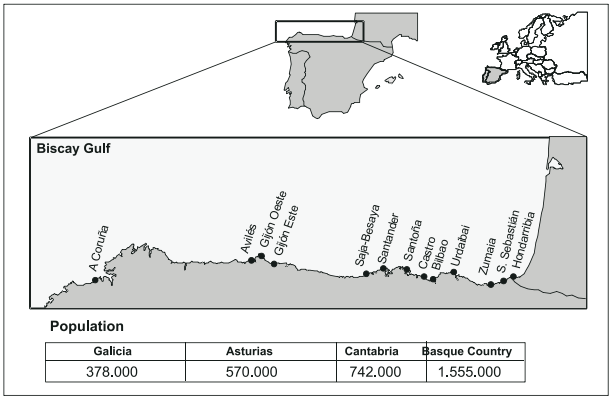

Figure 1: Location of the main sanitation systems in North Spain, with an estimation of the equivalent inhabitants in the sanitation systems of the four northern Regions

In spite of the local or regional differences observed along the North coast, there are some important similarities in the physical conditions (weather, hydrodynamics, tides...), the biological features (ecological structure and functionality of the estuarine and coastal ecosystems) and the traditional uses of water masses in this biogeographic area, known as the "Green Spain". Compliance with the EU 76/160/EEC Directive on bathing waters, and with the 79/923/EEC Directive on shellfish growing areas proved to be the most restrictive limitations for the technical approval of the modeled discharge alternatives, at all the different locations studied (Nikolov et al., 1994; Álvarez et al., 1999; Puente et al., 2002). Furthermore, oxygen depletion and eutrophication in estuarine waters were also important factors conditioning the acceptance of risks related to the discharges to those "sensitive"

ecosystems. In consequence, the discharge of dry weather treated effluents (High Load Activated Sludge Treatment, HLAST) through submarine outfalls has been the technical alternative finally adopted by most managers from the local and regional administrations involved. However, the influence of the combined sewer overflows on the exceedences of water quality thresholds in wet weather conditions (Nikolov et al., 1994; Schiff et al., 2003) justifies the need for managing sanitation as a whole, in both the spatial and the temporal scales.

Impact assessments carried out during the pre-commissioning stage, at both the planning (SEA) and the project levels (EIA), were based on the evaluation of risks (probability x consequences) estimated for different "sanitation schemes", taking advantage of the predictive power of mathematical models. However, experiences on ocean sewage outfalls in other geographic areas of the world (e.g. Mearns, 1992; Anderlini & Wear, 1992; Fagan et al., 1992; Otway et al., 1996; Bellan et al., 1999) have clearly demonstrated, first, that predictions are useless unless they can be tested at field and, secondly, that risk-free decision-making is an impossible goal. Thus, post-commissioning validation of the probabilistic predictions assumed by each sanitation project has been based on the corresponding Environmental Monitoring Program (EMP). In summary, SEA, EIA and EMP constituted the management tools available for providing the information that will enable suitable actions to be taken in order to protect the aquatic environment, its resources and human health.

As recommended by the U.S. National Research Council (NRC, 1990) and, more recently, by the Committee on Ocean Monitoring in the Canadian Department of Fisheries & Oceans (Strain & Macdonald, 2002), integration of those tools in case objective-oriented programs is a useful approach for evaluation of "ocean health", whose success depends on the ability to produce specific and accurate information to discriminate the effects of human disturbances from natural variability (Smith et al., 1988; Ferraro et al., 1991; Warwick & Clarke, 1991; Anderlini & Wear, 1992). In agreement with that procedure, site planning, environmental risk assessments of discharges and monitoring are the three main tasks supporting the decision making process related to the management of the new sanitation projects in North Spain (CHN, 1995).

The process for environmental validation of a sanitation system is made up of four consecutive stages: 1) Design and selection of integrated schemes (strategic assessment), 2) Risk evaluation for selected alternatives (impact assessment of projects), 3) Verification of adverse effects (objective-oriented monitoring) and 4) Action plan for mitigation of registered impacts (management of pollution events). In this paper, different methodological aspects regarding environmental impact assessment (1-2) and the monitoring of sewage discharges to coastal areas through submarine outfalls (3) are summarized.

2. Impact Assessments (SEA/EIA)

In the planning phase, possible sanitation schemes result as a consequence of the combination of the proposed locations for two elements: the treatment work and the discharge point of the treated effluents. Social and environmental concerns are usually the decisive factors for the acceptance of preliminary proposals, however, from a technical

point of view, the latter ones were previously the bottleneck for rejection of some alternatives. For instance, discharges of tertiary treated-disinfected dry weather effluents to estuarine areas have generally been discarded, in order to avoid unnecessary risks (i.e. shellfisheries contamination, eutrophication, long term recovery disturbances).

Regarding sewage outfalls, mathematical and statistical studies for the selection of appropriate points of discharge take into account the random nature of the factors that influence the dispersion and reaction of different contaminants in the sea (currents, tide, winds, radiation, temperature, turbidity…). Results for several projected alternatives are expressed in probabilistic terms, always referring to the lack of compliance with specific standards for different return periods, under a previously defined sampling design (Nikolov et al., 1994; Álvarez et al., 1999, Puente et al., 2002; Revilla et al., 2002). Depending on the stage of the analysis (planning vs. project design) and, consequently, the precision level needed to infer from the respective results, this procedure might support either the preliminary selection of alternatives (SEA) or the final design of the projected alternative (EIA).

As shown in Figure 2, a single-case analysis of the sewage plumes originated by two alternative outfalls for the Bilbao sewerage (Basque Country) may demonstrate their possible influence on the coastal waters of the neighboring region (Cantabria). Furthermore, results of a much more detailed spatially and temporally integrated study for the sewage outfall of Gijon (Asturias County), allowed the technical approval of different discharge alternatives (outfall flows) based on evaluation of acceptable risks (probability of non-compliance with the bathing water Directive) (Figure 3).

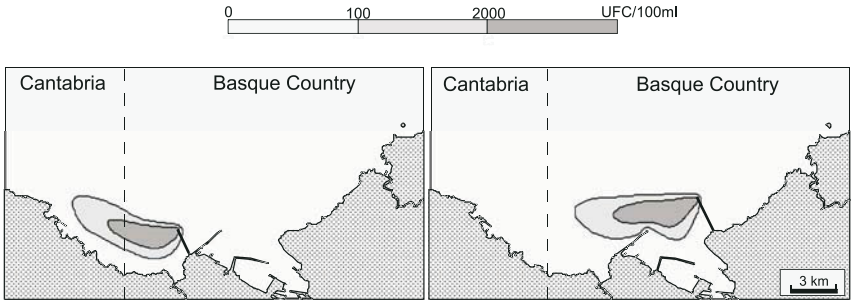

Figure 2: Simulations of sewage discharges from the two outfalls proposed for the sanitation system of Bilbao. Dashed lines indicate the administrative limits for the coastal waters of Cantabria and the Basque Country

Intensive predictive modeling studies have been an important time and labour-consuming task for the pre-commissioning stage. Moreover, fieldwork at that stage have included campaigns for calibration of hydrodynamics and sea level prediction routines (Revilla, 1999), implementation of models for the simulation of local process of oxygen evolution in shallow estuaries (García et al., 2002) and process of bacteriological inactivation (Canteras et al., 1995), establishment of sediment oxygen demand (SOD) rates (Revilla, 1999), proposal of sound sampling strategies of bathing waters (López et al., 2001), development of epidemiological tests (Prieto et al., 2003) and formulation of water quality criteria (Puente et al., 2002).

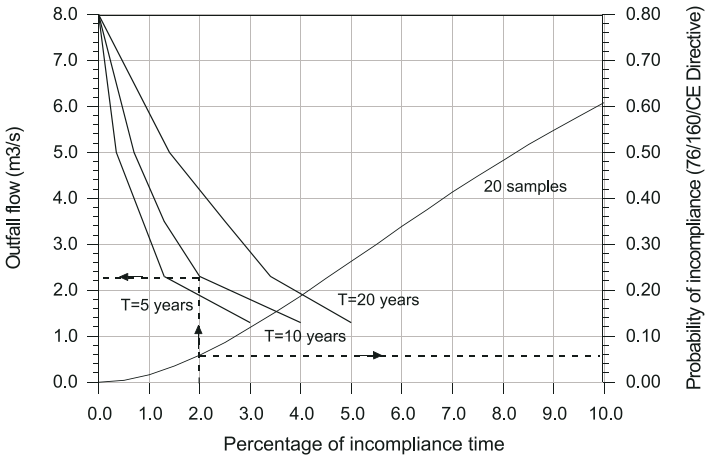

Figure 3: Design diagram for the sewage outfall of Gijon, for different return periods, considering a discrete sampling based on 20 samples through the bathing season

3. Environmental Monitoring Program

The design of EMPs of the sanitation systems followed the general model summarized by Juanes et al. (2002), whose main components are the definition of specific objectives, the accurate designs for data gathering and the generation of management-oriented information. Thus, monitoring programs were based on modeling predictions and assumptions about likely responses of a great variety of environmental compartments to disturbances. Uncertainties associated with some of those assumptions justified the need to establish an "adaptive monitoring design" (Ringold et al., 1996), through the implementation of a program of continuous measurements, that support both the definition of the specific objectives to be addressed and the more appropriate technical designs, in order to produce predefined management information useful for decision making. For that purpose, information from baseline studies, carried out at the pre-commissioning stage, and from previous regulatory surveillances (bathing waters, shellfisheries...) are the reference points for subsequent monitoring analyses.

4. Baseline Studies

At the beginning of the 90's, the scarce scientific information about the coastal ecosystems off the North coast of Spain underlined the limitations initially found for the development of predictions of responses of benthic and pelagic communities to wastewater discharges. For that reason, systematic and intensive baseline studies were carried out in the surroundings of the projected sanitation areas (Table 1). At present only 1 of the 12 sanitation systems is in full operation, that of the Bay of Santander, and three of them have implemented the EMP at the commissioning and post-commissioning stages of the outfall discharge.

The main objective of those studies was the establishment of the predischarge environmental conditions of the pelagic and benthic ecosystems, in the surroundings of

both the old uncontrolled points of discharge -some of them spatially coincident with the new overflows- and the designed ocean outfall discharges. To meet that objective, studies were designed to evaluate environmental conditions of the water column, the intertidal and the subtidal soft and rocky bottoms (cf. Revilla, 1999).

Table 1: Basic features of the sewage outfalls and information about the baseline studies in the pelagic (W) and the benthic systems (B). Bold figures indicate post-commissioning EMPs currently in course

Sanitation area	Submarine outfall		Effluent treatment	Baseline studies		Year of operation
	Depth (m)	Length (m)		Surveys W/B (year)	Stations W/B	
Hondarribia	20	350	Secondary	2/2 (1993)	9/9	**1999**
S. Sebastián	50	1200	HLAST	1/1 (1992)	21/28	**2001**
Zumaia	—	Direct	Secondary+UV	2/2 (1993)	9/9	2000
Urdaibai	10	100	Secondary+UV	4/2 (1998)	12/19	Project
Bilbao			Secondary			Project
Castro	25	1250	HLAST	—-	—-	2003
Santoña	23	2750	HLAST	4/2 (1998)	16/24	Project
Santander	36	3430	HLAST	4/2 (1998)	22/30	**2001**
Saja-Besaya	34	3075	HLAST	4/2 (1998)	22/31	Project
Gijón E	23	2600	HLAST	1/1 (1992)	20/22	1997
Gijón W	24	2100	HLAST	1/1 (1992)		Project
Avilés	36	3600	HLAST	1/1 (1992)	17/16	Construction
A Coruña	26	1620	HLAST	—	—	Project

5. Technical Design

5.1 Environmental Objectives

Stating clear monitoring objectives involves integrating public concerns and the predictions of the environmental designs with the legal and regulatory framework, through the use of scientific understanding, to identify relevant questions to be addressed (NRC, 1990). However, this is a difficult task due to the lack of clearly defined normative standards and the scarce scientific knowledge about many subjects, which restricts the establishment of appropriate reference and acceptable conditions. In a few cases, like that of bathing waters or shellfish growing areas, specific criteria have been enforced by law (Directives 76/160/EEC and 79/923/EEC). In most cases, quantitative criteria that take into account the global protection of either the pelagic or the benthic ecosystems do not exist. Furthermore, the discharge of hazardous substances is currently regulated for a limited number of them (Directive 76/464/EEC). These shortages imply that, many times, scientists must develop their own criteria (Nikolov et al., 1994; Puente et al., 2002).

Surveillance of the health of bathing waters and shellfish growing areas, aesthetic deterioration, trophic status of the coastal and estuarine water bodies, benthic pollution effects and bioaccumulation were the preliminary environmental objectives adopted by all

the EMPs (CHN; 1995). However, because of the adaptive design of the monitoring programs, case-specific modifications were already purposed. For instance, after three years of intensive monitoring of the discharges of the Santander outfall, the eutrophication in the surrounding coastal areas was evaluated as a quite unlikely risk, reducing the relevancy of this objective to a secondary level.

5.2 Sampling and Measurement Implementation

Field surveys for collecting data are among the most expensive and laborious process in environmental assessment and constitute a major element in EMP, whose effectiveness depends, to a large extent, on sampling design. Nevertheless, applicable normative do not usually specify the sampling and analytical procedures.

In order to ensure the fulfillment of the established objectives, EMPs were designed according to the specific physical (e.g. bathymetric profiles, substrates...), chemical (e.g. effluent characteristics), biological (e.g. special habitats and resources) and socioeconomic features (e.g. beaches, shellfisheries..) of each sanitation system. Regulatory surveillance programs currently developed in bathing zones and shellfish growing areas were also adjusted to fit the statistical requirements of the risk assessments used for the sanitation design (López et al, 2000; Puente et al., 2002). In general terms, the EMPs for sewage outfalls consider the control of water quality four times a year and the implementation of a single and extensive campaign of the benthos, every spring-summer season, because of its capacity to register the effects of discharges.

Anyway, working in the coastal environment complicates the establishment of general rules. Thus, initial sampling designs may be modified in order to achieve a better assessment of the actual effects. For instance, according to previous monitoring results (sediment dynamics, chemistry of sediments, benthic communities) obtained around the point of discharge of the Santander outfall, the sampling network for near-field impact assessment on benthic ecosystems, implemented at the post-commissioning stage, was later simplified in combination with the bioaccumulation studies (Figure 4).

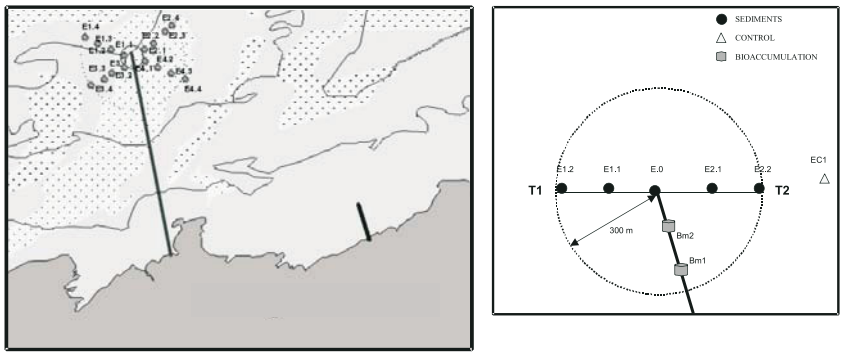

Figure 4: Preliminary sampling network implemented for near-field impact assessment on benthic ecosystems of the Santander outfall (left) and close-up of the adopted modification (right)

In a similar way, the preliminary proposal of monitoring indicators for analyses of water and benthos that was established in the general methodology (CHN, 1995) has been progressively modified. The schedule of variables included in the currently developed EMPs is shown in Table 2. Procedures for sampling and analysis of those variables in different matrices were standardized, following a specific monitoring manual for each sanitation system.

Table 2: Selected variables for the monitoring of water bodies and benthic ecosystems)

Indicators	Diagnostic	Warning	Fulfillment	Control*
Water	Salinity Temperature Detergents	Chlorophyll a pH Grease and oils	Dissolved oxygen Turbidity	DIN, DIP Suspend solids
Benthos	Granulometry Organic matter	Benthic communities	Heavy metals PCBs	Total N Total P

* Only in the case that annual average values of warning indicators exceed the normal ranges

5.3 Quality Assurance and Control

Standardization and validation of sampling and analytical techniques is one important problem to be solved in EMP design. Data that are not based on adequate quality assurance/quality control (QA/QC) may be erroneous, and their misuse can lead to wrong management decisions (Batley, 1999). In spite of this fact, the applicable normative and EMPs usually make little or no reference to quality control. However, it should be pointed out that some recent proposals include in their items the necessity of estimating the level of confidence and precision of the results provided by the monitoring programs (Directive 2000/60/CE, COM 2000/860). Thus, analytical performance is an important goal for implementation in the EMPs.

Main problems in this respect mainly arise because of most of biological determinations (e.g. taxonomic identification of species) that may be influenced by different error types (human factor, sampling representability, nomenclature). Based on the extensive monitoring work carried out all along the Biskay Gulf, different studies on the "taxonomic sufficiency" (Warwick, 1988) for detecting environmental impacts of sewage outfalls have been implemented (cf. Juanes & Canteras, 1995; Puente et al., 2002).

6. Synthesis and Interpretation of Data

The objective of the EMP is not to generate relevant technical or scientific information, but rather to provide the information needed by decision makers to address public concerns. As shown in Figure 5, management-oriented Geographic Information Bases, which combine environmental, socioeconomic and regulatory data, are useful tools for the synthesis and interpretation of data.

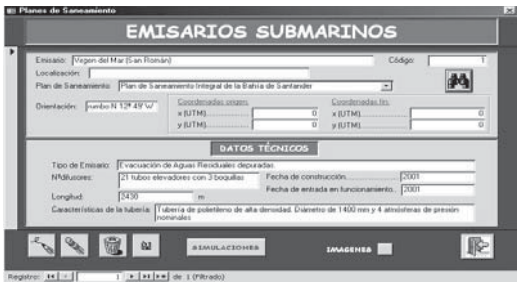

Figure 5: Example of the Geographic Information Base (GIB) developed for the management of information in the region of Cantabria (N Spain)

7. Conclusions

As a general conclusion of this work, it should be noted that environmental-oriented planning strategies for the design of sanitation systems in the coastal zone will be the only way to protect the aquatic environment, its resources and human health. For that purpose, SEA, EIA and EMP constituted the management tools available for providing the information that will enable the sustainable management of coastal areas.

Acknowledgements

Part of this work was supported by the National Plan of Research and Development (2000-2003) from the Spanish Ministry of Science and Technology (Project # REN2001-1225-C03) and by a "Ramón y Cajal" Research Grant to J.A. Juanes.

References

Álvarez, C. 1996. Aportaciones metodológicas al estudio de la contaminación litoral originada por vertidos y alivios procedentes de redes de saneamiento urbano. Ph. D.-Thesis, University of Cantabria (Spain): 253 pp.

Álvarez, C., Juanes, J.A., Revilla, J.A., Koev, K.N., Roldán, A., Ivanov, V. 1999. Environmental study of the alternatives for the sewer system of a small coastal community in the Bay of Biscay. *Wat. Sci. Tech.,* 39(8): 161-168

Anderlini, V. C. and Wear, R. G. 1992. The effects of sewage and natural seasonal disturbances on benthic macrofaunal communities in Fitzroy Bay, Wellington, New Zealand. *Mar. Pollut. Bull.*, 24: 21-26

Batley, G.E. 1999. Quality assurance in environmental monitoring. *Mar. Pollut. Bull.*, 39: 23-31

Bellan, G., Bourcier, M., Salen-Picard, C., Arnoux, A., Casserley, S. 1999. Benthic ecosystems changes associated with wastewater treatment at Marseille: implications for the protection and restoration of the Mediterranean coastal shelf ecosystem. *Water Environ. Res.*, 71(4): 483-493

Canteras, J.C., Juanes, J. A., Pérez, L., Nikolov, K.N. 1995. Modelling the coliforms inactivation rates in the Cantabrian sea (Gulf of Biskay) from "in situ" and laboratory determinations of T90. *Wat. Sci. Tech,* 32(2): 37-44

CHN.1995. Metodología de estudio de los saneamientos litorales. Confederación Hidrográfica del Norte (CHN), Dirección Técnica, Oviedo (España)

Fagan, P., Miskiewicz, A.G., Tate, P.M. 1992. An approach to monitoring sewage outfalls. A case study on the Sydney deepwater sewage outfalls. *Mar. Pollut. Bull.,* 25:172-180

Ferraro, S.P., Swartz, R.C., Cole, F.A., Schults, D.W. 1991. Temporal changes in the benthos along a pollution gradient: discriminating the effects of natural phenomena from sewage-industrial wastewater effects. *Estuar. Coast. Shelf Sci.,* 33: 383-407

García, A., Revilla, J.A., Medina, R., Álvarez, C., Juanes, J.A. 2002. A model for predicting the temporal evolution of dissolved oxygen concentration in shallow estuaries. *Hydrobiologia,* 475/476: 205-211

Juanes, J.A., Canteras, J.C. 1995. Monitoring of sewage outfalls in northern Spain: preliminary studies of benthic communities. *Wat. Sci Tech,* 32(2): 289-295

Juanes, J.A., Puente, A., Revilla, J.A., López, M., Alvarez, C., Medina, R. (2002) Monitoring programs design in coastal zones affected by combined sewer overflows and outfall discharges. Proc. II Int. Conference on Marine Waste Water Discharges. 8 pp.

López, B., Juanes, J.A., Revilla, J.A., Álvarez, C., Delgado, M. 2000. The bathing water quality control in the beaches of North Spain: proposal for a local protocol of monitoring. *Environm. Engin. & Health Sciences:* 255-265

Mearns, A.J. 1992. Ecological effects of ocean sewage outfalls: observations and lessons. *Oceanus,* 24: 45-54

National Resarch Council. 1990. Managing troubled waters. The role of marine environmental monitoring. National Academic Press. Washington, D.C. 125 pp.

Nikolov, K.N., Revilla, J.A., Alvarez, C., Luceño, A. 1994. A design methodology for combined sewer system elements with overflows in coastal zones. *J. Coastal Res.,* 10: 531-538

Otway, N.M., Gray, C.A., Craig, J.R., McVea, T.A., Ling, J.E. 1996. Assessing the impacts of deepwater sewage outfalls on spatially and temporally variable marine communities. *Mar. Environ. Research.*, 41(1): 45-71

Prieto, D., López, B., Juanes, J.A., Revilla, J.A., Llorca, J., Delgado, M. 2001. Recreation in coastal waters: Health risks associated with bathing in sea water. *J. Epidemiology & Community Health,* 55: 442-447

Puente, A., Juanes, J.A., García-Castrillo, G., Álvarez, C., Revilla, J.A., Gil, J.L. 2001. Baseline study of soft bottom benthic assemblages in the Bay of Santander (Gulf of Biscay). *Hydrobiologia,* 475/476: 141-149

Puente, A., Juanes, J.A., Revilla, J.A., Álvarez, C., Gómez, J., García, A. 2002. Desarrollo de un criterio aplicable a la vigilancia de la calidad bacteriológica de las aguas en las zonas de producción de moluscos de la Bahía de Santander. *Bol. Inst. Esp. Oceanogr.,* 18 (1-4): 67-73

Revilla, J.A. (dir.tec.) 1999. Estudios complementarios al estudio de alternativas e informe de impacto ambiental del saneamiento de las marismas de Santoña. Tech. Rep. Confederación Hidrográfica del Norte, Ministerio de Medio Ambiente, Madrid

Revilla, J.A., Álvarez, C., García, A., Medina R., Juanes, J.A. 2002. Environmental design of submarine outfall according to the European Water Framework Directive. Proc. 2nd Int. Conf. On Marine Waste Water Discharges. 12 pp.

Ringold, P.L., Alegría, J., Czaplewski, R.L., Mulder, B.S., Tolle, T., Burnett, K. 1996. Adaptive monitoring design for ecosystem management. *Ecol. Applic*., 6: 745-747

Schiff, K.C., Morton, J, Weisberg, S.B. 2003. Restrospective evaluation of shoreline water quality along Santa Monica Bay beaches. *Marine Environmental Research,* 56: 245-253

Smith, R. W., Bernstein, B.B. and Cimberg, R.L. 1988. Community-environmental relationships in the benthos: applications of multivariate analytical techniques. In: Marine organisms as indicators, D. F. Soule and G. S. Kleppel (eds.). Springer-Verlag, New York, pp. 247-326

Strain, P.M., Macdonald, R.W. 2002. Design and implementation of a program to monitor ocean health. *Ocean & Coastal Management,* 45: 325-355

Warwick, R. M. 1988. Analysis of community attributes of the macrobenthos of Frierfjord/Langesundfjord at taxonomic levels higher than species. *Mar. Ecol. Prog.* Ser., 46, 167-170

Warwick, R. M. and Clarke, K. R. 1991. A comparison of some methods for analyzing changes in benthic community structure. *J. Mar. Biol. Ass. U. K*., 71, 225-244

EVALUATION OF COASTAL DEFENCE STRATEGIES IN PORTUGAL

Rui Taborda
GeoFCUL/LATTEX, Lisbon University
Lisboa, Portugal

Fernando Magalhães
Instituto da Água, Divisão de Ordenamento e Protecção
Lisboa, Portugal

Carlos Ângelo
Urb. Portela, Paços de Brandão, Portugal

Abstract

In Portugal, coastal protection has proceeded largely in an *ad hoc* manner and has been based on the construction of hard engineering protection structures generally constructed to address emergency situations. This paper presents the results of two case studies that were used to compare the local and global cost-effectiveness of two coastal protection strategies: construction of groin fields and beach nourishment. According to the results of this study, beach nourishment is the most cost effective solution in the Algarve open beaches, with moderate energy conditions. In the high energetic environment of the Aveiro coast, beach nourishment was also shown to be cost effective when a significant fraction of the sediment cell is considered.

1. Introduction

Presently, most of the Portuguese sandy shorelines are affected by coastal erosion with retreat rates that, in some locations, reach several meters per year. This behavior is related with an important sand deficit that is mainly related to dam construction, sand and gravel exploitation and extensive estuarine dredging for navigation. Shoreline retreat is also enhanced locally by sand retention on coastal structures and by sea level rise although this last factor seems to play a secondary role (circa 10%, according to Ferreira et al., 1990, Andrade, 1990).

The combination of coastal erosion with the huge value of coastline properties and the economic importance of the coastal tourism industry has created a management problem that is very difficult to solve. This problem is generally addressed by three methods: hard stabilization, soft stabilization and relocation. The strategy adopted to cope with the coastal erosion problem should be technically sound, environmentally acceptable and economically viable.

In Portugal, coastal protection has until very recently, relied almost exclusively on the use of groin fields. This kind of strategy, which has been used in long-term erosional shorelines without any beach nourishment schemes, stands against the recommended practice. In fact,

C. Zimmermann et al. (eds.), Environmentally Friendly Coastal Protection, 255-265.

the use of groins as a shore protection method has a very restricted window of application; the fact that groins have been used so ubiquitously reflects a general misunderstanding about their functioning (Headland et al., 1999). This trend started to change in the last years and some alternative solutions have been attempted. However, these solutions have been used without an assessment of cost and benefits related to a particular solution and the first efforts to evaluate the cost-benefit ratio of different solutions are only now being developed, this work providing a re-iteration of the studies presented by Magalhães et al. (submitted). Due to the lack of suitable data, only direct costs for the "hard" and "soft" protection schemes were considered in this study. In the "hard" stabilization method only the costs related with groin construction were considered.

2. Approaches to Coastal Erosion

An adequate protective beach scheme is fundamental to any coastal protection plan. Beach protection can be obtained either by hard engineering structures that can be shore-normal (e.g., groins) or shore-parallel (e.g., seawalls or detached breakwaters) or by soft protection methods like beach nourishment. Shore-normal structures are generally used to prevent the cross-shore movement of sand that occurs during storms and the flooding of hinterland areas, while shore perpendicular structures are generally used to reduce longshore sediment transport (Headland et al., 1999). In this paper only groins will be discussed, since they are, by far, the most frequently used structure for coastal protection in Portugal.

2.1 Groin Fields

Groins interrupt littoral drift. Sands accumulate updrift and there is downdrift erosion induced by that blocking, which is sometimes felt several kilometers from the groin, leading, in most cases, to the construction of additional groin fields. Although it is difficult to estimate the extent to which a groin field will retard longshore sediment transport, the effectiveness of groins is most strongly related to the length of these structures with respect to the width of the surf zone. Feenstra et al. (1998) have shown that it will be most economical to built relatively short groins focusing on the reduction of the littoral drift in the inner surf zone during moderate wave conditions. These authors also discuss the situations in which groins may be applied and are cost-effective. According to them, these structures are not effective along, namely, steep reflective high-energy sand coasts and macro-tidal sand coasts. Nersesian et al. (1992) have concluded that groin fields can be used to reinforce or to hold protective beach fills and that bypassing of longshore sediment should be ensured.

One fundamental aspect of the functional design of groins is related to the ratio between groin spacing (gs) and groin length (gl). According to US Army Corps of Engineers (2002), a ratio of 2 – 3 is required for the proper functioning of shore-normal groins.

2.2 Beach Nourishment

As stated by Headland et al. (1999) "Beaches offer storm protection through a natural dynamic response to varing waves and water levels. Accordingly it is difficult to provide better shore protection than that offered by a beach". Since artificial nourishment emulates

nature itself, it is the most effective and friendly protection alternative. Beach nourishment is described in many papers and books, the excellent reviews by Dean (2002) and Douglass (2002) providing outstanding examples. Beach nourishment is a soft protective and remedial measure that leaves a beach in a more natural state than hard structures and preserves its recreational value. It is a popular option in highly developed areas with heavily used beaches and valuable beachfront real estate, especially during the early onset of erosion. This option has been the worldwide selected alternative for shore protection since the 1960s. A good example is Miami Beach, Florida, US, which was renourished over the period 1976 through 1981 at a cost of around 52×10^6€ . Attendance at the beach increased from 8 million in 1978 to 21 million in 1983. Globally, there was a 700 € return for every 1 € invested in beach nourishment (Houston, 1996).

In the cases where there is a systematic sediment deficit, where the coast suffers from a chronic erosion problem, artificial nourishment will be subject to the same erosion and the beach fill design should include recognition of the regular maintenance cost. This issue is related to a main weakness that is related with beach fill operations as the general public, if not properly informed, will considered the beach fill a failure and reclaim a more "visible" protection scheme.

In Portugal, soft protection schemes have been only been used in relatively sheltered beaches and, in general, with fixed structures to prevent end losses. Examples can be found in the Algarve: Praia da Rocha (Gomes and Weinholtz, 1971), Alvor (Teixeira, 1999), Cabanas Island (Dias et al., 2003), Cacela Peninsula (Ângelo, 2001, Dias et al., 2003); and in low-energy pocket and estuarine beaches on the west coast (Andrade et al., in press; Ministério do Ambiente, 1999).

3. Case Studies

Two case studies, which suffer from chronic coastal erosion problems, were used for the comparison of the local and global cost-effectiveness of coastal defence strategies: Costa Nova / Vagueira, south of Aveiro, in the west coast and Quarteira / Vale do Lobo, in the south coast (Figure 1). Both sites are located on open sandy coastal stretches and are characterized by large differences in energy levels and magnitudes of littoral drift processes.

Data used in this study were obtained from actual construction costs while maintenance costs were estimated from the available data and literature. In what concerns beach nourishment expenditure at these coastal stretches, beach nourishment costs were estimated taking into account the saturation of the littoral drift, the unit cost of sand for some nourishment projects in Portugal and the availability of offshore sand sources.

3.1 Quarteira/Vale do Lobo

The analyzed coastal stretch is represented by a narrow sand beach backed by medium to low height (10 to 15 m) cliffs which developed in poor consolidated red sandstones. These cliffs are the main source of sand that feeds the longshore drift, which has a net transport on the order of 10^4 to 10^5 m^3/y directed eastwards (Andrade, 1990). This coastal stretch suffered from chronic erosion problems which were reported at least since 1940, with

mean retreat rates for the period 1958/1969 in the order of 0.5 m/y (Correia et al., 1994). In order to stop coastal erosion at one of the largest tourist villages in Algarve, several groins were built in the decade of 1970 in front of Quarteira, inducing, along with the Vilamoura marina jetties, the interruption of the eastward littoral transport. As a consequence, there was a net increase in cliff retreat rates, which attained, during the period of 1974/80, a mean rate of up to 7.5 m/y downcoast of the groin field, at Forte Novo (Correia et al. 1994; Marques, 1997). Presently, the Quarteira groin field has 6 groins, 100 m to 140 m long, which protect a coastal stretch of approximately 1500 m (Figure 2).

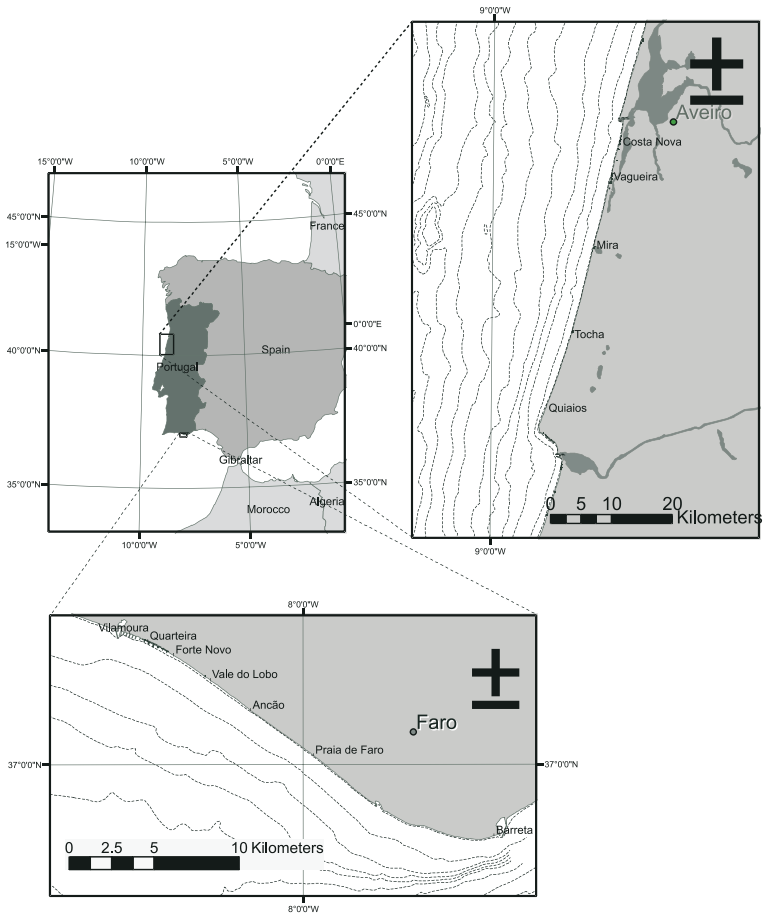

Figure 1: Location map of case studies: A) Costa Nova/Vagueira; B) Quarteira/Vale do Lobo

Due to the trapping of sand in the groin field the downcoast progressive erosion of the beach started to threaten other major tourist resorts, increasing the pressure to build protection structures. This could lead to a never ending spiral of protective structures that

begun with a rip-rap construction to protect Vale do Lobo swimming pool in 1984/85, and ultimately could lead to the construction of a groin field ending only at Barreta, approximately 25 km to the east.

Figure 2: Aerial view of coastal structures in front of Quarteira

To estimate the actual cost related with the building of protective hard structures in this coastal stretch, data from similar structures recently built in the Algarve coast were used. A mean building cost of 4,000 € per meter of structure groin was found, reasonably agreeing with Van Rijn (1998) estimates of 2,500 to 4,000 U$. Assuming that the maintenance of these structures increases their cost by a factor of 3 over 50 years (Van Rijn, 1998), an estimated cost of 12,000 € / meter structure is obtained. Using a value of 2 for the ratio gs/gl, meaning that each meter of groin should protect 2 meters of shoreline, which is about the same that is used to protect that coastal stretch in front of Quarteira, an estimated cost over 50 years of 6,000 € / m, which is equivalent to an average cost of 120 € per meter of shoreline per year.

Due to the tourist importance of the area, the political option for the coastal defence of this sandy stretch has changed and it was decided to artificially nourish these beaches. This option would enable the maintenance of the environmental values of the region and the width of the beaches and cliffs, one of the most valuable aspects of the region (Veloso-Gomes et al, 2003). The artificial sand nourishment began in 1998 and was finished in the first week of January 1999, involving the deposition of 600 000 m^3 of sand, pumped from offshore, from a distance of 4 km and depths between 16 m and 20 m, along 1400 m shoreline (Teixeira et al., 1998). The actual cost of this operation was 2.4 M €,

which should be supported, in equal shares, by government authorities and Vale do Lobo Resort.

Unfortunately, no monitoring program was conducted after the nourishment so the relevance of this operation for the protection cost estimation is limited; nevertheless, it can give some guidance on that matter. In this case, assuming the need for long term nourishment of a volume equal to the potential net longshore drift (100 000 m^3/yr) and a cost of sand of 2.5 € /m^3, the protection cost per year would be around 250 000 € /yr. The present estimate for sand cost, that was obtained directly from contractors, is somewhat lower than that obtained for the Vale do Lobo nourishment (4.0 €/m^3) but is roughly in the middle of the interval presented by Muñoz-Perez et al. (2001) for 38 restorations operations carried out in 28 beaches along the Gulf of Cadiz which have similar conditions. There is still a large uncertainty concerning the average longshore drift volume along the coast. While some authors estimate a volume of $10^3 m^3$/yr, others estimate a longshore drift two order of magnitude larger ($10^5 m^3$/yr), with most authors suggesting a value between 3×10^4 and 5×10^4 m^3/yr (Consulmar, 1995 in Teixeira et al., 1998). In order to have a conservative estimate, the larger value of the interval was used. This estimate agrees reasonably well with present field observations which indicate that the beach width is reaching its pre-fill stage (Pinto, personal communication). However, despite being "lost" after some time so far as Vale do Lobo beaches are concerned, sand is not lost to the system. Due to longshore drift, which operates throughout the entire littoral cell, the sand which was used to nourish this coastal stretch moves to eastward beaches. This means that the nourishment, as it stops the cause of erosion (the sand deficit) there, would ultimately protect the entire coastal sediment cell.

Considering the extension of the nourished coastal stretch, a value of 180 € per meter of shoreline per year is obtained. However, because of the role of nourishment in protecting the entire coastal sediment cell, the protection costs will be "diluted" when a larger coastal length is considered, meaning that the protection cost per unit length of sandy shore decreases as larger coastal stretches are taken into account. For example, when considering coastal stretches of 5 km (Quarteira / Vale-do-Lobo) and 20 km (Quarteira / Barreta), the maintenance cost will be reduced to 50 €/y/m and 12.5 €/y/m, respectively. These results show that even for relatively small coastal stretches the beach nourishments cost estimates are much lower that those obtained for the construction of a groin field.

The source of sand is one of the critical aspects concerning beach nourishment design. In this case, studies by Teixeira & Macedo (2001) have shown that the offshore sources of sand between Quarteira and Barra Nova do Ancão are estimated to be at least 5×10^6 m^3, which will be sufficient to saturate the littoral drift for several tens of years.

3.2 Costa Nova/Vagueira

This coastal stretch is located in the Aveiro district, south of Aveiro lagoon. The coast has a NNE-SSW orientation and corresponds to a linear low sandy coast. It is fully exposed to high energetic Atlantic swell, with a net southward longshore drift around 1×10^6 m^3 / yr (Oliveira et al., 1982). Presently this area is subject to severe erosion problems, due to the sand retention on the updrift side of Aveiro harbour jetties. Following construction of the jetties , shoreline retreat rates increased dramatically southward of these structures and a

retreat of 200 m up to 300 m was recorded between 1947 and 1978 (Veloso-Gomes et al., 2003), with mean rates that attained 8 m/yr. This situation has led to the construction of the Costa Nova groin field, which induced retreat values as high as 50 m in the two-year period after their construction (Dias, 1990). A total of eleven groins were built in the period 1972/73 to protect this coastal stretch (Oliveira et al., 1982; Oliveira, 1990). However, the present-day situation, as evident from the analysis of aerial photographs, is somewhat different, with 7 groins and almost 2 km of seawalls (Figure 3). The characteristics of the identifiable defence structures are given in Hidrotécnica Portuguesa (1997) and in Veloso-Gomes et al. (2002).

Figure 3: Aerial view of coastal structures in front of Vagueira

Despite this protection scheme, the recession in this stretch is more serious than previously. According to Veloso-Gomes et al. (2002), the shoreline is predicted to retreat to a position that will result in the formation of one or more new inlets in the Ria de Aveiro. This situation has been prevented by emergency works, which have been executed in the last few years by locals and by the local and central administration authorities in order to allow sufficient time to prepare more sound solutions. Presently this coastal stretch is protected by a very vulnerable dune system that needs to be artificially repaired or reconstructed otherwise it may result in flooding of the rich agricultural hinterland areas. If a new inlet forms , the southern lagoon system will suffer the direct influence of coastal waters and the agricultural lands will be saline with strong impacts on the ecosystems.

According to the Eurosion project (www.eurosion.org) coastal erosion in this area has already caused severe economic losses by reducing the visitation of beaches, estimated at

half a million people during summer in Aveiro. In the same period the cost for creating and maintaining efficient coastal protection works has resulted in lower value for land properties established along the coast (down by 80% of the initial value in some places).

To estimate the protection cost using a groin field, data from two 220 m – length groins were recently built south of Cost Nova in the ambit of the Portuguese Water Institute (INAG)'s Coastal Zone Management Plan, were used. Each groin cost about 2,000,000 €; that is the cost of each meter of these structures was around 9,000 €. This value is clearly above Quarteira / Vale do Lobo and Van Rijn (1998)'s estimates for groin cost (2,500-5,000 €/m structure) but is justified by the highly energetic characteristics of the coast. Assuming, that the maintenance of these structures increases their cost by a factor of 3 over 50 years (Van Rijn, 1998), an estimated cost of 27,000 €/m groin is obtained. Using a value of 3 for the ratio gs/gl meaning that each meter of groin should protect 3 meters of shoreline (the maximum value suggested by US Army Corps of Engineers, 2002 and similar to the one presently used for coastal protection in a Portuguese Coastal stretch with similar characteristics Espinho-Paramos), this leads to an estimated cost over 50 years of 9,000 €/m shoreline or 180 €/m/yr, which is considered a relatively high protection cost. On the other hand, the maintenance costs for the period 1975-1997 (Hidrotécnica Portuguesa, 1997) suggest that Van Rijn (1998)'s estimates for such costs are underestimated in the case of Costa Nova, meaning that value could be even higher.

In this highly energetic environment, the unit cost of nourishment sand should also be higher than the previous case, so the average cost was estimated as 3 €/m;. For an overall volume transport rate on the order of $10^6 m^3/y$ (the assumed littoral drift, not accounting for the present transposition at Aveiro inlet, which was hypothetically estimated by Oliveira (1997) to be around 2×10^5 m^3/yr) that is required for the system to become saturated, a global cost of 3×106 €/m^3/yr is expected. As discussed in the previous case, when the littoral drift becomes saturated at a given locality the same holds true for the entire downdrift coastal stretch. Considering littoral stretches of 5 km (Aveiro jetties / Vagueira Norte), 20 km (Aveiro jetties / Mira) and 50 km (Aveiro jetties / Quiaios), the corresponding protection costs are about 600 €/m/y, 150 €/m/y and 60 €/m/y, respectively. These results show, that even in this high energy coast with a large longshore drift magnitude, beach nourishment can be a cost-effective solution for coastal protection.

In this case, where huge values of sand are needed for beach nourishment maintenance, the offshore sand borrow site is one of the main concerns when considering the viability of this strategy. Several works carried out in the Portuguese mainland coast (e.g. Dias et al., 1980; Magalhães, 2001, 2003) have identified large amounts of sand and gravel deposits in the continental shelf offshore Aveiro coast, whose characteristics and depth of occurrence make them favorable borrow areas for such operations. In this situation offshore sand requirements could also be strongly reduced with the implementation of a sand bypassing system at Aveiro inlet.

4. Conclusions

In Portugal, the choice of the different options for coastal protection has relied on subjective criteria and not on objective cost-benefit analysis, which has resulted in inappropriate measures of coastal erosion mitigation. To address this issue two case

studies were used to compare the local and global cost-effectiveness of a "hard" and a "soft" approaches. The chosen sites are characterized by differences in energy levels and magnitudes of littoral drift processes. It should be point out that the figures presented in this work are based on available data; as more data will become available, cost estimates will be refined. Nevertheless, and despite present uncertainties, some general conclusions on cost-effectiveness of different approaches to coastal erosion at the studied sites can be drawn.

In the lower-energy littoral (Quarteira/Vale do Lobo), artificial nourishment becomes a solution that is very cost-effective, regardless of the length of the coastal stretch considered. In fact, when the all the littoral cell is considered the direct protection costs is one order of magnitude lower that of the groin field approach.

In a high energy littoral zone (Costa Nova/Vagueira), the protection of the coast by a groin field is more economical than artificial nourishment only when a small coastal stretch is considered. When the protection scheme includes at least a significant part of the littoral sediment cell, as environmentally advisable, beach nourishment becomes the most economical option.

These results show that even in a highly energetic coast, with high net longshore drift values, beach nourishment is not only the environmentally preferred method but also the most economic one. It also should be stressed that only direct construction and maintenance cost were considered in this study; if other costs, like recreational benefits, storm damage reduction and property appreciation benefits of the different defence methods, were also taken into account, probably beach nourishment would have an even better cost-benefit ratio compared to the hard stabilization scheme.

The main contribution of the present study is to hopefully increase the public and political awareness to a very serious problem which is related to a critical option concerning coastal erosion and our legacy to future generations.

Acknowledgments

This is a DISEPLA Group contribution and was partially supported by Fundação da Ciência e Tecnologia thought project PDCTM/P/MAR/15265/99 "CROP". The authors wish to acknowledge Irmãos Cavaco, S.A. for the Vagueira photograph.

References

Andrade, C., 1990. *O ambiente de barreira da Ria Formosa, Algarve - Portugal*. PhD thesis. Universidade de Lisboa, 627 pp. (*unpublished*)

Andrade, C., Freitas,M.C., Cachado, C., Cardoso, A., Monteiro, J., Brito, P. & Rebelo, L. 2002. *Coastal Zones*. In: Santos, F.D., Forbes, K. & Moita, R. (eds.) *Climate Change in Portugal. Scenarios, Impacts and Adaptation Measure.* Gradiva, Lisboa, 173-219

Ângelo, C. 2001. *Técnicas de protecção e de conservação da zona costeira. Uma estratégia de gestão operacional*. Tese de mestrado, Fac. Ciências Univ. Lisboa, 168 pp. (*unpublished*)

Andrade, C. (*in press*). Monitoring the Nourishment of Santo Amaro Estuarine Beach (Portugal). *Journal of Coastal Research*, SI 39

Bettencourt, P. 1997. Notas para uma estratégia de gestão da orla costeira. *Colectânea de ideias sobre a Zona Costeira de Portugal*. Associação Eurocoast, Portugal, 265-283

Correia, F., J.M.A. Dias & T. Boski. 1994. The retreat of eastern Quarteira cliffed coast and its possible causes (preliminary results). *Gaia* 9, 119-122

Dean, R.G. 2002. *Beach Nourishment. Theory and Practice*. Advanced Series on Ocean Engineering, World Scientific, 18, 399 pp.

Dias, J.M.A. 1990. A evolução actual do litoral portugês. *Geonovas*, 11, 15-29

Dias, J.M.A., J.H. Monteiro & L.C. Gaspar. 1980. Potencialidades em cascalhos e areias da plataforma continental portuguesa. *Com. Serv. Geol. Portugal*, 66: 227-240

Dias, J.M.A., Ferreira, Ó., Matias, A., Vila, A. e Sá-Pires, C. (2003). Evaluation of Soft Protection Techniques in Barrier Islands by Monitoring Programs: Case Studies from Ria Formosa (Algarve – Portugal). *Journal of Coastal Research*, SI 35, 117-131

Douglass, S.L. 2002. *Saving America's Beaches. The Causes of and Solutions to Beach Erosion*. Advanced Series on Ocean Engineering, 19, 91 pp.

Feenstra, J.F., I. Burton, J.B. Smith & R.S.J. Tool. 1998. *Handbook on methods for climate change impact assessment and adaptation strategies*. Nairobi and Amsterdam: UNEP and IES

Ferreira, Ó., J.M.A. Dias & R. Taborda. 1990. Importância relativa das acções antrópicas e naturais no recuo da linha de costa a sul de Vagueira. *Actas do 11 Simpósio sobre a Protecção e Revalorização da faixa costeira do Minho ao Liz*, 157-163

Gomes N. & M.B. Weinholtz. 1971. Evolução da embocadura do estuário do Arade (Portimão) e das praias adjacentes. Emagrecimento da praia da Rocha e sua reconstituição por deposição de areias dragadas no anteporto. *3as jornadas luso-brasileiras de engenharia civil*, III-4, 1-26

Headland, J., Smith, W.G., Kotulak, P., Alfageme, S. 1999. Coastal Protection Methods *in Handbook of Coastal Engineering*, Editor: J.B. Herbich, McGraw-Hill, 8.1-8.66

Hidrotécnica Portuguesa, 1997. *Plano de Ordenamento da Orla costeira Ovar-Marinha Grande. Estudos de Base*. Volume 2 – Dinâmica costeira e obras de defesa

Houston J.R. 1996. International tourism and U.S. beaches. *Shore and beach*, 67, 2-3

Magalhães, F. 2001. A cobertura sedimentar da plataforma continental portuguesa. Distribuição espacial. Contrastes temporais. Potencialidades económicas. *Doc. Técnico Inst. Hidrográfico*, 34, 287 p.

Magalhães, F. 2003. Aggregate deposits in the portuguese continental shelf. *Thalassas*, 19, 23-31

Magalhães, F., C. Ângelo & R. Taborda (*submitted to Thalassas*) - Towards the adoption of adequate coastal protection strategies in Portugal

Marques F. 1997. Sea cliff evolution: the importance of quantitative studies for hazard and risk assessment, and for planning of coastal areas. *Colectânea de ideias sobre a Zona Costeira de Portugal*. Associação Eurocoast, Portugal, p. 67-86

Ministério do Ambiente, 1999. *Programa Litoral/99*. 75 pp. Lisboa

Nersesian, G.K., N.C. Kraus & F.C. Carson. 1992. Functioning of groins at Westhampton Beach, Long Island, New York. *Proceedings 23rd International conference on coastal engineering*, ASCE, New York, 3357-3370

Oliveira, I. M. 1990. Erosão costeira no litoral norte. Considerações sobre a sua génese e controlo. *Actas do 11 Simpósio sobre a Protecção e Revalorização da faixa costeira do Minho ao Liz*, 201-221

Oliveira, I. M. 1997. Proteger ou não proteger ou sobre a vulnerabilidade de diferentes opções face à erosão costeira. *Colectânea de ideias sobre a Zona Costeira de Portugal*. Associação Eurocoast, Portugal, 205-227

Oliveira, I.M., Valle, A.F. & Miranda, F. 1982. Litoral problems in the portuguese west coast. *Proceedings International conference on coastal engineering, III, 1951-1969*

Teixeira, S.B. 1999. Alimentação artificial de praias do Algarve. *Cidades e Munícipios. Temática: Por um novo litoral*, 54-58

Teixeira, S.B.; Furtado A. & Gaspar, M. 1998. Avaliação do Impacte da Alimentação Artificial da Praia de Vale do Lobo nas Comunidades de Bivalves (Algarve-Portugal). *Seminário sobre Dragagens, Dragados e Ambientes Costeiros*: 47-56, Associação Eurocoast-Portugal, Porto

Teixeira, S. B. & Macedo, F. 2001. *Prospecção de manchas de empréstimo ao largo de Albufeira (Algarve)*. Relatório DRAOT Algave, 59 pp.

U.S. Army Corps of Engineers. 2002. *Coastal Engineering Manual. Engineer Manual* 1110-2-1100, U.S. Army Corps of Engineers, Washington, D.C. (in 6 volumes)

Van Rijn L.C. 1998. *Principles of Coastal Morphology*. Aqua Publications, Amsterdam.

Veloso-Gomes, F., F. Taveira Pinto, J.P. Barbosa, L. Neves & C. Coelho. 2002. Littoal 2002. Associação Eurocoast, Portugal: 411-422

CONCLUSIONS AND RECOMMENDATIONS OF THE WORKING GROUPS

On the last day of the workshop, discussions in three subgroups were held. The discussions focussed on Coastal Morphology, Engineering Structures and their Hydrodynamic Interactions and on Environmental Aspects and Integrated Modelling.

1. Coastal Morphology

Participants: Ping Dong, Dorina Dragancheva, Razvan Mateescu, Boyan Savov, Jens Schefferman, Rui Taborda, Ekaterina Trifonova, Claus Zimmermann, Robert Dean (chair)

The morphological working group adopted a scope of identifying needs to ensure the availability of: (1) An adequate understanding of the physics underlying coastal and nearshore processes, and (2) The associated information/data resources to provide guidance for future decisions related to coastal morphological changes. This scope encompasses effects of relative sea level change and reduction in sediment supply, each which can induce erosional pressure on the beach and nearshore systems and each of which can be due to both natural and/or anthropogenic causes. The array of possible responses to erosional pressure include: (1) Retreat, (2) Coastal armouring, (3) Beach nourishment, and (4) Combinations of these. The appropriate response for a particular scenario will require improved decision making tools than are now available and an incorrect response could be quite expensive, both monetarily and sociologically.

1.1 Data Collection and Processing

Long-term data should be organized, stored and made available for future generations and decision making. These data should include shoreline positions and nearshore bathymetry. I International level standards should be defined how to measure and how to store data. Surveys of available sediment resources with attention to both quality and quantity are needed. Also this information should be available via standardised databases. Take advantage of “Experiments of Opportunity” to develop a better understanding of nearshore processes.

1.2 Consultancy and Relation with Clients

Recognize the uncertainties in morphological prediction. Educate clients to have realistic expectations. Prior to recommending an approach, attempt to understand the system, i.e. is the shelf a source of sink of sand? Assume greater responsibility in developing and ensuring adherence to appropriate coastal legislation. Encourage multidisciplinary and integrated approaches. Coastal structures have the potential for substantial negative impacts to adjacent beach systems which should be considered in design. Consider the setting.

C. Zimmermann et al. (eds.), Environmentally Friendly Coastal Protection, 267-271.

1.3 Future Developments

Recognize the possibility of Global Climate Change and consider adaptive responses. Tools (models) are needed to evaluate coastal response to sea level rise and/or reduction in sediment supply without engineered responses. Methods are needed of separating the shoreline and nearshore effects of natural and anthropogenic causes. Also tools are needed to evaluate the effects of coastal protection structures and the maintenance. All tools should incorporate the best understanding of the relevant physics. It is therefore necessary to look for case studies which clarify and hopefully quantify the processes, for example of large interruptions in longshore sediment transport or reductions in sediment supply.

Finally the group concluded that workshops of this type should be continued to promote technology transfer and to ensure more consistency.

2. Discussion on Engineering Structures and their Hydrodynamic Interactions

Participants: Lorenzo Capietti, Sevket Cokgor, Kristjo Daskalov, Marcel van Gent, Pedro Lomonaco, Stig Magnar Lцves, Tomasz Marcinkowski, Valeri Penchev, Joan Pope, Panayotis Prinos, Francisco Sancho, Henk Jan Verhagen (chair)

From the discussion it followed that in general the main problem is not so much the limits in specialised knowledge, as well the implementation and application. In spite of this, some deficiencies were identified in the ongoing research programmes. The discussion addressed four relevant issues:

2.1 Research Issues

Within this issue, the discussion concentrated on the need for further research. Modern computational techniques make it very well possible to make mathematical descriptions of nearly all processes and to compute hydrodynamic behaviour in detail. Of course calibration of the mathematical models is essential, and is usually done using physical models. The continuous need for calibration and verification of mathematical models using physical models was stressed. Regarding the interaction of water and sand and/or mud beds, mathematical models are much more complicated, but still very possible. However, calibration and verification is much more complicated because of the difficulty to make physical models coupling the hydrodynamics with sediment transport. Consequently it was concluded that there is a lack of knowledge related to scour processes. Prediction of scour is essential for the stability of a structure. Therefore insight in scour processes is important. On the other hand, if well monitored, scour can be observed and in many cases scour can be stopped by using appropriate bed protection (dumping of stone).

Morphological models give at this moment very acceptable predictions for long term coastal protection; in order to apply these models some kind of "dominant wave climate" is used. However, it is questionable if the same mathematical models (especially the same calibration factors) can be used in case of extreme hydraulic loads, which is usually the design condition for an engineering structure.

In general it was concluded that for many research results it takes too much time before these results are implemented in the daily design routine. This is largely caused by the fact that researchers are usually not interested in contributing to design manuals, because research funding cannot be used for design manuals (Universities usually provide money to research groups related to the number of scientific publications, preferably in Journals, not read by designers; contributions to a design manual are often not considered as scientific publications, and therefore not appreciated accordingly).

2.2 Guidance for Structure Performance

It was concluded that often coastal managers lack guidance on when to apply a structure and if a structure can be applied, what is the best structure to be applied. Design guidelines for the structure are usually clear, but the morphological effects are difficult to generalise, they are very case dependent. So, regarding morphological effects of structures, one should always perform site specific studies. It is very important that managers realise that they should not try to solve local, isolated problems without considering the whole system.

Quite some guidance is needed for the managers of low crested structures. It is expected that the European DELOS program will provide the required knowledge. Of course there is now a need to disseminate the findings and conclusions in the form of guidelines to coastal managers.

2.3 Information to Decision Makers

It was concluded that communication with decision makers is often a problem. Very often this depends on the definition of "success". For example nearshore nourishments are considered successful to maintain the long term sediment balance for a coastal stretch, but they may not be successful in providing a wide beach during the next tourist season. It is important to define the performance standard. Project goals have to be defined clearly in terms understandable by the public. Results of research should be put in forms for both public and political understanding.

2.4 Failures

Failures are inherent to the construction process. However, failures are seldom reported in detail, especially when the failures are not too large, and no official enquiry is made. Even a greater problem are "non-functioning" structures. Many patented structures have been presented, and applied in some field tests. In cases where such structures did not provide the required results, usually no extensive report regarding this structure is presented. Consequently potential users elsewhere are not aware of the non-effective performance. It is therefore suggested that a database be developed containing results of experimental structures. The database should to be set up with care. It is not the intention to blame persons or organizations, but only to prevent that the same mistake is made twice.

The same database can be used to report on "experiments of opportunity". For example if a temporary structure for some reason is not removed and exposed to an overload, the behaviour of this structure may provide useful information. Reporting on such a case is important

3. Environmental Aspects and Integrated Modelling

Participants: Doina Botzan, Jose Cortezon, Jose Juanes, Gytautas Ignatavičus, Vitalij Ivanov, Anna Ivanova, Grzegorz Rozynski, Iwona Szalucka, Nicolaj Lissev, Margaret Johnsen, Stephan Mai, Dano Roelvink (chair)

The environmental working group tried to make an inventory of the status of environmental aspects and integrated modelling in the countries of the participants. This inventory was focussed on a number of aspects.

3.1 Climate Change

In Germany and Holland historical trends are accounted for as a minimum. In Holland the IPCC recommendations are taken into account; this leads to a special concern for the tidal inlets and near estuaries. In Germany no accelerated sealevel rise is considered, but a fixed additional safety factor of 50 cm for important hydraulic structures is taken into account. In Poland the issue is very controversial, in the US the government is minimising the discussion, it is there difficult to find consensus. The UK follows active planning and mitigation, e.g. Humber shoreline management plan.

3.2 Public Acceptance

The working group concluded that there is a need for improvement of the public acceptance of necessary coastal protection. This could be achieved by:

- Better information on risk of doing nothing;
- Integrated CZM, much participation;
- Long-term process to reduce mistrust of government;
- Educate children, in a balanced manner;
- Adapting to public concerns;
- Difficult to deal with very negative attitudes.

3.3 "Environmentally-Friendly Structures"?

It is difficult to give a good definition of an environmentally-friendly structure. Aesthetic aspects are extremely important but subjective. It should in any case have no negative effects on water quality and one should consider the role of the structure within the whole coastal cell. Some participants consider that a minimum requirement is to have a beach at all. In this respect EU directives on habitats are relevant for important habitats on sea bottom. Because of developments at the coast control of water quality is important. The effluent from hotels should always be treated before it is discharged into the sea. Hotel owners often look only to short term profit, and are therefore less interested in water quality control; they become only interested when they observe a decrease in guests because of the pollution, but at that moment measures are already too late. In Romania this is a significant problem.

The lack of land (e.g. at the Crimea) triggers reclamation works. When not properly designed, such works may also worsen the water quality. Mathematical modelling is in

such cases needed to predict the effects. Usually bad effects are predicted due to altered circulation, added effluents, problems related to dredging in sensitive areas. In situations with strong enough tidal currents, deep dredging pits may be preferable to wide shallow pits; this is not possible in other seas because of occurrence of anoxic situations.

3.4 Protection of Soft Cliff Coasts

On a number of places, notably in Poland, accelerated cliff erosion is observed due to increased storminess. In many cases the costs are very high in relation to the value of the land, so perhaps one should sacrifice the area in many cases. In some cases this results in an unofficial "do nothing" policy (e.g. in Romania, due to limited economic governmental resources and no interest with some private investors, like hotel owners).

In some cases retarding toe erosion may be a solution. In a few cases hard defences (e.g. at some places along the Bulgarian coast) have been constructed with the aim to stop toe erosion.

3.5 Integration

There is a strong need for further integration of physical, biological and social points of view for ICZM. Meetings and discussions are often too much mono-disciplinary (e.g. at this workshop there is only one biologist). However, it is difficult to establish communication between disciplines. Interdisciplinary research is not always accepted as "serious". In any case one should integrate disciplines within institutes. Accomplishment of this objective requires a critical mass.

AUTHORS INDEX

Fernando MAGALHÃES	Instituto da Água, Divisão de Ordenamento e Protecção, Lisboa	Portugal	255
Stephan MAI	Franzius-Institut for Hydraulic, Waterways and Coastal Engineering, University of Hannover	Germany	149
Tomasz MARCINOWSKI	Maritime Institute Gdansk	Poland	219
Andreas MATHEJA	Franzius-Institut for Hydraulic, Waterways and Coastal Engineering, University of Hannover	Germany	149
Kalin NIKOLOV	North Basin Water Authority; Spanish Ministry of Environment; Santander	Spain	243
Valeri PENCHEV *	Coastal Hydraulics Div., Bulgarian Ship Hydrodynamics Centre	Bulgaria	107
Joan POPE *	Coastal and Hydraulics Lab., US Army Engineer Research and Development Center	USA	41
Panayotis PRINOS	Aristotle University Thessaloniki Coastal Eng. Lab.-Hydraulics Lab.	Greece	177
Zbigniew PRUSZAK	Dept. Coastal Dynamics & Engineering., Institute of Hydroengineering, PAS, Gdańsk	Poland	129
A. PUENTE	Dept. of Water and Environment; University of Cantabria, Santander	Spain	243
José A. REVILLA	University of Cantabria	Spain	243
J.A. ROELVINK *	WL | Delft Hydraulics, Delft	Netherlands	93
Grzegorz ROZYNSKI *	Institute of Hydro-Engineering, Polish Academy of Sciences	Poland	129
Oliver STOSCHEK	Franzius-Institut for Hydraulic, Waterways and Coastal Engineering, University of Hannover	Germany	149
Marek SZMYTKIEWICZ	Dept. Coastal Dynamics & Engineering., Institute of Hydroengineering, PAS, Gdańsk	Poland	129
Rui TABORDA	Dept. of Geology, University of Lisbon	Portugal	255
Henk Jan VERHAGEN *	Delft University of Technology	Netherlands	57
Cesar VIDAL	Ocean & Coastal Research Group, University of Cantrabria, Santander	Spain	191
Claus ZIMMERMANN *	Franzius-Institut for Hydraulic, Waterways and Coastal Engineering, University of Hannover	Germany	11

** Key-note Speaker*

SUBJECT INDEX